Bright Ehijiele Amenkhienan

The Role of Iron Oxides in Organic Matter Preservation and Phosphate Sorption in New South Wales Soils

School of Life and Environmental Sciences

Faculty of Science

The University of Sydney

New South Wales, Australia

A thesis submitted to fulfill requirements for the degree of

Doctor of Philosophy

February 2026

Statement of originality

I certify that the intellectual content of this thesis is the product of my own work. This thesis has not been submitted for any degree or other purposes before and all the assistance received in preparing this thesis and sources have been duly acknowledged.

Name: Bright Ehijiele Amenkhienan

Date: 16 February 2026

Australian Government Support

This research was supported by the **Soil Science Challenge Grants Program** funded by the **Australian Government Department of Agriculture, Fisheries and Forestry** and this research contributes towards the **National Soil Strategy** and the implementation of the **National Soil Action Plan**.

Artificial Intelligence

No content produced by generative AI tools has been used in the preparation of this thesis.

Authorship attribution statement

Chapter 2 of this thesis is a review of literature published as Amenkhienan, B.E., Dijkstra, F., Warren, C. and Singh, B. (2024). Understanding extractable metal species relationships with phosphorus sorption and organic carbon in soils. *Soil Research 62 (8)*. https://doi.org/10.1071/SR24118.

I designed the study with co-authors, analysed the data and wrote the drafts of the manuscript.

Student name: Bright Ehijiele Amenkhienan

Date: 16 February 2026

In addition to the statement above, as a supervisor for this candidature, I can confirm that the authorship attribution statements above are correct.

Supervisor name: Balwant Singh

Date: 16 February 2026

Acknowledgements

I thank the Almighty God for giving me life, strength, courage and perseverance throughout my PhD journey despite hearing the shocking news from Nigeria about the death of my dad at the beginning of my research.

I am thankful to the Tertiary Education Trust Fund (TETFund) for their financial support in tuition fees and living expenses during my PhD research.

I am grateful to my supervisor Professor Balwant Singh, for his in-depth supervision of my PhD research. I highly appreciate his immeasurable support, valuable suggestions, critical review and constructive feedback he gave me during my research. I am thankful to my co-supervisor Professor Feike Dijkstra, for his support and constructive feedback offered to me during my PhD research. Many thanks to another of my co-supervisor Professor Charles Warren for his useful comments that helped in producing this thesis.

I would like to say a big thanks to my progression panel chair, Associate Professor Andrew Merchant and progression panel member Dr William Salter, for their support and suggestions during the yearly progress evaluation meetings in ensuring that my research is running smoothly and that I am well mentally and fit to complete my PhD programme.

I thank Sami Hoxha and Adriana Hoxha for their assistance in soil sampling, Nicholas Proschogo and Bernadeth Antonio for their technical assistance in the ICP-MS analysis, Samuel Duyker for his technical assistance in XRD and XRF analysis and, Jeremy Wykes for his help during data collection on the beamline at Australian Synchrotron. I am also thankful to the following technical staff; Iona Gyorgy, Hero Tahaei, Tatjana Matic, Evelyn Yin, Dominic Cross, and Bridie Stanfield for the immense support I received during my laboratory work.

A heartfelt and special thanks to my wife Laurette Chala whom I got married to during my PhD programme and my twins Eliana and Ezra who were given birth to during my PhD programme, for the energy, unending love and unwavering support to complete my research. I thank my sibling Stephen, relatives, and in-laws for their support.

I am grateful to the Nwanoka's family who picked me from the airport, supported and accommodated me for 3 months without paying any bills when I first arrived in Australia. Many thanks to my church family and Box family who supported my family and I right from when I came to Australia. A very big thanks to my friends in the office, Zongtang Yang, Andree Nenkam, Chinaza, Oscar Wang, Sandra Evangelista, Mikaela Tilse, James Hunt, Siska Syaranamual, Md Zillur Rahman, Shamim Mia, Ho Jun Jang (Jay), Christy Tsz Hung, Yu Mi, Marliana Widyastuti, Lloyd Huang, Anna Favaro, Rachel Yamamoto, and Yijia Tang for the enjoyable and shared experience during my PhD journey.

Table of Contents

List of Figures

List of Tables

Abstract

Evaluating the role of iron (Fe) and aluminium (Al) oxides in the preservation of soil organic carbon (SOC) and phosphate sorption is important for better management of soils and enhancing our knowledge on global soil C cycling and phosphate sorption in agricultural soils. Thirty-seven surface (0 – 20cm) and 37 subsurface (20 – 40cm) soil samples from 37 sites across different agricultural regions of New South Wales, Australia. Soil samples were subjected to three separate extractions, i.e., sodium pyrophosphate (PP) to extract organo-metal complexes, ammonium oxalate (OX) to extract poorly crystalline and short-range order (SRO) minerals and dithionite citrate bicarbonate (DCB) to extract total metal oxides and associated OC. X-ray absorption spectroscopy (XAS) was used to identify and quantify Fe in different minerals using 18 surface and subsurface bulk soil samples. Soil clay minerals and Fe oxides were examined by X-ray diffraction (XRD). Surface and subsurface soils with substantial Fe oxides contents from two sites i.e., Wagga Wagga and Tumbarumba were used to evaluate the adsorption of phosphate and DOC behaviour. Adsorption data were fitted into linear initial mass isotherms. Results showed that SOC was extracted in the sequence: $C_{PP} > C_{DCB} > C_{OX}$, with mean of 62 %, 41 % and 28 % C, respectively, of the TC in soils. C_{PP} and C_{DCB} were significantly greater in the surface than the subsurface soils. The extraction sequence for Fe was: $Fe_{DCB} > Fe_{OX} > Fe_{PP}$, with mean of 49 %, 9 % and 3 %, respectively, of the total Fe. The sequence for Al was: $Al_{DCB} > Al_{OX} > Al_{PP}$, with mean of 4 %, 3.9 % and 2 %, respectively, of the total Al. All extractable forms of Fe and Al showed significant positive correlations with extractable C, which suggested their role in the preservation of SOC. Linear combination fitting (LCF) analysis of the X-ray absorption near edge spectroscopy (XANES) and extended X-ray absorption fine structure (EXAFS) at the Fe-K edge revealed that crystalline Fe oxides (i.e. hematite and goethite) accounted for 60 % and 40 % respectively, of the proportion of total Fe present in the bulk soil samples. The predictions for ferrihydrite were reasonable from both

XANES and EXAFS. XAS predicted Fe content in various Fe phases was well correlated with the DCB extractable Fe. EXAFS predicted Fe contents in different phases better than XANES in bulk soils. The isotherm showed that both surface and subsurface soils from Tumbarumba had a greater phosphate adsorption capacity than the soils from Wagga Wagga. Phosphate adsorption was greater for the subsurface (m = 0.72) than the surface (m = 0.82) soil from Tumbarumba. The trend for surface and subsurface was opposite for Wagga Wagga soils, where phosphate adsorption capacity was greater for surface (m = 0.55) than the subsurface (m = 0.37) soils. The greatest capacity for DOC adsorption in both studied soils occurred in the subsurface soils. In the mixed solution of P and DOC, phosphate adsorption promoted DOC desorption in the surface and subsurface soils from Wagga Wagga and Tumbarumba. The findings from these studies are important in providing valuable insights for farmers, climate modelers, land managers and researchers in soil science in making informed decisions on the prediction of SOC and phosphate sorption.

Chapter One

Introduction

Soils contain approximately 75 % organic carbon (OC) pool in the terrestrial biosphere (Paul *et al.*, 2008). Globally, soil stores approximately 2340 petagram of OC in 0 - 30 cm topsoils, of this about 64 % of the OC is present in 0 - 10 cm topsoils (Jobbágy and Jackson, 2000; López-Ulloa *et al.*, 2005). Soil organic carbon (SOC) is dynamic in nature, and it is a significant component of biogeochemical C cycle (Lal *et al.*, 1999; Yu *et al.*, 2025). Soil OC plays important role in several physical, chemical and biological properties of soils (Watanabe, 2017). The preservation of SOC is pivotal in maintaining soil structure, increasing soil quality, soil fertility, agricultural productivity, mitigating global environmental challenges and maintaining ecosystem services (Milne *et al.*, 2015; Lal, 2016; Fujisaki *et al.*, 2018; Georgiou, 2025; Sabetizadeh *et al.*, 2025). The association of OC with minerals, termed as mineral-associated organic carbon (MAOC), has received significant attention in recent years, because it is recognised as a major mechanism in the long-term stabilisation and preservation of OC in soils (Sollins *et al.*, 1996; Torn *et al.*, 1997; Lützow *et al.*, 2006; Rasmussen *et al.*, 2006; Lehmann and Kleber, 2015; Hall and Thompson, 2022). Iron (Fe) and aluminium (Al) are considered the most important mineral components in the preservation of OC in MAOC (Wilson *et al.*, 2013; Watanabe, 2017; Wagai *et al.*, 2020; Jia *et al.*, 2024). A number of mechanisms, such as, co-precipitation, surface complexation, weak chemical interactions and cation bridging has been postulated in the formation of MAOC involving Fe/Al oxides in soils (Kögel-Knabner *et al.*, 2008; von Lützow *et al.*, 2008; Kleber *et al.*, 2015; Kang *et al.*, 2024). However, the nature of association and stability of OC with Fe/Al oxides in different soil types are not well understood.

Iron and Al are among the most abundant elements in soils (Cornell and Schwertmann, 2003). The formation of Fe and Al oxides including hydroxides, oxyhydroxides and oxides in soils is

primarily through weathering and dissolution of primary minerals (Chadwick and Chorover, 2001). These minerals possess higher specific surface area (SSA) and reactive hydroxyl sites which makes the minerals effective sorbents for dissolved OC (Kaiser and Guggenberger, 2000; Mikutta *et al.*, 2007). Iron bound OC contributes about 15 to 38 % of the total OC in sediments and soils (Cornell and Schwertmann, 2003; Wagai and Mayer, 2007; Zhao *et al.*, 2016). Surface hydroxyl groups of Fe oxides preferentially react with carboxylic functional groups of OC via ligand exchange in stabilising and preserving OC in soils (Gu *et al.*, 1994; Mikutta *et al.*, 2007; Kleber *et al.*, 2015; Chen *et al.*, 2020). The concentrations of Fe and Al oxides is commonly high in tropical and subtropical soils, which are highly leached and highly weathered (Singh and Gilkes, 1992; Mikutta *et al.*, 2009). Despite the prevalent occurrence of Fe oxides in Australia soils, the association of OC with Fe oxides has remained poorly understood in these soils (Davey *et al.*, 1975; Singh and Gilkes, 1992; Viscarra Rossel *et al.*, 2010). The relationship between SOC and extractable metals may provide insight into the role of different metal species in the formation of MAOC and preservation of OC in soils (Coward *et al.*, 2017). This perspective has been asserted by significant positive relationships between SOC and ammonium oxalate extractable Fe and Al, which suggested the significant role of poorly crystalline Fe/Al oxides or short range order (SRO) Fe/Al oxides in the formation of MAOC in soils (Kaiser and Guggenberger, 2000; Kleber *et al.*, 2005; Rasmussen *et al.*, 2006; von Fromm *et al.*, 2025). In addition, the abundance of crystalline Fe oxides has been reported to be the key driver of MAOC abundance in soils, with significant relationships between dithionite-citrate-bicarbonate extractable Fe/Al and SOC found in soils from different regions of world (Mu *et al.*, 2016; Zhao *et al.*, 2016; Yu *et al.*, 2019; Zhao *et al.*, 2023). The relationships between extractable forms of metals had been studied mostly using limited surface soils. More so, there is a lack of information on the role of different species of Fe and

Al in the SOC stabilisation and preservation in phosphorus (P) deficient soils, which occupy much of the tropic and subtropics regions and southern hemisphere including Australia.

The preservation of OC is significant in the context of P dynamics in soils. Phosphorus is an essential nutrient required by plants in large amounts in several important functions including photosynthesis, respiration and regulation of several enzymes (Hawkesford *et al.*, 2023). Phosphorus is released into soils from the weathering of primary P containing minerals such as apatite (Stewart *et al.*, 2005). The concentration of total P in soils ranges from 1.4 to 9639 mg/kg, with an average concentration of 584 mg/kg in surface (0 – 30 cm) soils (He *et al.*, 2021). The average total P concentration in slightly weathered, intermediately, and highly weathered soils, based on global and regional databases, is 719, 481 and 472 mg/kg, respectively (He *et al.*, 2021). Despite the substantial amount of total P present in most soils, crop productivity is often limited by P availability, because a small fraction (< 1 %) of the total P is present in soluble forms (Bünemann *et al.*, 2011; Balemi and Negisho, 2012). Plant roots absorb P from soil solution primarily as monobasic phosphate ($H_2PO_4^-$) and dibasic phosphate (HPO_4^{2-}) ions (Tiessen, 2005).

The concentration of phosphate in soil solution is controlled by various reactions that have been considered under three categories, which include (i) adsorption-desorption, (ii) dissolution-precipitation, and (iii) mineralisation-immobilisation (Sims and Pierzynski, 2005; Bünemann, 2015; Roberts and Johnston, 2015). In highly weathered soils of tropical and subtropical regions, P is the generally the most limiting plant nutrient because of their high P sorption capacity and low P use efficiency (Singh and Gilkes, 1991; Tiessen, 2005; De Campos *et al.*, 2016). In soils of the tropical and subtropical regions, phosphate sorption occurs on Fe and Al oxides surfaces through phosphate exchange with hydroxyl (OH^-) groups otherwise known as ligand exchange reactions (Parfitt *et al.*, 1975; Borggaard *et al.*, 1990; Torrent *et al.*, 1992; Torrent, 1997; Agbenin, 2003). Herndon *et al.* (2019) reported that almost half of soil

phosphate was sequestered by Fe oxides in shallow organic soils of low-lying areas from Artic and Boreal regions. Some studies have related chemically extractable forms of Fe and Al with phosphate sorption capacity of soils (Walker and Syers, 1976; Borggaard *et al.*, 1990; Singh and Gilkes, 1991).

There is a complex interaction among Fe/Al oxides, organic matter (OM), and P in soils. Phosphorus is an important component of SOC, because a large amount of P, necessary for the formation of organo-mineral complexes, is stored with SOC (Spohn, 2020). The presence of OM on surfaces of Fe and Al oxides can block P adsorption sites, thereby improving P availability in soils (Hunt *et al.*, 2007). Furthermore, they can also prevent the crystallisation of Fe and Al oxides (Schwertmann, 1966). Therefore, it is important to evaluate the role of Fe and Al oxides in P deficient soils that occupy much of the tropic and subtropics regions and southern hemisphere including Australia. This will enhance our understating of global soil C cycling, phosphate adsorption behaviour and assist in better management of agricultural soils of New South Wales (NSW), Australia. In addition, the identification and quantification of Fe oxides in soils is still a challenge, consequently, there is a need for a simple procedure in this regard. Considering all the above, the specific objectives of this study were to:

- ✓ examine relationships among the different fractions of extractable Fe and Al with SOC concentration and P adsorption capacity and the relationship between P adsorption capacity and SOC concentration from published literature
- ✓ determine the role of different fractions of metal(loid)s in preserving OC in both top and sub-soils of agricultural regions of New South Wales, Australia
- ✓ evaluate the use of X-ray absorption spectroscopy to quantify Fe in different minerals and organic phase in selected surface and subsurface soils
- ✓ examine the competitive adsorption behaviour of phosphate and dissolved organic carbon (DOC) in surface and subsurface soils rich in Fe oxides.

This thesis is organised into 6 chapters. Chapter 1 introduces the research topic and outlines the structure of the thesis.

Chapter 2 presents a review of literature evaluating the relationship between extractable Fe and Al and SOC concentration and P sorption capacity. Two key research questions were asked: (1) do extractable Fe and Al have any relationships with P sorption capacity and SOC concentration? and, (2) do P sorption capacity and SOC concentration have any relationship? To address these questions, data from 77 published article were systematically synthesised and analysed, research gap identified, and the chapter set the foundation for subsequent chapters. The chapter has been published in Soil Research Journal as; Amenkhienan, B.E., Dijkstra, F., Warren, C. and Singh, B., 2024. Understanding extractable metal species relationships with phosphorus sorption and organic carbon in soils. *Soil Research*, *62*(8).

Chapter 3 investigated extensively the role of different fractions of Fe, Al, Mn and Si in the preservation of OC in both top and sub-soils. The study hypothesised that SRO minerals of Fe, Al, Mn and Si contribute more to the preservation of OC in both top- and sub-soils. The study further hypothesised that concentration of Fe will be the most prominent amongst the metals in all extractions in both top- and sub-soils. The manuscript is prepared for submission to Geoderma Journal.

Chapter 4 focused on the use of X-ray absorption near edge and extended X-ray absorption fine structure spectroscopy at the Fe-K edge to identify and quantify Fe-containing minerals and Fe complexed with OM in bulk soils. The manuscript is prepared for submission to Clay and Clay Minerals Journal.

Chapter Five examined adsorption of phosphate, DOC, and competitive adsorption of both phosphate and DOC from mixed solutions of P and DOC on surface and subsurface soils with substantial Fe oxides. The study hypothesised that phosphate or DOC adsorption will be greater in the subsurface soils than the surface soils. The study further hypothesised that DOC would

inhibit phosphate adsorption in both surface and subsurface soils. The manuscript is prepared for submission to Frontiers in Soil Science Journal.

Chapter 6 provides the summary conclusions of this thesis and suggest areas where future research is needed.

References

Agbenin, J.O., 2003. Extractable iron and aluminum effects on phosphate sorption in a savanna Alfisol. *Soil Science Society of America Journal* **67**, 589-595.

Balemi, T., Negisho, K., 2012. Management of soil phosphorus and plant adaptation mechanisms to phosphorus stress for sustainable crop production: a review. *Journal of soil science and plant nutrition* **12**, 547-562.

Borggaard, O.K., Jdrgensen, S.S., Moberg, J.P., Raben-Lange, B., 1990. Influence of organic matter on phosphate adsorption by aluminium and iron oxides in sandy soils. *Journal of Soil Science* **41**, 443-449.

Bünemann, E.K., 2015. Assessment of gross and net mineralization rates of soil organic phosphorus–A review. *Soil Biology and Biochemistry* **89**, 82-98.

Bünemann, E.K., Oberson, A., Frossard, E., 2011. Phosphorus in action: Biological processes in soil phosphorus cycling. *Soil Biology* **26**.

Chadwick, O.A., Chorover, J., 2001. The chemistry of pedogenic thresholds. *Geoderma* **100**, 321-353.

Chen, C., Hall, S.J., Coward, E., Thompson, A., 2020. Iron-mediated organic matter decomposition in humid soils can counteract protection. *Nature Communications* **11**, 2255.

Cornell, R.M., Schwertmann, U., 2003. The iron oxides: structure, properties, reactions, occurrences, and uses. Wiley-vch Weinheim.

Coward, E.K., Thompson, A.T., Plante, A.F., 2017. Iron-mediated mineralogical control of organic matter accumulation in tropical soils. *Geoderma* **306**, 206-216.

Davey, B., Russell, J., Wilson, M., 1975. Iron oxide and clay minerals and their relation to colours of red and yellow podzolic soils near Sydney, Australia. *Geoderma* **14**, 125-138.

De Campos, M., Antonangelo, J.A., Alleoni, L.R.F., 2016. Phosphorus sorption index in humid tropical soils. *Soil and Tillage Research* **156**, 110-118.

Fujisaki, K., Chapuis-Lardy, L., Albrecht, A., Razafimbelo, T., Chotte, J.-L., Chevallier, T., 2018. Data synthesis of carbon distribution in particle size fractions of tropical soils: Implications for soil carbon storage potential in croplands. *Geoderma* **313**, 41-51.

Georgiou, K., 2025. Limits, controls, and vulnerability of mineral-associated soil organic carbon. EGU General Assembly, Vienna, Austria.

Gu, B., Schmitt, J., Chen, Z., Liang, L., McCarthy, J.F., 1994. Adsorption and desorption of natural organic matter on iron oxide: mechanisms and models. *Environmental Science & Technology* **28**, 38-46.

Hall, S.J., Thompson, A., 2022. What do relationships between extractable metals and soil organic carbon concentrations mean? *Soil Science Society of America Journal* **86**, 195-208.

Hawkesford, M.J., Cakmak, I., Coskun, D., De Kok, L.J., Lambers, H., Schjoerring, J.K., White, P.J., 2023. Chapter 6 - Functions of macronutrients. This chapter is a revision of the third edition chapter by M. Hawkesford, W. Horst, T. Kichey, H. Lambers, J. Schjoerring, I. Skrumsager Møller, and P. White, pp. 135–189. DOI: https://doi.org/10.1016/B978-0-12-384905-2.00006-6. In: Rengel, Z., Cakmak, I., White, P.J. (Eds.), Marschner's Mineral Nutrition of Plants (Fourth Edition). *Academic Press*, San Diego, pp. 201-281.

He, X., Augusto, L., Goll, D.S., Ringeval, B., Wang, Y., Helfenstein, J., Huang, Y., Yu, K., Wang, Z., Yang, Y., 2021. Global patterns and drivers of soil total phosphorus concentration. *Earth System Science Data* **13**, 5831-5846.

Herndon, E.M., Kinsman-Costello, L., Duroe, K.A., Mills, J., Kane, E.S., Sebestyen, S.D., Thompson, A.A., Wullschleger, S.D., 2019. Iron (oxyhydr)oxides serve as phosphate

traps in Tundra and Boreal peat soils. *Journal of Geophysical Research: Biogeosciences* **124**, 227-246.
Hunt, J.F., Ohno, T., He, Z., Honeycutt, C.W., Dail, D.B., 2007. Inhibition of phosphorus sorption to goethite, gibbsite, and kaolin by fresh and decomposed organic matter. *Biology and Fertility of Soils* **44**, 277-288.
Jia, N., Li, L., Guo, H., Xie, M., 2024. Important role of Fe oxides in global soil carbon stabilization and stocks. *Nature Communications* **15**, 10318.
Jobbágy, E.G., Jackson, R.B., 2000. The vertical distribution of soil organic carbon and its relation to climate and vegetation. *Ecological Applications* **10**, 423-436.
Kaiser, K., Guggenberger, G., 2000. The role of DOM sorption to mineral surfaces in the preservation of organic matter in soils. *Organic Geochemistry* **31**, 711-725.
Kang, J., Qu, C., Chen, W., Cai, P., Chen, C., Huang, Q., 2024. Organo–organic interactions dominantly drive soil organic carbon accrual. *Global Change Biology* **30**, e17147.
Kleber, M., Eusterhues, K., Keiluweit, M., Mikutta, C., Mikutta, R., Nico, P.S., 2015. Mineral–organic associations: formation, properties, and relevance in soil environments. *Advances in Agronomy* **130**, 1-140.
Kleber, M., Mikutta, R., Torn, M., Jahn, R., 2005. Poorly crystalline mineral phases protect organic matter in acid subsoil horizons. *European Journal of Soil Science* **56**, 717-725.
Kögel-Knabner, I., Guggenberger, G., Kleber, M., Kandeler, E., Kalbitz, K., Scheu, S., Eusterhues, K., Leinweber, P., 2008. Organo-mineral associations in temperate soils: Integrating biology, mineralogy, and organic matter chemistry. *Journal of Plant Nutrition and Soil Science* **171**, 61-82.
Lal, R., 2016. Feeding 11 billion on 0.5 billion hectare of area under cereal crops. *Food and Energy Security* **5**, 239-251.
Lal, R., Kimble, J.M., Stewart, B.A., Eswaran, H., 1999. Global climate change and pedogenic carbonates.
Lehmann, J., Kleber, M., 2015. The contentious nature of soil organic matter. *Nature* **528**, 60-68.
López-Ulloa, M., Veldkamp, E., De Koning, G., 2005. Soil carbon stabilization in converted tropical pastures and forests depends on soil type. *Soil Science Society of America Journal* **69**, 1110-1117.
Lützow, M.v., Kögel-Knabner, I., Ekschmitt, K., Matzner, E., Guggenberger, G., Marschner, B., Flessa, H., 2006. Stabilization of organic matter in temperate soils: mechanisms and their relevance under different soil conditions–a review. *European Journal of Soil Science* **57**, 426-445.
Mikutta, C., Wiederhold, J.G., Cirpka, O.A., Hofstetter, T.B., Bourdon, B., Von Gunten, U., 2009. Iron isotope fractionation and atom exchange during sorption of ferrous iron to mineral surfaces. *Geochimica et Cosmochimica Acta* **73**, 1795-1812.
Mikutta, R., Mikutta, C., Kalbitz, K., Scheel, T., Kaiser, K., Jahn, R., 2007. Biodegradation of forest floor organic matter bound to minerals via different binding mechanisms. *Geochimica et Cosmochimica Acta* **71**, 2569-2590.
Milne, E., Banwart, S.A., Noellemeyer, E., Abson, D.J., Ballabio, C., Bampa, F., Bationo, A., Batjes, N.H., Bernoux, M., Bhattacharyya, T., 2015. Soil carbon, multiple benefits. *Environmental Development* **13**, 33-38.
Mu, C., Zhang, T., Zhao, Q., Guo, H., Zhong, W., Su, H., Wu, Q., 2016. Soil organic carbon stabilization by iron in permafrost regions of the Qinghai-Tibet Plateau. *Geophysical Research Letters* **43**, 10,286-210,294.
Parfitt, R.L., Atkinson, R.J., Smart, R.S.C., 1975. The mechanism of phosphate fixation by iron oxides. *Soil Science Society of America Journal* **39**, 837-841.

Paul, S., Veldkamp, E., Flessa, H., 2008. Differential response of mineral-associated organic matter in tropical soils formed in volcanic ashes and marine Tertiary sediment to treatment with HCl, NaOCl, and Na4P2O7. *Soil Biology and Biochemistry* **40**, 1846-1855.

Rasmussen, C., Southard, R.J., Horwath, W.R., 2006. Mineral control of organic carbon mineralization in a range of temperate conifer forest soils. *Global Change Biology* **12**, 834-847.

Roberts, T.L., Johnston, A.E., 2015. Phosphorus use efficiency and management in agriculture. *Resources, conservation and recycling* **105**, 275-281.

Sabetizadeh, M., Zhou, Y., Heinesch, B., Longdoz, B., Beauclaire, Q., van Wesemael, B., 2025. Assessing Soil Organic Carbon Dynamics Across Croplands and Grasslands: A RothC Model Analysis with Varied Carbon Inputs. EGU General Assembly, Vienna, Austria.

Schwertmann, U., 1966. Inhibitory effect of soil organic matter on the crystallization of amorphous ferric hydroxide. *Nature* **212**, 645-646.

Sims, T.J., Pierzynski, G.M., 2005. Chemistry of phosphorus in soils. *Chemical processes in soils* **8**, 151-192.

Singh, B., Gilkes, R., 1991. Phosphorus sorption in relation to soil properties for the major soil types of south-western Australia. *Soil Research* **29**, 603-618.

Singh, B., Gilkes, R., 1992. Properties and distribution of iron oxides and their association with minor elements in the soils of south-western Australia. *Journal of Soil Science* **43**, 77-98.

Sollins, P., Homann, P., Caldwell, B.A., 1996. Stabilization and destabilization of soil organic matter: mechanisms and controls. *Geoderma* **74**, 65-105.

Spohn, M., 2020. Increasing the organic carbon stocks in mineral soils sequesters large amounts of phosphorus. *Global Change Biology* **26**, 4169-4177.

Stewart, W.M., Hammond, L.L., Van Kauwenbergh, S.J., 2005. Phosphorus as a natural resource. *Phosphorus: agriculture and the environment* **46**, 1-22.

Tiessen, H., 2005. Phosphorus Dynamics in Tropical Soils. Phosphorus: Agriculture and the Environment, pp. 253-262.

Torn, M.S., Trumbore, S.E., Chadwick, O.A., Vitousek, P.M., Hendricks, D.M., 1997. Mineral control of soil organic carbon storage and turnover. *Nature* **389**, 170-173.

Torrent, J., 1997. Interactions between phosphate and iron oxide. *Soils and environment: soil processes from mineral to landscape scale* **30**, 321-344.

Torrent, J., Schwertmann, U., Barrón, V., 1992. Fast and slow phosphate sorption by goethite-rich natural materials. *Clays and Clay Minerals* **40**, 14-21.

Viscarra Rossel, R., Bui, E., De Caritat, P., McKenzie, N., 2010. Mapping iron oxides and the color of Australian soil using visible–near-infrared reflectance spectra. *Journal of Geophysical Research: Earth Surface* **115**.

von Fromm, S.F., Jungkunst, H.F., Amenkhienan, B., Hall, S.J., Georgiou, K., Pries, C.H., Montaño-López, F., Quesada, C.A., Rasmussen, C., Schrumpf, M., Singh, B., Thompson, A., Wagai, R., Fiedler, S., 2025. Moisture and soil depth govern relationships between soil organic carbon and oxalate-extractable metals at the global scale. *Biogeochemistry* **168**, 20.

von Lützow, M., Kögel-Knabner, I., Ludwig, B., Matzner, E., Flessa, H., Ekschmitt, K., Guggenberger, G., Marschner, B., Kalbitz, K., 2008. Stabilization mechanisms of organic matter in four temperate soils: Development and application of a conceptual model. *Journal of Plant Nutrition and Soil Science* **171**, 111-124.

Wagai, R., Kajiura, M., Asano, M., 2020. Iron and aluminum association with microbially processed organic matter via meso-density aggregate formation across soils: organo-metallic glue hypothesis. *Soil* **6**, 597-627.

Wagai, R., Mayer, L.M., 2007. Sorptive stabilization of organic matter in soils by hydrous iron oxides. *Geochimica et Cosmochimica Acta* **71**, 25-35.

Walker, T., Syers, J.K., 1976. The fate of phosphorus during pedogenesis. *Geoderma* **15**, 1-19.

Watanabe, T., 2017. Significance of active aluminum and iron on organic carbon preservation and phosphate sorption/release in tropical soils. In: Funakawa, S. (Ed.), Soils, Ecosystem Processes, and agricultural development: Tropical Asia and Sub-Saharan Africa. *Springer* Tokyo, Japan, pp. 103-125.

Wilson, C.A., Cloy, J.M., Graham, M.C., Hamlet, L.E., 2013. A microanalytical study of iron, aluminium and organic matter relationships in soils with contrasting hydrological regimes. *Geoderma* **202-203**, 71-81.

Yu, M., Wang, Y., Jiang, J., Wang, C., Zhou, G., Yan, J., 2019. Soil organic Carbon Stabilization in the Three Subtropical Forests: Importance of Clay and Metal Oxides. *Journal of Geophysical Research: Biogeosciences* **124**, 2976-2990.

Yu, X., Wang, L., Wang, Q., Zhou, G., Sun, H., Guggenberger, G., Li, Y., Yakov, K., Luo, Y., Fu, Y., 2025. Faster soil organic carbon turnover in MAOM versus POM: straw input causes larger microbial driven soil organic carbon decomposition but higher straw accumulation in MAOM. *Soil and Tillage Research* **251**, 106549.

Zhao, B., Dou, A., Zhang, Z., Chen, Z., Sun, W., Feng, Y., Wang, X., Wang, Q., 2023. Ecosystem-specific patterns and drivers of global reactive iron mineral-associated organic carbon. *Biogeosciences Discussions* **2023**, 1-39.

Zhao, Q., Poulson, S.R., Obrist, D., Sumaila, S., Dynes, J.J., McBeth, J.M., Yang, Y., 2016. Iron-bound organic carbon in forest soils: quantification and characterization. *Biogeosciences* **13**, 4777-4788.

Chapter Two

Understanding extractable metal species relationships with phosphorus sorption and organic carbon in soils.

This chapter is published as:
Amenkhienan Bright E., Dijkstra Feike, Warren Charles and Singh Balwant (2024). Understanding extractable metal species relationships with phosphorus sorption and organic carbon in soils. *Soil Research 62*, SR24118. https://doi.org/10.1071/SR24118.

2.0 Abstract

Context

Iron (Fe) and aluminium (Al) oxides are important in phosphate sorption capacity of soils and preservation of soil organic carbon (SOC). However, there is a complex interplay between among Fe/Al oxides, SOC, and phosphorus (P) in soils.

Aims

Our objective was to further evaluate the relationships between extractable Fe and Al and SOC concentration and P sorption capacity using generalized additive mixed models (GAMMs).

Methods

We compiled and analysed data from 77 published articles from Scopus and Web of Science.

Key results

Ammonium oxalate extractable aluminium (Al_{ox}) and dithionite-citrate-bicarbonate extractable aluminium (Al_d) had a strong statistically significant relationship with P sorption capacity (R^2 = 0.92 Al_{ox}, $p<0.0001$, and R^2 = Al_d 0.93, $p<0.0001$), but Al_d had a stronger statistically significant relationship with P sorption capacity (R^2 = Al_d 0.93, AIC = 508). Further, a positive 1:1 relationship between Al_{ox} and Al_d (slope = 0.96, R^2 = 0.94), suggests that the pool of Al dissolved by ammonium oxalate and dithionite citrate bicarbonate (DCB) was nearly similar. A strong statistically significant relationship was found between ammonium oxalate extractable

iron (Fe_{ox}) and Al_{ox}, and SOC concentration (R^2 = 0.57 Fe_{ox}, 0.58 Al_{ox}, $p<0.0001$), but Al_{ox} had a stronger statistically significant relationship with SOC concentration (R^2 = Al_d 0.58, AIC = 645). This may be due to various interactions of SOC with Al oxides, which can directly or indirectly influence P sorption capacity in soils.

Conclusions

Extractable Fe and Al have significant relationships with P sorption capacity and SOC concentration. The DCB forms of extractable Al and ammonium oxalate extractable Al have stronger relationships with SOC concentration and P sorption capacity than extractable Fe. The concentration of ammonium oxalate extractable Al in the soil samples was significantly ($p<0.001$) greater than the concentration of ammonium oxalate extractable Fe. In this study, P sorption capacity had no relationship with SOC concentration.

Implications

DCB and ammonium oxalate extractable Fe (and Al) that represent Fe in crystalline and poorly crystalline, or amorphous form of Fe/Al may be used as a routine soil test and may be able to predict P sorption capacity and SOC preservation potential, particularly in acid soils.

Keywords: Iron, aluminium, soil organic carbon, relationship, phosphorus sorption capacity, ammonium oxalate, dithionite citrate bicarbonate, extractable metals.

2.1 Introduction

Soil organic matter (SOM) consists of about 50% carbon (C) and it is a critical component of soils (Banwart *et al.*, 2019). Soil OM plays very vital roles in the functioning and productivity of ecosystems, soil quality and health, soil fertility and productivity (Reeves, 1997; Watanabe, 2017). Soils are the largest reservoir of C, storing twice the amount of organic C that is present in the atmosphere and vegetation combined (Batjes, 1996, 2014). Soil OC is quite dynamic in nature, with continuous in and out fluxes that determine its net reserves in soils. It is important

to increase the net storage of C in the soil to stabilise CO_2 concentration in the atmosphere and to mitigate climate change, which has been the focus of scientific investigation in the last few decades (Lal, 2004; Banwart *et al.*, 2019).

The stabilisation of OM in soils is controlled by several mechanisms. Three primary mechanisms have been identified for the preservation of SOC, which include (i) accumulation of primary and secondary recalcitrant forms of organic molecules, (ii) inaccessibility of SOC against enzymes and microbial decomposition via occlusion in aggregates, and (iii) chemical interactions, involving adsorption and co-precipitation, with phyllosilicates and iron (Fe) and aluminium (Al) oxides (used for brevity the term includes oxides/hydroxides/oxyhydroxides) (Sollins *et al.*, 1996; Lützow *et al.*, 2006; Kleber *et al.*, 2015; Hemingway *et al.*, 2019). The association of SOM with minerals, particularly involving Fe and Al oxides, has been identified as a key mechanism for the long-term preservation of SOC (Kaiser and Guggenberger, 2000; Rasmussen *et al.*, 2006; Tamrat *et al.*, 2019; Hall and Thompson, 2022; Ye *et al.*, 2022), and thus, the necessity to better understand these interactions.

Iron and Al oxides are common constituents of most soils and thus very important in with the preservation of SOC via chemical interactions due to their large specific surface area (SSA) and reactive surfaces. During pedogenesis, Fe and Al containing primary minerals undergo chemical weathering, forming pedogenic species of Fe and Al (includes all secondary Fe and Al oxide and monomeric and polymeric species of Fe and Al in soil solution), which react with SOC. In monomeric forms, they bind with organic ligands (e.g., carboxylic functional groups) to form organo-metal complexes while in polymeric forms they can form polynuclear complexes and secondary minerals. Secondary minerals (including oxides, hydroxides, oxyhydroxides and hydrated oxides) are often small in size, and thus have a large SSA and sorption capacity, and ability to bind and stabilise OC in soils (Kaiser and Guggenberger, 2003; Wagai *et al.*, 2013; Kleber *et al.*, 2015; Rennert, 2019; Wagai *et al.*, 2020). This perspective

has been asserted by close and strong positive relationships between SOC and ammonium oxalate extractable Fe and Al, which suggest that SOC is preferably preserved by interaction with poorly crystalline minerals (Kaiser and Guggenberger, 2003; Kleber *et al.*, 2005; Wiseman and Püttmann, 2006; Rasmussen *et al.*, 2018; Yu *et al.*, 2021; Hall and Thompson, 2022).

The preservation of SOC is important in the context of phosphorus (P) dynamics in soils. Phosphorus is a major plant nutrient that plays a key role in photosynthesis, respiration, biosynthesis of nucleic acids and membranes, and regulation of several enzymes (Hawkesford *et al.*, 2023). Total P concentrations in natural soils of terrestrial ecosystems are highly variable, ranging from 1.4 to 9636 mg kg^{-1}, with an average concentration of 584 mg kg^{-1} in surface (0 – 30 cm) soils (He *et al.*, 2021). Weathering coupled with erosion and leaching depletes P that is present in soil primary minerals. Therefore, the total P concentration in soils decreases over the course of soil development (Walker and Syers, 1976; Crews *et al.*, 1995). He *et al.* (2021) reported mean total P concentration of 719, 481 and 472 mg kg^{-1} in slightly weathered, intermediately, and strongly weathered soils, based on global and regional databases, respectively. A negligible (<0.1 %) fraction of the total P in soils exists in soil solution that is in a plant available form (Raghothama and Karthikeyan, 2005). Organic soil P is the most important source of P in highly weathered soil. Organic P represents approximately 44% of total soil P in highly weathered soil (Cross and Schlesinger, 1995). Phosphate associated with soil minerals is not readily bioavailable, it is either strongly adsorbed to minerals or present in insoluble P compounds formed from the reactions of phosphate with Al, Fe, and calcium (De Schrijver *et al.*, 2012).

Similar to SOC, chemically extractable forms of Fe and Al have been identified as the key components in governing P sorption capacity of soils (Walker and Syers, 1976; Borggaard *et al.*, 1990; Singh and Gilkes, 1991). Phosphorus availability is widely considered to be the main constraint in limiting primary productivity in highly weathered soils because of their low P

contents and propensity of phosphate to strongly adsorb onto Fe and Al oxides (Cross and Schlesinger, 1995; Sanchez, 2019). The effectiveness of P fertilisers in cropping soils relies primarily on P sorption capacity, which is primarily related to the concentration of different forms of Fe and Al oxides, particularly in highly weathered soils of tropic and sub-tropic regions (De Campos *et al.*, 2016; Lin *et al.*, 2020). Iron and Al oxides are well known to bind phosphate and limit P bioavailability in soils from both temperate and tropical systems (Walker and Syers, 1976; Borggaard *et al.*, 1990; Singh and Gilkes, 1991; Vitousek *et al.*, 2010). Herndon *et al.* (2019) reported that Fe oxides sequester approximately half of soil phosphate in shallow organic soils of low-lying areas from Artic and Boreal regions. Phosphate sorption is known to occur on Fe and Al oxides surfaces via ligand exchange reactions and it may be immobilised through occlusion with ageing (Torrent *et al.*, 1992; Watanabe, 2017). In addition, soil P has been linked to soil C sequestration capacity in highly weathered soils (where organic C can sorb P via cation bridging mechanism, with cations such as Fe^{3+}, Al^{3+} and Ca^{2+} being involved in the process) because of continuous P fertilization, which can reduce SOC mineralization (Giardina *et al.*, 2004; Li *et al.*, 2006) although the relationship is not well understood under different soil environmental conditions.

There is a complex interplay among Fe/Al oxides, organic matter, and P in soils. Phosphorus is a significant component of SOC, because a large amount of P, necessary for the formation of organo-mineral complexes, is stored with SOC (Spohn, 2020). The OC:OP ratios of croplands indicate that approximately 13 and 22 kg P per ton of SOC are stored in the topsoil and subsoil of croplands, respectively (Spohn, 2020). Organic amendments have been shown to increase P availability in soils by reducing phosphate adsorption or increasing phosphate desorption or by directly supplying more P contained in the organic amendments (Hunt *et al.*, 2007; Zhang *et al.*, 2018; Ma *et al.*, 2019; Yang *et al.*, 2019). Under normal soil pH conditions, OM predominantly carries negative charge and can form surface-complexes with Fe and Al oxides

that carry positive surface charge (Singh *et al.*, 2016). Phosphorus can be adsorbed by reversible reactions on SOM, with some bonds being much more readily and rapidly broken than others (Sposito, 1989). The presence of OM on minerals can inhibit adsorption of negatively charged inorganic and organic P compounds and thus increase bioavailable P in soils (Hunt *et al.*, 2007). Jindo *et al.* (2023) summarised various competitive sorption reactions that occur between SOC and bioavailable P. Firstly, SOC carrying a negative charge is adsorbed on the surfaces of metal (Fe/Al) oxides, which are positively charged thereby blocking the surface charge sites and increasing P desorption. Secondly, SOC adsorbed on the surfaces of metal oxides enhances P repulsion and, increases bioavailable P. Lastly, SOC chelating with Fe adsorbed on surfaces of metal oxides leads to formation of Fe-SOC, which can be released from the surface sites, making the surface sites positively charged and available for P sorption in soils.

The abundance of crystalline (dithionite-citrate-bicarbonate) and poorly crystalline (ammonium oxalate) Fe and Al oxides are diverse in soils and, contribute to SOC preservation and stabilisation and P sorption. Therefore, a comprehensive evaluation of the role of Fe and Al oxides in the stabilisation of SOC and sorption of P will enhance our knowledge on global soil C cycling, and P sorption and help in better soil management. Studies have synthesised large datasets of soils, showing that acid ammonium oxalate extractable Al was the strongest predictor of SOC concentration (Rasmussen *et al.*, 2018; Von Fromm *et al.*, 2021; Yu *et al.*, 2021; Hall and Thompson, 2022; Zhao *et al.*, 2023) while Watanabe (2017) reported that ammonium oxalate extractable Fe and Al (active Fe + Al) were the strongest predictor of P sorption. Few studies have explored relationships between extractable metals and SOC concentration but has not considered relationship with P sorption capacity within the same datasets. This is the first study that has examined relationships among the different fractions of Fe and Al with SOC concentration and P sorption capacity simultaneously, thereby adding new

knowledge to the existing literature. In our study, we explored published data to evaluate the relationships among the different fractions of Fe and Al with SOC and P adsorption of soils. The main objective was to identify the role of different fractions of Fe and Al oxides in the SOC preservation and P availability in soils using a generalized additive mixed model (GAMM) approach. We have two key research questions: (1) do extractable Fe and Al have any relationships with P sorption capacity and SOC concentration? and, (2) does P sorption capacity and SOC concentration have any relationship?

2.2 Methodology

Peer-reviewed publications were searched on Scopus and Web of Science databases using the following key search terms: soil + iron oxides extract*+ "phosph*sorpt*"; soil + iron oxides extract* + "organic matter" OR "organic carbon"; soil + iron oxides + "phosph*sorpt*"; soil + iron oxides + "organic matter" OR "organic carbon". The key search terms did not only display chemically extractable Fe but also displayed chemically extractable Al, hence extractable Al was not included in the above key search terms. The preferred reporting items for systematic reviews and meta-analyses (PRISMA) diagram (Page *et al.*, 2021) were used for the identification and selection of pertinent published papers for this study. A total number of 5,717 publications resulted from the database searches, with 3,917 publications from Scopus and 1,836 from Web of Science. Publications that appeared as duplicate within the Scopus database and within the Web of Science database based on the different key search terms used were 251 and 1,031; this amounted to a total of 1,282 of duplicate within both databases while duplicate publications between databases (Scopus and Web of Science) were 565. In total, duplicate publications within and between the two databases removed were 1,847; that left a total number of 3,870 publications. Only publications having data for P sorption capacity (based on Langmuir model), organic C, and chemically extractable metal (Fe and Al) oxides were

selected, extracted, and analysed because they adequately focused or contributed to the main objective of our study. Therefore, with the above-mentioned criteria, a total number of 3,772 irrelevant publications were excluded, 18 publications were inaccessible and excluded while another 3 publications were also excluded because they were not in English. This resulted in a total of 77 relevant publications which were eligible and examined for this study. A summary of the identification and selection of relevant publications used for this study are shown in Figure 2.1.

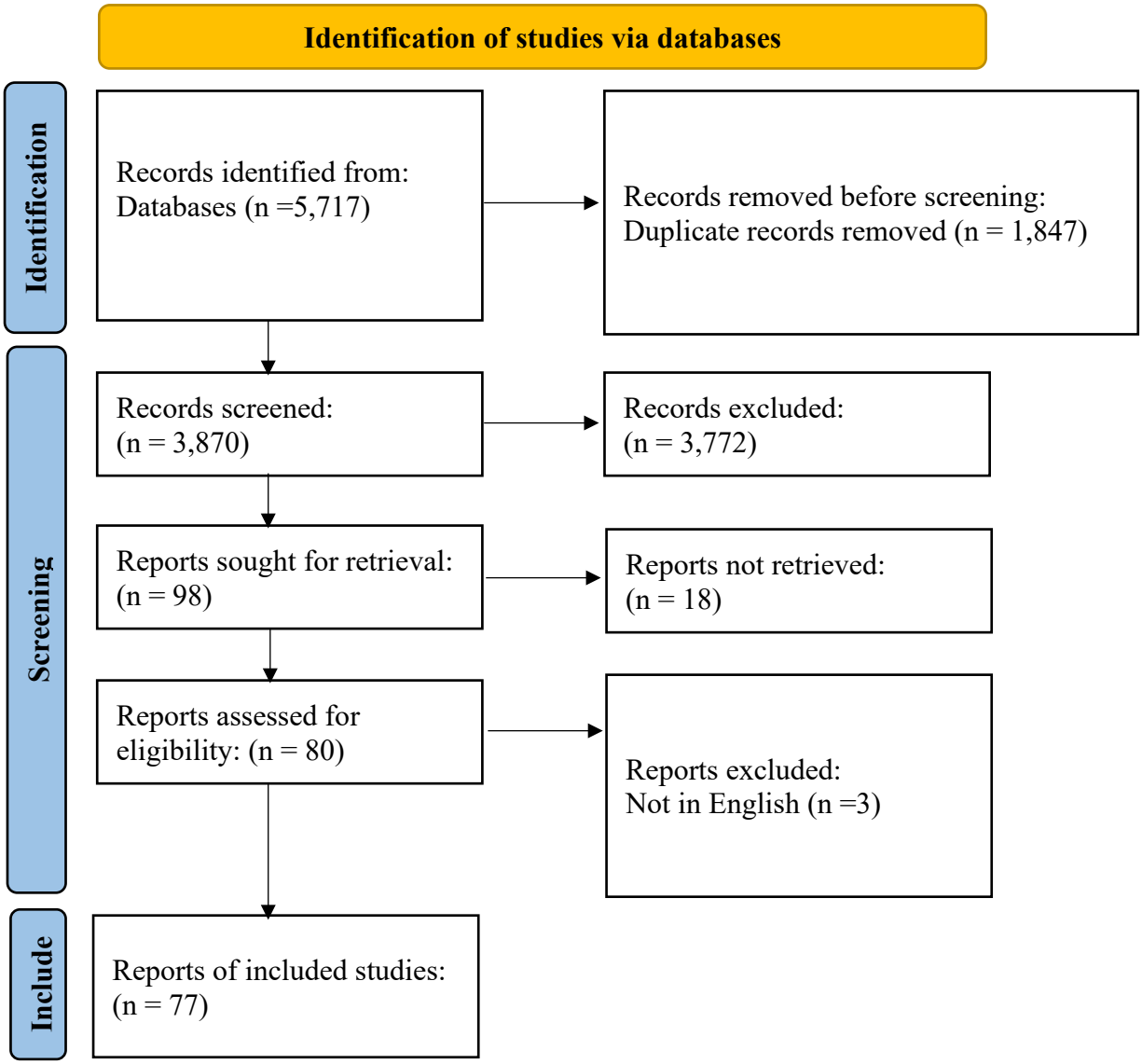

Figure 2.1. *Flow diagram for the identification of relevant publications using PRISMA, where n = number of papers.*

2.3 Data Analysis

The data extracted from selected journal papers were statistically analysed to examine the main drivers of P sorption capacity and SOC concentration using the *gamm* function within the *mgcv* package of generalized additive mixed models (GAMMs) (Wood, 2017). The response variables were SOC concentration and P sorption capacity. The predictor variables were chemically extractable forms of Fe and Al. Ammonium oxalate extractable iron (Fe_{ox}) and aluminium (Al_{ox}) consist of poorly crystalline minerals phases or short-range-ordered (SRO) mineral phases and organo-metal complexes. Dithionite-citrate-bicarbonate extractable iron (Fe_d) and aluminium (Al_d) consist of crystalline minerals phases or pedogenic phases. All response and predictor variables were log10 transformed to conform to assumptions of residual distribution in GAMM. The generalized additive mixed model accounts for non-linear relationships between response variables and the predictors by fitting penalized smooth functions to each predictor to minimise excessive "wiggliness" (Wood, 2017). The default K dimension of 10 (maximum degree of freedom) was used for each smooth function to dictate the flexibility of the relationship. The effective degree of freedom (edf) was used to express the plotted shape of the model. If the edf is equal to 1 then the smooth term is reduced from a flexible relationship to a simple linear relationship. We tested various smooth functions in the full model, which included the response variable, the extractable metals (Fe_{ox}, Fe_d, Al_{ox}, Al_d) and the interaction terms, however, the addition of interaction terms did not reduce the Akaike's information criterion (AIC), hence it was not included in the final model. The residuals approximately followed a Gaussian distribution; therefore, an identity link function was used. The F values were used to estimate the significance ($p<0.001$) of model terms. If the values of the response variables or the predictors were missing from the data, then those data were excluded from the GAMM analysis.

We initially fit two separate but single optimal GAMMs for each of the two response variables (i.e., SOC concentration and P sorption capacity), and all four predictor variables (Fe_{ox}, Fe_d, Al_{ox}, Al_d). The model assumptions were evaluated using residual plots. The single optimal GAMM showed relationships between each extractable metal and P sorption capacity, and between each extractable metal and SOC concentration. We observed that correlations between Fe and Al affected their relationships with P sorption capacity and SOC concentration, respectively (Supplementary Figure 2.1 and 2.2). In GAMM, this is known as concurvity, which also refers to collinearity where values greater than 0.8 indicate close relationship and instability of a parameter while 0 indicates no relationship with other variables (Wood, 2017). The limitation of the model is collinearity, which prevented running the single optimal GAMMs having all the predictor variables.

To avoid the problem of correlation among ammonium oxalate and dithionite-citrate-bicarbonate (DCB) extractable metals leading to concurvity, we fitted four separate additional GAMMs involving single extractable metals (Fe_{ox}, Fe_d, Al_{ox}, Al_d). The separate GAMMs were used to address questions on understanding the relationships between extractables forms of metals and P sorption capacity as well as SOC concentration. The additional GAMMs enable investigation of redundancy in various extractable metals as predictors of P sorption capacity and SOC concentration. The AIC values of each model fit by restricted maximum likelihood (REML), was used to compare the performance of models, with smaller AIC indicating better performance. The R^2 values presented in the results are adjusted R^2, adjusted for the number of predictors. The highest R^2 values indicate better performance of the models. The R^2 values of P sorption capacity is much higher compared to SOC concentration because the number of observations for P sorption capacity (n = 265) was higher than SOC (n =249). Furthermore, we used the GAMMs to explore the non-linear relationships of extractable metals and P sorption capacity and SOC concentration, while we used the reduced major axis (RMA) regression to

evaluate the linear relationships and slopes between extractable metals because assumptions weren't met. The "*lmodel2*" function was used for RMA regression (Figure 3). Paired t-test was used to test the differences between mean concentrations of extractable Al and Fe within depths. All analyses were performed using R studio statistical software version 4.4.1 (RCoreTeam, 2024).

2.4 Results and Discussion

2.4.1 Phosphorus sorption capacity versus extractable Fe and Al oxides

The relationship between P sorption capacity and metals extracted in acid ammonium oxalate (Fe_{ox} and Al_{ox}) and citrate dithionite bicarbonate (Fe_d and Al_d) are shown in Supplementary Figure 2.1. The single optimal GAMMs with all predictor variables, i.e., Fe_{ox}, Fe_d, Al_{ox} and Al_d, failed because of severe concurvity, i.e., the "concurvity" function was close to 1; Fe_{ox} = 0.99, Fe_d = 0.99, Al_{ox} = 0.98 and Al_d = 0.98 (Supplementary Figure 2.1), therefore additional four separate models were fitted.

In the four separate additional GAMMs involving single extractable metals, we observed that individual extractable metals (Fe_{ox}, Fe_d, Al_{ox} and Al_d) had statistically significant relationships with P sorption capacity (R^2 = 0.91 Fe_{ox}; $p<0.05$, R^2 = 0.90 Fe_d; $p<0.0001$, R^2 = 0.92 Al_{ox}; $p<0.0001$, and R^2 = Al_d 0.93, $p<0.0001$). Phosphorus sorption capacity increased with Fe_{ox}, Fe_d, Al_{ox} and Al_d, with curvilinear (non-linear) relationships (Figure 2.2 a, b, c, and d). Our results show that both Al_d and Al_{ox} were better predictor variables (AIC =508 and 532, respectively) of P sorption capacity in soils than Fe_d and Fe_{ox} (AIC =572 and 545, respectively), and Al_d was a better predictor variable of P sorption capacity than Al_{ox} (Figure 2.2 c and d). Several studies have reported significant correlations of P sorption capacity with Fe_{ox}, Al_{ox}, Fe_d and Al_d contents in different soil types (Syers *et al.*, 1971; Ping and Michaelson, 1986; Peña

and Torrent, 1990; Singh and Gilkes, 1991; Börling *et al.*, 2001; Agbenin, 2003; Wiriyakitnateekul *et al.*, 2005).

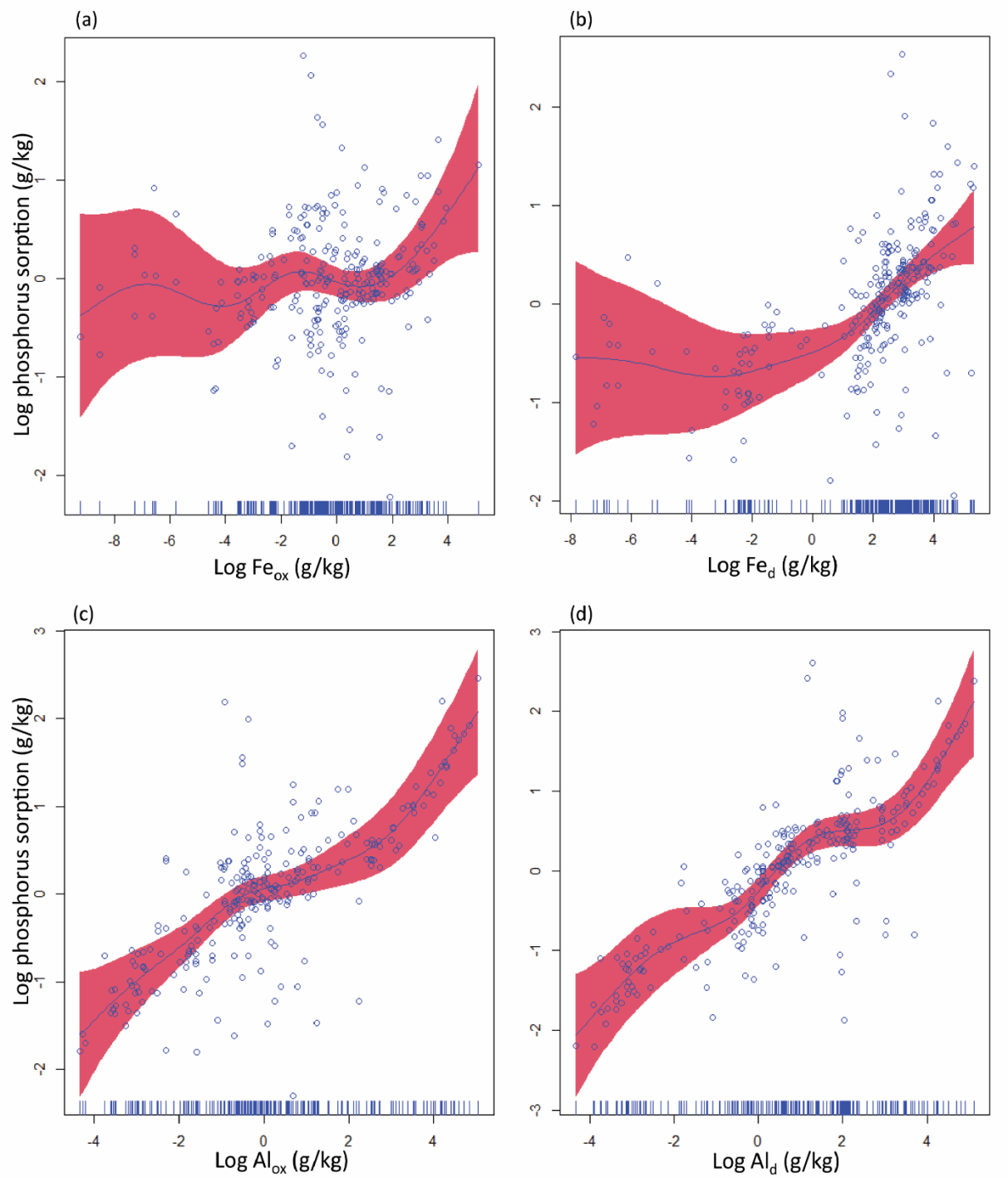

Figure 2.2. *Relationships between phosphorus sorption and individual extractable metals where each of the four metals extracted (ammonium oxalate extractable iron [Fe_{ox}], dithionite-citrate-bicarbonate extractable iron [Fe_d], ammonium oxalate extractable [Al_{ox}], and dithionite-citrate-bicarbonate extractable aluminium [Al_d]) was used separately in the generalized additive mixed models (GAMMs). These results are different from the model in Supplementary Figure 2.1, where Fe_{ox}, Fe_d, Al_{ox}, and Al_d were included in a single GAMM model. Akaike's information criterion values for Fe_{ox}, Fe_d, Al_{ox}, and Al_d in the GAMM model (using each extracted metal separately) were 545, 572, 532 and 508, respectively. The respective F-statistic values were 10, 2, 12, and 17; and R^2 values were 0.91, 0.90, 0.92 and 0.93. The shaded red region around the smooth lines represents the 95% confidence intervals.*

The higher P sorption capacity of extractable Al than the extractable Fe may be due to its greater SSA and, high density of reactive hydroxyl sites. Phosphate sorption on Al oxides occurs through ligand exchange reactions where singly coordinated hydroxyl (OH) groups are exchanged by phosphate anions (Borggaard *et al.*, 1990). These results are consistent with several previous studies on different soil types (Bromfield, 1965; Singh and Gilkes, 1991; Börling *et al.*, 2001; Agbenin, 2003), where Al_{ox} and Al_d were found to be more strongly correlated with P sorption capacity than Fe_{ox} and Fe_d irrespective of their total contents in soils. The relative contribution of Al_d in P sorption capacity has been estimated to be 3 to 5 times greater than Fe_d in acid soils from Australia and Nigeria (Bromfield, 1965; Singh and Gilkes, 1991; Agbenin, 2003). Acid ammonium oxalate extracts non-crystalline or amorphous and short-range order Al oxides and organically complexed Al (McKeague and Day, 1966; Dahlgren, 1994; Rennert, 2019). Poorly crystalline and nano-sized crystalline goethite and hematite particles can also be dissolved during acid ammonium oxalate extraction (Acebal *et al.*, 2000). In the DCB extraction, in addition to the Al forms extracted by acid ammonium oxalate solution, Al substituting for Fe in the structure of well crystalline Fe oxides (i.e., goethite and hematite) is also extracted. The contribution of Al released from the dissolution of Al-substituted goethite and hematite during the DCB extraction may explain the slightly better prediction of P sorption capacity with Al_d than Al_{ox}. The substitution of Al for Fe in Fe oxides is common in soils, with up to one-third (Al/(Al+Fe)) = 0.33) in goethite and half of that in hematite (Singh and Gilkes, 1992). The crystal size of Fe oxides has been known to decrease with increasing degree of Al substitution in their structures, thereby increasing SSA and, P sorption capacity (Borggaard, 1983).

Furthermore, our findings do not negate the importance of different forms of Fe oxides on P sorption capacity even though they are not the strongest predictors of P sorption capacity. As mentioned earlier, Fe_{ox} and Fe_d showed statistically significant relationships with P sorption

capacity (Figure 2.2 a and b). High P sorption capacity has been found in Oxisols and Alfisols, which have a high concentration of Al_d and Fe_d (De Campos *et al.*, 2016). Several other studies have reported significant relationships between different forms of extractable Fe and Al and P sorption capacity in soils from tropical and temperate regions of the world (Ahenkorah, 1968; Loganathan and Fernando, 1980; Peña and Torrent, 1984, 1990; Singh and Gilkes, 1991; Freese *et al.*, 1992; Agbenin, 2003; Li *et al.*, 2007; Bortoluzzi *et al.*, 2015; Watanabe, 2017).

Table 2.1 shows the mean concentrations of Fe and Al in soils extracted by acid ammonium oxalate and DCB extractants at three soil depths. Figure 2.3 shows the pairwise 1:1 relationship between extractable metals. The RMA regression of all the relationships were statistically significant ($p < 0.0001$) but not all the relationships were strong (Figure 2.3). Ammonium oxalate Al and Al_d had a nearly 1:1 relationship in the soil samples (Figure 2.3 b). Although, few samples (encircled in Figure 2.3 b) appear to deviate from this relationship, where additional Al (substituting for Fe) might have been released from the structure of Fe oxides during the DCB extraction. Our results are consistent with the results reported by Hall and Thompson (2022) for a large North American soil dataset. The linear relationship between Fe_{ox} and Fe_d was weak ($R^2 = 0.29$; Figure 2.3 a), and as expected, Fe_d was generally greater than Fe_{ox} (RMA regression slope = 0.27 ± 0.02), which indicates ammonium oxalate extracted about 27% of the Fe extracted by DCB. Similar results, showing a weak relationship between Fe_{ox} and Fe_d was reported by (Hall and Thompson, 2022). The weak relationship between Fe_d and Al_d, and between Fe_{ox} and Al_d (Figure 2.3 d and e), may indicate different environmental conditions, mineral composition, and degree of Al substitution in Fe oxides in the soils. The Fe and Al extracted in ammonium oxalate and DCB had a weak and variable relationship with each other (Figure 2.3 c and f).

Table 2.1. *Mean concentrations of Al and Fe at three depths (0-20cm, 20 – 50cm, and > 50cm). The values in parentheses are standard deviations in the concentrations. Fe_{ox}, ammonium oxalate extractable iron; Fe_d, dithionite-citrate-bicarbonate extractable iron; Al_{ox}, ammonium oxalate extractable aluminium; Al_d, dithionite-citrate-bicarbonate extractable aluminium.*

Soil Depth (cm)[A]	**Fe_{ox}**	**Fe_d**	**Al_{ox}**	**Al_d**
	← g/kg →			
0-20 (n=204)	3.09 (5.80)b	19.89 (29.25)a	3.29 (7.97)a	5.57 (8.91)b
20-50 (n=102)	5.03 (18.04)b	19.95 (28.46)a	8.38 (24.87)a	10.14 (25.85)b
>50 (n=42)	4.97 (7.79)b	16.10 (19.45)a	18.36 (30.88)a	19.28 (32.77)b

[A.] The number of individual soil horizon samples from each soil depth are listed in parentheses. Different letters on the rows indicate significant ($p<0.001$) differences in the mean values between ammonium oxalate Fe and Al and between dithionite-citrate-bicarbonate Fe and Al within each depth based on paired t-test.

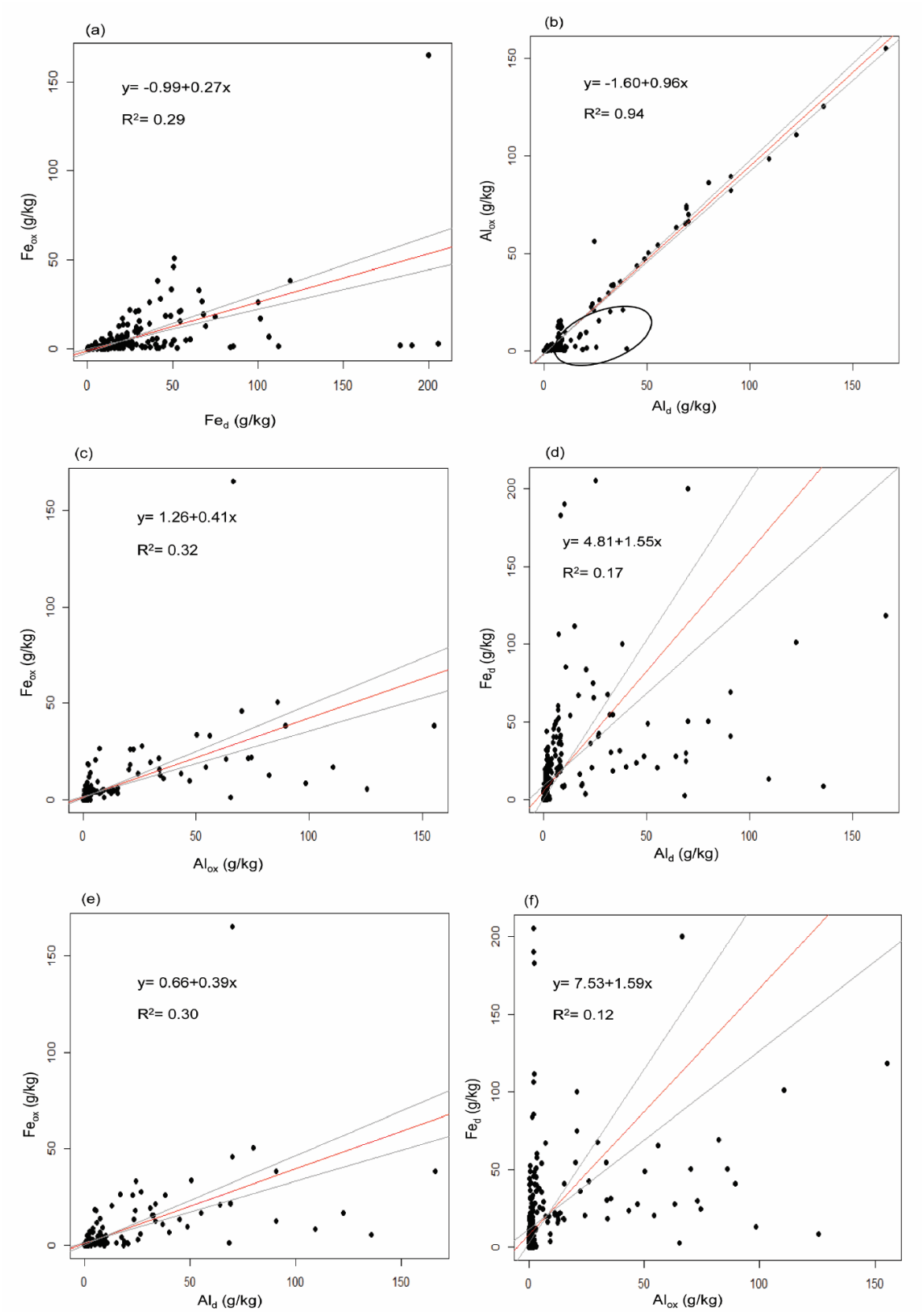

Figure 2.3. *Relationships between various forms of Al and Fe extracted in ammonium oxalate and dithionite-citrate-bicarbonate solutions. Lines in red indicate reduced major axis (RMA) regression, and lines (in grey) indicate confidence intervals for the RMA regression line, R^2 values and RMA regression equation are given in each plot. All regression slopes were statistically significant at $p<0.0001$. Fe_{ox}, ammonium oxalate extractable iron; Fe_d, dithionite-citrate-bicarbonate extractable iron; Al_{ox}, ammonium oxalate extractable aluminium; Al_d, dithionite-citrate-bicarbonate extractable aluminium.*

2.4.2 Soil Organic Carbon (SOC) versus extractable Fe and Al oxides

Supplementary Figure 2.2 shows the relationships between soil organic carbon (SOC) and Al and Fe extracted in acid ammonium oxalate (Al_{ox} and Fe_{ox}) and dithionite citrate bicarbonate (Al_d and Fe_d). All predictor variables (Fe_{ox}, Fe_d, Al_{ox} and Al_d) failed in the single optimal GAMM because of severe concurvity i.e. Fe_{ox} = 0.94, Fe_d = 0.95, Al_{ox} = 0.99 and Al_d = 0.99. In the four separate GAMMs involving each of the four extractable metals, we observed a statistically significant relationship of each metal with SOC concentration (R^2 = 0.57 Fe_{ox}, 0.54 Fe_d, 0.58 Al_{ox} and Al_d 0.52, $p<0.0001$). The SOC concentration increased with Fe_{ox}, Fe_d, and Al_{ox}, with curvilinear (non-linear) relationships (Figure 2.4 a, b, and c) while Al_d had a linear relationship with SOC (edf = 1) (Figure 2.4 d). In the GAMM plots, we observed that when these variables increased non-linearly, SOC was plateaued (i.e SOC did not show any further increase). This may suggest that many soils are not yet saturated with SOC hence, these soils have additional capacity for SOC adsorption onto Al and Fe oxides. These results are consistent with the observations from the NEON soil dataset where an increase in the metals (Al_{ox} and ammonium acetate exchangeable calcium plus exchangeable magnesium [Ca_{xe} + Mg_{ex}) did not further increase the SOC (Yu *et al.*, 2021). Our results show that oxalate extractable metals (Fe_{ox} and Al_{ox}) are better predictor variables of SOC than DCB extracted metals (Fe_d and Al_d) and Al_{ox} was a slightly stronger predictor variable than Fe_{ox} as shown by the AIC (Al_{ox} = 645 vs Fe_{ox} = 658) (Figure 2.4). Recent studies, consisting of larger soil datasets from North America, have consistently revealed that Al_{ox} exhibited stronger predictive power for SOC concentrations compared to Fe_{ox} and Fe_d (Rasmussen *et al.*, 2018; Yu *et al.*, 2021; Hall and Thompson, 2022). Watanabe (2017) reported a significant correlation between Fe + Al oxides and SOC and concluded that the major components of SOC preservation is through binding with Fe and Al oxides. The RMA regression showed statistically significant ($p < 0.01$) relationship between SOC concentration and Fe_{ox} + Al_{ox} (Supplementary Figure 2.3). In this

study, Fe_{ox} + Al_{ox} explained 29 % of the variability in the SOC concentration. Kleber *et al.* (2005) observed that Fe_{ox} + Al_{ox} explained 78% of the variability ($p < 0.001$) in SOC concentration in acid soils and suggested that SOC concentration in acid soils is positively and linearly correlated to the concentration of poorly crystalline minerals. In contrast to these, Percival *et al.* (2000) reported a significant correlation between Al pyrophosphate (Al_{pp}) (pyrophosphate extracts organo-Al complexes) and SOC, and observed that Al_{pp} was the best predictor of SOC concentration.

Soil organic C stabilisation by poorly crystalline oxides (i.e., Al_{ox} and Fe_{ox}) may be due to the possession of extensive SSA and increased reactive sites. The formation of stable organic-metal complexes (Al and Fe) occurs through ligand exchange reactions between carboxyl groups of SOC and singly coordinated hydroxyl (OH) groups at the metal surfaces (Kaiser and Guggenberger, 2000). The interaction between SOC and Al/Fe oxides can lead to less susceptibility of SOC to desorption, oxidative degradation, biodegradation and greater long-term preservation of SOC in soils (Kaiser and Guggenberger, 2003; Zimmerman *et al.*, 2004). There was a weak relationship between Fe_{ox} and Al_{ox} in soil samples (Figure 2.3 c), and Al_{ox} was significantly ($p<0.001$) greater than Fe_{ox} (Table 2.1). This was possibly due to greater solubility of Al than Fe at low pH in soils and the weak tendency of Al oxides to crystalise as compared to Fe (Shang and Tiessen, 1998; Watanabe, 2017). During acid-mediated mineral weathering, Al phases (gibbsite and aluminosilicates) are known to dissolve at higher pH values than the Fe oxides (goethite, hematite and ferrihydrite) (Chadwick and Chorover, 2001). The soluble Al^{3+} outperform base cations on the cation exchange sites, thereby maintaining the soil pH within the range of 4.0 to 5.5, which in turn, restricts the dissolution of Fe (Chadwick and Chorover, 2001). Also, the greater abundance of Al than Fe in the parent material might favour the higher Al concentration than Fe ions in the soil solution (Hall and Thompson, 2022).

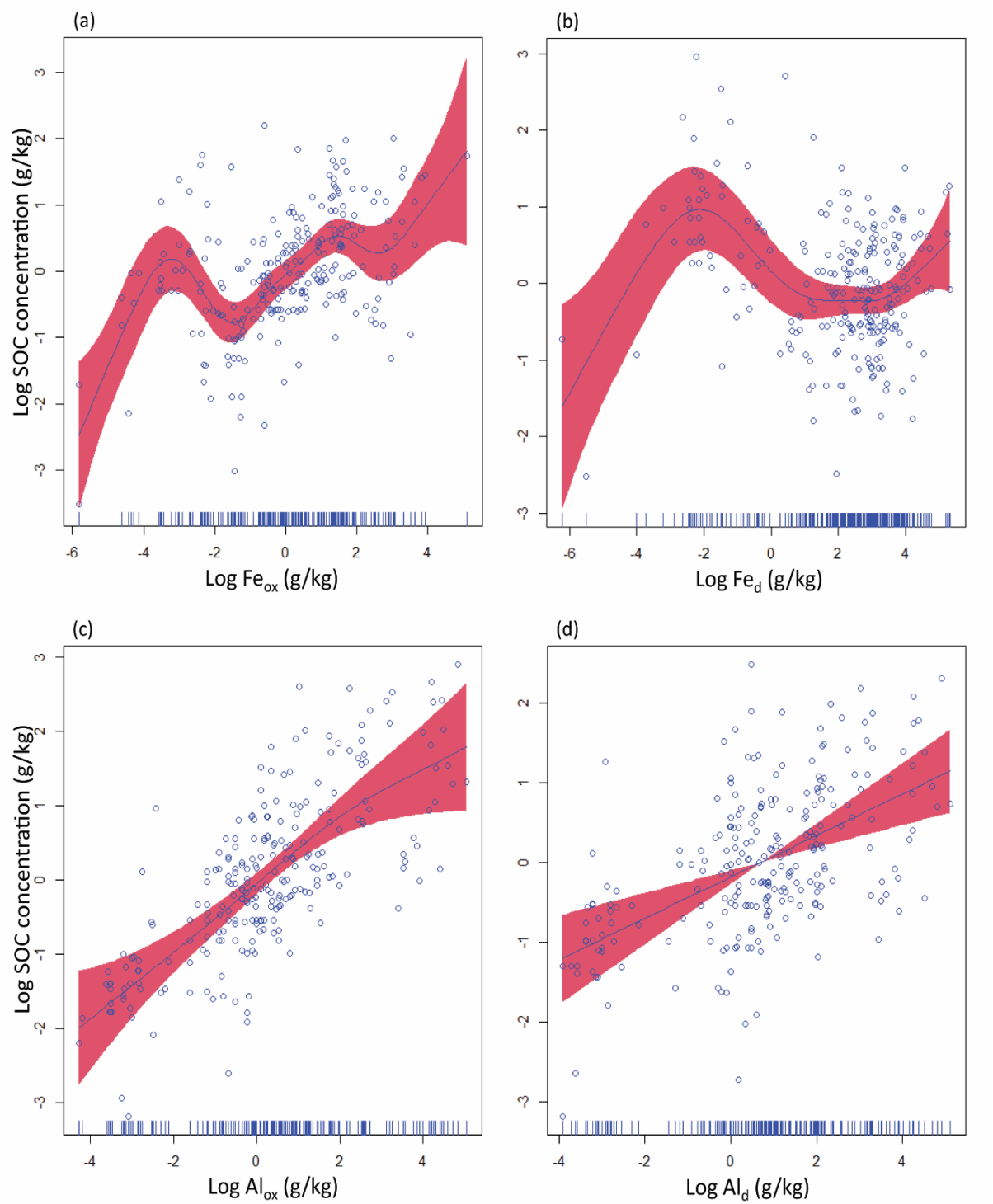

Figure 2.4. *Relationships between soil organic carbon (SOC) and individual extractable metals where each of the four metals extracted, (ammonium oxalate extractable iron [Fe_{ox}], dithionite-citrate-bicarbonate extractable iron [Fe_d], ammonium oxalate extractable aluminium [Al_{ox}], dithionite-citrate-bicarbonate extractable aluminium [Al_d]) was used in the generalized additive mixed models (GAMMs). These results are different from the model in Supplementary Figure 2.2, where Fe_{ox}, Fe_d, Al_{ox}, and Al_d were included in a single model. Akaike's information criterion values for separate models that included either Fe_{ox}, Fe_d, Al_{ox}, Al_d, were 658, 672, 645 and 670, respectively; F-statistic values for the individual predictors were 7, 6, 23, and 19; R^2 values for the full models were 0.57, 0.54, 0.58 and 0.52. The shaded red areas around the smooth lines represent the 95% confidence intervals.*

Our results do not refute the significant role of crystalline oxides (Fe_d or Al_d) in protecting SOC. Crystalline oxides play an important role in the preservation of SOC when present in the soil in substantial amounts (Mikutta *et al.*, 2006; Yeasmin *et al.*, 2017). A strong positive significant correlation between SOC and crystalline Fe oxides has been observed in soils (Mikutta *et al.*, 2006; Yeasmin *et al.*, 2017). Contrary to this, negative relationships between Fe_d (crystalline Fe) and SOC concentrations have also been reported in some studies, which has been related to the smaller SSA of crystalline Fe oxides as compared to SRO Fe phases (Fe_{ox}) (Percival *et al.*, 2000; Hall and Silver, 2015).

The rate of SOC mineralisation is controlled by its association with extractable metals. Few studies have quantified SOC mineralisation of OC sorbed onto minerals (Mikutta *et al.*, 2007; Schneider *et al.*, 2010; Saidy *et al.*, 2012). Saidy *et al.* (2012) studied the influence of Fe oxides (including ferrihydrite, goethite, hematite) and imogolite on C mineralisation in an illitic clay. They reported that C mineralisation was significantly reduced by ferrihydrite with increased SSA than goethite, hematite and imogolite, and the illitic clay-ferrihydrite association provided greater stabilisation of SOC. Mikutta *et al.* (2007) reported that mineral associated organic matter primary held by ligand exchange exhibited resistance to mineralisation compared to organic matter bound by van der Waals forces. Likewise, OC bound to poorly crystalline Al hydroxides reduced the rate of OC mineralisation in soils (Schneider *et al.*, 2010). Soils dominated by poorly crystalline minerals have a tendency to reduce SOC mineralisation because of the stabilisation of SOC by chemical sorption of SOC while it may not be applicable to soils dominated by crystalline minerals (Parfitt *et al.*, 2002; Rasmussen *et al.*, 2006).

2.4.3 SOC and P sorption capacity

The linear regression relationship between the two response variables (SOC and P sorption capacity) of our study is shown in Figure 2.5. The relationship between SOC concentration and P sorption capacity was weak, and non-significant ($R^2 = 0.01$, Figure 2.5). This may be due to

various interactions of SOC with SRO, which can directly or indirectly influence P sorption capacity in soils (Guppy *et al.*, 2005; Yan *et al.*, 2016; Hawkins *et al.*, 2022). Studies have reported a weak and non-significant correlation between SOC and P sorption capacity (Villapando and Graetz, 2001; Yan *et al.*, 2013), and a non-significant direct effect of SOC on P sorption capacity in a path analysis (Ige *et al.*, 2007; Kang *et al.*, 2009).

Iron/Al oxides are important for SOC stabilisation and sorption of P (Gérard, 2016). Competitive sorption occurs between SOC and phosphate for adsorption sites of Fe/Al oxides because both are negatively charged and utilize the same adsorption sites (Antelo *et al.*, 2010; Jindo *et al.*, 2023). The presence of high concentration of SOC in the soil can decrease P sorption capacity and increase P bioavailability in soils. The sorbed SOC can block the adsorption sites which leads to decreased phosphate sorption and repulsion, thereby increasing bioavailability P (Hunt *et al.*, 2007; Jindo *et al.*, 2023). The bioavailability of P in soils has been reported to be enhanced through the application of organic and inorganic fertilizers (Hunt *et al.*, 2007; Ma *et al.*, 2019; Yang *et al.*, 2019). Conversely, some studies have observed increased P sorption capacity and decreased bioavailability of P in soils with increasing SOC contents (Guppy *et al.*, 2005; Chase *et al.*, 2018).

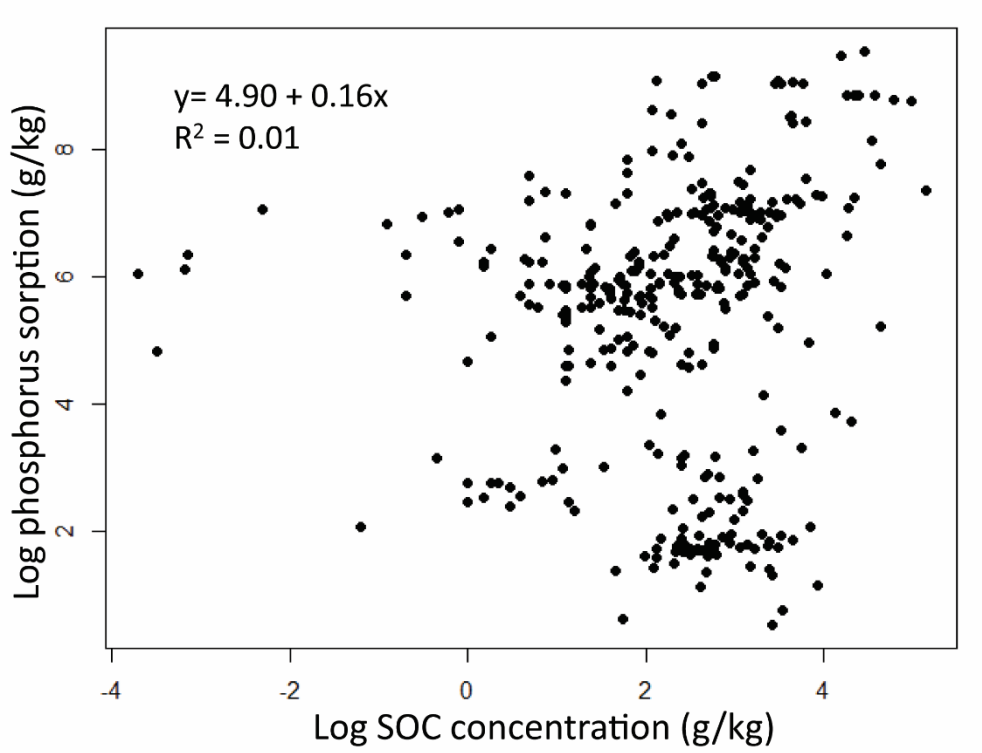

Figure 2.5. *Relationship between phosphorus sorption and soil organic carbon (SOC), R^2 values and regression equation are given in plot. Regression slope was not statistically significant.*

2.5 Conclusions

Oxalate extractable and dithionite extractable metals are important indicators of the P sorption capacity of soils and SOC preservation. The analysis of the data from the published studies demonstrates that $Al_{ox,}$ and Al_d are strong predictor variables of P sorption capacity of soils, but Al_d was a better predictor variable than Al_{ox} of the P sorption capacity of soils. Further, a positive 1:1 relationship between Al_{ox} and Al_d suggests that the pool of Al dissolved by ammonium oxalate and DCB was nearly the same, although small deviations from this relationship, might indicate release of additional Al substituting for Fe from the structure of Fe oxides during the DCB extraction. Similarly, we found that Fe_{ox} and Al_{ox} are good predictor variables of SOC, but Al_{ox} is a better predictor variable of SOC. From the above, we deduce that extractable Fe and Al have significant relationships with P sorption capacity and SOC concentration. The DCB forms of extractable Al and ammonium oxalate extractable Al have

stronger relationships with SOC concentration and P sorption capacity than extractable Fe. The concentration of ammonium oxalate extractable Al in the soil samples was significantly ($p<0.001$) greater than the concentration of ammonium oxalate extractable Fe. Although, the data used from the published literature do not show a relationship between P sorption capacity and SOC concentration, further research is needed on this aspect, particularly in acid soils.

2.6 Implications

The DCB and ammonium oxalate extractable Fe (and Al) represent Fe in crystalline and poorly crystalline, or amorphous form of Fe/Al may be used as a routine soil test, and these may be able to predict P sorption capacity and SOC preservation potential, particularly in acid soils.

2.6 Declaration of Funding

I acknowledge the **Soil Science Challenge Grants Program** funded by the **Australian Government Department of Agriculture, Fisheries and Forestry** and this chapter contributes towards the **National Soil Strategy** and the implementation of the **National Soil Action Plan**.

I am thankful to the Tertiary Education Trust Fund (TETFund), Nigeria for the financial support in tuition fees and living expenses.

2.7 Supporting Information

***Supplementary Table 2.1**. Selected publications/papers used for this study.*

Authors, year	Title of publications/papers
Bromfield 1965	Studies of the relative importance of iron and aluminum in the sorption of phosphate by some Australian soils
Lopez-Hernandez and Burnham 1974	The covariance of phosphate sorption with other soil properties in some British and tropical soils
Leger et al. 1979	The effects of organic matter, iron oxides and moisture on the color of two agricultural soils of Quebec
Loganathan and Fernando 1980	Phosphorus sorption by some coconut-growing acid soils of Sri Lanka and its relationship to selected soil properties
Jeanroy and Guillet 1981	The occurrence of suspended ferruginous particles in pyrophosphate extracts of some soil horizons
Peña, and Torrent 1984	Relationships between phosphate sorption and iron oxides in alfisols from a river terrace sequence of mediterranean Spain
Borggaard, et al. 1990	Influence of organic matter on phosphate adsorption by aluminium and iron oxides in sandy soils
Goldberg 1990	Effect of aluminum and iron oxides and organic matter on flocculation and dispersion of arid zone soils
Peña, and Torrent 1990	Predicting phosphate sorption in soils of mediterranean regions
Singh, 1991	Mineralogical and chemical characteristics of soils from South-Western Australia
Colombo et al. 1991	The contrasting effect of goethite and hematite on phosphate sorption and desorption by Terre Rosse
Soon 1991	Solubility and retention of phosphate in soils of the northwestern Canadian prairie
Walbridge et al. 1991	Vertical distribution of biological and geochemical phosphorus subcycles in two southern Appalachian Forest soil
Espejo and Cox 1992	Factors affecting phosphorus sorption in palexerults of western Spain
Torrent et al. 1992	Fast and Slow Phosphate Sorption by Goethite-Rich Natural Material
Jorgensen and Borggaard 1992	A Preliminary investigation of sorption and mobility of phosphate in a Danish spodosol
Osodeke et al. 1993	Phosphorus sorption characteristics of some soils of the rubber belt of Nigeria
Afif et al. 1993	Availability of phosphate applied to calcareous soils of West Asia and North-Africa
Arduino et al 1993	Phosphorus status of certain agricultural soils of Lesotho, Southern Africa
Demesquita and Torrent 1993	Phosphate sorption as related to mineralogy of a hydrosequence of soils from the Cerrado region (Brazil)
Mubiru and Karathanasis 1994	Phosphorus-sorption characteristics of intensely weathered soils in South-Central Kentucky
Yuan and Lavkulich 1994	Phosphate sorption in relation to extractable iron and aluminum in Spodosols

Wang and Tzou 1995	Phosphate sorption by calcite, and iron-rich calcareous soils
Indiati et al. 1995	Soil phosphorus sorption and availability as a function of high phosphorus fertilizer additions
Jugsujinda et al. 1995	Influence of extractable iron, aluminum, and manganese on p-sorption in flooded acid sulfate soils
Anghinoni et al. 1996	Phosphorus sorption isotherm characteristics and availability parameters of Appalachian acidic soils
Tsadilas et al. 1996	Phosphate sorption by red mediterranean soil from Greece
OwusuBennoah et al. 1996	Phosphate sorption in relation to aluminum and iron oxides of oxisols from Ghana
Zhou et al. 1997	Phosphorus sorption characteristics of Bh and Bt horizons horn sandy coastal plain soils
De Mello et al. 1998	Phosphorus and iron mobilization in flooded soils from Brazil
Van Ranst et al. 1998	Charge characteristics in relation to free iron and organic matter of soils from Bambouto mountains, Western Cameroon
Hansen et al. 1999	Phosphate sorption to matrix and fracture wall materials in a Glossaqualf
Osei and Singh 1999	Electrophoretic mobility of some tropical soil clays: effect of iron oxides and organic matter
Uusitalo and Tuhkanen 2000	Phosphorus saturation of Finnish soils: evaluating an easy oxalate extraction method
Börling et al. 2001	Phosphorus sorption in relation to soil properties in some cultivated Swedish soils
Dubus and Becquer 2001	Phosphorus sorption and desorption in oxide-rich ferralsols of New Caledonia
Villapando and Graetz 2001	Phosphorus sorption and desorption properties of the spodic horizon from selected Florida spodosols
Agbenin 2003	Extractable iron and aluminum effects on phosphate sorption in a savanna alfisol
Duiker et al. 2003	Iron (hydr)oxide crystallinity effects on soil aggregation
Eusterhues et al. 2003	Stabilization of soil organic matter by interactions with minerals as revealed by mineral dissolution and oxidative degradation
Pizarro et al. 2003	Influence of organic matter on iron oxides mineralogy of volcanic soils
Hartono et al. 2005	Phosphorus sorption-desorption characteristic of selected acid upland soils in Indonesia
Li et al. 2007	Phosphorus sorption-desorption by purple soils of China in relation to their properties
Ranno et al. 2007	Phosphorus adsorption capacity in lowland soils of Rio Grande do Sul State
Tsaousidou et al. 2008	Iron oxides in four Red Mediterranean soils on metarhyolite and metadolerite in Kilkis, Greece
Spielvogel et al. 2008	Soil organic matter stabilization in acidic forest soils is preferential and soil type-specific
Lair et al. 2009	Phosphorus sorption-desorption in alluvial soils of a young weathering sequence at the Danube River

Igwe et al. 2010	Fe and Al oxides distribution in some ultisols and inceptisols of southeastern Nigeria in relation to soil total phosphorus
Heiberg et al. 2010	A comparative study of phosphate sorption in lowland soils under oxic and anoxic conditions
Janardhanan and Daroub 2010	Phosphorus sorption in organic soils in South Florida
Rezapour et al. 2010	Distribution of iron oxides forms on a transect of calcareous soils, North-West of Iran
Chakraborty et al. 2012	Compositional differences between alaquods and paleudults affecting phosphorus sorption-desorption behavior
Ketrot et al. 2013	Interactive effects of iron oxides and organic matter on charge properties of red soils in Thailand
Wang et al. 2013	Phosphorus adsorption by soils from four land use patterns
Wissing et al. 2013	Management-induced organic carbon accumulation in paddy soils: The role of organo-mineral associations
Pinto et al. 2013	P-sorption and desorption in savanna Brazilian soils as a support for phosphorus fertilizer management
Cloy et al. 2014	Stabilization of organic carbon via chemical interactions with Fe and Al oxides in gley soils
Fink et al. 2014	Mineralogy and phosphorus adsorption in soils of south and central-west Brazil under conventional and no-tillage systems
Bortoluzzi et al. 2015	Occurrence of iron and aluminum sesquioxides and their implications for the P sorption in subtropical soils
Guareschi et al. 2015	Adsorption of P and forms of iron in no-tillage areas in the 'Cerrado' biome
Guedes et al. 2015	Maximum phosphorus adsorption capacity adjusted to isotherm models in representative soils of Eastern Amazon
Jonczak et al. 2015	Characteristics of iron and aluminium forms and quantification of soil forming processes in chernozems in western Slovakia
Rezapour et al. 2015	Changes in forms and distribution pattern of soil iron oxides due to long-term cropping in the Northwest of Iran
Hanke et al. 2015	Influence of organic matter on mean size of clay minerals in basalt soils in Southern Brazil
De Campos et al. 2016	Phosphorus sorption index in humid tropical soils
Estevez et al. 2016	Poorly crystalline components in aggregates from soils under different land use and parent material
Souza et al. 2017	Al/Fe (hydr)oxides organic carbon associations in Oxisols - From ecosystems to submicron scales
Zhao et al. 2017	Aggregate stability and size distribution of red soils under different land uses integrally regulated by soil organic matter, and iron and aluminum oxides
Jafarzadeh-Haghighi et al. 2017	Preservation of organic matter in soils of a climo-biosequence in the main range of Peninsular Malaysia
Gonzalez-Rodriguez and Fernandez-Marcos 2018	Phosphate sorption and desorption by two contrasting volcanic soils of equatorial Africa

Durn et al. 2019	Impact of iron oxides and soil organic matter on the surface physicochemical properties and aggregation of Terra Rossa and calcocambisol subsoil horizons from Istria (Croatia)
Fang et al. 2019	Paddy cultivation significantly alters phosphorus sorption characteristics and loss risk in a calcareous paddy soil chronosequence
Xue et al. 2019	Roles of soil organic carbon and iron oxides on aggregate formation and stability in two paddy soils
Ye et al. 2019	Controls on mineral-associated organic matter formation in a degraded oxisol
Yu et al. 2019	Soil organic carbon stabilization in the three subtropical forests: importance of clay and metal oxides
Biswas et al. 2020	Organic carbon content and Fe-organo association in soils under rice dominant cropping system in Bangladesh
Chen et al. 2022	Increased interactions between iron oxides and organic carbon under acid deposition drive large increases in soil organic carbon in a tropical forest in southern China

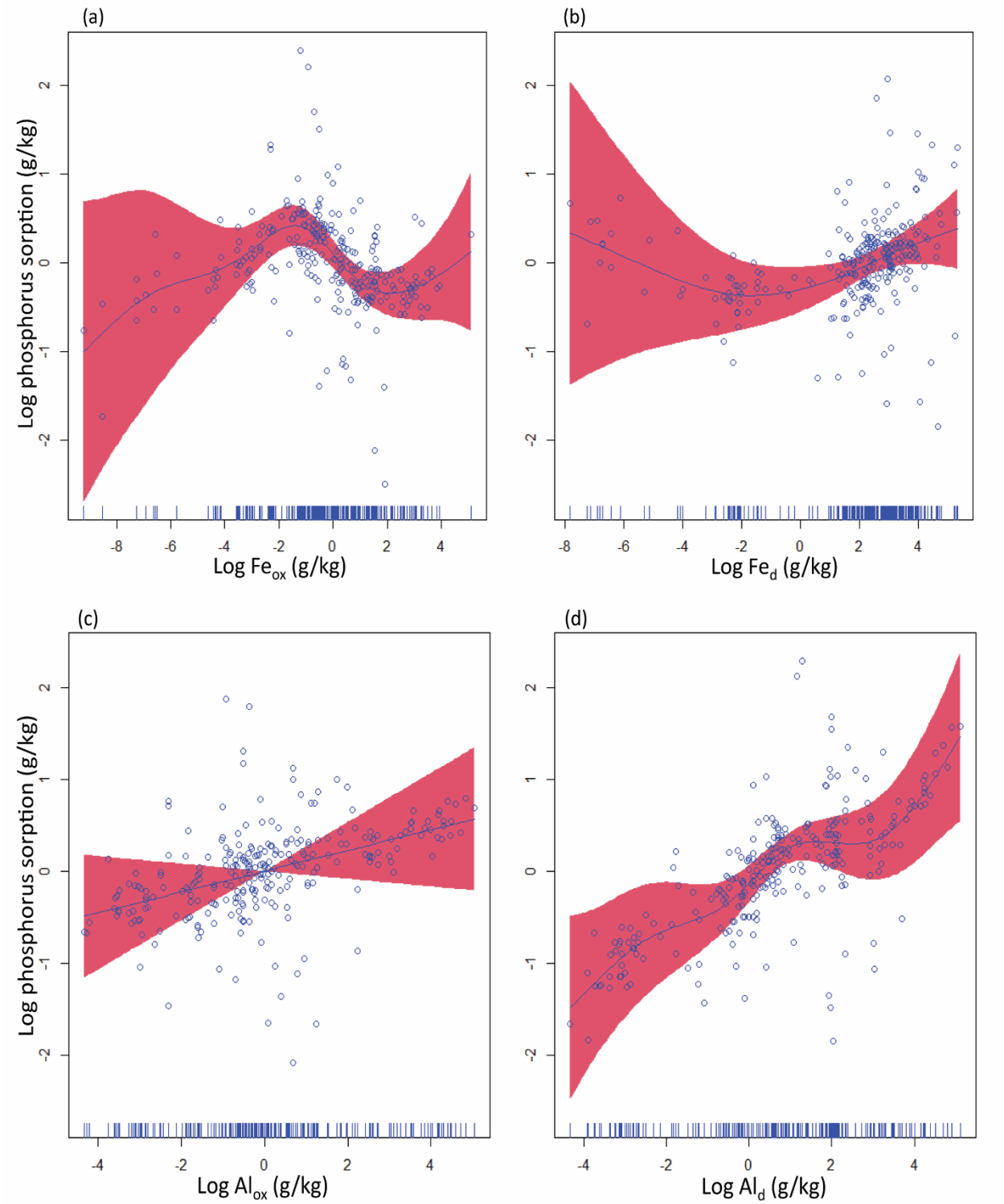

Supplementary Figure 2.1. *Relationships between phosphorus sorption and ammonium oxalate extractable iron (Fe_{ox}) (a), dithionite-citrate-bicarbonate extractable iron (Fe_d) (b), ammonium oxalate extractable aluminium (Al_{ox}) (c), and dithionite-citrate-bicarbonate extractable aluminium (Al_d) in the single optimal generalized additive mixed model (GAMM) (R^2 = 0.93). All predictors were significant at P<0.001. Shaded regions indicate two SEs from the mean predicted value.*

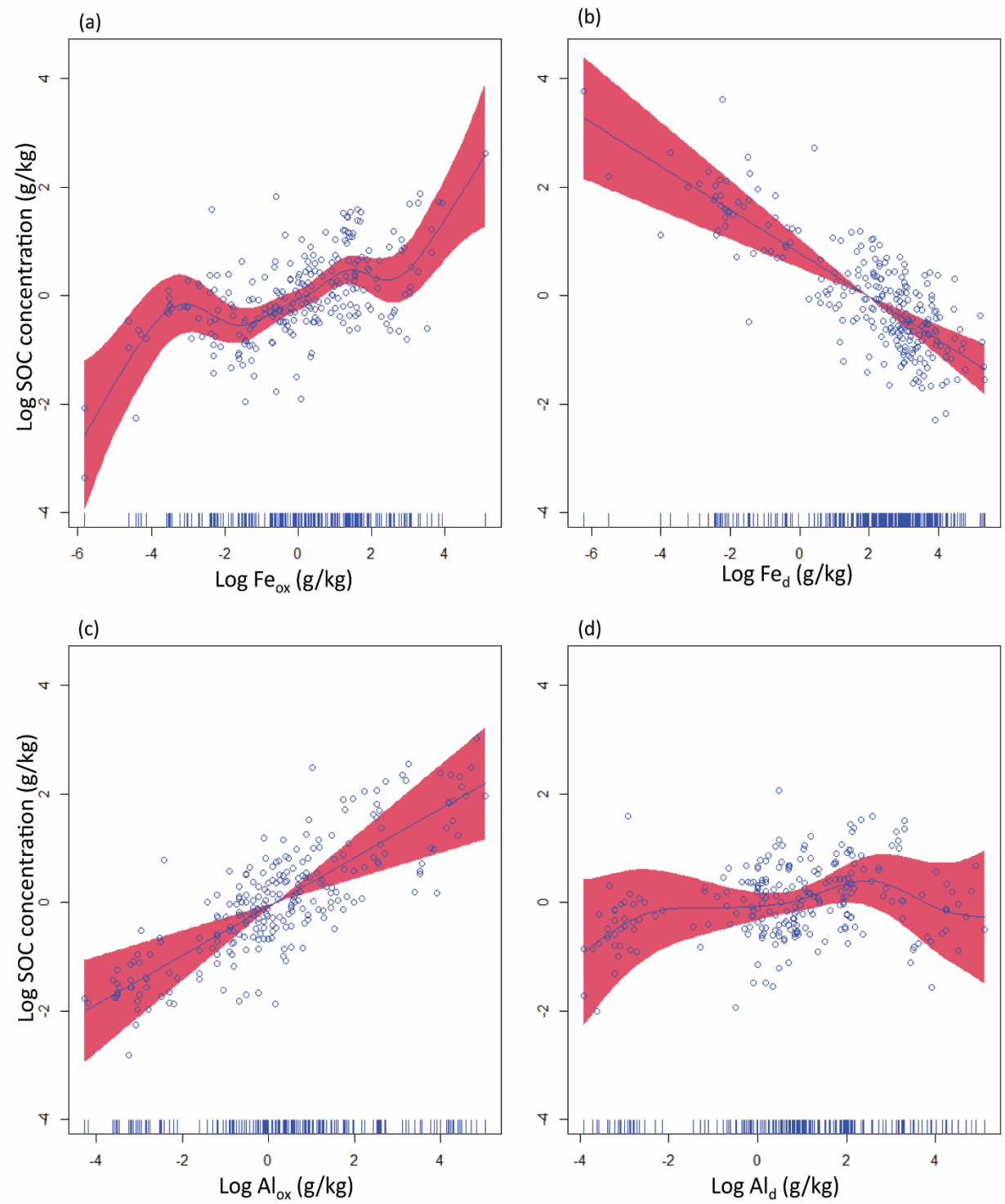

Supplementary Figure 2.2. *Relationships between soil organic carbon (SOC) concentration and ammonium oxalate extractable iron (Fe_{ox}) (a), dithionite-citrate-bicarbonate extractable iron (Fe_{d}) (b), ammonium oxalate extractable aluminium (Al_{ox}) (c), dithionite-citrate-bicarbonate extractable aluminium (Al_{d}) in the single optimal generalized additive mixed model (GAMM) (R^2 = 0.69). All predictors were significant at P<0.001. Shaded regions indicate two SEs from the mean predicted value.*

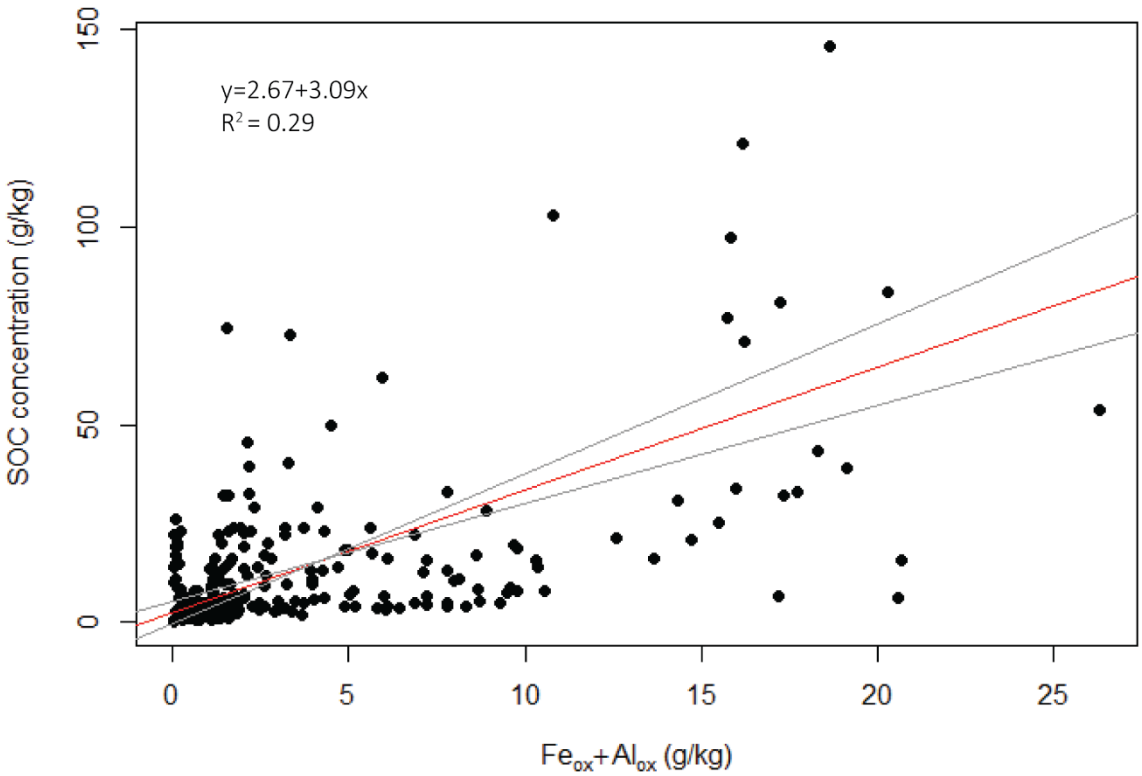

Supplementary Figure 2.3. *Relationship between soil organic carbon (SOC) concentration and ammonium oxalate extractable iron (Fe_{ox}) + ammonium oxalate extractable aluminium (Al_{ox}). Lines in red indicate reduced major axis (RMA) regression, and lines (in grey) indicate confidence intervals for the RMA regression line, R^2 values and RMA regression equation are given in each plot. Regression slope was statistically significant at $p<0.01$.*

References

Acebal SG, Mijovilovich A, Rueda EH, Aguirre ME, Saragovi C (2000) Iron-oxide mineralogy of a mollisol from Argentina: A study by selective-dissolution techniques, x-ray diffraction, and Mössbauer spectroscopy. *Clays and Clay Minerals* **48**, 322-330.

Agbenin JO (2003) Extractable iron and aluminum effects on phosphate sorption in a savanna Alfisol. *Soil Science Society of America Journal* **67**, 589-595.

Ahenkorah YAW (1968) Phosphorus-retention capacities of some cocoa-growing soils of Ghana and thier relationship with soil properties. *Soil Science* **105**, 24-30.

Antelo J, Fiol S, Pérez C, Mariño S, Arce F, Gondar D, López R (2010) Analysis of phosphate adsorption onto ferrihydrite using the CD-MUSIC model. *Journal of Colloid and Interface Science* **347**, 112-119.

Banwart SA, Nikolaidis NP, Zhu Y-G, Peacock CL, Sparks DL (2019) Soil Functions: Connecting Earth's Critical Zone. *Annual Review of Earth and Planetary Sciences* **47**, 333-359.

Batjes NH (1996) Total carbon and nitrogen in the soils of the world. *European Journal of Soil Science* **47**, 151-163.

Batjes NH (2014) Total carbon and nitrogen in the soils of the world. *European Journal of Soil Science* **65**, 10-21.

Borggaard O (1983) The influence of iron oxides on phosphate adsorption by soil. *Journal of Soil Science* **34**, 333-341.

Borggaard OK, Jdrgensen SS, Moberg JP, Raben-Lange B (1990) Influence of organic matter on phosphate adsorption by aluminium and iron oxides in sandy soils. *Journal of Soil Science* **41**, 443-449.

Börling K, Otabbong E, Barberis E (2001) Phosphorus sorption in relation to soil properties in some cultivated swedish soils. *Nutrient Cycling in Agroecosystems* **59**, 39-46.

Bortoluzzi EC, Pérez CAS, Ardisson JD, Tiecher T, Caner L (2015) Occurrence of iron and aluminum sesquioxides and their implications for the P sorption in subtropical soils. *Applied Clay Science* **104**, 196-204.

Bromfield SM (1965) Studies of the relative importance of iron and aluminium in the sorption of phosphate by some Australian soils. *Australian Journal of Soil Research* **3**, 31-44.

Chadwick OA, Chorover J (2001) The chemistry of pedogenic thresholds. *Geoderma* **100**, 321-353.

Chase AJ, Erich MS, Ohno T (2018) Bioavailability of phosphorus on iron (oxy) hydroxide not affected by soil amendment–derived organic matter. *Agricultural and Environmental Letters* **3**, 170042.

Crews TE, Kitayama K, Fownes JH, Riley RH, Herbert DA, Mueller-Dombois D, Vitousek PM (1995) Changes in soil phosphorus fractions and ecosystem dynamics across a long chronosequence in Hawaii. *Ecology* **76**, 1407-1424.

Cross AF, Schlesinger WH (1995) A literature review and evaluation of the. Hedley fractionation: Applications to the biogeochemical cycle of soil phosphorus in natural ecosystems. *Geoderma* **64**, 197-214.

Dahlgren RA (1994) Quantification of allophane and imogolite. In: J.E. Amonette, J.W. Stucki (eds) Quantitative Methods in Soil Mineralogy. *Soil Science Society of America*, pp 430-451.

De Campos M, Antonangelo JA, Alleoni LRF (2016) Phosphorus sorption index in humid tropical soils. *Soil and Tillage Research* **156**, 110-118.

De Schrijver A, Vesterdal L, Hansen K, De Frenne P, Augusto L, Achat DL, Staelens J, Baeten L, De Keersmaeker L, De Neve S (2012) Four decades of post-agricultural forest

development have caused major redistributions of soil phosphorus fractions. *Oecologia* **169**, 221-234.
Freese D, van der Zee SEATM, van Riemsdijk WH (1992) Comparison of different models for phosphate sorption as a function of the iron and aluminium oxides of soils. *Journal of Soil Science* **43**, 729-738.
Gérard F (2016) Clay minerals, iron/aluminum oxides, and their contribution to phosphate sorption in soils - A myth revisited. *Geoderma* **262**, 213-226.
Giardina CP, Binkley D, Ryan MG, Fownes JH, Senock RS (2004) Belowground carbon cycling in a humid tropical forest decreases with fertilization. *Oecologia* **139**, 545-550.
Guppy CN, Menzies N, Moody PW, Blamey F (2005) Competitive sorption reactions between phosphorus and organic matter in soil: a review. *Soil Research* **43**, 189-202.
Hall SJ, Silver WL (2015) Reducing conditions, reactive metals, and their interactions can explain spatial patterns of surface soil carbon in a humid tropical forest. *Biogeochemistry* **125**, 149-165.
Hall SJ, Thompson A (2022) What do relationships between extractable metals and soil organic carbon concentrations mean? *Soil Science Society of America Journal* **86**, 195-208.
Hawkesford MJ, Cakmak I, Coskun D, De Kok LJ, Lambers H, Schjoerring JK, White PJ (2023) Chapter 6 - Functions of macronutrients. This chapter is a revision of the third edition chapter by M. Hawkesford, W. Horst, T. Kichey, H. Lambers, J. Schjoerring, I. Skrumsager Møller, and P. White, pp. 135–189. In: Rengel Z, Cakmak I, White PJ (eds) Marschner's Mineral Nutrition of Plants (Fourth Edition). *Academic Press*, San Diego, pp 201-281.
Hawkins J, Vermeiren C, Blackwell M, Darch T, Granger S, Dunham S, Hernandez-Allica J, Smolders E, McGrath S (2022) The effect of soil organic matter on long-term availability of phosphorus in soil: Evaluation in a biological P mining experiment. *Geoderma* **423**, 115965.
He X, Augusto L, Goll DS, Ringeval B, Wang Y, Helfenstein J, Huang Y, Yu K, Wang Z, Yang Y (2021) Global patterns and drivers of soil total phosphorus concentration. *Earth System Science Data* **13**, 5831-5846.
Hemingway JD, Rothman DH, Grant KE, Rosengard SZ, Eglinton TI, Derry LA, Galy VV (2019) Mineral protection regulates long-term global preservation of natural organic carbon. *Nature* **570**, 228-231.
Herndon EM, Kinsman-Costello L, Duroe KA, Mills J, Kane ES, Sebestyen SD, Thompson AA, Wullschleger SD (2019) Iron (oxyhydr)oxides serve as phosphate traps in Tundra and Boreal peat soils. *Journal of Geophysical Research: Biogeosciences* **124**, 227-246.
Hui W, Jun Z, Qing-Ling F, Xiong JW, Can H, Hong-Qing H, Violante A (2015) Adsorption of phosphate onto ferrihydrite and ferrihydrite-humic acid complexes. *Pedosphere* **25**, 405-414.
Hunt JF, Ohno T, He Z, Honeycutt CW, Dail DB (2007) Inhibition of phosphorus sorption to goethite, gibbsite, and kaolin by fresh and decomposed organic matter. *Biology and Fertility of Soils* **44**, 277-288.
Ige D, Akinremi O, Flaten D (2007) Direct and indirect effects of soil properties on phosphorus retention capacity. *Soil Science Society of America Journal* **71**, 95-100.
Jindo K, Audette Y, Olivares FL, Canellas LP, Smith DS, Paul Voroney R (2023) Biotic and abiotic effects of soil organic matter on the phytoavailable phosphorus in soils: A review. *Chemical and Biological Technologies in Agriculture* **10**, 1-12.
Kaiser K, Guggenberger G (2000) The role of DOM sorption to mineral surfaces in the preservation of organic matter in soils. *Organic Geochemistry* **31**, 711-725.
Kaiser K, Guggenberger G (2003) Mineral surfaces and soil organic matter. *European Journal of Soil Science* **54**, 219-236.

Kang J, Hesterberg D, Osmond DL (2009) Soil organic matter effects on phosphorus sorption: a path analysis. *Soil Science Society of America Journal* **73**, 360-366.
Kleber M, Eusterhues K, Keiluweit M, Mikutta C, Mikutta R, Nico PS (2015) Mineral–organic associations: formation, properties, and relevance in soil environments. *Advances in Agronomy* **130**, 1-140.
Kleber M, Mikutta R, Torn M, Jahn R (2005) Poorly crystalline mineral phases protect organic matter in acid subsoil horizons. *European Journal of Soil Science* **56**, 717-725.
Lal R (2004) Soil carbon sequestration impacts on global climate change and food security. *Science* **304**, 1623-1627.
Li M, Hou YL, Zhu B (2007) Phosphorus sorption-desorption by purple soils of China in relation to their properties. *Australian Journal of Soil Research* **45**, 182-189.
Li Y, Xu M, Zou X (2006) Effects of nutrient additions on ecosystem carbon cycle in a Puerto Rican tropical wet forest. *Global Change Biology* **12**, 284-293.
Lin Y, Gross A, O'connell CS, Silver WL (2020) Anoxic conditions maintained high phosphorus sorption in humid tropical forest soils. Biogeosciences 17, 89-101.
Loganathan P, Fernando WT (1980) Phosphorus sorption by some coconut-growing acid soils of Sri Lanka and its relationship to selected soil properties. *Journal of the Science of Food and Agriculture* **31**, 709-717.
Lützow Mv, Kögel-Knabner I, Ekschmitt K, Matzner E, Guggenberger G, Marschner B, Flessa H (2006) Stabilization of organic matter in temperate soils: mechanisms and their relevance under different soil conditions–a review. *European Journal of Soil Science* **57**, 426-445.
Ma Y, Ma J, Peng H, Weng L, Chen Y, Li Y (2019) Effects of iron, calcium, and organic matter on phosphorus behavior in fluvo-aquic soil: farmland investigation and aging experiments. *Journal of Soils and Sediments* **19**, 3994-4004.
McKeague J, Day J (1966) Dithionite-and oxalate-extractable Fe and Al as aids in differentiating various classes of soils. *Canadian Journal of Soil Science* **46**, 13-22.
Mikutta R, Kleber M, Torn MS, Jahn R (2006) Stabilization of soil organic matter: association with minerals or chemical recalcitrance? *Biogeochemistry* **77**, 25-56.
Mikutta R, Mikutta C, Kalbitz K, Scheel T, Kaiser K, Jahn R (2007) Biodegradation of forest floor organic matter bound to minerals via different binding mechanisms. *Geochimica et Cosmochimica Acta* **71**, 2569-2590.
Page MJ, McKenzie JE, Bossuyt PM, Boutron I, Hoffmann TC, Mulrow CD, Shamseer L, Tetzlaff JM, Akl EA, Brennan SE, Chou R, Glanville J, Grimshaw JM, Hróbjartsson A, Lalu MM, Li T, Loder EW, Mayo-Wilson E, McDonald S, McGuinness LA, Stewart LA, Thomas J, Tricco AC, Welch VA, Whiting P, Moher D (2021) The PRISMA 2020 statement: An updated guideline for reporting systematic reviews. *Systematic Reviews* **10**.
Parfitt R, Parshotam A, Salt G (2002) Carbon turnover in two soils with contrasting mineralogy under long-term maize and pasture. *Soil Research* **40**, 127-136.
Peña F, Torrent J (1984) Relationships between phosphate sorption and iron oxides in Alfisols from a river terrace sequence of Mediterranean Spain. *Geoderma* **33**, 283-296.
Peña F, Torrent J (1990) Predicting phosphate sorption in soils of mediterranean regions. *Fertilizer Research* **23**, 173-179.
Percival HJ, Parfitt RL, Scott NA (2000) Factors controlling soil carbon levels in New Zealand grasslands is clay content important? *Soil Science Society of America Journal* **64**, 1623-1630.
Ping C, Michaelson G (1986) Phosphorus sorption by major agricultural soils of Alaska. *Communications in Soil Science and Plant Analysis* **17**, 299-320.
Raghothama K, Karthikeyan A (2005) Phosphate acquisition. *Plant and Soil* **274**, 37-49.

Rasmussen C, Heckman K, Wieder WR, Keiluweit M, Lawrence CR, Berhe AA, Blankinship JC, Crow SE, Druhan JL, Hicks Pries CE, Marin-Spiotta E, Plante AF, Schädel C, Schimel JP, Sierra CA, Thompson A, Wagai R (2018) Beyond clay: towards an improved set of variables for predicting soil organic matter content. *Biogeochemistry* **137**, 297-306.

Rasmussen C, Southard RJ, Horwath WR (2006) Mineral control of organic carbon mineralization in a range of temperate conifer forest soils. *Global Change Biology* **12**, 834-847.

R Core Team (2024) R: A language and environment for statistical computing. R Foundation for Statistical Computing, Vienna, Austria. URL https://www.R-project.org/.

Reeves DW (1997) The role of soil organic matter in maintaining soil quality in continuous cropping systems. *Soil and Tillage Research* **43**, 131-167.

Rennert T (2018) Wet-chemical extractions to characterise pedogenic Al and Fe species–a critical review. *Soil Research* **57**, 1-16.

Saidy AR, Smernik RJ, Baldock JA, Kaiser K, Sanderman J, Macdonald LM (2012) Effects of clay mineralogy and hydrous iron oxides on labile organic carbon stabilisation. *Geoderma* **173-174**, 104-110.

Sanchez PA (2019) Properties and managment of soils in the tropics. 2nd edn. Cambridge University Press, Cambridge, United Kingdom.

Schneider MPW, Scheel T, Mikutta R, van Hees P, Kaiser K, Kalbitz K (2010) Sorptive stabilization of organic matter by amorphous Al hydroxide. *Geochimica et Cosmochimica Acta* **74**, 1606-1619.

Shang C, Tiessen H (1998) Organic matter stabilization in two semiarid tropical soils: size, density, and magnetic separations. *Soil Science Society of America Journal* **62**, 1247-1257.

Singh B, Gilkes R (1991) Phosphorus sorption in relation to soil properties for the major soil types of south-western Australia. *Soil Research* **29**, 603-618.

Singh B, Gilkes R (1992) Properties and distribution of iron oxides and their association with minor elements in the soils of south-western Australia. *Journal of Soil Science* **43**, 77-98.

Singh M, Sarkar B, Biswas B, Churchman J, Bolan NS (2016) Adsorption-desorption behavior of dissolved organic carbon by soil clay fractions of varying mineralogy. *Geoderma* **280**, 47-56.

Sollins P, Homann P, Caldwell BA (1996) Stabilization and destabilization of soil organic matter: mechanisms and controls. *Geoderma* **74**, 65-105.

Spohn M (2020) Increasing the organic carbon stocks in mineral soils sequesters large amounts of phosphorus. *Global Change Biology* **26**, 4169-4177.

Sposito G (1989) Soil adsorption phenomena. In: The chemistry of soils. Oxford University Press.

Syers J, Evans T, Williams J, Murdock J (1971) Phosphate sorption parameters of representative soils from Rio Grande do Sul, Brazil. *Soil Science* **112**, 267-275.

Tamrat WZ, Rose J, Grauby O, Doelsch E, Levard C, Chaurand P, Basile-Doelsch I (2019) Soil organo-mineral associations formed by co-precipitation of Fe, Si and Al in presence of organic ligands. *Geochimica et Cosmochimica Acta* **260**, 15-28.

Torrent J, Schwertmann U, Barrón V (1992) Fast and slow phosphate sorption by goethite-rich natural materials. *Clays and Clay Minerals* **40**, 14-21.

Villapando RR, Graetz DA (2001) Phosphorus sorption and desorption properties of the spodic horizon from selected Florida Spodosols. *Soil Science Society of America Journal* **65**, 331-339.

Vitousek PM, Porder S, Houlton BZ, Chadwick OA (2010) Terrestrial phosphorus limitation: mechanisms, implications, and nitrogen–phosphorus interactions. *Ecological applications* **20**, 5-15.

Von Fromm SF, Hoyt AM, Lange M, Acquah GE, Aynekulu E, Berhe AA, Haefele SM, McGrath SP, Shepherd KD, Sila AM, Six J, Towett EK, Trumbore SE, Vågen TG, Weullow E, Winowiecki LA, Doetterl S (2021) Continental-scale controls on soil organic carbon across sub-Saharan Africa. *Soil* **7**, 305-332.

Wagai R, Kajiura M, Asano M (2020) Iron and aluminum association with microbially processed organic matter via meso-density aggregate formation across soils: organo-metallic glue hypothesis. *Soil* **6**, 597-627.

Wagai R, Mayer LM, Kitayama K, Shirato Y (2013) Association of organic matter with iron and aluminum across a range of soils determined via selective dissolution techniques coupled with dissolved nitrogen analysis. *Biogeochemistry* **112**, 95-109.

Walker T, Syers JK (1976) The fate of phosphorus during pedogenesis. *Geoderma* **15**, 1-19.

Watanabe T (2017) Significance of active aluminum and iron on organic carbon preservation and phosphate sorption/release in tropical soils. In: Funakawa S (ed) Soils, Ecosystem Processes, and agricultural development: Tropical Asia and Sub-Saharan Africa. Springer Japan, Tokyo, pp 103-125.

Wiriyakitnateekul W, Suddhiprakarn A, Kheuruenromne I, Gilkes RJ (2005) Extractable iron and aluminium predict the P sorption capacity of Thai soils. *Soil Research* **43**, 757-766.

Wiseman C, Püttmann W (2006) Interactions between mineral phases in the preservation of soil organic matter. *Geoderma* **134**, 109-118.

Wood SN (2017) Generalized Additive Models: An introduction with R. 2nd edn. Chapman and Hall/CRC press, Boca Raton, Florida, United States.

Yan J, Jiang T, Yao Y, Lu S, Wang Q, Wei S (2016) Preliminary investigation of phosphorus adsorption onto two types of iron oxide-organic matter complexes. *Journal of Environmental Sciences (China)* **42**, 152-162.

Yan X, Wang D, Zhang H, Zhang G, Wei Z (2013) Organic amendments affect phosphorus sorption characteristics in a paddy soil. *Agriculture, ecosystems and environment* **175**, 47-53.

Yang X, Chen X, Yang X (2019) Effect of organic matter on phosphorus adsorption and desorption in a black soil from Northeast China. *Soil and Tillage Research* **187**, 85-91.

Ye C, Huang W, Hall SJ, Hu S (2022) Association of organic carbon with reactive iron oxides driven by soil pH at the global scale. *Global Biogeochemical Cycles* **36**, e2021GB007128.

Yeasmin S, Singh B, Johnston CT, Sparks DL (2017) Organic carbon characteristics in density fractions of soils with contrasting mineralogies. *Geochimica et Cosmochimica Acta* **218**, 215-236.

Yu W, Weintraub SR, Hall SJ (2021) Climatic and geochemical controls on soil carbon at the continental scale: interactions and thresholds. *Global Biogeochemical Cycles* **35**, e2020GB006781.

Zhang L, Ding X, Peng Y, George TS, Feng G (2018) Closing the loop on phosphorus loss from intensive agricultural soil: a microbial immobilization solution? *Frontiers in Microbiology* **9**, 104.

Zhao B, Dou A, Zhang Z, Chen Z, Sun W, Feng Y, Wang X, Wang Q (2023) Ecosystem-specific patterns and drivers of global reactive iron mineral-associated organic carbon. *Biogeosciences Discussions* **2023**, 1-39.

Zimmerman AR, Chorover J, Goyne KW, Brantley SL (2004) Protection of mesopore-adsorbed organic matter from enzymatic degradation. *Environmental Science and Technology* **38**, 4542-4548.

Chapter Three

This chapter is under review as:

Identifying the role of different forms of metal(loid)s in the preservation of organic carbon in Australian soils

Bright E. Amenkhienan, Feike A. Dijkstra, Charles Warren, and Balwant Singh.

School of Life and Environmental Sciences, The University of Sydney, NSW 2015, Australia.

3.0 Abstract

A strong association of organic carbon (OC) with metal oxides, especially iron (Fe) and aluminium (Al) oxides has been reported in several recent studies. However, the role of various species of Fe, Al, manganese (Mn) and silicon (Si) in the preservation of OC in Australian soils remains poorly understood. To address this, we collected topsoil (0-20 cm) and subsoil (20-40 cm) soil samples from 37 sites across different agricultural regions of New South Wales, Australia. Soil samples were subjected to three separate extractions, i.e., sodium pyrophosphate (PP) to extract organo-metal complexes, ammonium oxalate (OX) to extract poorly crystalline and short-range order (SRO) minerals and dithionite citrate bicarbonate (DCB) to extract total metal oxides and associated OC. Soil organic carbon (SOC) was extracted in the sequence: C_{PP} > C_{DCB} > C_{OX}, with mean of 62 %, 41 % and 28 % C, respectively, of the TC in soils. C_{PP} and C_{DCB} were significantly greater in the topsoils than the subsoils. The extraction sequence for Fe was: Fe_{DCB} > Fe_{OX} > Fe_{PP}, with mean of 49 %, 9 % and 3 %, respectively, of the total Fe. Fe_{PP} was significantly greater in the topsoils than the subsoils. The sequence for Al was: Al_{DCB} > Al_{OX} > Al_{PP}, with mean of 4 %, 3.9 % and 2 %, respectively, of the total Al. Manganese was extracted in the sequence - Mn_{OX} > Mn_{DCB} > Mn_{PP}, with an average of 78 %, 65 % and 43 %, respectively, of the total Mn. All forms of extractable Mn were significantly greater in the topsoils than the subsoils. All extractants dissolved < 1% of the total Si. All extractable forms of Fe and Al showed significant positive correlations with extractable C, which suggested their role in the preservation of SOC. The large fraction of OC extracted by PP suggests that most

of the SOC was present in organic-Fe/Al complexes in the studied soils. The significant amount of OC extracted by OX also indicates that a substantial portion of the SOC was present in association with SRO and poorly crystalline Fe oxides, while a relatively small proportion of OC extracted by DCB (because it extracts C associated with both crystalline and amorphous Fe) suggests a limited role of crystalline Fe/Al oxides in the OC preservation.

Keywords: Soil organic carbon, iron, aluminium, manganese, silicon, extraction, sodium pyrophosphate, ammonium oxalate, dithionite citrate bicarbonate, extractable metals.

3.1 Introduction

A large fraction of organic carbon (OC) in the terrestrial ecosystems is stored in soils (SOC), which is more than the combined together in the atmosphere and vegetation (Batjes, 2014). The abundance of SOC is important to the physico-chemical and biological properties of soils (Watanabe, 2017). Soil OC is also an important component of the biogeochemical cycle of C (Lal *et al.*, 1999). A small change in the total globally SOC pool can substantially increase or decrease atmospheric CO_2 concentration and thus has potential to accelerate or mitigate global warming (Lal, 2004; Crowther *et al.*, 2016). Managing soils to boost OC stocks has been suggested as a strategy to mitigate the increase in atmospheric CO_2 concentration (Mikutta *et al.*, 2006). The association of OC with minerals has received significant attention in recent decades, because it is recognised as a key mechanism in the stabilisation and long-term storage of OC in soils (Sollins *et al.*, 1996; Torn *et al.*, 1997; Lützow *et al.*, 2006; Kögel-Knabner *et al.*, 2008; Kleber *et al.*, 2015; Lehmann and Kleber, 2015). Several mechanisms, such as surface complexation, cation bridging, weak chemical interactions and co-precipitation, have been postulated in the formation of mineral-associated organic carbon (MAOC) in soils (Kögel-Knabner *et al.*, 2008; von Lützow *et al.*, 2008; Kleber *et al.*, 2015). Chemical

interactions of OC with minerals decrease its susceptibility towards oxidative attack and microbial mineralisation, which subsequently results in the stabilisation and accumulation of OC in soils (Kaiser and Guggenberger, 2003; Kalbitz *et al.*, 2005; Kögel-Knabner *et al.*, 2008). The nature of association and stability of the MAOC in different soil types are not well understood.

Iron (Fe) and aluminium (Al) are among the most prevalent elements in soils (Cornell and Schwertmann, 2003). Iron and Al oxides (the term 'oxides' used for brevity, it includes hydroxides, oxyhydroxides and oxides) are formed in soils from the weathering and dissolution of primary minerals (Chadwick and Chorover, 2001). These minerals are effective sorbents for dissolved OC because of their high specific surface area (SSA) and reactive surfaces (Kaiser and Guggenberger, 2000). Iron bound C has been estimated to contribute 15 to 38 % of the total OC in sediments and soils (Cornell and Schwertmann, 2003; Wagai and Mayer, 2007; Zhao *et al.*, 2016). The concentration of Fe and Al oxides is generally high in intensively weathered soils of tropical and subtropical regions (Singh and Gilkes, 1992; Mikutta *et al.*, 2009). The surface hydroxyl groups of Fe oxides are capable of interacting with carboxyl or hydroxamate groups of SOC via ligand exchange, thus stabilise and protect SOC against microbial mineralisation (Gu *et al.*, 1994; Mikutta *et al.*, 2007; Kleber *et al.*, 2015; Chen *et al.*, 2020). The reaction between Fe oxides and organic functional groups have been studied and it has been found that Fe oxides preferentially bind with aromatic and carboxylic functional groups of OC (Gu *et al.*, 1994; Kaiser, 2003; Chen *et al.*, 2014; Yeasmin *et al.*, 2014). Co-precipitation of dissolved OC with polyvalent cations such as Fe and Al in organo-metal complexes also stabilises SOC (Baldock and Skjemstad, 2000; Scheel *et al.*, 2007; Eusterhues *et al.*, 2011; Mikutta *et al.*, 2014). Co-precipitation may occur due to changes in soil pH or redox conditions (Wagai and Mayer, 2007; Fritzsche *et al.*, 2015). For example, in temporarily waterlogged paddy soils, upon aeration, dissolved Fe (II) is rapidly oxidised to relatively

insoluble Fe (III) and large amount of OC co-precipitate with Fe (Chen *et al.*, 2014; Song *et al.*, 2022). Some studies have revealed that co-precipitation (organo-metal complexes) was more effective in sequestering dissolved OC than adsorption (Mikutta *et al.*, 2011; Chen *et al.*, 2014; Mikutta *et al.*, 2014). Despite the wide-spread occurrence of Fe oxides in Australian soils, the association of OC with Fe oxides remains poorly understood in these soils (Davey *et al.*, 1975; Singh and Gilkes, 1992; Viscarra Rossel *et al.*, 2010).

Manganese (Mn) is a redox-active element that can strongly interact with organic functional groups, thus influencing the preservation of SOC (Li *et al.*, 2021). Relative to bulk soils, Mn oxides could be strongly enriched in OC (Rennert *et al.*, 2014). Mn oxides in particular the poorly crystalline Mn oxides possess relatively large SSA and higher adsorption capacity for organic (Estes *et al.*, 2017; Stuckey *et al.*, 2018; Li *et al.*, 2021), and inorganic compounds such as heavy metals (Feng *et al.*, 2007) thereby stabilising and protecting OC against decomposition (Li *et al.*, 2021). Mn oxides have several properties similar to Fe oxides (Li *et al.*, 2021), but the association of OC with Mn oxides in Australian soils is understudied. Silicon (Si) plays a significant role in regulating the biogeochemical C cycle and stabilization of SOC. In the terrestrial ecosystem, the behaviours of Fe and Al maybe regulated by biogeochemical Si cycle through Si-Fe and Si-Al feedback (Pokrovski *et al.*, 2003; Matus *et al.*, 2014). Consequently, this may play a significant role in stabilising SOC (Song *et al.*, 2018), either through direct preservation of SOC by chemical interaction with amorphous Si (phytolith) or through indirect stabilisation of MAOC and soil aggregates (Pokrovski *et al.*, 2003; Matus *et al.*, 2014; Zhang *et al.*, 2016).

The relationship between SOC and extractable metals can determine the role of different forms or species of metals in the formation of MAOC and preservation of OC in soils. Other techniques, such as, X-ray diffraction and vibrational spectroscopy, are unable to distinguish association of OC with different species of Fe and Al oxides (Coward *et al.*, 2017). Despite

some overlaps and non-selectivity, extraction techniques offer the best option for the assessment of OC association with Fe, Al, Mn, and Si. Numerous studies have used extraction procedures to understand the role of Fe and Al oxides in the stabilisation of SOC in relatively young soils from temperate soils (Kaiser and Guggenberger, 2000; Kleber *et al.*, 2005; Wiseman and Püttmann, 2006; Kaiser *et al.*, 2007; Wagai and Mayer, 2007; Rasmussen *et al.*, 2018; Ashida *et al.*, 2021). Studies have revealed significant positive relationships between SOC and ammonium oxalate (OX), that highlights the important role of poorly crystalline Fe/Al oxides or short range order (SRO) Fe/Al oxides in the formation of MAOC in both surface (Rasmussen *et al.*, 2006) and sub-surface soils (Kaiser and Guggenberger, 2000; Kleber *et al.*, 2005; von Fromm *et al.*, 2025). Likewise, crystalline Fe oxides abundance have been reported to be the major drivers of MAOC abundance in soils and a close relationship between dithionite-citrate-bicarbonate (DCB) extractable Fe/Al and SOC have been reported in soils from different regions (Mu *et al.*, 2016; Zhao *et al.*, 2016; Yu *et al.*, 2019; Zhao *et al.*, 2023). Many other studies have reported a significant relationship between sodium pyrophosphate (PP) extractable Fe/Al and SOC in a wide range of soils, suggesting the relevance of organo-metal complexes in the stabilisation of SOC (Percival *et al.*, 2000; Wagai and Mayer, 2007; Wagai *et al.*, 2013; Lawrence *et al.*, 2015; Hall and Thompson, 2022; Yu *et al.*, 2023). The relationships between forms of metals are done largely on a limited samples and surface soils. Also, there is a general lack of information on the role of different species of Fe, Al, Mn and Si in phosphorus deficient soils that occupy much of the tropic and subtropics and southern hemisphere including Australia.

In this study, we used PP (pH 10), OX (pH 3) and DCB to extract organo-metal complexes, SRO and/or poorly crystalline metal phases and crystalline or free metal oxides, respectively, from a range of soil types with varying Fe concentrations. Also, we used both top and sub-soils

for this study. Soil OC associated with each of the extractable form was also determined. The main aim of this study was to determine the role of different fractions (or species) of metal(loid)s in preserving OC in top and sub-soils of agricultural regions of New South Wales, Australia. We hypothesised that SRO minerals of Fe, Al, Mn and Si contribute more to the preservation of OC in both top- and sub-soils. We further hypothesised that concentration of Fe will be the most prominent amongst the metals in all extractions in both top- and sub-soils.

3.2 Materials and Methods

3.2.1 Soil samples and handling

Topsoil (0 – 20 cm) and subsoil (20 – 40 cm) samples were collected from 37 sites across New South Wales, Australia (Figure 3.1). The location names, coordinates, and Australian Soil Classification (ASC) of the soil samples are presented in Supplementary Table 3.1. Soil samples were air-dried, crushed, passed through a 2 mm sieve and stored at room temperature for laboratory analysis.

3.2.2 Soil physical and chemical properties

Soil pH and electrical conductivity (EC) were measured in 1:5 of soil and water extracts using a combined glass electrode pH meter and EC meter, respectively (Rayment and Lyons, 2011). Particle size analysis (PSA) was determined by the hydrometer method (Gee and Or, 2002). Cation exchange capacity (CEC) was determined by the silver thiourea method (Rayment and Lyons, 2011). Total nitrogen (TN) was analysed using vario MACRO cube Elementar CHN analyser. Total Fe, Al, Mn, and Si were analysed using a PANalytical Minipal 4 X-Ray Florescence (XRF) spectrometer.

3.2.3 Selective extraction procedure and analyses

Soil samples were subjected to three separate chemical extractions to dissolve different Fe phases (Table 3.1). Aluminium, Mn and Si were also measured in these extractions, however, the extractants are most specific to Fe phases. All soil samples (in duplicates) were separately extracted by sodium pyrophosphate (PP, pH 10), ammonium oxalate (OX, pH 3), and dithionite-citrate-bicarbonate (DCB). To validate the quantification of extracted C, a subset of 10 samples (with a wide range in Fe content) were also extracted by sodium pyrophosphate (PP, pH 7.5), dithionite-hydrochloric acid (DH) and Hydrochloric acid-hydroxylamine (HH), as described in more detail in Section 3.2.7. The concentrations of Fe, Al, Si and Mn in supernatants from each extraction were analysed using PerkinElmer Nexion 300x inductively coupled plasma-mass spectrometer (ICP-MS). The residues after each extraction were analysed for total C to determine the C extracted by each reagent.

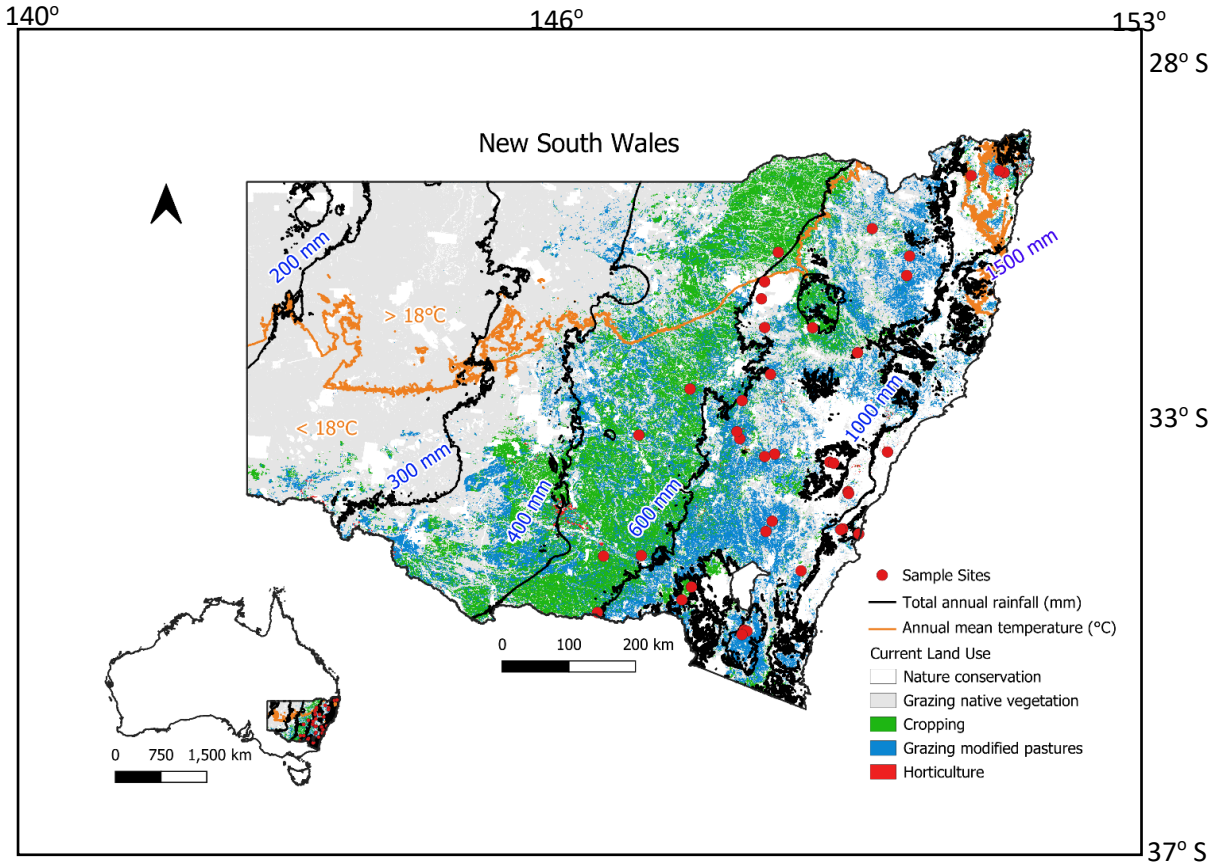

Figure 3.3.1. *Map of New South Wales showing sampling (red dots) locations of soil samples, current land use, total annual rainfall and annual mean temperature.*

Table 3.1. *A summary of chemical extraction procedures and targeted phases.*

Solvent	Concentration	Solvent pH	Target phases	Number of soil samples
Sodium pyrophosphate (PP)	0.1 M	10	Organic matter- complexed metals	74
Sodium pyrophosphate (PP)	0.1 M	7.5	Organic matter- complexed metals	10
Ammonium oxalate (OX)	0.2 M	3	Non-crystalline, amorphous, short-range-ordered (SRO) minerals and poorly crystalline minerals	74
Dithionite-citrate-bicarbonate (DCB)	0.3M, 1 M	8	Total 'free' oxides or pedogenic or crystalline metal oxides	74
Dithionite-Hydrochloric acid (DH)	0.05 M, 0.05 M	2.3	Total 'free' oxides or pedogenic phases or crystalline metal oxides	10
Hydrochloric acid-hydroxylamine (HH)	0.25 M 0.25 M	0.8	Non-crystalline, amorphous, short-range-ordered (SRO) minerals and poorly crystalline minerals	10

3.2.4 Sodium pyrophosphate (PP) at pH 10

Pyrophosphate extraction provides an estimate organic complexed or bound Fe and Al in soils (Loveland and Digby, 1984). We used the procedure described by McKeague (1967) to extract organic C complexed with Fe and Al, for this 500 mg of soil was mixed with 50 ml of 0.1 M PP solution (pH 10) in 55 ml centrifuge tubes. The samples were shaken for 16 hours and centrifuged at 3280 × *g* and the supernatants filtered through a 0.2 µm PES membrane syringe filter (Merck Millipore, Millex-GP, 33 mm diameter) for ICP-MS analysis.

3.2.5 Acid ammonium oxalate (OX)

Extraction with 0.2 M ammonium oxalate (pH 3.0) in the dark dissolves SRO and poorly crystalline minerals (Schwertmann, 1964). For this extraction, 500 mg of soil was mixed with 30 ml of 0.2 M ammonium oxalate (pH 3.0) in 55 ml centrifuge tubes, and the mixture was shaken for 4 hours in the dark (McKeague and Day, 1966). The suspensions were then

centrifuged at 3280 × *g* for 10 minutes. The supernatants were filtered through a 0.2 µm PES membrane syringe filter for ICP-MS analysis.

3.2.6 Dithionite-citrate-bicarbonate (DCB)

Dithionite-citrate-bicarbonate extraction was used to extract pedogenic Fe and Al phases in soils (Mehra and Jackson, 1960). Briefly, 1 g of soil was mixed with 40 ml of 0.3 M sodium (Na)-citrate and 5 ml of 1 M Na-bicarbonate, in 55 ml centrifuge tubes. The tubes were heated in a water bath to 80 ºC for 10 min, then 1 g of sodium dithionite was added and stirred immediately for 1 min and then occasionally 5 min. After the digestion, 10 mL of saturated sodium chloride (NaCl) solution was added to promote flocculation. The samples were centrifuged at 3280 × *g*, and the supernatants were filtered through Whatman 42 filter paper for the analysis. The extraction procedure was repeated twice for some of the soil samples, where brown or red colouration was observed.

3.2.7 Extractable C methodology validation

Two of the extraction procedures involve C containing reagents (i.e., oxalate, citrate, and bicarbonate), hence we compared the residual total C in soils after OX and DCB extractions with comparable procedures, i.e. HH and DH, respectively, which do not employ C compounds in the extraction procedure (Heckman *et al.*, 2018).

3.2.8 Sodium pyrophosphate (PP) at pH 7.5

Selective samples (with a range of total Fe content) were extracted with PP at pH 7.5 in duplicate to determine the peptization of Fe oxides at pH 10 (Parfitt and Childs, 1988; Rennert, 2019). The procedure of McKeague (1967) as described earlier was followed, except the PP solution pH was adjusted to 7.5 with hydrochloric acid (HCl). Selective samples containing a range of PP extractable Fe were used in the extraction.

3.2.9 Hydrochloric acid-hydroxylamine (HH)

Inorganic HH extraction targets SRO and/or amorphous Fe and Al oxides (Chao and Zhou, 1983; Ross *et al.*, 1985). Acidified hydroxylamine is capable of extracting Fe phases (Chao and Zhou, 1983) that closely align with SRO minerals extraction procedure using acid ammonium oxalate (McKeague and Day, 1966). Acidified hydroxylamine is a C-free alternative to OX and the residual soil C analysis after this extraction was used to compare with the OX extractant soil residues. For this extraction, we weighed 500 mg soil into a 55 mL centrifuge tube, mixed with 30 ml of HH solution, the mixture was shaken for 16 hours and then centrifuged at 3280 × *g*. The supernatant was filtered through a 0.2 µm PES membrane syringe filter for ICP-MS analysis.

3.2.10 Dithionite-hydrochloric acid (DH)

Dithionite-hydrochloric acid is a C-free alternative to DCB to extract pedogenic Fe and Al phases just like DCB (Wagai and Mayer, 2007; Wagai *et al.*, 2013). This extraction was performed on selective samples to compare the DH extractable C values to DCB extractable C values. 500 mg of soil was mixed with 30 ml of 57.4 mM sodium dithionite, shaken for 16 hours and centrifuged at 3280 × *g* for 40 mins. The supernatants were filtered through a 0.2 µm PES membrane syringe filter into another 50 ml centrifuge tubes. Soil residues were rinsed with 10 ml of 0.05 M HCl, shaken for 1 hour and then centrifuged again. The supernatants were filtered as before and combined with Na dithionite extracts.

3.2.11 Post-extraction procedure and analysis

The soil residues after extractions were washed twice with ultrapure water to remove entrained solutions, centrifuged, dried overnight, lightly ground manually and weighed for total carbon (C) analysis. Total C concentrations of the soil samples before and after extraction were analysed in duplicates using a vario MACRO cube Elementar CHN analyser. Total C

concentrations represented OC concentrations because most of studied soils had acidic pH values. The presence of carbonate was also tested by adding hydrochloric acid to the soil samples.

3.2.12 Data Analysis

Paired t-test was used to determine differences in the concentrations of extractable metal(loid)s (Fe, Al, Mn and Si) and extractable C between samples from the two depths. Correlations between physical and chemical properties of soils were performed using Spearman's rho correlation. The generalised linear mixed model (GLMM) regression was used to determine relationships between extractable metal concentrations and other soil properties. In GLMM regression, we used extractable metal concentrations and soil properties as the fixed effects and soil types as the random effects. After running the model with all soil properties first, the non-significant variables were removed from the fixed effects and the model was re-run to obtain variables that were significant in the model. For data analysis, we used JMP Pro software (Version 17.0, SAS Institute Incorporation, Cary, NC, USA).

3.3 Results

3.3.1 Soil physical and chemical characteristics

A summary of soil physical and chemical properties is shown in Table 3.2. Soil pH was strongly acidic to near neutral, with values ranging from 4.7 to 7.6. The electrical conductivity (EC) values of soils were small for all samples ranging from 1.33 mS/m to 42.6 mS/m in the topsoils and 1.24 mS/m to 13.7 mS/m in the subsoils. Cation exchange capacity (CEC) of soils was mostly small ranging between 69.8 $mmol_c/kg$ and 99.7 $mmol_c/kg$ in the topsoils and 47.4 $mmol_c/kg$ and 99.7 $mmol_c/kg$ in the subsoils. The clay content in soils increased with depth and ranged from 3 to 54 % in the topsoils and 6 to 59 % in the subsoils. Total Al increased significantly with depth, while total Fe, Mn and Si concentration remained similar.

The concentrations of TC and TN were significantly ($p<0.05$) greater in the topsoils (TC: 25.0±2.3 g/kg and TN: 1.2±0.2 g/kg) than the subsoils (TC: 17.5±1.6 and TN: 0.7±0.1 g/kg) as shown in Figure 3.2. A linear relationship was observed between TC and TN in the topsoils (R^2 = 0.60, $p<0.001$), subsoils (R^2 = 0.78, $p<0.001$), and all samples combined (topsoils and subsoils) (R^2 = 0.75, $p<0.001$) (Supplementary Figure 3.1). The C:N ratio significantly ($p<0.05$) increased with soil depth, from 23.3±1.3 g/g in the topsoils to 28.7±1.8 g/g in the subsoils.

Table 3.2. *Summary of important chemical and physical properties of the studied soils (n = 74)*

Properties	**Topsoil**			**Subsoil**		
	Range	**Mean ± SE**	**Median**	**Range**	**Mean**	**Median**
pH $_{(1:5\ water)}$	4.70 – 7.38	5.92±0.11a	5.85	4.87 – 7.60	6.15±0.13a	6.14
$EC_{1:5}$ (mS/m)	1.33 – 42.6	6.73±1.13a	4.99	1.24 – 13.7	4.18±0.44b	3.43
CEC ($mmol_c/kg$)	69.8 – 99.7	94.0±1.3a	97.9	47.4 – 99.7	92.5±2.1a	98.3
Exchangeable Ca ($mmol_c/kg$)	1.3 – 37.9	18.0±1.9a	20.9	0.6 – 39.8	15.7±1.9a	13.4
Exchangeable Mg ($mmol_c/kg$)	2.3 – 34.7	16.0±1.4a	16.4	1.8 – 49.9	18.3±1.8a	15.4
Exchangeable Na ($mmol_c/kg$)	0.1 – 13.4	1.5±0.4a	1	0.1 – 23	3.8±0.9b	1.3
Exchangeable K ($mmol_c/kg$)	0.4 – 7.6	2.5±0.3a	2.2	0.1 – 6.1	1.5±0.2b	1.1
Sand (%)	36 – 95	61.7±2.9a	64	26 – 90	56.9±2.9a	59
Silt (%)	2 – 30	13.2±1.0a	14	2 – 30	11.9±1.1a	11
Clay (%)	3 – 54	25.1±2.6a	20	6 – 59	31.2±2.7a	30
Total Fe (g/kg)	9.34 – 161.97	50.12±5.91a	35.12	11.26– 136.96	53.29±5.17a	40.83
Total Al (g/kg)	18.08– 125.79	76.54±3.99a	77.72	40.18– 132.91	87.31±3.34b	88.16
Total Mn (g/kg)	0 – 3.1	0.78±0.13a	0.5	0 – 3.6	0.60±0.13a	0.3
Total Si (g/kg)	148.54– 384.73	251.42±9.35a	258.32	153.39– 356.31	237.33±8.26a	235.71

Similar letters in the same row indicate non-significant differences between mean values ($P < 0.05$) while different letters indicate significant differences between mean values ($P < 0.05$) of soil properties.

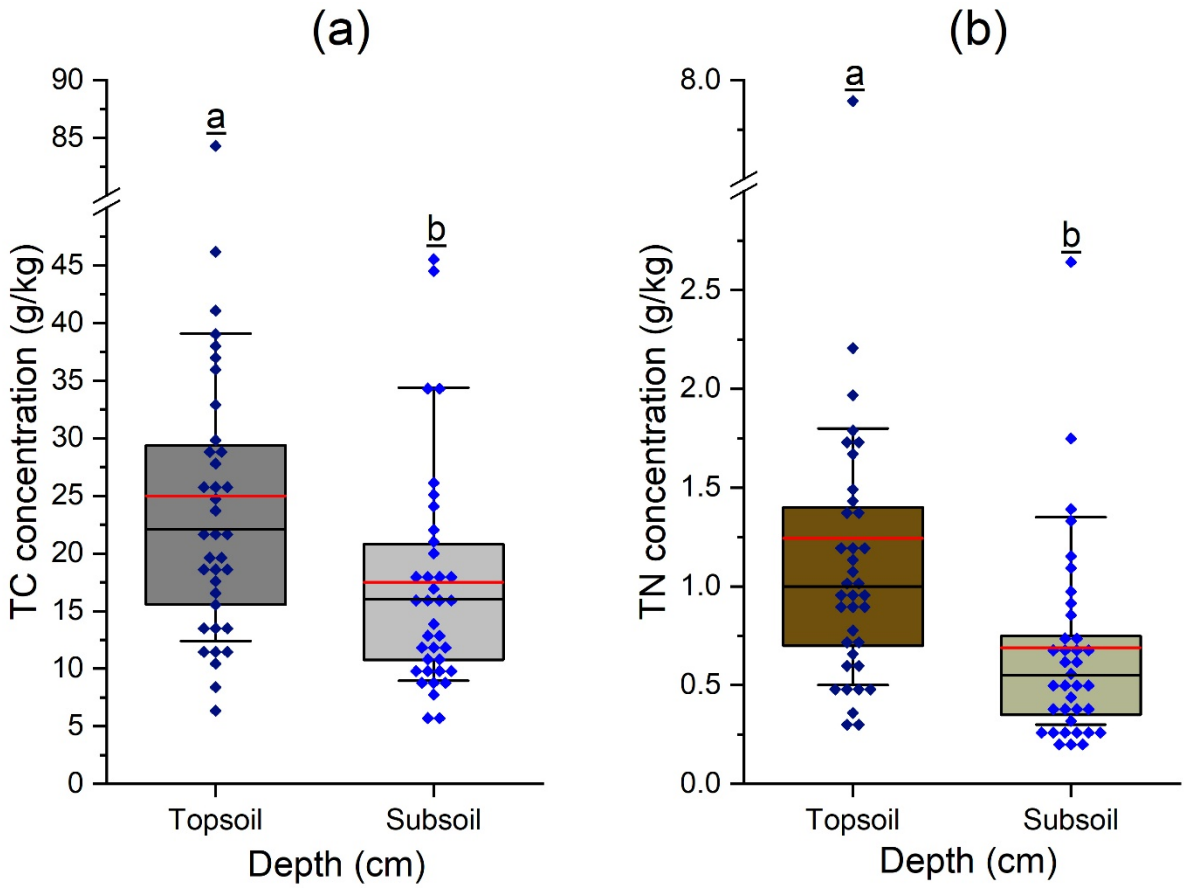

Figure 3.2. *Concentrations of total carbon (TC) and total nitrogen (TN) in topsoils (0-20 cm) and subsoils (20-40 cm). Boxes comprise of the 25th and 75th percentiles, whiskers extend from the 10th to 90th percentiles. Red and black bars indicate the mean and the median values, respectively. Dark blue and navy-blue diamonds show the data for individual samples, the symbols are displaced horizontally to avoid overlaps. Different letters indicate significant differences in the mean values of samples from different depths based on Tukey-Kramer HSD test ($p<0.01$).*

The correlation coefficients between soil physical and chemical properties are shown in Table 3.3. The CEC showed a significant positive correlation with clay ($r = 0.70$, $p<0.01$) and a significant negative correlation with sand ($r = - 0.64$, $p<0.01$). Soil pH showed significant positive correlations with CEC, exchangeable Ca, exchangeable Mg, exchangeable Na, and clay content. Soil EC had significant positive relationships with TC, TN, exchangeable Ca, exchangeable K, and CEC.

Total Fe and Al showed significant positive correlations with clay and CEC. Total Mn had significant positive relationships with pH, EC, TC, TN, exchangeable Ca, exchangeable K, CEC, and total Fe. Total Si showed a significant positive relationship with sand content ($r = 0.71$, $p<0.01$).

Table 3.3. *Spearman's rho correlation coefficients for relationships between soil physical and chemical properties.*

	pH	EC	TC	TN	Ca	Mg	Na	K	CEC	Sand	Silt	Clay	Total Fe	Total Al	Total Mn
EC	0.25*														
TC	-0.06	0.40**													
TN	<0.1	0.58**	0.84**												
Ca	0.58**	0.51**	0.18	0.39**											
Mg	0.38**	0.13	-0.04	-0.01	0.14										
Na	0.24*	-0.03	-0.06	-0.11	-0.08	0.56**									
K	0.05	0.61**	0.36**	0.54**	0.47**	-0.02	-0.13								
CEC	0.57**	0.23*	0.02	0.11	0.51**	0.73**	0.44**	0.04							
Sand	-0.22	0.05	0.01	-0.05	-0.22	-0.55**	-0.27*	0.22	-0.64**						
Silt	<-0.1	0.22	0.24*	0.29*	0.20	0.13	0.14	0.23*	0.22	-0.50**					
Clay	0.27*	-0.08	-0.06	<-0.1	0.25*	0.60**	0.30**	-0.24*	0.70**	-0.94**	0.22				
Total Fe	0.32**	-0.03	0.07	0.12	0.29*	0.56**	0.18	-0.28*	0.69**	-0.76**	0.16	0.81**			
Total Al	0.14	-0.31**	-0.06	-0.14	-0.04	0.47**	0.19	-0.40**	0.42**	-0.73**	0.03	0.81**	0.75**		
Total Mn	0.49**	0.33**	0.27*	0.53**	0.66**	0..08	-0.16	0.34**	0.30**	-0.12	0.23	0.08	0.25*	-0.13	
Total Si	-0.25*	0.07	-0.14	-0.11	-0.22	-0.48**	-0.14	0.30**	-0.60**	0.71**	-0.07	-0.78**	-0.89**	-0.84**	-0.14

**Correlation is significant at P < 0.05.*
***Correlation is significant at P < 0.01.*

3.3.2 Extractable Fe, Al, Mn and Si concentrations

The concentration of Fe, Al, Mn and Si extracted by the three main extractants (DCB, OX and PP) varied across soil depths (Figure 3.3). The concentration of Fe extracted by the three extractants was in the sequence – $Fe_{DCB} > Fe_{OX} > Fe_{PP}$ (Figure 3.3a). The concentration of Fe_{PP} in soil samples ranged from 0.01 g/kg to 5.80 g/kg, with a significantly ($p<0.001$) greater mean concentration in the topsoils (1.10±0.11 g/kg) than the subsoils (0.85±0.12 g/kg). The Fe_{OX} concentration varied between 0.68 g/kg and 12.81 g/kg, and the topsoils (4.15±0.33 g/kg) and subsoils (3.99±0.33 g/kg) having a similar mean concentration. Fe_{DCB} concentration in soil samples ranged from 2.92 g/kg to 79.87 g/kg, and similar to the Fe_{OX}, the mean Fe_{DCB} concentration was similar in the topsoils (23.46±1.87 g/kg) and the subsoils (25.76±1.94 g/kg) (Figure 3.3a). On an average, PP, OX and DCB extracted 3 %, 9 % and 49 % of the total Fe respectively, across both soil depths.

The concentration of Al dissolved by the three extractants was in the order: $Al_{DCB} > Al_{OX} > Al_{PP}$ (Figure 3.3b). The Al_{PP} concentration ranged between 0.27 g/kg and 6.47 g/kg, with similar average concentrations in the topsoils (1.41±0.11 g/kg) and the subsoils (1.39±0.13 g/kg). Al_{OX} concentration varied from 0.34 g/kg to 8.0 g/kg, with a significantly ($p=0.003$) greater concentration in the subsoils (3.31±0.21 g/kg) than the topsoils (3.00±0.20 g/kg). The Al_{DCB} concentration in soils ranged from 0.28 g/kg to 10.26 g/kg, with a mean of 2.94±0.2 g/kg in the topsoils and 3.50±0.25 g/kg in the subsoils. The subsoils had a significantly ($p=0.008$) greater mean concentration of Al_{DCB} than the topsoils. PP constituted a mean of 2 % of the total Al, OX and DCB constituted a mean proportion of 3.9% and 4 %, respectively, of the total Al across both depths.

Manganese was dissolved by the three extractants in the order – $Mn_{OX} > Mn_{DCB} > Mn_{PP}$ (Figure 3.3c). The concentration of Mn in all three extractions was generally very low, with values < 1 g/kg in all samples. The Mn_{PP} concentration ranged from <0.01 g/kg to 1.07 g/kg. The mean

concentration of Mn_{PP} in the topsoils (0.25±0.03 g/kg) was significantly ($p<0.001$) greater than the subsoils (0.11±0.01 g/kg). The concentrations of Mn_{OX} in soil samples varied from 0.001 to 2.93 g/kg and it was significantly ($p<0.001$) greater in the topsoils (mean = 0.60±0.08 g/kg) than the mean concentration in the subsoils (0.45±0.08 g/kg). DCB extracted Mn concentration ranged from 0.01 g/kg to 3.62 g/kg, and like Mn_{PP} and Mn_{OX}, the topsoils (0.47±0.07 g/kg) had a significantly ($p=0.04$) greater mean concentration of Mn_{DCB} than the subsoils (0.36±0.07 g/kg). PP, OX and DCB extracted on an average 43, 78 and 65 % of the total Mn, respectively, across both soil depths.

The concentration of Si dissolved by the three extractants occurred in the sequence – $Si_{DCB} > Si_{OX} > Si_{PP}$ (Figure 3.3d). The concentration of Si_{PP} ranged from 0.19 g/kg to 2.45 g/kg, with similar concentrations in the topsoils (0.69±0.03 g/kg) and subsoils (0.66±0.05 g/kg). Si_{OX} concentrations varied between 0.05 g/kg and 3.03 g/kg, with significantly ($p=0.006$) greater concentration in the subsoils (0.81±0.07 g/kg) than the topsoils (0.70±0.06 g/kg). The concentration of Si_{DCB} ranged from 0.28 g/kg to 4.35 g/kg, and the subsoils (1.76±0.11 g/kg) had a significantly ($p=0.07$) greater mean concentration of Si_{DCB} than the topsoils (1.52±0.08 g/kg). PP extracted 0.3 % (mean) of the total Si, OX extracted 0.4 % of the total Si, and DCB extracted 0.7 % of the total Si across both depths.

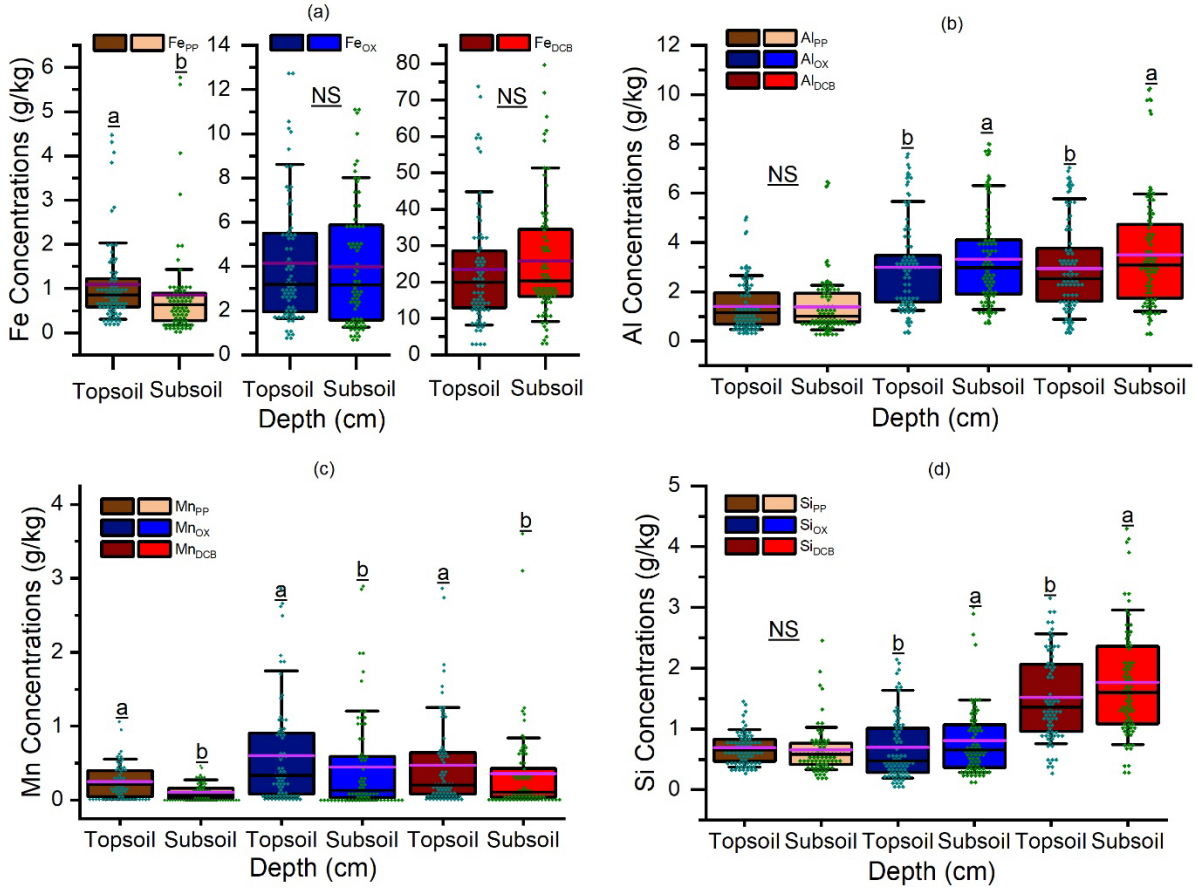

Figure 3.3. *Concentrations of iron (Fe), aluminium (Al), manganese (Mn) and silicon (Si) in topsoils and subsoils extracted by sodium pyrophosphate (PP), ammonium oxalate (OX), and dithionite-citrate-bicarbonate (DCB) procedures. Boxes comprise of the 25th and 75th percentiles, whiskers extend from the 10th to 90th percentiles. Purple and black bars signify the mean and the median values, respectively. Dark cyan and green diamonds indicate data for individual samples, the symbols are displaced horizontally to avoid overlaps. Different letters indicate significant differences in the mean values between samples from different soil depths based on paired T-test ($p<0.05$). NS means non-significant difference.*

3.3.3 Relationship between extractable metal(loid)s

The Pearson correlation coefficients between extractable metals are shown in Table 3.4. Fe_{OX} showed a significant positive correlation with all other extractable forms of Fe, Al, Si, and Mn. Fe_{DCB} was positively and significantly correlated with Al_{OX}, Al_{DCB}, Mn_{OX}, Mn_{DCB}, Mn_{PP}, Si_{OX}, Si_{DCB}, and negatively and significantly correlated with Si_{PP}. Fe_{PP} showed significant positive correlations with Al_{OX} and Al_{PP}.

Al_{OX} had significant positive relationships with Al_{DCB}, Al_{PP}, and Si_{OX}. Al_{DCB} showed significant positive relationships with Al_{PP}, Si_{OX}, Si_{DCB} and a significant negative relationship with Si_{PP}. Al_{PP} was negatively and significantly correlated with Mn_{OX}, Mn_{DCB}, and Si_{DCB}.

Mn_{OX} had a significant positive correlation with Mn_{DCB}, Mn_{PP}, Si_{OX}, and Si_{DCB} while Mn_{DCB} had a significant positive correlation with Mn_{PP}.

Si_{OX} and Si_{PP} showed a significant positive relationship with Si_{DCB}.

Table 3.4. *Pearson correlation coefficients for relationships between different extractable metal(loid)s in soils*

	Fe_{OX}	Fe_{DCB}	Fe_{PP}	Al_{OX}	Al_{DCB}	Al_{PP}	Mn_{OX}	Mn_{DCB}	Mn_{PP}	Si_{OX}	Si_{DCB}
Fe_{DCB}	0.61**										
Fe_{PP}	0.41**	0.04									
Al_{OX}	0.64**	0.50**	0.24*								
Al_{DCB}	0.48**	0.83**	0.16	0.69**							
Al_{PP}	0.26*	0.06	0.64**	0.65**	0.40**						
Mn_{OX}	0.46**	0.39**	0.01	-0.07	0.05	-0.30**					
Mn_{DCB}	0.42**	0.34**	0.06	-0.10	0.05	-0.27*	0.93**				
Mn_{PP}	0.36**	0.29*	0.22	-0.17	-0.05	-0.23	0.77*	0.63**			
Si_{OX}	0.71**	0.44**	-0.10	0.51**	0.30**	-0.11	0.29*	0.19	0.09		
Si_{DCB}	0.35**	0.45**	-0.21	0.20	0.26*	-0.23*	0.25*	0.21	0.05	0.55**	
Si_{PP}	<0.01	-0.24*	0.12	-0.17	-0.37**	-0.03	0.10	0.02	0.16	0.13	0.32**

** Correlation is significant at the 0.05 probability level (2-tailed).*
*** Correlation is significant at the 0.01 probability level (2-tailed).*

3.3.4 Extractable C concentrations

Mean concentration of C dissolved by the three extractants was in the sequence – $C_{PP} > C_{DCB} > C_{OX}$ (Figure 3.4). The PP extractable C (C_{PP}) ranged from 2.8 to 31.0 g/kg with a mean of 13.3±1.17 g/kg in the topsoils and 11.9±1.14 g/kg in the subsoils. The mean C_{PP} concentration was significantly greater (p=0.004) in the topsoils than the subsoils. Sodium pyrophosphate extracted on an average 62 % of the total soil C across both soil depths.

The concentration of DCB extractable C (C_{DCB}) ranged from 0.5 g/kg to 28.4 g/kg in all samples, with a significantly (p=0.025) greater mean concentration in the topsoils (9.8±1.25

g/kg) than in the subsoils (8.5±1.11 g/kg) (Figure 3.4). The extractable C_{DCB} constituted 41 % (mean) of the total soil C across both depths.

The OX extractable C (C_{OX}) concentration varied between 0.5 g/kg and 26.5 g/kg across the two depths. The concentration was similar in the topsoils (6.4±1.08 g/kg) and subsoils (6.3±1.11 g/kg) (Figure 3.4). The C_{OX} represented on an average 28 % of the total C in all samples.

The concentration of the DCB extractable C minus OX extractable C ($C_{DCB} - C_{OX}$), i.e., C associated with crystalline forms of Fe oxides was similar in the topsoils (3.3±0.55 g/kg) and the subsoils (2.29±0.28 g/kg) (Figure 3.4). The $C_{DCB} - C_{OX}$ constituted on the average 13% of the total soil C across both depths.

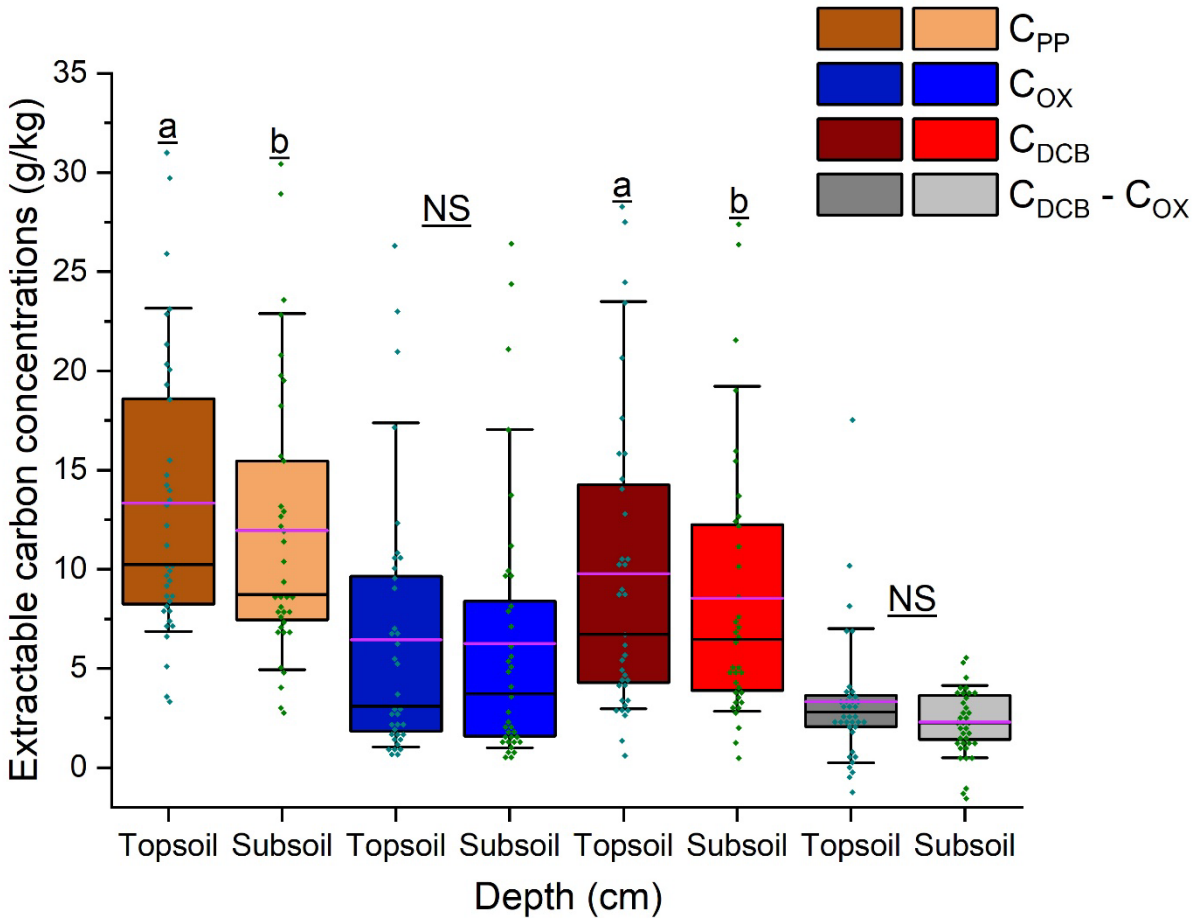

Figure 3.4. *Concentrations of carbon (C) in topsoils and subsoils extracted by sodium pyrophosphate (PP), ammonium oxalate (OX), dithionite-citrate-bicarbonate (DCB) reagents, and concentration of carbon extracted by dithionite-citrate-bicarbonate (DCB) minus concentration of carbon extracted by ammonium oxalate (OX). Boxes comprise of the 25th and 75th percentiles, whiskers extend from the 10th to 90th percentiles. Purple and black bars signify the mean*

and the median values, respectively. Dark cyan and green diamonds indicate data for individual samples, the symbols are displaced horizontally to avoid overlaps. Different letters indicate significant differences in the mean values of samples from different soil depths based on paired T-test ($p<0.05$). NS means non-significant difference.

3.3.5 Relationship between extractable metal phases, soil properties and extractable C

The relationships between extractable metal phases, soil properties and extractable C using the generalized linear mixed model (GLMM) regression are shown in Tables 3.5 and 3.6. In Table 3.5, the TC was included as a fixed effect term into the model and we observed that with the inclusion of TC into the model, the different forms of extractable metals showed no significant relationship with the different forms of extractable C in both top- and sub-soils but Fe_{OX} (topsoil), Al_{OX} and Al_{DCB} (subsoil) had significant negative relationship with extractable C. However, the TC showed significant ($p<0.001$) relationships with the different forms of extractable C in both topsoils and subsoils (Table 3.5). In addition, pH had a significant ($p=0.005$, $p=0.004$ and $p=0.04$, respectively) relationship with the different forms of extractable C in the topsoils. Similarly, clay content showed a significant ($p=0.007$ and $p=0.03$) relationship with the different forms of extractable C in the subsoils. However, silt showed a significant ($p<0.001$ and $p=0.01$) relationship with C_{OX} and C_{DCB}, respectively, in topsoils.

In Table 3.6, TC was excluded from the generalized linear mixed model (GLMM), where C extracted by three reagents showed positive relationships with pH, silt or clay and extractable Fe and Al (Table 3.6). For example, Fe_{PP}, pH, and silt showed statistically significant ($p<0.001$, $p<0.001$, and $p=0.0004$, respectively) relationships with C_{PP} in the topsoils. Similarly, Fe_{OX} and pH had significant positive ($p<0.001$ and $p=0.026$, respectively) relationships with C_{OX} in the topsoils, and Fe_{OX}, pH, and silt ($p<0.001$) had significant positive relationships with C_{OX} in the subsoils. Also, Al_{DCB} ($p<0.001$) and pH ($p=0.002$) showed significant positive relationships with C_{DCB} in the topsoils; and Fe_{DCB} ($p<0.001$) and silt ($p=0.0006$) showed significant positive relationships with C_{DCB} in the subsoils. Extractable Mn and Si were excluded from the GLMM because they showed no statistically significant relationship with the extractable C.

Table 3.5. *Fixed effects parameter estimates in the topsoils and subsoils obtained from the generalized linear mixed model. The extractable metals and soil properties (including TC) were used as the fixed effect terms, soil types as the random effect and sodium pyrophosphate extractable C, ammonium oxalate extractable C and dithionite-citrate-bicarbonate extractable C as the dependent variables. The standard errors are given in parentheses.*

	Depth	**Fixed effects term**	**Regression coefficient**	**95 % Lower**	**95% Upper**	**F Ratio**	**Prob>F**
C_{PP}	Topsoil	Fe_{PP}	0.06 (0.06)	-0.06	0.19	1.06	0.31
		pH	0.26 (0.08)	0.08	0.43	9.51	0.005
		TC	0.02 (0.003)	0.01	0.03	31.58	<0.001
		Intercept	0.002 (0.01)	-0.02	0.02		
	Subsoil	Fe_{PP}	0.05 (0.09)	-0.24	0.14	0.31	0.58
		Al_{PP}	0.08 (0.07)	-0.22	0.17	1.22	0.28
		Clay	0.01 (0.004)	8.08	0.003	0.02	0.007
		TC	0.05 (0.01)	0.04	0.07	48.57	<0.001
		Intercept	-0.001 (0.01)	-0.02	0.02		
C_{OX}	Topsoil	Fe_{OX}	-0.09 (0.04)	-0.16	-0.01	5.99	0.02
		pH	0.56 (0.130	19.84	0.26	0.87	0.004
		Silt	0.06 (0.01)	0.04	0.09	25.80	<0.001
		TC	0.04 (0.01)	0.02	0.05	38.18	<0.001
		Intercept	0.004 (0.03)	-0.05	0.06		
	Subsoil	Fe_{OX}	-0.11 (0.04)	-0.19	-0.02	7.21	0.011
		Al_{OX}	-0.15 (0.06)	-0.26	-0.03	6.32	0.017
		Clay	0.02 (0.01)	0.01	0.03	8.40	0.007
		TC	0.09 (0.01)	0.07	0.11	86.31	<0.001
		Intercept	0.05 (0.06)	-0.07	0.16		
C_{DCB}	Topsoil	Fe_{DCB}	0.02 (0.01)	-0.01	0.02	0.52	0.47
		Al_{DCB}	-0.10 (0.09)	-0.29	0.09	1.13	0.30
		pH	0.26 (0.12)	0.01	0.52	4.78	0.04
		EC	-0.06 (0.01)	-0.08	-0.04	29.11	<0.001
		Silt	0.03 (0.01)	0.01	0.05	7.79	0.01
		TC	0.06 (0.01)	0.05	0.07	92.56	<0.001
		Intercept	0.01 (0.02)	-0.03	0.05		
	Subsoil	Fe_{DCB}	-0.001 (0.01)	-0.01	0.01	0.05	0.83
		Al_{DCB}	-0.10 (0.05)	-0.21	0.01	3.50	0.07
		Clay	0.01 (0.01)	0.001	0.02	5.26	0.03
		TC	0.06 (0.01)	0.05	0.07	77.69	<0.001
		Intercept	0.05 (0.05)	-0.05	0.15		

Table 3.6. *Fixed effects parameter estimates in the topsoils and subsoils obtained from the generalized linear mixed model. The extractable metals and soil properties (excluding the TC) were used as the fixed effect terms, soil types as the random effect and sodium pyrophosphate extractable C, ammonium oxalate extractable C and dithionite-citrate-bicarbonate extractable C as the dependent variables. The standard errors are given in parentheses*

	Depth	**Fixed effects term**	**Regression coefficient**	**95 % Lower**	**95% Upper**	**F Ratio**	**Prob>F**
C_{PP}	Topsoil	Fe_{PP}	0.23 (0.03)	0.17	0.30	53.96	<0.001
		pH	0.27 (0.06)	0.16	0.38	22.56	<0.001
		Silt	0.02 (0.01)	0.01	0.03	14.12	0.0004
		Intercept	0.37 (0.37)	-0.37	1.11		
	Subsoil	Fe_{PP}	0.30 (0.04)	0.21	0.38	44.45	<0.001
		Al_{PP}	0.14 (0.05)	0.23	0.44	8.67	0.004
		Clay	0.01 (0.003)	0.002	0.01	7.34	0.009
		Intercept	2.17 (0.11)	1.92	2.41		
C_{OX}	Topsoil	Fe_{OX}	0.08 (0.02)	0.04	0.12	18.03	<0.001
		pH	0.18 (0.08)	0.02	0.34	5.16	0.026
		Intercept	0.30 (0.51)	-0.72	1.33		
	Subsoil	Fe_{OX}	0.14 (0.02)	0.09	0.18	33.09	<0.001
		Si_{OX}	-0.52 (0.19)	-0.77	-0.27	17.76	<0.001
		pH	0.35 (0.08)	0.19	0.52	18.44	<0.001
		Silt	0.04 (0.01)	0.02	0.06	29.84	<0.001
		Intercept	-1.15 (0.53)	-2.22	-0.09		
C_{DCB}	Topsoil	Al_{DCB}	0.22 (0.04)	0.15	0.29	36.47	<0.001
		pH	0.24 (0.07)	0.09	0.39	10.22	0.002
		EC	0.03 (0.01)	0.01	0.04	20.98	<0.001
		Clay	-0.01 (0.003)	-0.02	-0.002	5.92	0.018
		Intercept	-0.16 (0.58)	-1.33	1.02		
	Subsoil	Fe_{DCB}	0.02 (0.003)	0.01	0.02	23.48	<0.001
		Silt	0.02 (0.01)	0.01	0.04	13.08	0.0006
		Intercept	1.33 (0.24)	0.78	1.87		

3.3.6 Extractable C: metal molar ratio

The molar ratio of C to metals (M) (C: Fe+Al) extracted by each reagent in the samples from two depths are presented in Figure 3.5. In the PP extracts, the C:M molar ratio varied between 1.2 and 40.9 for all soil samples. The C:M molar ratio was similar in the topsoils (9.4±1.3) and subsoils (9.6±1.4) (Figure 3.5a). The OX extracts had C:M molar ratio ranging from 0.1 to 10.7, with a similar mean value of 1.6±0.3 and 1.4±0.3 for the topsoils and the subsoils (Figure 3.5b), respectively. The C:M molar ratios in the DCB extracted fractions ranged from 0.03 to 8.5 in all samples, with similar ratios in the topsoils (1.0±0.2) and subsoils (0.7±0.1) (Figure 3.5c).

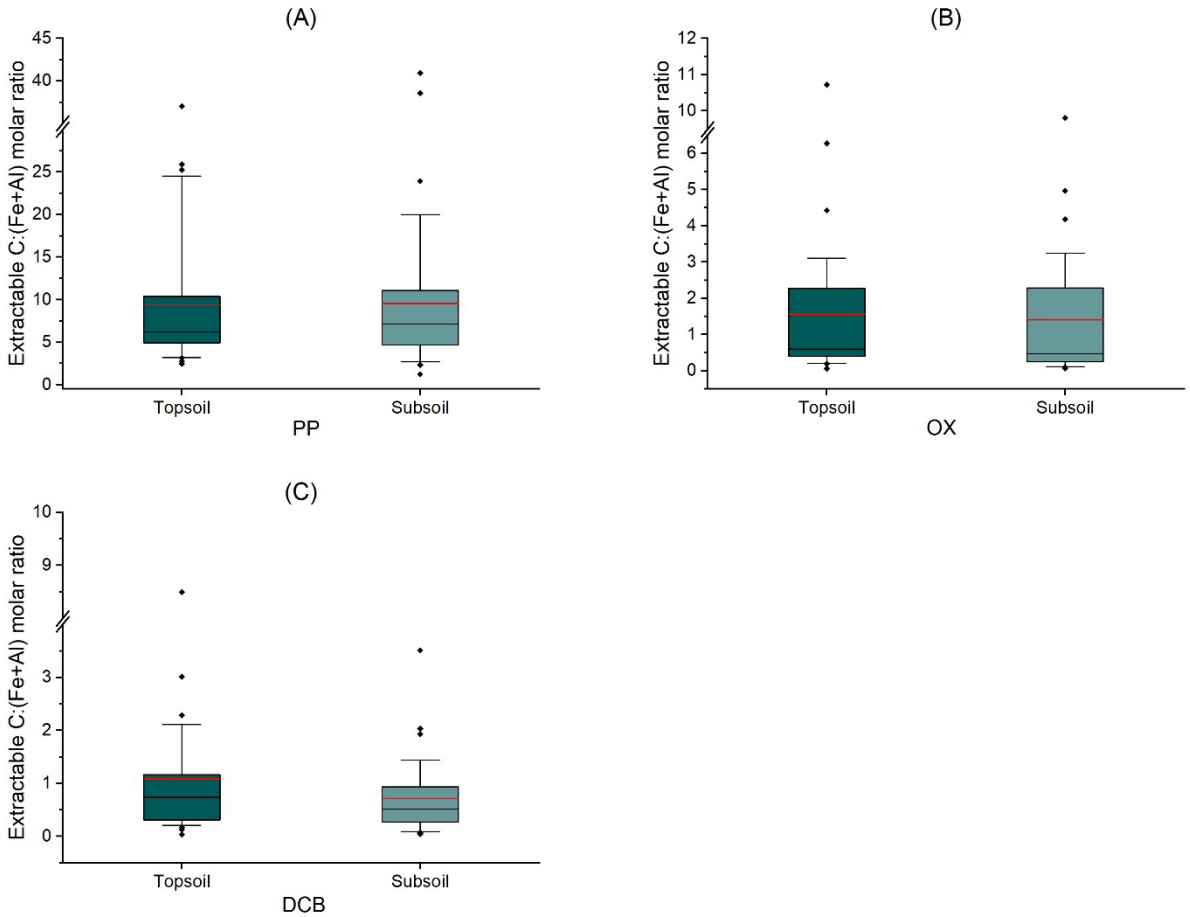

Figure 3.5. *Boxplots of C:(Fe+Al) molar ratios in the extracts of sodium pyrophosphate (PP), ammonium oxalate (OX), and dithionite-citrate-bicarbonate (DCB) of topsoils and subsoils. Boxes comprise of the 25th and 75th percentiles, whiskers extend from the 10th to 90th percentiles, red bars signify mean, black bars signify median, and black dots show the outliers.*

3.4 Discussion

3. 4.1 Soil physicochemical properties in relation to OC

The association of OC with Fe and Al oxides can be affected by soil pH, which influences the mineral phases of Fe/Al oxides, surface charge characteristics of metal oxides, and interactions between OC and metal oxides (Zhao *et al.*, 2016; Ye *et al.*, 2022). Most of our samples had acidic pH and soil pH showed a positive significant relationship with extractable C (Tables 3.5 and 3.6). Both Fe and Al oxides carry a net positive charge in the acidic to near neutral pH range, as the point of zero charge of these minerals range from 7.8 to 10 (Sparks *et al.*, 2024). Also, the negative charge on soil organic matter would be expected to increase with increasing pH due to deprotonation of acidic functional groups, such as carboxyls, quinones and enols (Sparks *et al.*, 2024). Other studies have observed a significant correlation between soil pH and Fe/Al associated OC, which implies that soil pH regulates the propensity of Fe and Al oxides to associate with OC (Wang *et al.*, 2017; Zhao *et al.*, 2019; Ye *et al.*, 2022).

The significant positive relationships between extractable C, clay and silt (Table 3.5 and 3.6) shows the important role of clay and silt fractions in preserving OC in soils. These results are consistent with several other studies (Six *et al.*, 2002; Yu *et al.*, 2019). Clay mineralogy as well as soil clay content is important in stabilising OC, with its ability to protect OC via physical and chemical interactions and other indirect factors. Oades (1988) speculated that finer textured soils have more cation bridges (Ca^{2+} in neutral, Fe^{3+} and Al^{3+} in acidic soils) to bind organic molecules to soil clay particles. While Christensen (1992) supported the idea of increased binding of organic molecules via cation bridges in clayey soils, he proposed that the principal effect of higher clay (or clay + silt) contents occurred via stabilisation of microbially processed of organic residues, that are readily lost in sandy soils. In contrast, Feller *et al.* (2020) concluded that greater biomass inputs or aggregation in finer textured soils caused correlations between SOC and clay concentrations in the tropical soils. It has been reported that there is a greater

amount of mineral-associated OM in soils with increased clay and silt contents, and hence increased OM storage through binding to mineral surfaces in soils (Stewart *et al.*, 2007; Laganiere *et al.*, 2010; Vos *et al.*, 2018). Others have suggested increased occlusion of particulate OM in soil aggregates rich in clay-size minerals that restricts access for microbial degradation (McCarthy *et al.*, 2008; Steffens *et al.*, 2017; Schweizer *et al.*, 2021). Jindaluang *et al.* (2013) reported that organic compounds with aromatic and amide functional groups are selectively preserved in fine textured soils, while recalcitrant aliphatic-C exists in the coarse textured soils. Hassink (1997) proposed that C associated with organo-mineral complexes are protected chemically and the level of protection increased with increased silt fraction of the soil. It is possible that all or many of these mechanisms occur simultaneously, but the adsorption of organic compounds to clay surfaces perhaps is a major factor in the preservation of SOM.

3.4.2 Extractable metal(loid)s

The dissolution of metal(loid)s obtained by PP, OX and DCB extractions provides an approximation of their specific phases in soils and these extractions are not completely selective, with often some overlaps in the extracted fractions of metal(loid)s (Parfitt, 2009; Rennert, 2019). Nevertheless, chemical extraction procedures offer the best option to evaluate the association of OC with different chemical and mineralogical forms of metal(loid)s in soils. The extracted concentration of Fe, Al, and Si followed the same sequence (i.e., PP < OX < DCB), while Mn was extracted in the sequence: PP < DCB < OX. These results showed that Fe was extracted at higher concentrations than Al, Mn and Si, and hence was likely a more important binding phase. This support our hypothesis that concentration of extractable Fe will be the most prominent element in all extractions in both top- and sub-soils. Furthermore, the global mean values (3.09 g/kg for Fe_{OX} and 19.89 g/kg for Fe_d, see Table 2.1) for topsoil was similar with the mean values (4.15 g/kg for Fe_{OX} and 23.46 g/kg for Fe_d) for topsoil used in

this study. This shows that crystalline Fe oxide content in Australian soils is relatively more important for binding OC. This did not fully support our hypothesis that SRO phases of Fe, Al, Mn and Si contribute most to the preservation of OC in these soils.

The DCB procedure is known to extract pedogenic or free Fe oxides (and Al substituted in the structure of goethite and hematite) and SRO Fe/Al oxides (McKeague and Day, 1966; Shang and Zelazny, 2008). The large proportion of the total Fe extracted by the DCB procedure showed the high concentration of secondary Fe oxides in the soils. The DCB procedure also extract some organic complexed Fe from soils (Bascomb, 1968) while some Fe oxides (such as magnetite and maghemite) and Fe sulfides are only partially or not extracted in the DCB extraction procedure (Pansu and Gautheyrou, 2006; Rennert and Lenhardt, 2024). In the oxalate extraction procedure, Fe present in non-crystalline, poorly ordered and short-range ordered (such as ferrihydrite) and a fraction of Al/Fe in organic complexes is dissolved (Schwertmann, 1964; McKeague and Day, 1966; Bascomb, 1968; Loeppert and Inskeep, 1996; Mikutta *et al.*, 2006). The OX extracted Fe had often been used to estimate ferrihydrite, a short range ordered Fe oxide concentrations in soils (Carlson and Schwertmann, 1981; Schwertmann *et al.*, 1982). The decreasing ratio of Fe_{OX}:Fe_{DCB}, referred at as active Fe ratio, indicates the degree of crystallinity of Fe oxides in soils (McKeague and Day, 1966). In topsoils and subsoils, the mean value of Fe_{OX}:Fe_{DCB} ratio was 0.18 and 0.16 (< 0.2), respectively, which suggest that most of the Fe was present in crystalline Fe oxides (i.e., goethite and hematite) in soils and the content of poorly crystalline Fe phases was small irrespective of soil depth (Mikutta *et al.*, 2006). The significant correlation between Fe_{DCB} and Fe_{OX} (Table 3.4), may be due to some overlap in the phases extracted by the two procedures. The DCB method is known to extract both crystalline and SRO (and poorly crystalline) Fe oxides (McKeague and Day, 1966; Shang and Zelazny, 2008). Similarly in addition to the SRO Fe oxides, oxalate dissolves crystalline Fe oxides such as magnetite, maghemite, lepidocrocite, and poorly crystalline and

nano-crystalline goethite and hematite (Childs and Wilson, 1983; Walker, 1983; Mansfeldt *et al.*, 2012). The close relationship between Fe_{DCB} and Fe_{OX} may also suggest that both Fe forms were function of similar pedogenic processes (Rezapour *et al.*, 2015).

PP (at pH 10) has been considered as a good extractant for organic Fe and Al complexes and 'active' amorphous inorganic forms of Fe from soils (Bascomb, 1968; Loveland and Digby, 1984; Pansu and Gautheyrou, 2006). The Fe_{PP} concentration in soils was generally low and decreased with soil depth (Figure 3.3a), a trend similar to the OC concentration in soils (Figure 3.2). These results are consistent with the published data for non-podzolic soils (Bascomb, 1968; Daly, 1982; Parfitt and Childs, 1988). Large variations in the Fe_{PP} concentration with different centrifuge speeds and/or use of flocculating agents have been reported in several past studies (Jeanroy and Guillet, 1981; McKeague and Schuppli, 1982; Schuppli *et al.*, 1983; Loveland and Digby, 1984; Skjemstad *et al.*, 1990). The variability in the Fe_{PP} concentration had been attributed to peptization of micro-crystalline goethite (including Al-substituted goethite) and ferrihydrite on which organic matter had been adsorbed (Borggaard, 1988; Parfitt and Childs, 1988; Rennert, 2019). There was no clear evidence for the presence of any solid phase in the supernatant in the procedure with medium-speed centrifugation (3280 × *g*) followed by micro-filtration (0.2 μm). The Fe_{PP} concentration data were consistent with the results obtained in other studies that used high-speed centrifugation and/or ultrafiltration (Schuppli *et al.*, 1983; Loveland and Digby, 1984). The significant correlation between Fe_{PP} and Fe_{OX} (Table 4) suggests some overlapping extractions of amorphous and SRO phases and Fe-organic complexes by the two reagents (Bascomb, 1968; Higashi *et al.*, 1981; Jeanroy and Guillet, 1981).

The differences between the mean Al_{PP}, Al_{OX} and Al_{DCB} values are much smaller compared with the mean Fe concentrations extracted by the three extractants (Figure 3.3a and b) and similar results have been obtained in previous studies (Skjemstad *et al.*, 1990; Singh and

Gilkes, 1991; Wiriyakitnateekul *et al.*, 2005). The Al_{DCB} and Al_{OX} concentrations are similar, with the mean value of Al_{OX}:Al_{DCB} ratio in the topsoils and subsoils being 1.02 and 0.95, respectively. These results are consistent with the published data (Hall and Thompson, 2022). Crystalline Al oxides are generally not dissolved during the DCB extraction and Al in DCB extracts results from various sources, such as Al-organic complexes, Al adsorbed on Fe oxides, and Al-substituted in the structure of Fe oxides (Rennert, 2019). A significant positive correlation was found between Al_{DCB} and Al_{OX} fractions (Table 3.4), which reflects that the two reagents might have extracted some similar Al-phases, such as, organo-Al complexes (Evans and Smillie, 1976; Parfitt and Childs, 1988; Dahlgren, 1994). The Al_{DCB} concentration showed a very strong correlation with Fe_{DCB} (Table 3.4), which was possibly due to a concurrent release of Al and Fe from the dissolution of crystalline Fe oxides (i.e., goethite and hematite) during the DCB extraction. Such observations have been made in other studies and Al substitution in goethite (up to 35 mol%) and hematite (up to 23 mol%) is well known in acidic and highly weathered soils (Bigham *et al.*, 1978; Fitzpatrick and Schwertmann, 1982; Childs and Wilson, 1983; Parfitt and Childs, 1988; Singh and Gilkes, 1992). The significant relationship observed between Al_{PP} and Al_{OX} (Table 3.4), implies that oxalate may have dissolved Al from organic complexes (McKeague and Day, 1966; Parfitt and Henmi, 1982; Farmer *et al.*, 1983).

Mn oxides in soils often occur in small concentration and poorly crystalline forms (Scheinost and Singh, 2023); and our results were consistent with this assertion, with Mn mostly being present in poorly crystalline forms that were slightly more efficiently extracted by the oxalate procedure than the DCB procedure. Jarvis (1984) also observed greatest Mn extraction with oxalate from soils in a study, where several extractants including DCB and PP were used. It was speculated that during oxalate extraction Mn was released from the reduction of relatively unweathered, highly crystalline oxides, or from mixed forms of Mn-Fe oxides. Manganese has been found to be strongly associated (adsorbed or substituted in structures) with natural Fe

oxides (Singh and Gilkes, 1992). Structural substitution of Mn in synthetic goethite and hematite has been confirmed by extended X-ray absorption fine structure spectroscopy (Singh and Gilkes, 1992; Manceau *et al.*, 2000; Singh *et al.*, 2000; Singh *et al.*, 2002). The order of Mn concentration extracted by the three extractants in our study is similar to the order obtained for several soils from England (Jarvis, 1984). However, the trend with greater Mn concentrations in the topsoils than the subsoils in our study is opposite to the earlier study, which might be due to the occurrence of poor drainage and periodic waterlogging in English soils. A significant relationship was observed between Mn_{PP} and Mn_{OX} (Table 3.4) that is similar to an earlier study; however, the relationship of Mn_{OX} was stronger with Mn_{DCB} than Mn_{PP} (Jarvis, 1984).

The Si concentrations were small in all three extracts (Figure 3.3d). These results indicate that allophane was absent and there was little or no dissolution of aluminosilicates in the soils (Parfitt and Childs, 1988). The sequence of Si extracted is consistent with the limited published data for the three extractions (Paterson *et al.*, 1993). The highest Si concentration was found in the DCB extracts, which might have released from different sources including adsorbed Si on the surfaces of SRO and crystalline Fe oxides, Si occluded in Fe oxides, and some Si dissolved from alumino-silicate clay minerals and quartz (Weaver *et al.*, 1968; Gamble and Daniels, 1972; Parfitt and Childs, 1988). Hall and Thompson (2022) reported greater Si in DCB extract than OX extract in soils from all soil orders except Andisols, where the trend was opposite. Fe_{OX} showed a significant correlation with Si_{OX} (Table 3.4), which indicate that Si_{OX} was primarily adsorbed onto the surfaces of SRO Fe phases and small amounts may also have been extracted from SRO Fe silicates (Parfitt and Henmi, 1982; Colombo and Torrent, 1991). Non-crystalline Si is not dissolved during the ammonium oxalate extraction (Wada, 1977).

3.4.3 Organic C association with different fractions of extractable metals

Sodium pyrophosphate is generally assumed to dissolve organo-metal complexes (Bascomb, 1968; Takahashi and Dahlgren, 2016). Pyrophosphate extracted the least amount of Fe, Al, Mn and Si amongst the three extractants (Figure 3.3) but dissolved the highest concentration of OC (Figure 4). Pyrophosphate extractable C constituted on average 62 % (range = 19 - 90 %) of the total SOC content across all samples from both soil depths. Yu *et al.* (2023) reported 39 to 60 % contribution from C_{PP} to the total SOC whereas 30 - 43 % contribution to the total SOC was reported in other studies (Wagai *et al.*, 2013; Heckman *et al.*, 2018). A significant positive relationship between Fe_{PP} and C_{PP} in both topsoils and subsoils (Table 3.6) suggests that organo-Fe complexes were predominantly extracted in the PP procedure. Several other studies have observed significant correlations of Fe_{PP} and Al_{PP} with SOC (Masiello *et al.*, 2004; Wagai *et al.*, 2013; Lawrence *et al.*, 2015; Takahashi and Dahlgren, 2016; Heckman *et al.*, 2018). The association of significant amount of SOC in Fe-organic complexes limits desorption, oxidative degradation, and biodegradation of OC (Parfitt *et al.*, 2002; Kaiser and Guggenberger, 2003; Zimmerman *et al.*, 2004; Rasmussen *et al.*, 2006).

The interpretation of PP extraction data requires some caution due to the dissolution of alkali-induced peptised organic matter (OM) from other fractions (Wagai *et al.*, 2013; Coward *et al.*, 2017). A limited number of samples containing a range of total Fe were extracted with PP at pH 7.5 to evaluate the dissolution of OC due to peptization of Fe/Al oxides adsorbed with organic matter at pH 10 (Parfitt and Childs, 1988; Rennert, 2019). The C_{PP10} and $C_{PP7.5}$ were similar in the four replications of the analysed samples (regression slope = 1.02±0.04, R^2 = 0.97; Supplementary Figure 3.2a). However, the PP at pH 10 extracted nearly three times greater Fe as compared to PP at pH 7.5 (regression slope = 2.88±0.57, R^2 = 0.59; Supplementary Figure 3.2b). The other three elements showed variable behaviour, with no consistent trend or relationship between $Al_{PP7.5}$ and Al_{PP10} (Supplementary Figure 3.2c), while

Mn_{PP10} and $Mn_{PP7.5}$ concentrations were almost similar (regression slope = 0.85±0.18, R^2 = 0.55; Supplementary Figure 3.2d), and PP at pH 10 extracted about half of the Si concentration as compared to the Si concentration in PP extract at pH 7.5 (regression slope = 0.48±0.09, R^2 = 0.57; Supplementary Figure 3.2e). These results show that some dispersion of non-target particles, particularly Fe oxides, occurred at pH 10, however, this did not release any additional OC from the dispersed phases. Parfitt and Childs (1988) reported that dispersion typically occurs in clayey soils (> 40 % clay content) containing goethite and ferrihydrite; soils in our study generally had > 40 % clay content, with kaolinite and hydroxy-interlayered vermiculite as the dominant phyllosilicates in the clay fraction.

Short-range-order Fe phases such as ferrihydrite have the capacity to adsorb high concentrations of SOC due to their extensive specific surface area and the presence of reactive sites for OC adsorption. The significant positive relationship between C_{OX} and Fe_{OX} in the soils (Table 3.6) suggests that SRO and poorly crystalline Fe oxides contributed substantially to the OC accumulation in the studied soils. About 28 % of the total SOC was solubilised during the OX extraction across both depths. Positive correlations between Fe_{OX} and C_{OX} have been reported in several other studies (Kaiser and Guggenberger, 2003; Kleber *et al.*, 2005; Wiseman and Püttmann, 2006; Rasmussen *et al.*, 2018; Yu *et al.*, 2021; Hall and Thompson, 2022; Amenkhienan *et al.*, 2024). Oxalate extractable Si had a significant negative relationship with the C_{OX} in subsoils (Table 3.6), which suggests that soil samples were devoid of poorly-crystalline aluminosilicates (e.g., allophane and imogolite), these SRO minerals are common in Andosols and Spodosols (Dahlgren, 1994).

Oxalate is a C based complexing agent, hence residual C in soils after OX extraction was compared with C in soils after HH extraction, which does not have C compounds (Heckman *et al.*, 2018). The C extracted by the two reagents in selected samples was quite similar (regression slope between C_{OX} and C_{HH} = 1.18±0.07, R^2 = 0.94; Supplementary Figure 3.3a), which

supported the significant association of C with SRO described above. In addition, HH and OX extracted similar Fe (regression slope = 1.06±0.07, R^2 = 0.94; Supplementary Figure 3.3b), Al (regression slope = 0.99±0.03, R^2 = 0.98; Supplementary Figure 3.3c) and Mn (regression slope = 0.93±0.02, R^2 = 0.99; Supplementary Figure 3.3d) concentrations, while more Si was extracted in the HH extraction (regression slope = 0.62±0.05, R^2 = 0.88; Supplementary Figure 3.3e). Hydroxylamine Hydrochloric acid and OX have been reported to have similar ability to extract SRO minerals (Chao and Zhou, 1983), which is consistent with our results.

The C_{DCB} is expected to be C associated with secondary crystalline Fe oxides including SRO phases. In the DCB procedure, 41 % (mean) of the total SOC was extracted from soil samples from both depths. Since DCB extracts both SRO and crystalline Fe and Al oxides, if the proportion of C_{OX} (28 %) is excluded from the C_{DCB} (41 %), on an average only 13 % of the total SOC was actually associated with crystalline Fe and Al oxides. The results indicate a relatively small role of crystalline Fe oxides in the preservation of OC in the studied soils. The relatively small contribution of crystalline Fe oxides in the preservation of OC might be related to smaller SSA and reduced hydroxyl surface sites of crystalline Fe oxides than to SRO Fe and Al oxides (Mikutta *et al.*, 2006; Heckman *et al.*, 2013; Newcomb *et al.*, 2017; Heckman *et al.*, 2018). Consequently, despite the high concentration of DCB extractable Fe and other elements in the studied soils (Figure 3.3a), the C_{DCB} portion was small. In the GLM model, the significant positive relationship between C_{DCB} and Al_{DCB} in topsoils (Table 3.6), was possibly due to Al substitution in the structure of crystalline Fe oxides (e.g. goethite and hematite) in soils, which dissolved during the DCB extraction. In the subsoils that have small OC concentration, a significant positive relationship existed between C_{DCB} and Fe_{DCB}. In both the top- and sub-soils, Fe_{DCB} showed a similar significant positive relationship with Al_{DCB}, which suggests Al occurred in the structures of goethite and hematite and dissolved during the DCB extraction. Significant positive correlations between OC and Fe_{DCB}, in soils dominated by crystalline Fe

oxides have been observed in past studies (Mikutta *et al.*, 2006; Yeasmin *et al.*, 2017). The C_{DCB} and C_{DH} were similar in the selected samples (regression slope = 1.04±0.05, R^2 = 0.97; Supplementary Figure 3.4a), which showed that no additional C was introduced in soil residues during the DCB extraction. The DH extracted lot less Fe and Al as compared to DCB (Supplementary Figure 3.4b, 3.4c). This is expected because DH procedure involves shaking for 16 hours at room temperature, whereas the DCB method requires heating for 15 minutes at 80^{o}C. However, Mn_{DCB} and Mn_{DH} were similar (Supplementary Figure 3.4d), and the DCB method extracted nearly 1.6 times Si as compared to the DH extraction (Supplementary Figure 3.4e).

3.4.4 Extractable C: metal molar ratio and the nature of potential binding mechanism

The molar ratio of C:M had been used to describe binding mechanisms between C and Fe + Al metals. The C:M molar ratio provides information on the potential nature and structure of organo-metal associations in the dissolved phases (Kaiser *et al.*, 2007; Huang *et al.*, 2021; Li *et al.*, 2025). Adsorption and co-precipitation experiments have demonstrated that Fe and Al oxides preferentially bind to organic functional group (Eusterhues *et al.*, 2014; Han *et al.*, 2019; Jardine and Zelazny, 2020; Vance *et al.*, 2020; Li *et al.*, 2023). Adsorption experiments showed that a C:M molar ratio of 1.0 (C:M = 1.0) indicates the maximum sorption capacity of metals oxides for natural OC (Wagai and Mayer, 2007; Lalonde *et al.*, 2012; Zhao *et al.*, 2016; Coward *et al.*, 2017). Molar ratio values less than 1.0 (C:M < 1.0) indicate the formation of the Fe/Al–associated OC complex via inner-sphere adsorption mechanism (Coward *et al.*, 2018), while C:M values > 1.0, indicate both adsorption and co-precipitation in forming Fe/Al-associated OC complexes. Specifically, C:M values > 6.0, indicate co-precipitation or chelation of organic ligands, generating low-density, organic-rich structures, forming Fe/Al–associated OC complexes (Higashi, 1983; Guggenberger and Kaiser, 2003; Wagai and Mayer, 2007; Zhao *et al.*, 2016; Coward *et al.*, 2017; Jeewani *et al.*, 2021). Our extraction results suggest the presence

of mixed association mechanisms between C and (Fe+Al) phases in the studied soils. In the PP fractions, high C:M molar ratios indicate the formation of precipitates of Fe/Al-associated OC complexes in both the top- and sub-soils. The PP extraction liberated C from low-density organic dominated structures (Coward *et al.*, 2017; Coward *et al.*, 2018; Jeewani *et al.*, 2021). The OX fractions had C:M molar ratio > 1, suggesting the occurrence of both adsorption and co-precipitation (in organo-metal complexes) processes. In contrast, the relatively low C:M molar ratios in the DCB fraction indicate the adsorption of OC on to crystalline Fe/Al oxides, possibly via inner-sphere complexation mechanisms (Coward *et al.*, 2017; Jeewani *et al.*, 2021; Yu *et al.*, 2023).

3.5 Conclusions

In this study, we determined the association of OC with different fractions of Fe, Al, Mn and Si in top- and sub-soils of NSW, Australia. The results do not fully support our hypothesis that SRO phases of Fe, Al, Mn and Si contribute most to the preservation of OC in these soils. We found that the largest portion (62 %) of the total OC was present in organo-metal complexes (co-precipitation) and about 28% of the total OC was associated with SRO phases in the studied soils. Crystalline Fe/Al oxides appear to play a relatively small role in the preservation of OC in the studied soils.

The results also showed that among the elements extracted, the concentration of Fe_{DCB} was the highest in the both top- and sub-soils. DCB and OX extracted almost similar Al concentrations, which might indicate release of additional Al, that substituted for Fe in the structure of Fe oxides, during DCB extraction. Crystalline Fe oxides (i.e., goethite and hematite) were dominant in both topsoils and subsoils, and SRO of Al and Si were absent in the soils.

The C:M molar ratio > 6.0 in the PP extracts suggested the co-precipitation of OC with metals by forming complexes with Fe and Al. The mean C:M molar ratio of about 1.5 in the OX fraction indicates that OC was associated with SRO Fe/Al by both adsorption and co-

precipitation processes. In contrast, the C:M molar ratio ≤ 1 in the DCB fraction suggested that OC was chemically adsorbed on the surface crystalline Fe/Al oxides via inner-sphere complexation. Organic carbon in the studied soils was preserved via both organo-metal complexes and adsorption processes.

3.6 Declaration of Funding

I acknowledge the **Soil Science Challenge Grants Program** funded by the **Australian Government Department of Agriculture, Fisheries and Forestry** and this chapter contributes towards the **National Soil Strategy** and the implementation of the **National Soil Action Plan**.

I am thankful to the Tertiary Education Trust Fund (TETFund), Nigeria for the financial support in tuition fees and living expenses.

I thank Sami Hoxha and Adriana Hoxha for their assistance in soil sampling, and Nicholas Proschogo and Bernadeth Antonio for their technical assistance in the ICP-MS analysis.

3.7 Supplementary Information

Supplementary Table 3.1. *Sampling locations and coordinates of the sampling sites*

Australia Soil Classification (ASC)	Location	Land use	Latitude	Longitude
Chromosol	Westwood (Cobbitty)	Unimproved pasture	-33.9959200	150.6543300
Dermosol	Landsdowne (Cobbitty)	Uncultivated land	-34.0235600	150.6630700
Tenosol	Narrabri (W2)	Conservational forest	-30.1355780	149.5337300
Brown Sodosol	Nowley (L Paddock)	Pasture	-31.3524340	150.0848330
Kandosol	Kiama	Grassland	-34.6770976	150.8258704
Chromosol	Braidwood	Native vegetation	-35.2730061	149.8993475
Dermosol	Cooma 1	Native pasture	-36.2300804	148.9899509
Dermosol	Cooma 2	Native pasture	-36.2459748	149.0307088
Dermosol	Coolringdon	Pasture	-36.3014335	148.9491106
Kandosol	Batlow	Forest	-35.5328325	148.1400089
Ferrosol	Tumbarumba	Pasture	-35.7406295	147.9849792
Chromosol	Wagga Wagga	Wheat field	-35.0274214	147.3338049
Kandosol	Sandigo (Narrandera)	Lucerne field	-35.9445395	146.6295168
Chromosol	Boree Creek	Canola field	-35.0357503	146.7280297
Kurosol	Grabben Gullen	Pasture	-34.6376901	149.3349216
Kurosol	Crookwell	Pasture	-34.4716016	149.4360090
Tenosol	Bathurst 1	Pasture	-33.3905737	149.4757577
Tenosol	Bathurst 2	Pasture	-33.4300890	149.3162021
Chromosol	Molong 1	Pasture	-33.1414672	148.9169831
Chromosol	Molong 2	Wheat field	-33.0292863	148.8694772
Dermosol	Wellington	Native grassland	-32.5274320	148.9528288
Dermosol	Dunedoo	Wheat field	-32.1047098	149.4090662
Tenosol	Mount Wilson	Conservational forest	-33.5188875	150.3604813
Ferrosol	Mount Tomah	Conversational forest	-33.5372431	150.4240973
Kandosol	Condobolin	Conservation forest	-33.0836540	147.2947170
Kandosol	Narromine	Pasture	-32.3409570	148.1184690
Kandosol	Coonabarabran	Forest	-31.3494030	149.3154480
Tenosol	Baradine	Forest (National Park)	-30.8857431	149.2635272
Tenosol	The Pilliga	Forest (National Park)	-30.6107310	149.3147380
Ferrosol	Inverell	Forest	-29.7538058	151.0428390
Ferrosol	Tabulam	Pasture	-28.9001668	152.6331904
Ferrosol	Clovass	Olive plantation	-28.8510260	153.1617260
Ferrosol	Casino	Forest	-28.8193435	153.0806690
Ferrosol	Guyra	Pasture	-30.1968190	151.6428116
Ferrosol	Armidale	Pasture	-30.5119000	151.5974604
Dermosol	Murrurundi	Pasture	-31.7544310	150.8060334
Tenosol	Somersby	Forest	-33.3556950	151.2879754

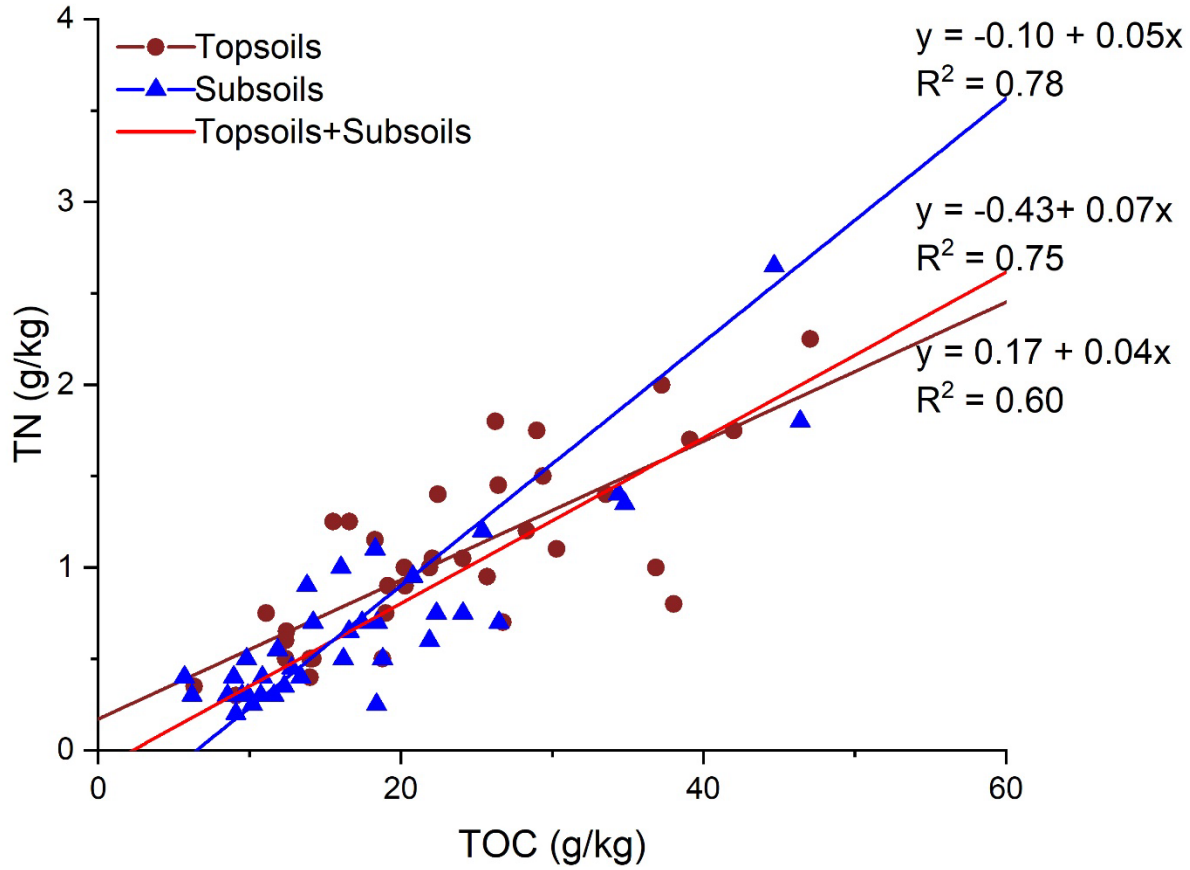

Supplementary Figure 3.1. *Relationship between concentration of total organic carbon (TOC) and total nitrogen (TN) in soils. The brown filled circles and brown line indicate data points and regression line, respectively, for the topsoils. The blue triangles and blue line indicate data points and regression line, respectively, for the subsoils while the red line indicate regression line for both the topsoils and subsoils. An outlier was removed from the topsoils.*

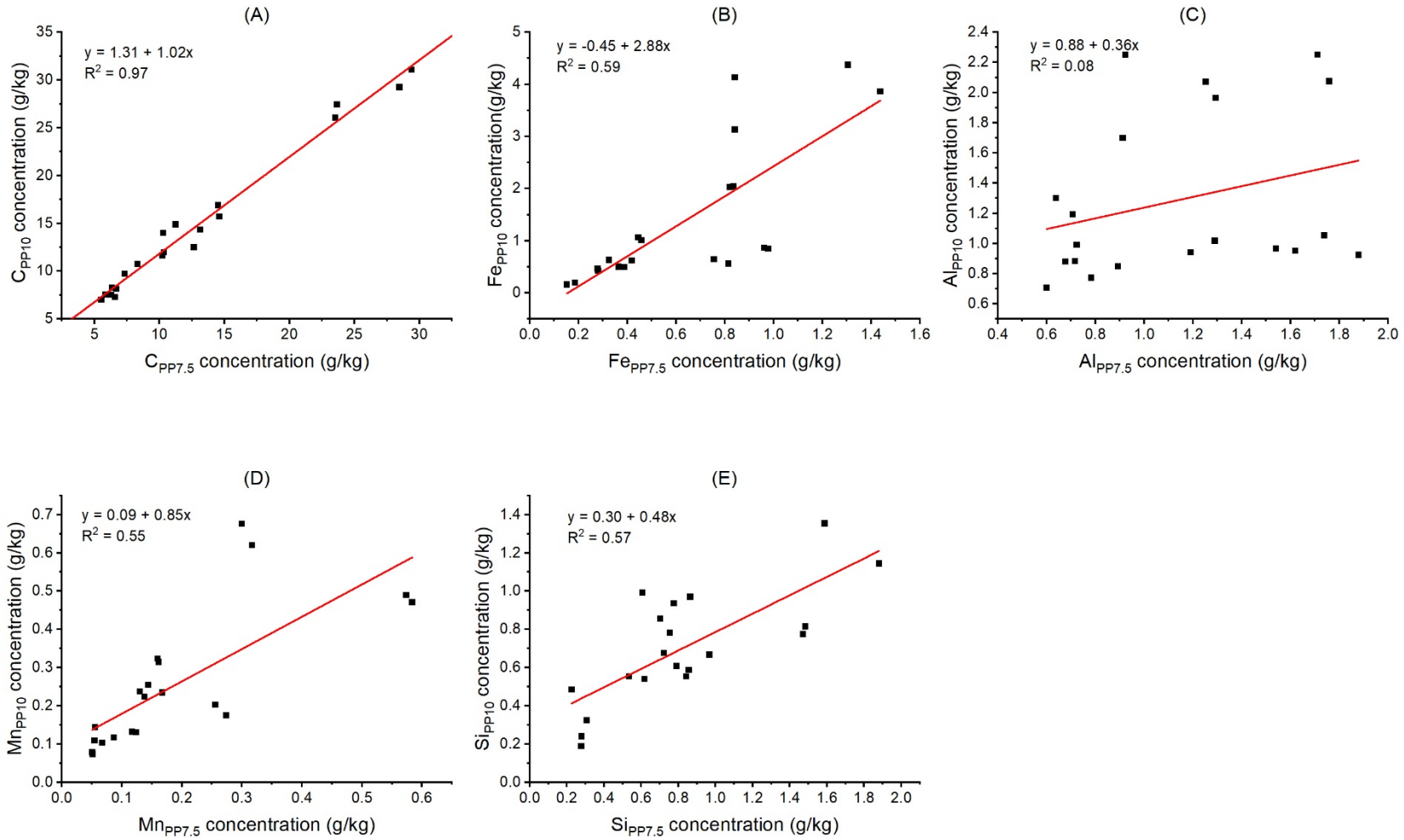

Supplementary Figure 3.2. *Linear regression showing relationships between C_{PP10} and $C_{PP7.5}$, and between the extractable metals at pH 10 and pH 7.5. All regression slopes were statistically significant at p <0.001 except for the regression slope of Al_{PP}. C_{PP10}; sodium pyrophosphate extractable carbon at pH 10, $C_{PP7.5}$; sodium pyrophosphate extractable carbon at pH 7.5, Fe_{pp10}; sodium pyrophosphate extractable iron at pH 10, $Fe_{pp7.5}$; sodium pyrophosphate extractable iron at pH 7.5, Al_{pp10}; sodium pyrophosphate extractable aluminium at pH 10, $Al_{pp7.5}$; sodium pyrophosphate extractable aluminium at pH 7.5, Mn_{pp10}; sodium pyrophosphate extractable manganese at pH 10, $Mn_{pp7.5}$; sodium pyrophosphate extractable manganese at pH 7.5, Si_{pp10}; sodium pyrophosphate extractable silicon at pH 10, $Si_{pp7.5}$; sodium pyrophosphate extractable silicon at pH 7.5. Red line indicates the regression line in the figures.*

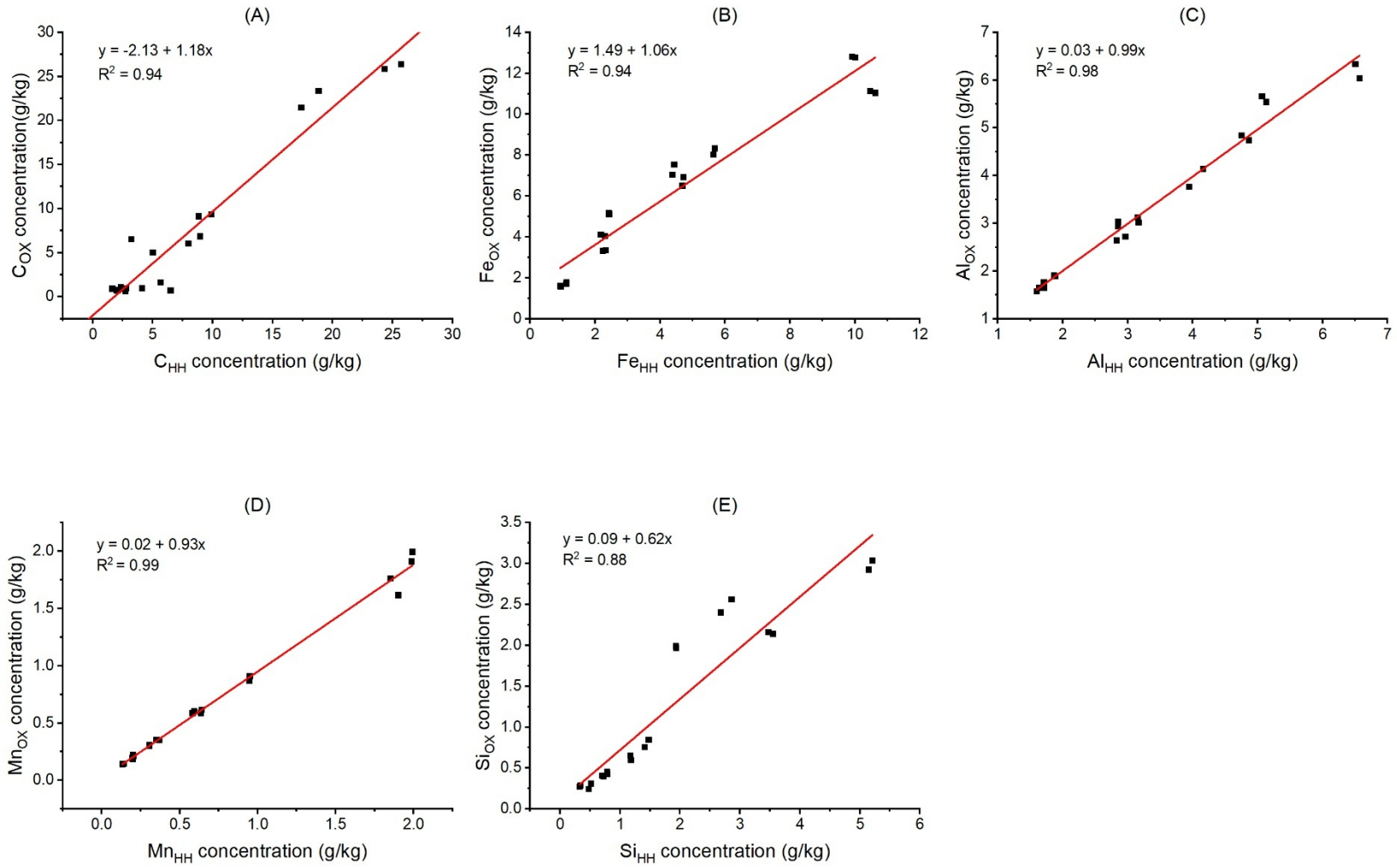

Supplementary Figure 3.3. *Linear regression showing relationships between C_{OX} and C_{HH}, and between the extractable metals. All regression slopes were statistically significant at $p < 0.001$. C_{OX}; ammonium oxalate extractable carbon, C_{HH}; hydrochloric acid-hydroxylamine extractable carbon, Fe_{OX}; ammonium oxalate extractable iron, Fe_{HH}; hydrochloric acid-hydroxylamine extractable iron, Al_{OX}; ammonium oxalate extractable aluminium, Al_{HH}; hydrochloric acid-hydroxylamine extractable aluminium, Mn_{OX}; ammonium oxalate extractable manganese, Mn_{HH}; hydrochloric acid-hydroxylamine extractable manganese, Si_{OX}; ammonium oxalate extractable silicon, Si_{HH}; hydrochloric acid-hydroxylamine extractable silicon. Red line indicates the regression line in the figures.*

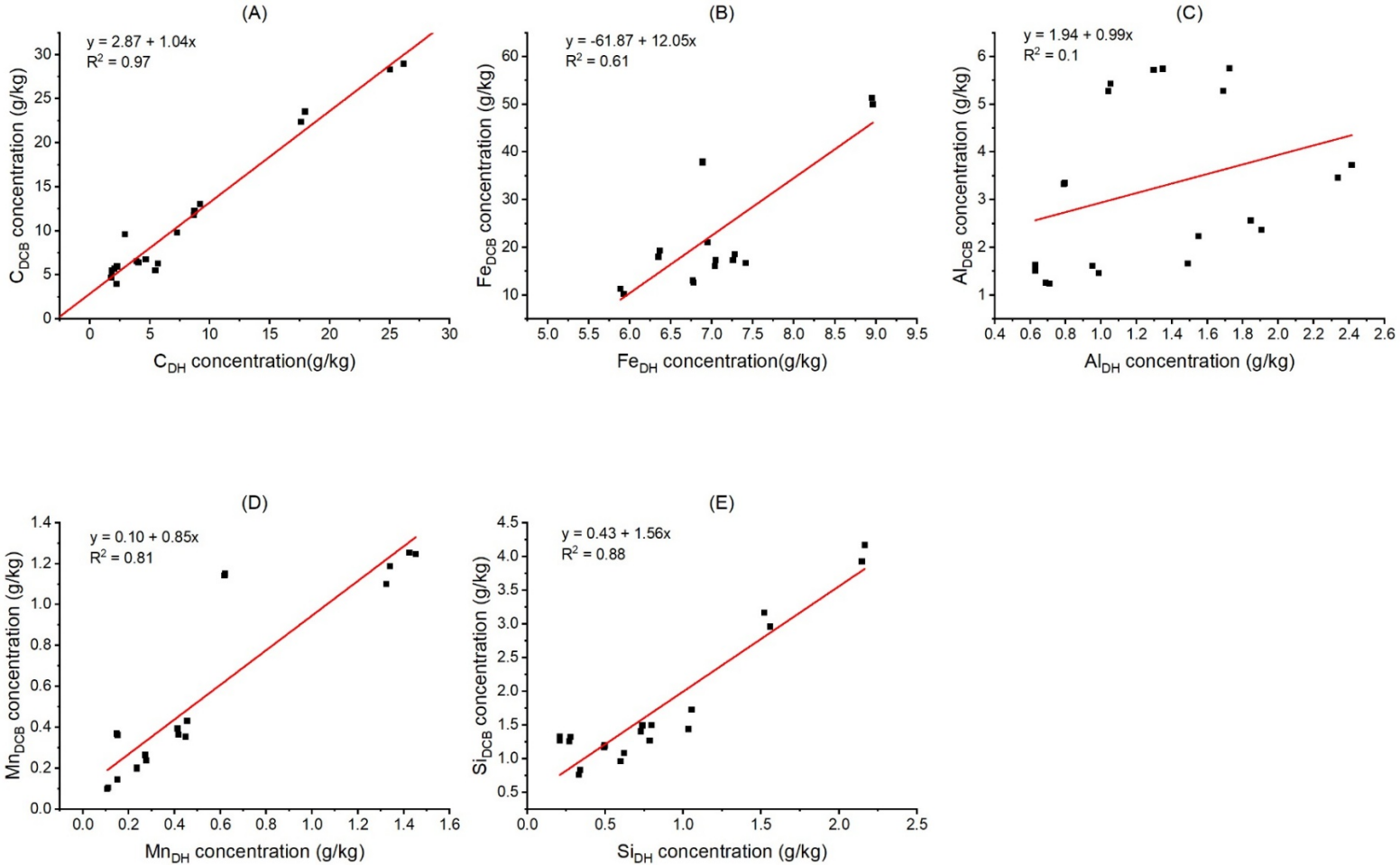

Supplementary Figure 3.4. *Linear regression showing relationships between C_{DCB} and C_{DH}, and between the extractable metals. All regression slopes were statistically significant at p <0.001 except for Fe and Al slopes. C_{DCB}; dithionite-citrate-bicarbonate extractable carbon, C_{DH}; dithionite-hydrochloric acid extractable carbon, Fe_{DCB}; dithionite-citrate-bicarbonate extractable iron, Fe_{DH}; dithionite-hydrochloric acid extractable iron, Al_{DCB}; dithionite-citrate-bicarbonate extractable aluminium, Al_{DH}; dithionite-hydrochloric acid extractable aluminium, Mn_{DCB}; dithionite-citrate-bicarbonate extractable manganese, Mn_{DH}; dithionite-hydrochloric acid extractable manganese, Si_{DCB}; dithionite-citrate-bicarbonate extractable silicon, Si_{DH}; dithionite-hydrochloric acid extractable silicon. Red line indicates the regression line in the figures.*

References

Amenkhienan, B.E., Dijkstra, F., Warren, C., Singh, B., 2024. Understanding extractable metal species relationships with phosphorus sorption and organic carbon in soils. *Soil Research* **62**.

Ashida, K., Watanabe, T., Urayama, S., Hartono, A., Kilasara, M., Mvondo Ze, A.D., Nakao, A., Sugihara, S., Funakawa, S., 2021. Quantitative relationship between organic carbon and geochemical properties in tropical surface and subsurface soils. *Biogeochemistry* **155**, 77-95.

Baldock, J., Skjemstad, J., 2000. Role of the soil matrix and minerals in protecting natural organic materials against biological attack. *Organic geochemistry* **31**, 697-710.

Bascomb, C.L., 1968. Distribution of Pyrophosphate-Extractable Iron and Organic Carbon in Soils of Various Groups. *Journal of Soil Science* **19**, 251-268.

Batjes, N.H., 2014. Total carbon and nitrogen in the soils of the world. *European Journal of Soil Science* **65**, 10-21.

Bigham, J., Golden, D., Bowen, L., Buol, S., Weed, S., 1978. Iron Oxide Mineralogy of Well-drained Ultisols and Oxisols: I. Characterization of Iron Oxides in Soil Clays by Mössbauer Spectroscopy, X-ray Diffractometry, and Selected Chemical Techniques. *Soil Science Society of America Journal* **42**, 816-825.

Borggaard, O.K., 1988. Phase identification by selective dissolution techniques. Iron in Soils and Clay Minerals. *Springer*, pp. 83-98.

Carlson, L.t., Schwertmann, U., 1981. Natural ferrihydrites in surface deposits from Finland and their association with silica. *Geochimica et Cosmochimica Acta* **45**, 421-429.

Chadwick, O.A., Chorover, J., 2001. The chemistry of pedogenic thresholds. *Geoderma* **100**, 321-353.

Chao, T., Zhou, L., 1983. Extraction techniques for selective dissolution of amorphous iron oxides from soils and sediments. *Soil Science Society of America Journal* **47**, 225-232.

Chen, C., Dynes, J.J., Wang, J., Sparks, D.L., 2014. Properties of Fe-organic matter associations via coprecipitation versus adsorption. *Environmental Science & Technology* **48**, 13751-13759.

Chen, C., Hall, S.J., Coward, E., Thompson, A., 2020. Iron-mediated organic matter decomposition in humid soils can counteract protection. *Nature Communications* **11**, 2255.

Childs, C., Wilson, A., 1983. Iron oxide minerals in soils of the Ha'apai group, Kingdom of Tonga. *Soil Research* **21**, 489-503.

Christensen, B.T., 1992. Physical fractionation of soil and organic matter in primary particle size and density separates. *Advances in Soil Science* **20**, 1-90.

Colombo, C., Torrent, J., 1991. Relationships between aggregation and iron oxides in Terra Rossa soils from southern Italy. *Catena* **18**, 51-59.

Cornell, R.M., Schwertmann, U., 2003. The iron oxides: structure, properties, reactions, occurrences, and uses. Wiley-vch Weinheim.

Coward, E.K., Ohno, T., Plante, A.F., 2018. Adsorption and Molecular Fractionation of Dissolved Organic Matter on Iron-Bearing Mineral Matrices of Varying Crystallinity. *Environmental Science & Technology* **52**, 1036-1044.

Coward, E.K., Thompson, A.T., Plante, A.F., 2017. Iron-mediated mineralogical control of organic matter accumulation in tropical soils. *Geoderma* **306**, 206-216.

Crowther, T.W., Todd-Brown, K.E.O., Rowe, C.W., Wieder, W.R., Carey, J.C., Machmuller, M.B., Snoek, B.L., Fang, S., Zhou, G., Allison, S.D., Blair, J.M., Bridgham, S.D., Burton, A.J., Carrillo, Y., Reich, P.B., Clark, J.S., Classen, A.T., Dijkstra, F.A., Elberling, B., Emmett, B.A., Estiarte, M., Frey, S.D., Guo, J., Harte, J., Jiang, L., Johnson, B.R., Kröel-

Dulay, G., Larsen, K.S., Laudon, H., Lavallee, J.M., Luo, Y., Lupascu, M., Ma, L.N., Marhan, S., Michelsen, A., Mohan, J., Niu, S., Pendall, E., Peñuelas, J., Pfeifer-Meister, L., Poll, C., Reinsch, S., Reynolds, L.L., Schmidt, I.K., Sistla, S., Sokol, N.W., Templer, P.H., Treseder, K.K., Welker, J.M., Bradford, M.A., 2016. Quantifying global soil carbon losses in response to warming. *Nature* **540**, 104-108.

Dahlgren, R.A., 1994. Quantification of allophane and imogolite. In: J.E. Amonette, J.W. Stucki (Eds.), Quantitative Methods in Soil Mineralogy. *Soil Science Society of America*, pp. 430-451.

Daly, B., 1982. Identification of podzols and podzolised soils in New Zealand by relative absorbance of oxalate extracts of A and B horizons. *Geoderma* **28**, 29-38.

Davey, B., Russell, J., Wilson, M., 1975. Iron oxide and clay minerals and their relation to colours of red and yellow podzolic soils near Sydney, Australia. *Geoderma* **14**, 125-138.

Estes, E., Andeer, P., Nordlund, D., Wankel, S., Hansel, C., 2017. Biogenic manganese oxides as reservoirs of organic carbon and proteins in terrestrial and marine environments. *Geobiology* **15**, 158-172.

Eusterhues, K., Hädrich, A., Neidhardt, J., Küsel, K., Keller, T.F., Jandt, K.D., Totsche, K.U., 2014. Reduction of ferrihydrite with adsorbed and coprecipitated organic matter: microbial reduction by Geobacter bremensis vs. abiotic reduction by Na-dithionite. *Biogeosciences* **11**, 4953-4966.

Eusterhues, K., Rennert, T., Knicker, H., Kogel-Knabner, I., Totsche, K.U., Schwertmann, U., 2011. Fractionation of Organic Matter Due to Reaction with Ferrihydrite: Coprecipitation versus Adsorption. *Environmental Science & Technology* **45**, 527-533.

Evans, L., Smillie, G., 1976. Extractable iron and aluminium and their relationship to phosphate retention in Irish soils. *Irish Journal of Agricultural Research*, 65-73.

Farmer, V., Russell, J., Smith, B., 1983. Extraction of inorganic forms of translocated Al, Fe and Si from a podzol Bs horizon. *Journal of Soil Science* **34**, 571-576.

Feller, C., Albrecht, A., Tessier, D., 2020. Aggregation and organic matter storage in kaolinitic and smectitic tropical soils. Structure and organic matter storage in agricultural soils. CRC Press, pp. 309-359.

Feng, X.H., Zhai, L.M., Tan, W.F., Liu, F., He, J.Z., 2007. Adsorption and redox reactions of heavy metals on synthesized Mn oxide minerals. *Environmental Pollution* **147**, 366-373.

Fitzpatrick, R.W., Schwertmann, U.v., 1982. Al-substituted goethite—an indicator of pedogenic and other weathering environments in South Africa. *Geoderma* **27**, 335-347.

Fritzsche, A., Schroder, C., Wieczorek, A.K., Handel, M., Ritschel, T., Totsche, K.U., 2015. Structure and composition of Fe-OM co-precipitates that form in soil-derived solutions. *Geochimica Et Cosmochimica Acta* **169**, 167-183.

Gamble, E., Daniels, R., 1972. Iron and silica in water, acid ammonium oxalate, and dithionite extracts of some North Carolina coastal plain soils. *Soil Science Society of America Journal* **36**, 939-943.

Gee, G.W., Or, D., 2002. 2.4 Particle-size analysis. *Methods of soil analysis: part 4 physical methods* **5**, 255-293.

Gu, B., Schmitt, J., Chen, Z., Liang, L., McCarthy, J.F., 1994. Adsorption and desorption of natural organic matter on iron oxide: mechanisms and models. *Environmental Science & Technology* **28**, 38-46.

Guggenberger, G., Kaiser, K., 2003. Dissolved organic matter in soil: challenging the paradigm of sorptive preservation. *Geoderma* **113**, 293-310.

Hall, S.J., Thompson, A., 2022. What do relationships between extractable metals and soil organic carbon concentrations mean? *Soil Science Society of America Journal* **86**, 195-208.

Han, L., Sun, K., Keiluweit, M., Yang, Y., Yang, Y., Jin, J., Sun, H., Wu, F., Xing, B., 2019. Mobilization of ferrihydrite-associated organic carbon during Fe reduction: Adsorption versus coprecipitation. *Chemical Geology* **503**, 61-68.

Hassink, J., 1997. The capacity of soils to preserve organic C and N by their association with clay and silt particles. *Plant and Soil* **191**, 77-87.

Heckman, K., Grandy, A.S., Gao, X., Keiluweit, M., Wickings, K., Carpenter, K., Chorover, J., Rasmussen, C., 2013. Sorptive fractionation of organic matter and formation of organo-hydroxy-aluminum complexes during litter biodegradation in the presence of gibbsite. *Geochimica et Cosmochimica Acta* **121**, 667-683.

Heckman, K., Lawrence, C.R., Harden, J.W., 2018. A sequential selective dissolution method to quantify storage and stability of organic carbon associated with Al and Fe hydroxide phases. *Geoderma* **312**, 24-35.

Higashi, T., 1983. Characterization of Al/Fe—humus complexes in dystrandepts through comparison with synthetic forms. *Geoderma* **31**, 277-288.

Higashi, T., De Coninck, F., Gelaude, F., 1981. Characterization of some spodic horizons of the Campine (Belgium) with dithionite-citrate, pyrophosphate and sodium hydroxide-tetraborate. *Geoderma* **25**, 131-142.

Huang, X., Liu, X., Liu, J., Chen, H., 2021. Iron-bound organic carbon and their determinants in peatlands of China. *Geoderma* **391**, 114974.

Jardine, P.M., Zelazny, L.W., 2020. Surface reactions of aqueous aluminum species. The environmental chemistry of aluminum. CRC Press, pp. 221-270.

Jarvis, S., 1984. The forms of occurrence of manganese in some acidic soils. *Journal of Soil Science* **35**, 421-429.

Jeanroy, E., Guillet, B., 1981. The occurrence of suspended ferruginous particles in pyrophosphate extracts of some soil horizons. *Geoderma* **26**, 95-105.

Jeewani, P.H., Ling, L., Fu, Y., Van Zwieten, L., Zhu, Z., Ge, T., Guggenberger, G., Luo, Y., Xu, J., 2021. The stoichiometric C-Fe ratio regulates glucose mineralization and stabilization via microbial processes. *Geoderma* **383**, 114769.

Jindaluang, W., Kheoruenromne, I., Suddhiprakarn, A., Singh, B.P., Singh, B., 2013. Influence of soil texture and mineralogy on organic matter content and composition in physically separated fractions soils of Thailand. *Geoderma* **195**, 207-219.

Kaiser, K., 2003. Sorption of natural organic matter fractions to goethite (α-FeOOH): effect of chemical composition as revealed by liquid-state 13C NMR and wet-chemical analysis. *Organic Geochemistry* **34**, 1569-1579.

Kaiser, K., Guggenberger, G., 2000. The role of DOM sorption to mineral surfaces in the preservation of organic matter in soils. *Organic Geochemistry* **31**, 711-725.

Kaiser, K., Guggenberger, G., 2003. Mineral surfaces and soil organic matter. *European Journal of Soil Science* **54**, 219-236.

Kaiser, K., Mikutta, R., Guggenberger, G., 2007. Increased stability of organic matter sorbed to ferrihydrite and goethite on aging. *Soil Science Society of America Journal* **71**, 711-719.

Kalbitz, K., Schwesig, D., Rethemeyer, J., Matzner, E., 2005. Stabilization of dissolved organic matter by sorption to the mineral soil. *Soil Biology and Biochemistry* **37**, 1319-1331.

Kleber, M., Eusterhues, K., Keiluweit, M., Mikutta, C., Mikutta, R., Nico, P.S., 2015. Mineral–organic associations: formation, properties, and relevance in soil environments. *Advances in Agronomy* **130**, 1-140.

Kleber, M., Mikutta, R., Torn, M., Jahn, R., 2005. Poorly crystalline mineral phases protect organic matter in acid subsoil horizons. *European Journal of Soil Science* **56**, 717-725.

Kögel-Knabner, I., Guggenberger, G., Kleber, M., Kandeler, E., Kalbitz, K., Scheu, S., Eusterhues, K., Leinweber, P., 2008. Organo-mineral associations in temperate soils:

Integrating biology, mineralogy, and organic matter chemistry. *Journal of Plant Nutrition and Soil Science* **171**, 61-82.
Laganiere, J., Angers, D.A., Pare, D., 2010. Carbon accumulation in agricultural soils after afforestation: a meta-analysis. *Global change biology* **16**, 439-453.
Lal, R., 2004. Soil carbon sequestration impacts on global climate change and food security. *Science* **304**, 1623-1627.
Lal, R., Kimble, J.M., Stewart, B.A., Eswaran, H., 1999. Global climate change and pedogenic carbonates.
Lalonde, K., Mucci, A., Ouellet, A., Gélinas, Y., 2012. Preservation of organic matter in sediments promoted by iron. *Nature* **483**, 198-200.
Lawrence, C.R., Harden, J.W., Xu, X., Schulz, M.S., Trumbore, S.E., 2015. Long-term controls on soil organic carbon with depth and time: A case study from the Cowlitz River Chronosequence, WA USA. *Geoderma* **247**, 73-87.
Lehmann, J., Kleber, M., 2015. The contentious nature of soil organic matter. *Nature* **528**, 60-68.
Li, H., Santos, F., Butler, K., Herndon, E., 2021. A Critical Review on the Multiple Roles of Manganese in Stabilizing and Destabilizing Soil Organic Matter. *Environmental Science & Technology* **55**, 12136-12152.
Li, Q., Hu, W., Li, L., Li, Y., 2023. Interactions between organic matter and Fe oxides at soil micro-interfaces: Quantification, associations, and influencing factors. *Science of The Total Environment* **855**, 158710.
Li, Y., Wang, C.-c., Zou, C., Zhao, Y., Wei, P., Liu, Y.-y., Zhao, X.-j., Lin, D.-m., He, X.-j., Huang, J.-l., Guo, J.-s., Zhu, G.-y., 2025. Effects of iron/aluminum mineral phases on soil organic carbon storage in different clay soils of subtropical acidic forests. *Catena* **252**, 108853.
Loeppert, R., Inskeep, K., 1996. Methods of Soil Analysis: Part III. Chemical Methods. In: D.L. Sparks, A.L.P., P.A. Helmke, R.H. Loeppert, P.N. Soltanpour, M.A. Tabatabai, C.T. Johnston, M.E. Sumner (Ed.). *Soil Science Society of America*, Madison, WI, pp. 639-664.
Loveland, P., Digby, P., 1984. The extraction of Fe and Al by 0.1 M pyrophosphate solutions: a comparison of some techniques. *Journal of Soil Science* **35**, 243-250.
Lützow, M.v., Kögel-Knabner, I., Ekschmitt, K., Matzner, E., Guggenberger, G., Marschner, B., Flessa, H., 2006. Stabilization of organic matter in temperate soils: mechanisms and their relevance under different soil conditions–a review. *European Journal of Soil Science* **57**, 426-445.
Manceau, A., Schlegel, M., Musso, M., Sole, V., Gauthier, C., Petit, P., Trolard, F., 2000. Crystal chemistry of trace elements in natural and synthetic goethite. *Geochimica et Cosmochimica Acta* **64**, 3643-3661.
Mansfeldt, T., Schuth, S., Häusler, W., Wagner, F.E., Kaufhold, S., Overesch, M., 2012. Iron oxide mineralogy and stable iron isotope composition in a Gleysol with petrogleyic properties. *Journal of soils and sediments* **12**, 97-114.
Masiello, C., Chadwick, O., Southon, J., Torn, M.S., Harden, J., 2004. Weathering controls on mechanisms of carbon storage in grassland soils. *Global Biogeochemical Cycles* **18**, GB4023.
Matus, F., Rumpel, C., Neculman, R., Panichini, M., Mora, M.L., 2014. Soil carbon storage and stabilisation in andic soils: A review. *CATENA* **120**, 102-110.
McCarthy, J.F., Ilavsky, J., Jastrow, J.D., Mayer, L.M., Perfect, E., Zhuang, J., 2008. Protection of organic carbon in soil microaggregates via restructuring of aggregate porosity and filling of pores with accumulating organic matter. *Geochimica et Cosmochimica Acta* **72**, 4725-4744.

McKeague, J., 1967. An evaluation of 0.1 M pyrophosphate and pyrophosphate-dithionite in comparison with oxalate as extractants of the accumulation products in podzols and some other soils. *Canadian Journal of Soil Science* **47**, 95-99.

McKeague, J., Day, J., 1966. Dithionite-and oxalate-extractable Fe and Al as aids in differentiating various classes of soils. *Canadian Journal of Soil Science* **46**, 13-22.

McKeague, J., Schuppli, P., 1982. Changes in concentration of iron and aluminum in pyrophosphate extracts of soil and composition of sediment resulting from ultracentrifugation in relation to spodic horizon criteria. *Soil Science* **134**, 265-270.

Mehra, O., Jackson, M., 1960. Iron oxide removal from soils and clays by a dithionite–citrate system buffered with sodium bicarbonate. *Clays and clay minerals*. *Elsevier*, pp. 317-327.

Mikutta, C., Wiederhold, J.G., Cirpka, O.A., Hofstetter, T.B., Bourdon, B., Von Gunten, U., 2009. Iron isotope fractionation and atom exchange during sorption of ferrous iron to mineral surfaces. *Geochimica et Cosmochimica Acta* **73**, 1795-1812.

Mikutta, R., Kleber, M., Torn, M.S., Jahn, R., 2006. Stabilization of soil organic matter: association with minerals or chemical recalcitrance? *Biogeochemistry* **77**, 25-56.

Mikutta, R., Lorenz, D., Guggenberger, G., Haumaier, L., Freund, A., 2014. Properties and reactivity of Fe-organic matter associations formed by coprecipitation versus adsorption: Clues from arsenate batch adsorption. *Geochimica et Cosmochimica Acta* **144**, 258-276.

Mikutta, R., Mikutta, C., Kalbitz, K., Scheel, T., Kaiser, K., Jahn, R., 2007. Biodegradation of forest floor organic matter bound to minerals via different binding mechanisms. *Geochimica et Cosmochimica Acta* **71**, 2569-2590.

Mikutta, R., Zang, U., Chorover, J., Haumaier, L., Kalbitz, K., 2011. Stabilization of extracellular polymeric substances (Bacillus subtilis) by adsorption to and coprecipitation with Al forms. *Geochimica et Cosmochimica Acta* **75**, 3135-3154.

Mu, C., Zhang, T., Zhao, Q., Guo, H., Zhong, W., Su, H., Wu, Q., 2016. Soil organic carbon stabilization by iron in permafrost regions of the Qinghai-Tibet Plateau. *Geophysical Research Letters* **43**, 10,286-210,294.

Newcomb, C.J., Qafoku, N.P., Grate, J.W., Bailey, V.L., De Yoreo, J.J., 2017. Developing a molecular picture of soil organic matter–mineral interactions by quantifying organo–mineral binding. *Nature communications* **8**, 396.

Oades, J., 1988. The retention of organic matter in soils. *Biogeochemistry* **5**, 35-70.

Pansu, M., Gautheyrou, J., 2006. Handbook of soil analysis. Springer: Berlin, Germany.

Parfitt, R., 2009. Allophane and imogolite: role in soil biogeochemical processes. *Clay minerals* **44**, 135-155.

Parfitt, R., Childs, C., 1988. Estimation of forms of Fe and Al-a review, and analysis of contrasting soils by dissolution and Mossbauer methods. *Soil Research* **26**, 121-144.

Parfitt, R., Henmi, T., 1982. Comparison of an oxalate-extraction methon and an infrared spectroscopic method for determining allophane in soll clays. *Soil Science and Plant Nutrition* **28**, 183-190.

Parfitt, R., Parshotam, A., Salt, G., 2002. Carbon turnover in two soils with contrasting mineralogy under long-term maize and pasture. *Soil Research* **40**, 127-136.

Paterson, E., Clark, L., Birnie, A., 1993. Sequential selective dissolution of iron, aluminium, and silicon from soils. *Communications in soil science and plant analysis* **24**, 2015-2023.

Percival, H.J., Parfitt, R.L., Scott, N.A., 2000. Factors controlling soil carbon levels in New Zealand grasslands is clay content important? *Soil Science Society of America Journal* **64**, 1623-1630.

Pokrovski, G.S., Schott, J., Farges, F., Hazemann, J.-L., 2003. Iron (III)-silica interactions in aqueous solution: Insights from X-ray absorption fine structure spectroscopy. *Geochimica et Cosmochimica Acta* **67**, 3559-3573.

Rasmussen, C., Heckman, K., Wieder, W.R., Keiluweit, M., Lawrence, C.R., Berhe, A.A., Blankinship, J.C., Crow, S.E., Druhan, J.L., Hicks Pries, C.E., Marin-Spiotta, E., Plante, A.F., Schädel, C., Schimel, J.P., Sierra, C.A., Thompson, A., Wagai, R., 2018. Beyond clay: towards an improved set of variables for predicting soil organic matter content. *Biogeochemistry* **137**, 297-306.

Rasmussen, C., Southard, R.J., Horwath, W.R., 2006. Mineral control of organic carbon mineralization in a range of temperate conifer forest soils. *Global Change Biology* **12**, 834-847.

Rayment, G.E., Lyons, D.J., 2011. *Soil chemical methods: Australasia*. CSIRO publishing.

Rennert, T., 2019. Wet-chemical extractions to characterise pedogenic Al and Fe species–a critical review. *Soil Research* **57**, 1-16.

Rennert, T., Händel, M., Höschen, C., Lugmeier, J., Steffens, M., Totsche, K., 2014. A NanoSIMS study on the distribution of soil organic matter, iron and manganese in a nodule from a stagnosol. *European Journal of Soil Science* **65**, 684-692.

Rennert, T., Lenhardt, K.R., 2024. Potential pitfalls when using popular chemical extractions to characterize Al-and Fe-containing soil constituents. *Journal of Plant Nutrition and Soil Science*.

Rezapour, S., Azhah, H., Momtaz, H.R., Ghaemian, N., 2015. Changes in forms and distribution pattern of soil iron oxides due to long-term cropping in the Northwest of Iran. *Environmental Earth Sciences* **73**, 7275-7286.

Ross, G., Wang, C., Schuppli, P., 1985. Hydroxylamine and ammonium oxalate solutions as extractants for iron and aluminum from soils. *Soil Science Society of America Journal* **49**, 783-785.

Scheel, T., Doerfler, C., Kalbitz, K., 2007. Precipitation of Dissolved Organic Matter by Aluminum Stabilizes Carbon in Acidic Forest Soils. *Soil Science Society of America Journal* **71**, 64-74.

Scheinost, A.C., Singh, B., 2023. Metal oxides. In: Goss, M.J., Oliver, M. (Eds.), Encyclopedia of Soils in the Environment (Second Edition). Academic Press, Oxford, pp. 135-148.

Schuppli, P., Ross, G., McKeague, J., 1983. The effective removal of suspended materials from pyrophosphate extracts of soils from tropical and temperate regions. *Soil Science Society of America Journal* **47**, 1026-1032.

Schweizer, S.A., Mueller, C.W., Höschen, C., Ivanov, P., Kögel-Knabner, I., 2021. The role of clay content and mineral surface area for soil organic carbon storage in an arable toposequence. *Biogeochemistry* **156**, 401-420.

Schwertmann, U., 1964. Differenzierung der eisenoxide des bodens durch extraktion mit ammoniumoxalat-Lösung. *Zeitschrift für Pflanzenernährung, Düngung, Bodenkunde* **105**, 194-202.

Schwertmann, U., Schulze, D., Murad, E., 1982. Identification of ferrihydrite in soils by dissolution kinetics, differential x-ray diffraction, and Mössbauer spectroscopy. *Soil Science Society of America Journal* **46**, 869-875.

Shang, C., Zelazny, L.W., 2008. Selective dissolution techniques for mineral analysis of soils and sediments. *Methods of Soil Analysis Part 5—Mineralogical Methods* **5**, 33-80.

Singh, B., Gilkes, R., 1991. Phosphorus sorption in relation to soil properties for the major soil types of south-western Australia. *Soil Research* **29**, 603-618.

Singh, B., Gilkes, R., 1992. Properties and distribution of iron oxides and their association with minor elements in the soils of south-western Australia. *Journal of Soil Science* **43**, 77-98.

Singh, B., Sherman, D., Gilkes, R., Wells, M., Mosselmans, J., 2000. Structural chemistry of Fe, Mn, and Ni in synthetic hematites as determined by extended X-ray absorption fine structure spectroscopy. *Clays and Clay Minerals* **48**, 521-527.

Singh, B., Sherman, D., Gilkes, R., Wells, M., Mosselmans, J., 2002. Incorporation of Cr, Mn and Ni into goethite (α-FeOOH): mechanism from extended X-ray absorption fine structure spectroscopy. *Clay Minerals* **37**, 639-649.

Six, J., Conant, R.T., Paul, E.A., Paustian, K., 2002. Stabilization mechanisms of soil organic matter: implications for C-saturation of soils. *Plant and soil* **241**, 155-176.

Skjemstad, J., Bushby, H., Hansen, R., 1990. Extractable Fe in the surface horizons of a range of soils from Queensland. *Soil Research* **28**, 259-266.

Sollins, P., Homann, P., Caldwell, B.A., 1996. Stabilization and destabilization of soil organic matter: mechanisms and controls. *Geoderma* **74**, 65-105.

Song, X., Wang, P., Van Zwieten, L., Bolan, N., Wang, H., Li, X., Cheng, K., Yang, Y., Wang, M., Liu, T., 2022. Towards a better understanding of the role of Fe cycling in soil for carbon stabilization and degradation. *Carbon Research* **1**, 5.

Song, Z., Liu, C., Müller, K., Yang, X., Wu, Y., Wang, H., 2018. Silicon regulation of soil organic carbon stabilization and its potential to mitigate climate change. *Earth-Science Reviews* **185**, 463-475.

Sparks, D.L., Singh, B., Siebecker, M.G., 2024. Environmental soil chemistry. Elsevier.

Steffens, M., Rogge, D.M., Mueller, C.W., Höschen, C., Lugmeier, J., Kölbl, A., Kögel-Knabner, I., 2017. Identification of distinct functional microstructural domains controlling C storage in soil. *Environmental science & technology* **51**, 12182-12189.

Stewart, C.E., Paustian, K., Conant, R.T., Plante, A.F., Six, J., 2007. Soil carbon saturation: concept, evidence and evaluation. *Biogeochemistry* **86**, 19-31.

Stuckey, J.W., Goodwin, C., Wang, J., Kaplan, L.A., Vidal-Esquivel, P., Beebe, T.P., Sparks, D.L., 2018. Impacts of hydrous manganese oxide on the retention and lability of dissolved organic matter. *Geochemical Transactions* **19**, 1-19.

Takahashi, T., Dahlgren, R.A., 2016. Nature, properties and function of aluminum–humus complexes in volcanic soils. *Geoderma* **263**, 110-121.

Torn, M.S., Trumbore, S.E., Chadwick, O.A., Vitousek, P.M., Hendricks, D.M., 1997. Mineral control of soil organic carbon storage and turnover. *Nature* **389**, 170-173.

Vance, G.F., Stevenson, F.J., Sikora, F.J., 2020. Environmental chemistry of aluminum–organic complexes. The environmental chemistry of aluminum. CRC Press, pp. 169-220.

Viscarra Rossel, R., Bui, E., De Caritat, P., McKenzie, N., 2010. Mapping iron oxides and the color of Australian soil using visible–near-infrared reflectance spectra. *Journal of Geophysical Research: Earth Surface* **115**.

von Fromm, S.F., Jungkunst, H.F., Amenkhienan, B., Hall, S.J., Georgiou, K., Pries, C.H., Montaño-López, F., Quesada, C.A., Rasmussen, C., Schrumpf, M., Singh, B., Thompson, A., Wagai, R., Fiedler, S., 2025. Moisture and soil depth govern relationships between soil organic carbon and oxalate-extractable metals at the global scale. *Biogeochemistry* **168**, 20.

von Lützow, M., Kögel-Knabner, I., Ludwig, B., Matzner, E., Flessa, H., Ekschmitt, K., Guggenberger, G., Marschner, B., Kalbitz, K., 2008. Stabilization mechanisms of organic matter in four temperate soils: Development and application of a conceptual model. *Journal of Plant Nutrition and Soil Science* **171**, 111-124.

Vos, C., Jaconi, A., Jacobs, A., Don, A., 2018. Hot regions of labile and stable soil organic carbon in Germany–Spatial variability and driving factors. *Soil* **4**, 153-167.

Wada, K., 1977. Allophane and imogolite, Minerals in soil environments. *Soil Science Society of America, Madison, WI*, 603-638.

Wagai, R., Mayer, L.M., 2007. Sorptive stabilization of organic matter in soils by hydrous iron oxides. *Geochimica et Cosmochimica Acta* **71**, 25-35.

Wagai, R., Mayer, L.M., Kitayama, K., Shirato, Y., 2013. Association of organic matter with iron and aluminum across a range of soils determined via selective dissolution techniques coupled with dissolved nitrogen analysis. *Biogeochemistry* **112**, 95-109.

Walker, A.L., 1983. The Effects of Magnetite on Oxalate- and Dithionite-Extractable Iron. *Soil Science Society of America Journal* **47**, 1022-1026.

Wang, Y., Wang, H., He, J.-S., Feng, X., 2017. Iron-mediated soil carbon response to water-table decline in an alpine wetland. *Nature Communications* **8**, 15972.

Watanabe, T., 2017. Significance of active aluminum and iron on organic carbon preservation and phosphate sorption/release in tropical soils. In: Funakawa, S. (Ed.), Soils, Ecosystem Processes, and agricultural development: Tropical Asia and Sub-Saharan Africa. *Springer* Tokyo, Japan, pp. 103-125.

Weaver, R., Syers, J., Jackson, M., 1968. Determination of silica in citrate-bicarbonate-dithionite extracts of soils. *Soil Science Society of America Journal* **32**, 497-501.

Wiriyakitnateekul, W., Suddhiprakarn, A., Kheuruenromne, I., Gilkes, R.J., 2005. Extractable iron and aluminium predict the P sorption capacity of Thai soils. *Soil Research* **43**, 757-766.

Wiseman, C., Püttmann, W., 2006. Interactions between mineral phases in the preservation of soil organic matter. *Geoderma* **134**, 109-118.

Ye, C., Huang, W., Hall, S.J., Hu, S., 2022. Association of organic carbon with reactive iron oxides driven by soil pH at the global scale. *Global Biogeochemical Cycles* **36**, e2021GB007128.

Yeasmin, S., Singh, B., Johnston, C.T., Sparks, D.L., 2017. Organic carbon characteristics in density fractions of soils with contrasting mineralogies. *Geochimica et Cosmochimica Acta* **218**, 215-236.

Yeasmin, S., Singh, B., Kookana, R.S., Farrell, M., Sparks, D.L., Johnston, C.T., 2014. Influence of mineral characteristics on the retention of low molecular weight organic compounds: A batch sorption–desorption and ATR-FTIR study. *Journal of colloid and interface science* **432**, 246-257.

Yu, M., Wang, Y., Jiang, J., Wang, C., Zhou, G., Yan, J., 2019. Soil organic Carbon Stabilization in the Three Subtropical Forests: Importance of Clay and Metal Oxides. *Journal of Geophysical Research: Biogeosciences* **124**, 2976-2990.

Yu, M., Wang, Y.P., Jiang, J., Cao, N., Chang, Z., Zhang, S., Yan, J., 2023. Soil Organic Carbon Stabilization Is Dominated by Non-Sorptive Process Among the Subsoils From Different Parent Material. *Journal of Geophysical Research: Biogeosciences* **128**, e2022JG007286.

Yu, W., Weintraub, S.R., Hall, S.J., 2021. Climatic and geochemical controls on soil carbon at the continental scale: interactions and thresholds. *Global Biogeochemical Cycles* **35**, e2020GB006781.

Zhang, X., Song, Z., McGrouther, K., Li, J., Li, Z., Ru, N., Wang, H., 2016. The impact of different forest types on phytolith-occluded carbon accumulation in subtropical forest soils. *Journal of soils and sediments* **16**, 461-466.

Zhao, B., Dou, A., Zhang, Z., Chen, Z., Sun, W., Feng, Y., Wang, X., Wang, Q., 2023. Ecosystem-specific patterns and drivers of global reactive iron mineral-associated organic carbon. *Biogeosciences Discussions* **2023**, 1-39.

Zhao, Q., Poulson, S.R., Obrist, D., Sumaila, S., Dynes, J.J., McBeth, J.M., Yang, Y., 2016. Iron-bound organic carbon in forest soils: quantification and characterization. *Biogeosciences* **13**, 4777-4788.

Zhao, Y., Xiang, W., Ma, M., Zhang, X., Bao, Z., Xie, S., Yan, S., 2019. The role of laccase in stabilization of soil organic matter by iron in various plant-dominated peatlands: degradation or sequestration? *Plant and Soil* **443**, 575-590.

Zimmerman, A.R., Chorover, J., Goyne, K.W., Brantley, S.L., 2004. Protection of mesopore-adsorbed organic matter from enzymatic degradation. *Environmental Science and Technology* **38**, 4542-4548.

Chapter Four

Iron speciation in different minerals and other phases in bulk soils using X-ray absorption spectroscopy

4.0 Abstract

Iron (Fe) is a major element that influences numerous geochemical processes in soils but the procedures for the identification and quantification of various Fe forms in bulk soils has remained cumbersome. Over the past 20 years, synchrotron-based X-ray absorption spectroscopy (XAS) including both X-ray absorption near edge (XANES) and extended X-ray absorption fine structure (EXAFS) spectroscopy has become a valuable tool for Fe speciation in soils. In this study we used XANES and EXAFS at the Fe-K edge to quantify Fe-containing minerals and Fe complexed with organic matter (OM) in bulk soils (n = 36). Seven Fe-containing minerals and an organic Fe compound were used as reference compounds for the XAS analysis. Linear combination fitting (LCF) using XANES and EXAFS spectra were used for the quantification of Fe in different phases. LCF analysis of the XANES and EXAFS data revealed that crystalline Fe oxides (i.e., hematite and goethite) accounted for 60 % and 40 %, respectively, of the total Fe in the bulk soil samples. The predictions for ferrihydrite were reasonable from both XANES and EXAFS. XAS predicted Fe content in various Fe phases was well correlated with the DCB extractable Fe. EXAFS predicted Fe contents in different phases better than XANES in bulk soils. XAS showed good results for quantification of Fe phases in bulk soils, which can be improved using closely matching reference materials in the analysis. The procedure could potentially be used in routine soil analysis considering the emergence of bench top laboratory based XAS spectrometers where longer acquisition time is affordable.

Keywords: Iron, Fe K-edge, spectra, XANES, EXAFS, XAS, LCF, XRD

4.1 Introduction

Iron (Fe) is the second most abundant metal and fourth most abundant element in the Earth's crust, constituting 6.3 % of the crust by mass (Frey and Reed, 2012). In soils, Fe is released from the weathering of primary Fe-bearing minerals, especially the Fe (II) bearing silicates and sulphides, such as olivine, biotite, pyroxene and pyrite. The concentration of Fe in soils ranges from <1 g/kg to 500 g/kg and the median concentration is about 30 g/kg, depending on the extent of weathering, redox conditions and parent material (Murad and Fischer, 1988; Scheinost and Singh, 2023). Iron plays a significant role in numerous geochemical processes, such as adsorption, desorption and redox reactions, in soils (Sundman *et al.*, 2014). Secondary Fe (III) oxides (including oxides, hydroxides and oxyhydroxides of Fe) can precipitate after the hydrolysis and oxidation of Fe that is released from the weathering of primary minerals (Scheinost and Singh, 2023). In soils, Fe oxides exist in poorly crystalline, nanocrystalline or highly crystalline forms. Goethite, hematite and ferrihydrite are the most common secondary Fe oxides found in soils (Schwertmann and Taylor, 1989; Bigham *et al.*, 2002; Scheinost and Singh, 2023). Iron oxides have a major influence on several physical, chemical and biological properties of soils, particularly in soils from the subtropical and tropical regions (Schwertmann and Taylor, 1989; Bigham *et al.*, 2002). The presence of Fe oxides, even at low concentrations, in soils is visibly noticeable due to their strong pigmenting determining the colour of many soils (Schwertmann and Lentze, 1966; Schwertmann and Taylor, 1989; Scheinost and Schwertmann, 1999). Soil colours, particularly those between red, brown, and yellow, are due to the presence of Fe oxides. Depending on the soil forming factors, Fe oxides can be evenly distributed in the soil profile or concentrated in a specific soil horizon (Cornell and Schwertmann, 2003). Iron oxides are important and useful in classifying soils and identifying pedogenic processes such as podzolisation, gleysation and lessivage (Blume and Schwertmann, 1969; Schwertmann, 1993).

Secondary Fe oxides in soils form under the influence of common soil-forming factors and processes, such as temperature, moisture, pH, redox potential, and therefore reflect the pedo-environmental conditions under which the secondary Fe oxides are formed (Schwertmann and Taylor, 1989). The poorly ordered mineral ferrihydrite is a secondary Fe oxide that forms in soil environments containing Fe^{2+} that is rapidly oxidised in the presence of high concentrations of organic carbon and/or silicate compounds, which hinder the formation of highly crystalline Fe oxides such as goethite and hematite (Cornell and Schwertmann, 1979; Carlson and Schwertmann, 1981; Schwertmann and Taylor, 1989). Ferrihydrite occurs globally in many soil environments that includes ochreous precipitates resulting from the oxidation of Fe^{2+}-containing waters, in volcanic ash soils, in the B horizons of podzols and in the placic horizons (Schwertmann and Fischer, 1973; Adams and Kassim, 1984; Campbell and Schwertmann, 1984; Parfitt *et al.*, 1988). Goethite is the most widespread crystalline Fe oxide in soils. It is generally present as the sole Fe oxide in cool and temperate zone soils, whereas it co-exists with hematite in soils from tropical and subtropical regions (Ségalen, 1971; Schwertmann and Taylor, 1989; Cornell and Schwertmann, 2003). Hematite has thermodynamic stability similar to goethite and is the second most abundant Fe oxide in soils (Diakonov *et al.*, 1994). However, in contrast to goethite, hematite is restricted to soils in warmer, predominantly subtropical and tropical climates (Kämpf and Schwertmann, 1983; Schwertmann, 1988).

Iron oxides in soils often have a large (50 to 450 m^2/g) specific surface area (SSA) and abundant reactive surfaces, and thus they exert a significant influence on the chemical behaviour and cycling of nutrients and pollutants (Schwertmann and Taylor, 1989; Kaiser and Guggenberger, 2000; Cornell and Schwertmann, 2003; Scheinost and Singh, 2023). More recently, Fe oxides have been recognised as the soil key component in the preservation of soil organic carbon (SOC) through their chemical interactions with OC and physical encapsulation of OC in soil aggregates (Kleber *et al.*, 2015; Coward *et al.*, 2017; Heckman *et al.*, 2018; Kirsten *et al.*, 2021;

Amenkhienan *et al.*, 2024; von Fromm *et al.*, 2025). Owing to their significant role in many key soil processes, identification and quantification of Fe oxides is important to estimate the adsorption capacity of soils with respect to trace metallic cations, oxyanions, organic matter and organic and inorganic contaminants, and understand pedogenic processes.

Over the years, different techniques and procedures have been used for the identification and quantification of Fe oxides in soils. These include X-ray diffraction (XRD), Mössbauer spectroscopy (MS), differential thermal analysis (DTA) (Schwertmann *et al.*, 1982), Raman spectroscopy (RS) (De Faria *et al.*, 1997; De Faria and Lopes, 2007; Hanesch, 2009), sequential selective chemical extraction (Mehra and Jackson, 1960; Schwertmann, 1964; McKeague, 1967), vis-NIR spectroscopy (Viscarra Rossel *et al.*, 2010) and soil colour (Scheinost and Schwertmann, 1999). However, many of these techniques are pertinent to crystalline phases of Fe and imposes specific analytical constraints in identifying poorly crystalline Fe-bearing minerals and/or are not sensitive enough to detect low concentration of Fe minerals including oxides (Prietzel *et al.*, 2007; Giannetta *et al.*, 2022). Mössbauer spectroscopy allows the characterisation of Fe speciation including oxidation state, and it can detect low concentrations of Fe minerals including poorly crystalline ferrihydrite, but it is not widely available and is very time consuming, and thus not be feasible for analysing large number of samples (Schwertmann *et al.*, 1982; Murad, 2010). Selective extraction techniques have limited utility in the identification and quantification of Fe oxides, with acid ammonium oxalate (and hydroxylamine hydrochloride) being useful only to estimate non-crystalline, poorly crystalline and short-range ordered iron oxides while dithionite-citrate-bicarbonate extracts total free Fe oxides (Loeppert and Inskeep, 1996).

Synchrotron-based XAS, including both EXAFS and XANES, has emerged as a valuable tool for characterising and quantifying Fe phases in soils and sediments (Singh *et al.*, 2010; Sundman *et al.*, 2014; Giannetta *et al.*, 2022; ThomasArrigo and Kretzschmar, 2022). It is a

versatile element-specific technique that can provide information on the local atomic environment, oxidation state and bonding characteristics of the Fe within crystalline and non-crystalline materials (O'day *et al.*, 2004; ThomasArrigo and Kretzschmar, 2022). Previously published XAS studies have mostly considered pure minerals or limited and/or selective fractions of sediments and soils. Prietzel *et al.* (2007) used linear combination fitting of XANES spectra to approximately quantify the influence of groundwater on the Fe(II) and Fe(III) phases in soils. Formenti *et al.* (2014) also used linear combination fit of XANES spectra to apportion Fe among goethite, hematite, illite and smectite in mineral dust transported over Western Africa. More recently, Giannetta *et al.* (2022) used linear combination fitting of both XANES and EXAFS spectra to quantify Fe species in few karst sediments. To the best of our knowledge, this is the first study that has used XANES and EXAFS spectroscopy to speciate Fe, in different minerals, using bulk soil samples. We have used surface and sub-surface soil samples representing several soil types and different environmental conditions of New South Wales, Australia in this study. The specific aim of this study was to determine the distribution of Fe in different minerals using bulk soil samples.

4.2 Materials and Methods

4.2.1 Soil samples

We selected 18 surface soil (0 – 20 cm) and 18 subsurface soil (20 – 40 cm) samples from different sites across New South Wales, Australia for this study as described in Chapter 3 (3.2.1). The soil types of the selected samples include Cambisol, Luvisol, Ferralsol, Arenosol, Alisol, and Acrisol soil orders according to the IUSS Working Group WRB (2022). The samples were dried in an oven at 40°C, crushed, and sieved through a 2 mm mesh sieve.

4.2.2 Extraction of selective Fe phases

Total free Fe oxide concentration was determined using the dithionite-citrate-bicarbonate (DCB) extraction procedure described by Mehra and Jackson (1960). The concentration of short-range ordered (and poorly crystalline) Fe oxides was measured by extracting 500 mg soil with 30 mL of 0.2 M ammonium oxalate (pH 3.0) in the dark for 4 h (McKeague and Day, 1966). The concentration of Fe complexed with organic matter (OM) was determined using the sodium pyrophosphate (PP) extraction procedure described by McKeague (1967). Iron concentration in all extracts was analysed using PerkinElmer Nexion 300x inductively coupled plasma-mass spectrometer (ICP-MS).

4.2.3 Total Fe in soil

Soil samples were finely ground to 100 µm to achieve a homogenous powder. The homogenous powder samples were placed into cup polyethylene sample cells with mylar film covering one end of the cup. Total Fe in the samples was measured using a PANalytical Minipal benchtop Energy Dispersive (ED)-X-Ray Florescence (XRF) spectrometer.

4.2.4 X-Ray Diffraction (XRD)

For XRD analysis, the clay fraction (<2 µm) was separated after dispersing the soil samples using 0.01 M sodium hydroxide. Oriented clays were prepared by depositing clay suspensions onto porous ceramic tiles and phyllosilicates were identified by XRD analysis following standard pretreatments (Brown and Brindley, 1980). X-ray diffraction patterns were obtained using a PANalytical X'Pert PRO instrument (40 kV and 40 mA) with CuKa radiation. Powder XRD patterns, measured from randomly orientated samples, were used for the identification of non-phyllosilicate minerals in the samples. Such data were measured using MoKα radiation with a STOE Stadi P powder diffractometer (50 kV and 40 mA) to avoid Fe fluorescence. Considering the high Fe concentration in many clay samples, which fluorescence under CuKa

radiation creating a polychromatic signal resulting in poor XRD patterns, we used MoKα radiation for the random powder XRD analysis.

4.2.5 X-ray absorption spectroscopy

Seven Fe-containing minerals and one organic Fe compound relevant to the soil samples were used as reference compounds for the XAS analysis. The details of the reference compounds are presented in Table 4.1. Illite and montmorillonite were obtained from the Source Clays Repository of the Clay Minerals Society, USA. Kaolinite had been isolated from a highly weathered soil in Western Australia (Singh and Gilkes, 1992). Goethite was synthesized using by rapidly adding 5 M of KOH solution into a 1 M $Fe(NO_3)_3$ solution, and hematite was prepared by heating goethite to 800°C (Schwertmann and Cornell, 2008). Two–line ferrihydrite was synthesized using the procedures described by Schwertmann and Cornell (2008), by adding 1 M KOH solution into 40 g $Fe(NO_3)_3$ solution to bring the pH to 7 – 8. Fe (III) citrate was purchased from Merck and was used a model compound for Fe- OM complexes.

Table 4.1. *Relevant information about the reference minerals (including a compound) used in the XAS analysis*

Reference minerals	Formula	Source	Iron content (%)
Goethite	α-FeOOH	Synthesized	62.85
Hematite	α-Fe_2O_3	Synthesized	69.94
Ferrihydrite	$Fe_5HO_8 \cdot 4H_2O$	Synthesized	66.21
Illite (IMt-2)	$(K_{1.37},Mg_{0.09},Ca_{0.06})$ $(Al_{2.69},Fe[III]_{0.67},Fe[II]_{0.06},Mg_{0.43},Ti_{0.06})$ $(Si_{6.77},Al_{1.23})O_{20}(OH)_4$	Silver Hill, Montana	5.12
Montmorillonite	$(Ca_{0.12},Na_{0.32},K_{0.05})$ $(Al_{3.01},Fe[III]_{0.41},Mn_{0.01},Mg_{0.54},Ti_{0.02})$ $(Si_{7.98},Al_{0.02})O_{20}(OH)_4$	Crook Country, Wyoming	2.34
Kaolinite (#235)	$(Al_{3.82}\ Fe_{0.18})Si_4O_{10}(OH)_8$	Singh and Gilkes, 1992	2.50
Fe(III) citrate	$C_6H_5FeO_7$	Merck and Sigma-Aldrich	17.50

Soil samples and standards were homogenously diluted with cellulose to obtain a total absorption jump of ~2.0 absorption length at the K-edge. Diluted powdered samples were manually pressed into 7 mm pellets (resulting in pellets sample weight of ~ 30 mg) and placed in perspex sample holders sealed with Kapton tape for the XAS analysis.

Two different mineral mixtures were prepared from goethite, hematite, ferrihydrite, kaolinite, illite and montmorillonite for testing the linear combination fitting (LCF) procedure. The first mixture was a quinary mixture of 50 % goethite, 15 % hematite, 5 % ferrihydrite, 25 % kaolinite, and 5 % illite (hereafter referred as G50H15F5K25I5 in this article). The second mixture was a senary mixture of 30 % goethite, 5 % hematite, 5 % ferrihydrite, 40 % kaolinite, 15 % illite and 5 % montmorillonite (hereafter referred as G30H5F5K40I15M5 in this article). The mixtures were thoroughly homogenized by hand grinding using an agate mortar before being diluted with cellulose and pressed into a pellet for the XAS analysis.

Iron K-edge XAS spectra of soil and standard samples were collected at the Medium Energy X-ray Spectroscopy Beamline (MEX1) of the Australian Synchrotron. The MEX1 beamline has a 1.3 tesla bend magnet source. Collimation and harmonic rejections were achieved by a Rh-coated mirror at ~4.75 mrad to the incident beam, further harmonic rejection was achieved by an elliptically bent Rh-coated mirror downstream of the monochromator, also at ~4.75 mrad. The harmonic content was less than 1 in 1E5. The incident energy was selected by a water-cooled dual crystal monochromator equipped with Si [1,1,1] crystals with an azimuthal angle of 30 degrees. The beam size was defined by slits ~2 m upstream of the of sample with a slit size of 3.0 mm H and 2.0 mm V. The size of the beam at the sample was determined during the experimental setup, via knife-edge scans to have a full width at half maximum (FWHM) of ~3.1 mm H and ~0.4 mm V. The incident beam energy was calibrated by defining the first peak in the first derivative of the absorption spectrum of an Fe metal foil, measured in transmission mode, to be 7110.75 eV (Kraft *et al.*, 1996). Energy drift at the MEX1 beamline has been

demonstrated to be of the order of 10s of meV over the timescale of an experiment. Samples were measured in transmission mode using 15 cm Ionitech gridded ion chambers filled with nitrogen gas at a pressure of 2 bar. The ion chamber currents were amplified by Stanford Research Systems SR570 current amplifiers; the resulting voltage was recorded by a d-tAcq ACQ430 at a sampling rate of 128 kHz and averaged for the acquisition time at each energy. Iron K-edge XANES spectra were acquired between 6912 and 7790 eV with variable step sizes, as fine as 0.1 eV with an acquisition time of 1 second per point. Three replicate scans were collected for all samples to confirm the absence of beam induced damage and enhance the signal-to-noise ratio. Replicate XAS spectra were merged, energy calibrated, background subtracted, and normalized using Athena (Ravel and Newville, 2005). Linear combination fitting (LCF) of the XANES spectra was performed using 306 data points ranging from 7092 eV to 7162 eV corresponding to -20 to 50 eV of the Fe-K edge. The weights were forced between 0 and 1 and the weights summed to 1. The LCF was applied to the first derivatives XANES spectra of the soil samples and reference minerals. Linear combination fit analysis of k^3-weighted Fe-K edge EXAFS spectra was performed over the k range from 2 to 12 $Å^{-1}$. The number of reference minerals selected in the LCF analysis was based on the XRD data. Furthermore, to determine the number of reference minerals to include in the LCF, the k^3-weighted Fe-K edge XANES spectra were analysed by principal component analysis (PCA) followed by a target transformation (TT) on each reference mineral (Supplementary Table 1 and Supplementary Figure 1).

4.3 Results and Discussion

4.3.1 Extractable Fe in soil samples

The concentrations of total, DCB extractable and ammonium oxalate (OX) extractable Fe in the soil samples are presented in Table 4.2. The DCB procedure extracts total or free Fe oxides,

including crystalline and short range or poorly ordered Fe oxides, and to some degree organically bound Fe (Jackson *et al.*, 1986; Loeppert and Inskeep, 1996). The ratio of DCB extractable Fe to total Fe (Fe_{DCB}:Fe_{Total}) ranged from 0.24 to 0.92, with a median of 0.45 indicating that a large fraction of the total Fe was present as secondary Fe oxides in the soil samples (Table 4.2). Ammonium oxalate dissolves short-ranged-order (SRO) or poorly crystalline forms of Fe. Fe_{OX} was higher in Ferrosols compared to other soils, however, one Kandosol (#29, #30) also had a higher Fe_{OX}. The OX extractable Fe to DCB extractable Fe (Fe_{OX}:Fe_{DCB}) ratio varied between 0.08 and 0.54, with a median of 0.16 (Table 4.2). Small values (< 0.1) of Fe_{OX}:Fe_{DCB} indicate a high degree of crystallinity of the Fe oxides (Blume and Schwertmann, 1969; Fitzpatrick and Schwertmann, 1982; Prasetyo and Gilkes, 1994), while values greater than 0.7 suggest low crystallinity of Fe oxides (Walker, 1983; Ashida *et al.*, 2021). In our samples, the ratio of Fe_{OX}:Fe_{DCB} was generally small indicating that highly crystalline Fe oxides, such as hematite and goethite, were the dominant Fe oxides in the soils. Sodium pyrophosphate dissolves Fe complexed with organic compounds. The PP extractable Fe (Fe_{PP}) ranged from 0.11 to 5.72 g/kg, with a median of 0.68 g/kg (Table 4.2).

4.3.2 X-ray diffraction (XRD)

Basally oriented XRD patterns of the clay fraction (< 2 μm) showed the dominance of kaolinite, together with variable, but generally small, amounts of hydroxy-interlayered vermiculite and illite in most samples. In addition, crystalline Fe oxides – goethite and hematite were identified in the XRD patterns of most samples. Anatase and quartz were also present in the clay fraction of most soil samples, though in small amounts (Table 4.2). The whole soil fraction XRD patterns were overwhelmingly dominated by quartz peaks and did not show the presence of any additional minerals, except for feldspar in few samples.

Table 4.2. *Clay mineralogy, total Fe, dithionite-citrate-bicarbonate extractable Fe (Fe_{DCB}), ammonium oxalate extractable Fe (Fe_{OX}), sodium pyrophosphate extractable Fe (Fe_{PP}), ratios of Fe_{DCB}:Total Fe, and Fe_{OX}:Fe_{DCB} in the soil samples.*

Soil sample ID	Soil Types	Minerals in clay fraction	Total Fe (%)	Fe_{DCB} (%)	Fe_{OX} (%)	Fe_{PP} (%)	Fe_{DCB}: Total Fe	Fe_{OX}: Fe_{DCB}
#29	Cambisol	H, G, K, S, I, A, Q	5.03	2.37	1.04	0.28	0.47	0.44
#30	Cambisol	H, G, K, S, I, A, Q	5.48	2.91	1.06	0.20	0.53	0.37
#31	Luvisol	G, H, K, I, HIV, A, Q	4.07	1.92	0.18	0.05	0.47	0.09
#32	Luvisol	G, H, K, I, HIV, A, Q	3.48	0.91	0.13	0.08	0.26	0.15
#33	Alisol	G, H, K, I, HIV, A, Q	4.83	2.46	0.41	0.07	0.51	0.16
#34	Alisol	G, H, K, I, HIV, A, Q	4.24	1.83	0.32	0.04	0.43	0.17
#41	Ferralsol	G, H, K, HIV, I, A, Q	8.53	4.17	0.77	0.07	0.49	0.18
#42	Ferralsol	G, H, K, HIV, I, A, Q	9.26	3.90	0.74	0.02	0.42	0.19
#45	Cambisol	G, H, K, I, HIV, A, Q	2.80	1.33	0.20	0.07	0.47	0.15
#46	Cambisol	G, H, K, I, HIV, A, Q	3.47	1.81	0.29	0.08	0.52	0.16
#49	Acrisol	G, H, K, I, HIV, A, Q	3.51	2.92	0.29	0.09	0.83	0.10
#50	Acrisol	G, H, K, I, HIV, A, Q	3.60	3.32	0.26	0.08	0.92	0.08
#53	Arenosol	G, H, K, I, A, Q	1.10	0.33	0.08	0.04	0.30	0.24
#54	Arenosol	G, H, K, I, A, Q	1.13	0.31	0.07	0.02	0.28	0.22
#57	Luvisol	G, H, K, I, HIV, A, Q	4.23	2.08	0.34	0.06	0.49	0.17
#58	Luvisol	G, H, K, I, HIV, A, Q	4.37	2.06	0.49	0.06	0.47	0.24
#59	Luvisol	G, H, K, I, A, Q	8.46	3.26	0.58	0.06	0.39	0.18
#60	Luvisol	G, H, K, S, A, Q	8.97	3.70	0.59	0.05	0.41	0.16
#61	Alisol	G, H, K, I, HIV, A, Q	6.30	2.57	0.27	0.02	0.41	0.11
#62	Alisol	G, H, K, I, HIV, A, Q	6.12	2.72	0.24	0.01	0.44	0.09
#63	Alisol	G, H, K, S, I, A, Q	8.71	2.96	0.31	0.02	0.34	0.11
#64	Alisol	G, H, K, S, I, A, Q	9.25	2.47	0.33	0.02	0.27	0.13
#67	Ferralsol	G, K, HIV, I, A, Q	4.01	1.60	0.86	0.43	0.40	0.54
#68	Ferralsol	G, K, HIV, I, A, Q	3.87	1.93	0.88	0.57	0.50	0.45
#71	Cambisol	G, K, I, HIV, A, Q	2.50	0.81	0.22	0.12	0.32	0.27
#72	Cambisol	G, K, I, HIV, A, Q	2.50	0.78	0.17	0.16	0.31	0.21
#75	Arenosol	G, H, K, HIV, A, Q	3.20	1.78	0.20	0.04	0.56	0.11
#76	Arenosol	G, H, K, HIV, A, Q	3.31	1.85	0.14	0.02	0.56	0.08
#83	Ferralsol	G, H, S, A, Q	10.24	2.46	0.55	0.08	0.24	0.22
#84	Ferralsol	G, H, S, A, Q	10.88	3.43	0.59	0.06	0.32	0.17
#87	Ferralsol	G, H, K, A, Q	16.20	7.29	0.99	0.19	0.45	0.14
#88	Ferralsol	G, H, K, A, Q	13.70	7.60	0.80	0.07	0.55	0.10
#89	Ferralsol	G, H, K, A, Q	12.29	6.06	0.55	0.07	0.49	0.09
#90	Ferralsol	G, H, K, A, Q	11.74	6.41	0.60	0.07	0.55	0.09
#93	Arenosol	G, H, K, HIV, A, Q	2.79	1.01	0.18	0.14	0.36	0.18
#94	Arenosol	G, H, K, HIV, A, Q	2.60	1.18	0.09	0.09	0.45	0.08
Mean			6.02	2.68	0.44	0.10	0.45	0.18
±SE			0.63	0.30	0.05	0.02	0.02	0.02
Median			4.31	2.42	0.32	0.07	0.45	0.16
Range			1.10-16.20	0.31-7.60	0.07-1.06	0.01-0.57	0.24-0.92	0.08-0.54

H= Hematite, G = Goethite, K = Kaolinite, I = Illite, S = Smectite, HIV = Hydroxyl Interlayer Vermiculite, A = Anatase, Q = Quartz

4.3.3 XAS for standard and soil samples

The energy positions of the normalised pre-edge peak centroids, inflection point of the absorption edge and edge peak of the reference compounds are shown in Table 4.3. The normalised peak centroid energy (PCE) of the reference minerals are positioned between 7113.5 and 7114.9 eV, which is consistent with earlier studies (Wilke *et al.*, 2001; Formenti *et al.*, 2014; Giannetta *et al.*, 2022). The pre-edge region has been assigned to a 1s → 3d transition (Westre *et al.*, 1997). The pre-edge centroid position, splitting and intensity of the pre-edge peaks vary systematically in Fe compounds, with the pre-edge centroid position being strongly dependent on the Fe oxidation state, whereas the pre-edge intensity is largely influenced by the Fe coordination geometry (Westre *et al.*, 1997; Wilke *et al.*, 2001). The average centroid of Fe^{2+} minerals is close to 7112.1 eV compared to 7113.5 eV for Fe^{3+} minerals (Wilke *et al.*, 2001). Evidently, the Fe in the reference minerals was solely, or mostly, in the Fe (III) oxidation state.

Normalised Fe K-edge XANES spectra and the corresponding first derivative spectra (obtained from normalised data using Gaussian Filter smoothing algorithm) for the reference compounds are shown in Figure 4.1. Some unique features were observed in the XANES spectra of the reference minerals, which support the use of XAS for Fe speciation in mineral mixtures. In the first derivative spectra, 3 – 4 peaks of varying heights were observed between 7110 and 7134 eV in the reference minerals. A single-peak structure corresponding to the edge region at 7125 eV was observed for Fe (III) citrate. In the XANES region, a second peak was observed between 7131 and 7136 eV for all reference minerals except for ferrihydrite, and Fe (III) citrate. These results are similar to those described by Formenti *et al.* (2014), who found a double-peak structure at 7124 and 7128 eV for hematite, goethite, illite, and montmorillonite in the first derivatives spectra, and a second peak between 7132 and 7136 eV for all minerals, except goethite.

The k^3-weighted chi [$k^3\chi(k)$] EXAFS spectra of the reference minerals and corresponding Fourier transforms are shown in Figure 4.2. The $k^3\chi(k)$ maximum peak was observed between 6.0 and 6.2 $Å^{-1}$ for all reference minerals, except for illite and montmorillonite where the $k^3\chi(k)$ maximum peak was observed at 4.0 $Å^{-1}$. Giannetta *et al.* (2022) observed an intense peak between 6.0 and 6.2 $Å^{-1}$ for goethite, hematite, ferrihydrite and Fe (III) citrate, and at 4.0 $Å^{-1}$ for illite in the $k^3\chi(k)$. In the Fourier transformed spectra, the second peak of hematite was greater in magnitude at 2.5 Å than the first peak. The highest intensity peak for goethite, ferrihydrite, illite, montmorillonite and Fe (III) citrate was observed at ~1.5 Å. The $k^3\chi(k)$ spectrum of kaolinite, not presented here, was relatively noisy and of poor quality.

Table 4.3. *Energy positions of the normalised pre-edge peak centroid, inflection point of the absorption edge and edge peak of Fe-K edge XANES spectra for the reference minerals and a compound.*

Standard compound	Fe oxidation state	Centroid pre-edge peak	Inflection point absorption edge	Edge peak
		Energy position / eV		
Goethite	+3	7115.0	7127.4	7131.2
Hematite	+3	7114.0	7125.6	7132.9
Ferrihydrite	+3	7114.5	7125.6	7132.0
Illite	+3	7113.8	7126.5	7131.3
Montmorillonite	+3	7113.5	7126.9	7132.4
Kaolinite	+3	7114.3	7126.4	7132.1
Fe (III) citrate	+3	7114.0	7124.9	7133.7

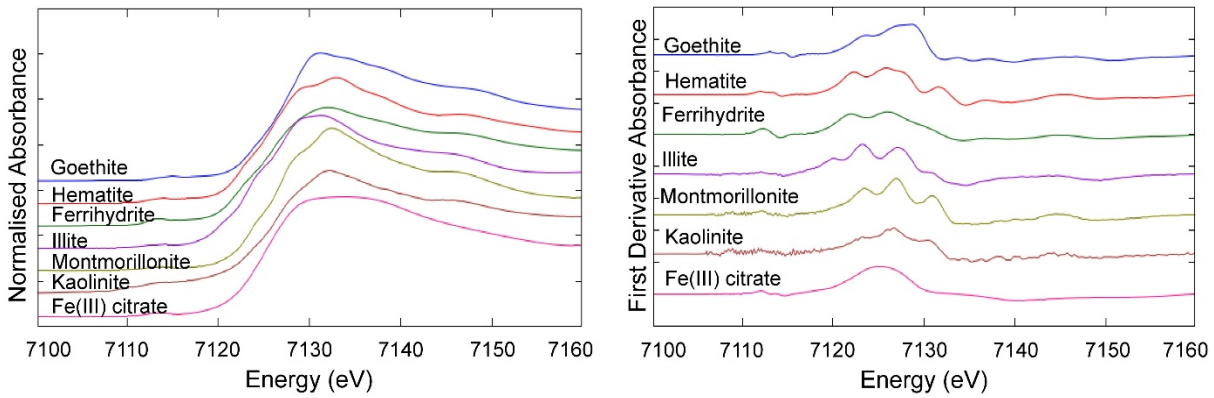

Figure 4.1. *Normalised XANES spectra (left) and their first derivative spectra (right) of the reference minerals and a compound used in the study. The intensities are presented in arbitrary units on a linear scale.*

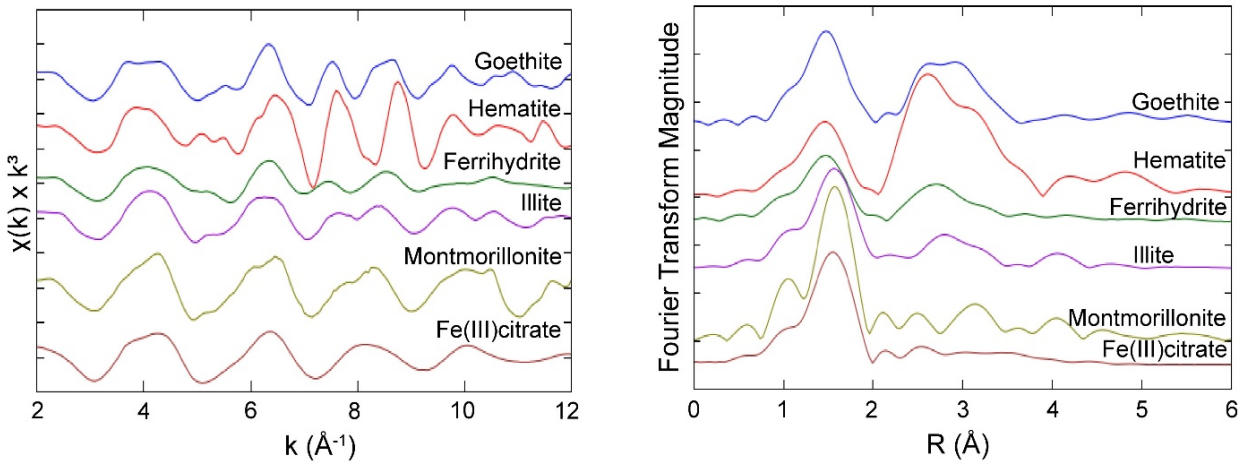

Figure 4.2. *k^3- weighted Fe-K edge EXAFS spectra (left) and their corresponding Fourier transformed magnitude (right) of the reference minerals, and a compound used in the study. The intensities are presented in arbitrary units on a linear scale.*

Linear combination fitting (LCF) was performed on the first derivative of Fe-K edge XANES and on the k^3-weighted Fe-K edge EXAFS spectra of both the mineral mixtures and on the soil samples. The LCF estimated Fe proportion in the minerals of the two mixtures was poor for the XANES spectra as compared to the EXAFS spectra. The proportion of Fe present in goethite in the two mixtures was substantially underestimated and the proportion in hematite and illite was overestimated as compared to the actual values in the mixtures (Table 4.4). In G50H15F5K25I5, XANES overestimated the proportion of Fe in ferrihydrite whereas the estimated and actual proportion of Fe were in reasonable agreement (11 vs 12 %) in G30H5F5K40I15M5 (Table 4.4). In both mixtures the amount of Fe present in the minerals as estimated from the XANES spectra showed a much weaker correlation than the values estimated from the EXAFS spectra, which provided a better agreement with the actual values of Fe present in both mixtures (Figure 4.3 a and b).

Table 4.4. *The actual proportion of Fe and values obtained by linear combination fitting of XANES and EXAFS spectra in the two reference mixtures of Fe minerals.*

Mineral	G50H15F5K25I5			G30H5F5K40I15M5		
	Actual	XANES	EXAFS	Actual	XANES	EXAFS
Goethite	68.0	32.0	68.0	68.5	35.0	83.0
Hematite	23.0	36.0	25.0	12.7	36.0	11.0
Ferrihydrite	7.0	14.0	4.0	12.0	11	5.0
Kaolinite	1.4	0	0	3.6	0	0
Illite	0.6	18	3.0	2.8	18	0
Montmorillonite	0	-	-	0.4	0	1.0
R-Factor		0.0173498	0.0012472		0.0189202	0.0040201
Un-normalised sum (%)		100.5	102.7		105.8	97.1

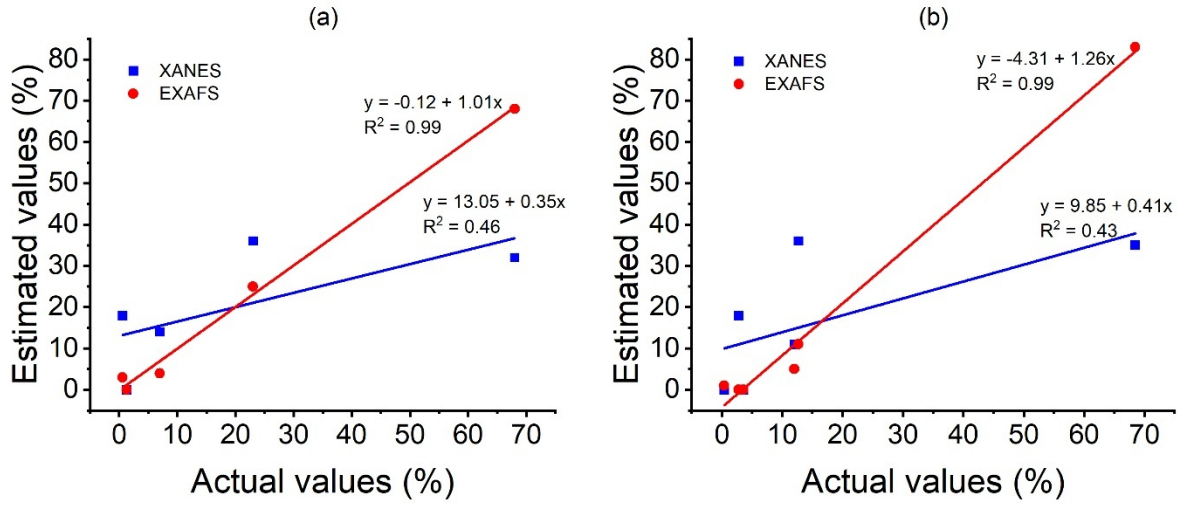

Figure 4.3. *Relationship between XANES and EXAFS estimated values of Fe and the actual values of Fe present in (a) G50H15F5K25I5 (quinary mixtures) (b) G30H5F5K40I15M5 (senary mixtures).*

Normalised XANES spectra and their corresponding first derivatives for the soil samples are presented in Figure 4.4. The spectra of all soil samples appeared similar, however, some differences became obvious in their first derivatives, where a double-peak structure, with varying intensity, was observed between 7122 and 7127 eV. The intensity of the second peak was greater than the first peak for most of the soil samples except for the samples #31 and #32, where the second peak was less intense than the first peak. In the XANES region, a sharp second peak was found between 7136 and 7137 eV for some soil samples (#30, #33, #34, #71 and #72). The XANES spectra of soil samples showed similarity to those of the reference minerals spectra, except for montmorillonite.

The pre-edge region in the first derivative spectra for most soil samples was characterised by a double-peak structure, which is assigned to the 1s → 3d and 1s → 4p transitions, where the 3d character was dominant (Dräger *et al.*, 1988; Westre *et al.*, 1997; Yamamoto, 2008). Table 4.5 shows the energy positions of the normalised pre-edge peak centroids, the inflection points of the absorption edge and the edge peak for the soil samples. The normalised pre-edge peak centroids of soil samples were positioned between 7113.3 and 7114.0 eV, suggesting that Fe was largely in the +3 oxidation state (Galoisy *et al.*, 2001; Wilke *et al.*, 2001; Giannetta *et al.*, 2022).

The $k^3\chi(k)$ spectra, and their corresponding Fourier transforms, of the soil samples are shown in Figure 4.5. The $k^3\chi(k)$ spectra all appeared similar between 2.0 to 10.0 $Å^{-1}$, however, some differences were obvious between 10.0 to 12.0 $Å^{-1}$. As found for the reference minerals, an intense peak was observed between 6.0 and 6.2 $Å^{-1}$ for all soil samples. The highest peak for all soil samples was observed at 1.5 Å in the Fourier transformed spectra.

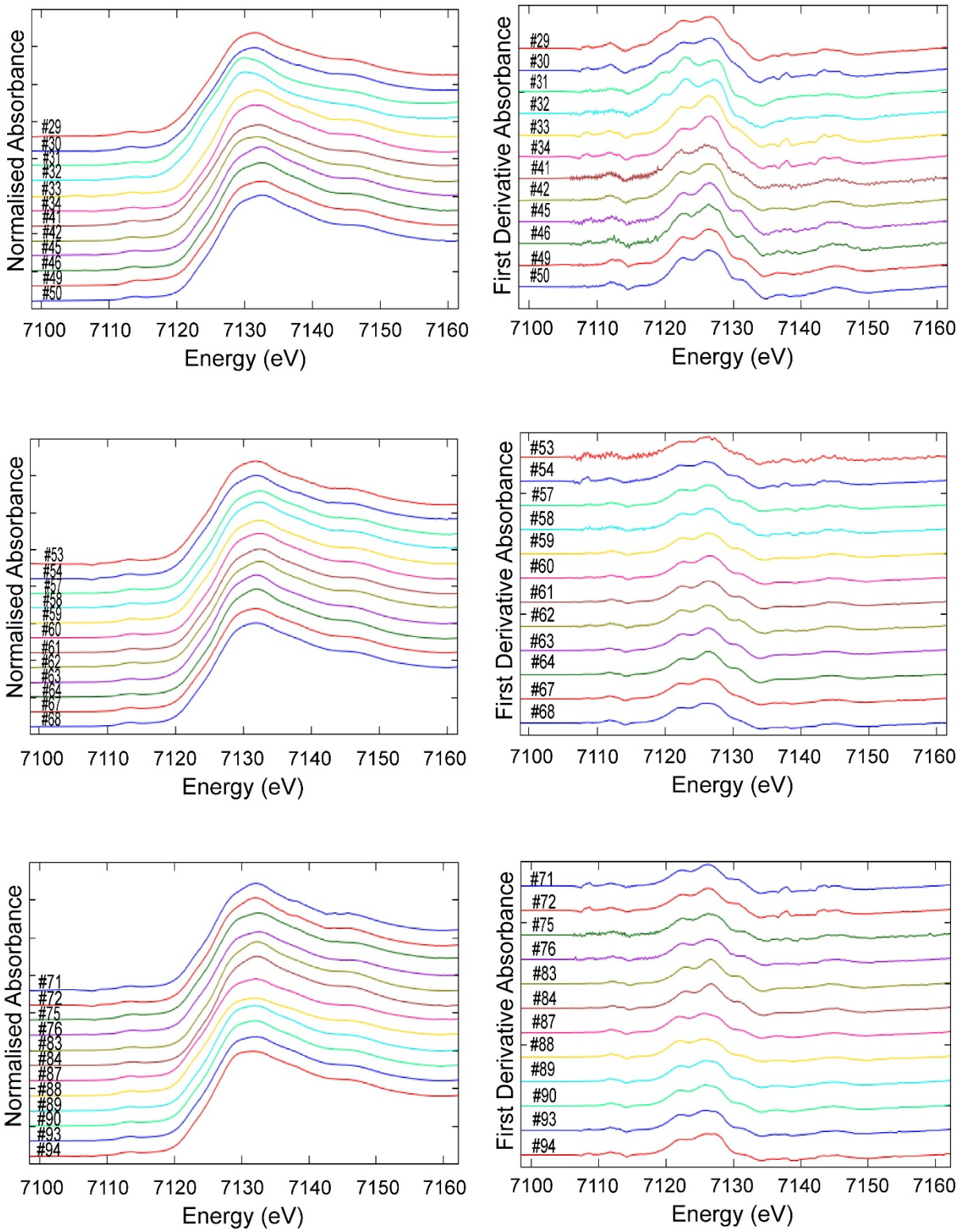

Figure 4.4. *Normalised XANES spectra (left) and their first derivative spectra (right) for the soil samples. The intensities are presented in arbitrary units on a linear scale.*

Table 4.5. *Energy positions of the normalised pre-edge peak centroids, inflection point of the absorption edge and edge peak in the Fe-K edge XANES spectra of soil samples.*

Soil sample ID	Centroid pre-edge peak	Inflection point absorption edge	Edge peak
	← Energy position / eV →		
#29	7113.3	7126.7	7131.5
#30	7113.3	7126.7	7131.4
#31	7113.8	7123.0	7129.9
#32	7113.9	7123.2	7130.0
#33	7113.6	7126.5	7131.8
#34	7113.6	7126.7	7131.5
#41	7113.6	7126.5	7132.2
#42	7113.6	7126.7	7131.9
#45	7114.0	7126.5	7132.5
#46	7113.9	7126.5	7132.6
#49	7114.3	7126.5	7132.4
#50	7114.0	7126.5	7132.5
#53	7113.5	7126.7	7131.9
#54	7113.3	7126.0	7131.8
#57	7113.9	7126.5	7132.2
#58	7113.9	7127.2	7132.4
#59	7113.9	7126.5	7132.3
#60	7113.9	7126.5	7132.3
#61	7113.9	7126.7	7132.4
#62	7113.9	7126.7	7132.4
#63	7113.6	7126.5	7131.9
#64	7113.6	7126.5	7131.9
#67	7113.5	7126.0	7131.8
#68	7113.5	7126.5	7131.9
#71	7113.5	7126.5	7132.1
#72	7113.6	7126.5	7132.0
#75	7114.0	7126.5	7131.7
#76	7114.0	7127.0	7132.6
#83	7113.9	7126.7	7132.2
#84	7113.9	7126.7	7132.2
#87	7113.5	7125.7	7132.1
#88	7113.6	7125.7	7132.0
#89	7113.5	7126.0	7132.0
#90	7113.5	7126.0	7132.0
#93	7113.5	7125.7	7132.1
#94	7113.5	7126.5	7131.8

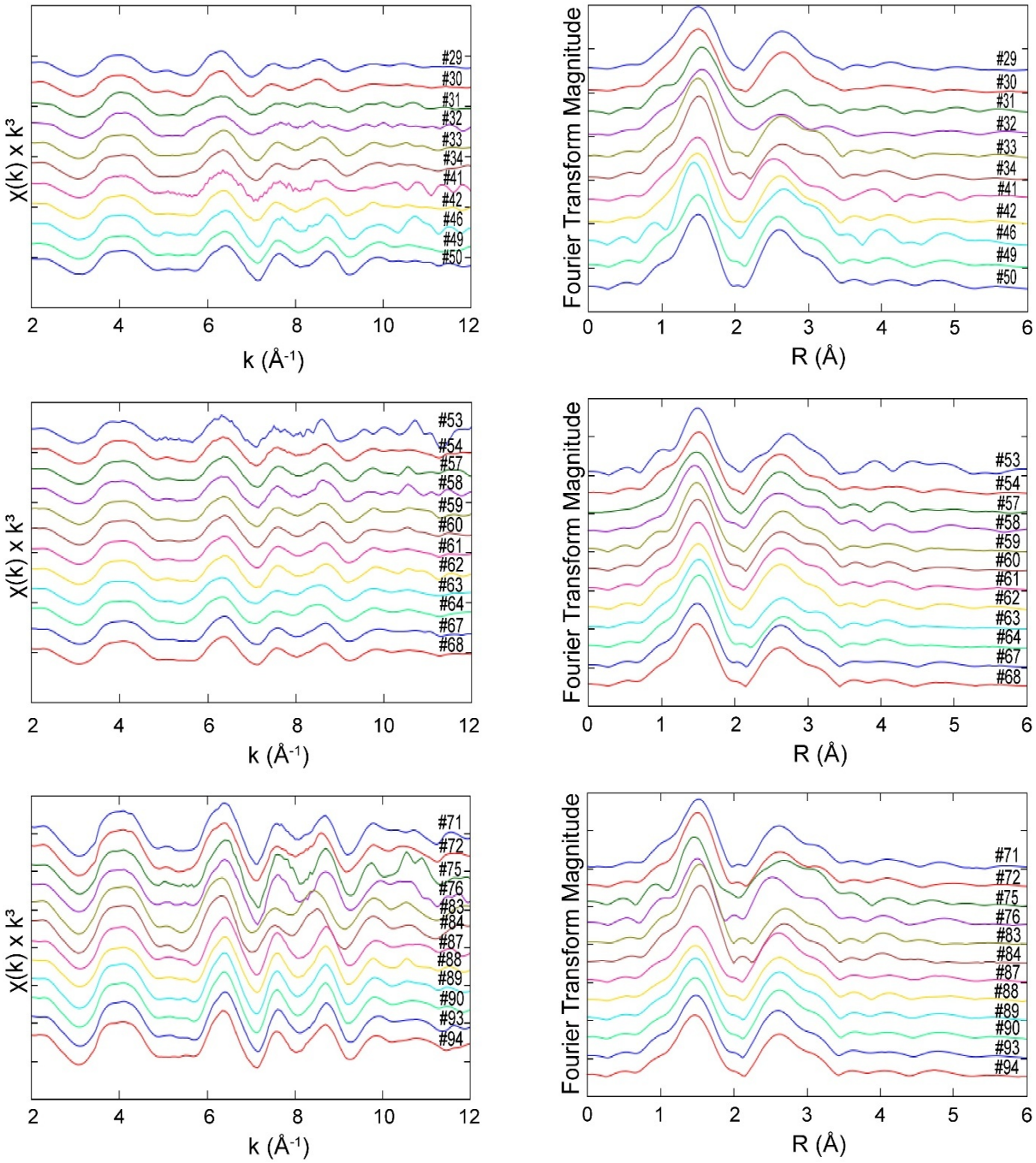

Figure 4.5. *k^3- weighted Fe-K edge EXAFS spectra (left) and their corresponding Fourier transformed magnitude (right) for the soil samples. The intensities are presented in arbitrary units on a linear scale.*

Similar to standard mixtures, we performed LCF using the first derivatives Fe K-edge XANES spectra of the soil samples and the proportions of Fe estimated in different minerals are presented in Table 4.6. The first derivative XANES spectra capture subtle spectral variability better than the normalised XANES spectra (O'day *et al.*, 2004; Formenti *et al.*, 2014). The median proportion of Fe was the highest in hematite (47%) and lowest in Fe associated with

organic matter (Fe-OM) (Table 4.6). In both illite and ferrihydrite the proportion of Fe was 15 %, whereas the median value in goethite and kaolinite was 14% and 11 %, respectively.

The LCF results of k^3-weighted Fe-K edge EXAFS spectra are shown in Table 4.7. The LCF Fe-K edge EXAFS results showed that ferrihydrite (median = 33 %) contained the most Fe followed by illite (median = 21 %) and goethite and hematite (median for both = 20 %) and least in Fe-OM (median = 15 %). Kaolinite could not be determined in this analysis as the spectrum was very noisy, and an unusual peak at 0.5 Å was present in the sample.

We calculated the total Fe content in the minerals and Fe-OM complexes in soils from their estimated values obtained by LCF of XANES and EXAFS spectra; and then this was evaluated against the extractable Fe measured in soil samples. The summed Fe content in goethite, hematite, ferrihydrite and Fe (III) citrate estimated by XANES ($p < 0.001$, $R^2 = 0.87$) and EXAFS ($p < 0.001$, $R^2 = 0.92$) showed significant and positive relationships with the Fe_{DCB} (Figure 4.6 a, b), with the relationship being slightly better and less scattered with the EXAFS estimated Fe than the XANES estimated Fe values. However, the slope values (1.75 and 1.93) suggested overestimation of Fe content by XAS analysis. This could be explained by several reasons. Firstly, natural Fe oxides have significant Al substitution in their structure, thus predictions based on pure minerals overestimated Fe contents in the minerals. Goethite and hematite in soils have been reported to contain up to 35 mol% and 23 mol% Al substitution in their structures (Bigham *et al.*, 1978; Fitzpatrick and Schwertmann, 1982; Singh and Gilkes, 1992). Secondly, DCB may not have extracted all of the Fe associated with the pedogenic Fe oxides and Fe-complexed with organic matter. Lastly, some errors in the total Fe content data obtained by handheld XRF may be possible. Chen *et al.* (2020) reported some inconsistencies ($R^2 = 0.90$) between Fe concentration obtained by a handheld XRF and ICP-OES analysis of acid digested samples, with XRF underestimating (4-5%) Fe concentration. The relationship between the extractable Fe measured in the soil samples and the Fe content present in the

minerals and Fe-OM complexes as estimated from XANES and EXAFS showed that few samples were within the 1:1 equality line (Supplementary Figure 2 and Supplementary Table 2)

Table 4.6. *The proportion of Fe present in different minerals and Fe-OM complexes as estimated by the linear combination fitting analysis of the first derivative XANES spectra and the un-normalised sum of fit of the soil samples.*

Soil sample ID	R-Factor	Illite (%)	Kaolinite (%)	Fe (III) citrate (%)	Ferrihydrite (%)	Goethite (%)	Hematite (%)	Un-normalised sum (%)
#29	0.0107108	43	7	5	45	-	-	100.3
#30	0.0126785	44	6	5	45	-	-	100.6
#31	0.0197620	85	-	5	10	-	-	98.2
#32	0.0166436	82	-	8	8	2	-	100
#33	0.0158070	20	4	9	6	14	47	107.7
#34	0.0176885	21	4	10	-	19	46	107.4
#41	0.0171355	17	6	12	39	-	26	99.7
#42	0.0079536	21	-	12	16	13	38	103.9
#45	0.0109710	8	17	-	-	14	61	107.3
#46	0.0105848	12	-	3	-	19	66	104.7
#49	0.0043865	10	4	2	8	20	56	101.2
#50	0.0026414	8	-	3	5	21	63	103.1
#53	0.0432561	27	15	6	25	-	27	105.2
#54	0.0221854	28	15	-	35	-	22	105.1
#57	0.0040292	11	11	2	14	13	49	103.6
#58	0.0106777	11	16	-	5	16	52	107.5
#59	0.0032973	13	10	-	15	14	48	103.6
#60	0.0063658	11	6	3	-	23	57	105.4
#61	0.0045221	10	12	-	6	14	58	104.8
#62	0.0071766	11	15	-	6	11	57	107
#63	0.0173140	28	10	-	9	11	42	110.2
#64	0.0210553	23	12	-	1	16	48	111.6
#67	0.0075832	18	-	11	26	11	34	105.1
#68	0.0076172	17	-	10	27	12	34	105.7
#71	0.0233604	14	21	-	18	2	45	109.1
#72	0.0259601	15	23	-	14	5	43	110.4
#75	0.0137083	9	7	4	7	14	59	104.7
#76	0.0047384	8	5	5	12	15	55	100.9
#83	0.0193772	11	18	-	-	21	50	109.4
#84	0.0173489	12	13	-	-	24	51	109.3
#87	0.0051105	11	-	11	47	-	31	101.5
#88	0.0086784	11	-	15	57	-	17	97.6
#89	0.0094701	15	-	12	18	9	46	105.4
#90	0.0092449	15	-	10	22	8	45	105.2
#93	0.0076549	15	-	12	23	7	43	104.2
#94	0.0152388	19	-	15	7	14	45	105.4
Median		15	11	9	15	14	47	

Dash (-) represent absent

Table 4.7. *The proportion of Fe present in different minerals and Fe-OM complexes estimated by the linear combination fitting analysis of the k^3-weighted Fe-K edge EXAFS spectra and the un-normalised sum of fit of the soil samples.*

Soil sample ID	R-Factor	Illite (%)	Fe (III) citrate (%)	Ferrihydrite (%)	Goethite (%)	Hematite (%)	Un-normalised sum (%)
#29	0.0626161	26	-	61	9	4	94.2
#30	0.0570873	24	-	63	13	-	95.6
#31	0.1039503	55	5	36	-	4	85.6
#32	0.1109910	50	9	38	-	3	88.1
#33	0.0120075	17	21	22	25	15	101.1
#34	0.0166062	21	29	12	30	8	98.8
#41	0.1176062	11	14	57	-	18	95.4
#42	0.0168118	9	12	38	23	18	100.2
#46	0.0795425	5	19	20	18	38	101.3
#49	0.0188276	4	23	28	18	27	96.8
#50	0.0092752	-	27	23	14	36	99.8
#53	0.1946085	36	-	28	28	8	98.0
#54	0.0233844	29	3	42	7	19	102.3
#57	0.0357697	23	7	37	9	24	99.3
#58	0.0585418	16	3	39	19	23	100.2
#59	0.0251987	10	14	33	25	18	102.2
#60	0.0162663	18	16	24	23	19	106.2
#61	0.0144663	19	13	26	20	22	100.9
#62	0.0203277	21	10	25	19	25	102.3
#63	0.0293208	32	17	26	22	3	99.0
#64	0.0265450	30	21	20	28	1	102.2
#67	0.0087187	-	19	41	22	18	104.5
#68	0.0084890	6	15	42	20	17	101.4
#71	0.0166031	23	19	20	13	25	103.0
#72	0.0243285	22	25	21	15	17	105.0
#75	0.0732394	12	10	25	16	37	99.0
#76	0.0578774	10	19	31	5	35	93.9
#83	0.0448180	46	18	8	28	-	109.7
#84	0.0449027	47	13	7	33	-	111.2
#87	0.0073802	-	8	49	11	32	98.8
#88	0.0083839	2	7	49	15	27	93.5
#89	0.0053488	-	13	34	25	28	104.0
#90	0.0057837	-	11	36	25	28	103.9
#93	0.0154319	-	21	38	10	31	103.3
#94	0.0177273	-	17	34	29	20	100.1
Median		21	15	33	20	20	

Dash (-) represent absent

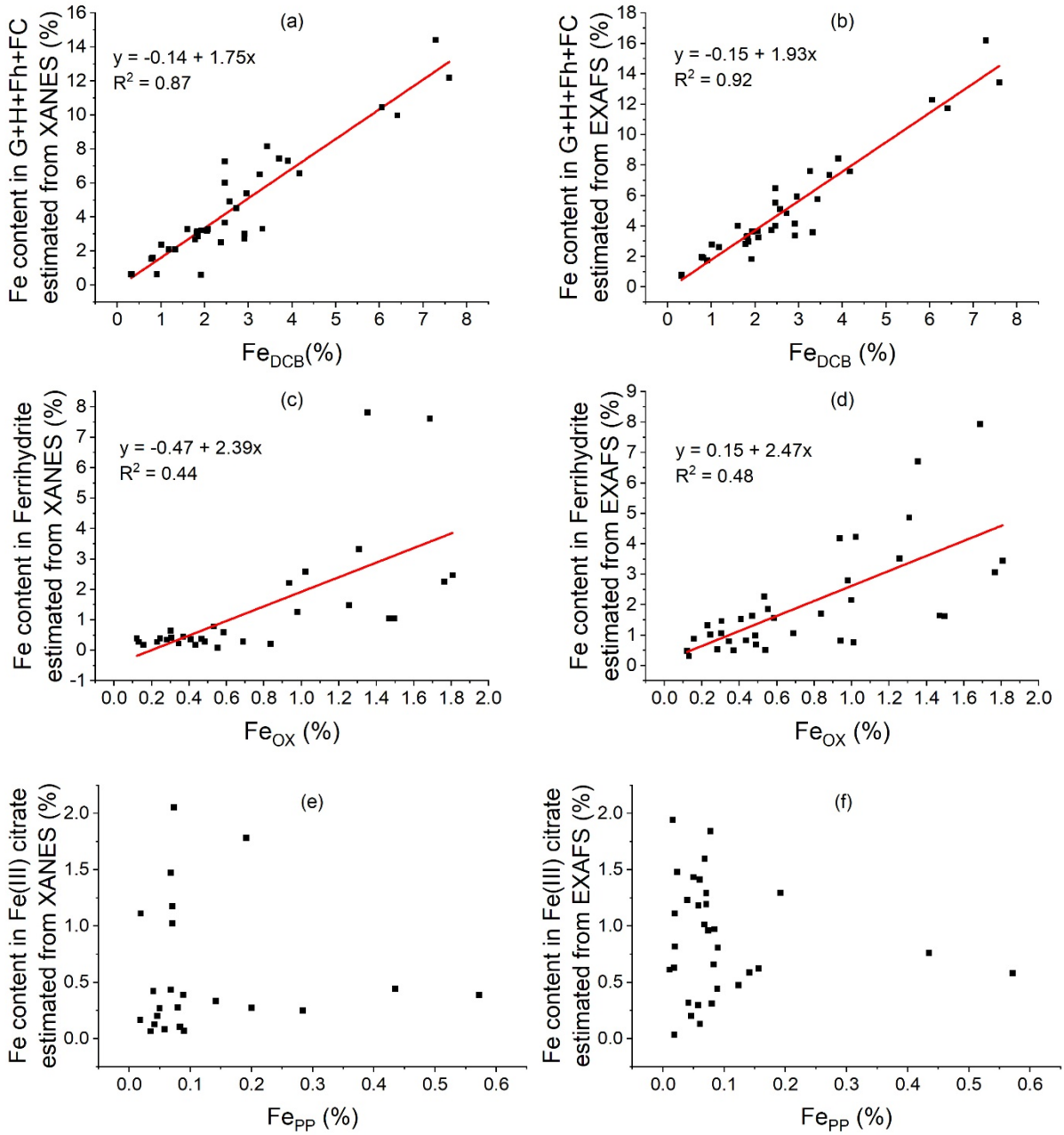

Figure 4.6. *Relationship between dithionite citrate bicarbonate extractable iron (Fe_{DCB}) content and summed Fe content present in goethite (G), hematite (H), ferrihydrite (Fh) and Fe (III) citrate (FC) estimated from (a) XANES and (b) EXAFS. Relationship between ammonium oxalate extractable iron (Fe_{OX}) content and Fe content present in ferrihydrite as estimated from (c) XANES and (d) EXAFS, and sodium pyrophosphate extractable iron (Fe_{PP}) content and Fe content present in Fe complexed with organic matter estimated from (e) XANES and (f) EXAFS.*

The Fe content estimated to be in goethite from the EXAFS showed a significant ($p < 0.001$, $R^2 = 0.70$) relationship with Fe content estimated to be in goethite from the XANES (Supplementary Figure 4.3a), while this relationship was weak ($p < 0.001$, $R^2 = 0.40$) for hematite content estimated by two procedures (Supplementary Figure 4.3b).

Iron content estimated from XANES and EXAFS was relatively poor. Although Fe content in ferrihydrite both estimated from XANES ($p < 0.001$, $R^2 = 0.44$) and EXAFS ($p < 0.001$, $R^2 = 0.48$) showed positive correlation with the Fe_{OX} content (Figure 4.6 c), the predictions were relatively poor. The Fe_{OX} content was multiplied by 1.7 to estimate ferrihydrite contents in soils (Childs, 1985; Parfitt and Childs, 1988). The Fe content estimated to be in ferrihydrite from the EXAFS was slightly better predictor of Fe_{OX} content than XANES. The quantification of ferrihydrite has been reported to be more accurate in EXAFS (Sun *et al.*, 2018; Giannetta *et al.*, 2022). However, ferrihydrite content predicted values from EXAFS were more scattered than XANES predicted values and XANES values significantly ($p < 0.001$, $R^2 = 0.59$) improved when two outliers were excluded. Oxalate extraction is not very specific for ferrihydrite extraction, as it is known to extract small amount of Fe-nanocrystalline and Fe-OM complexes (McKeague and Day, 1966; Parfitt and Henmi, 1982; Farmer *et al.*, 1983; Mansfeldt *et al.*, 2012). Fe content in ferrihydrite estimated from EXAFS showed a significant ($p < 0.001$, $R^2 = 0.88$) correlation with the ferrihydrite content estimated from XANES (Supplementary Figure 4.3c). Both XANES and EXAFS predicted values for Fe in Fe (III) citrate (i.e., complexed with organic matter (OM) showed no relationship with sodium pyrophosphate extractable Fe (Fe_{PP}) (Figure 4.6 e and f). This is probably because PP does not only extract organic complexed Fe, but also extract some poorly crystalline Fe (Bascomb, 1968; Higashi *et al.*, 1981; Jeanroy and Guillet, 1981; Skjemstad *et al.*, 1990). Furthermore, Fe(III) citrate may not have well represented the Fe complexed with organic matter in soils. The relationship between Fe content in Fe (III) citrate estimated from XANES and EXAFS

was poor (Supplementary Figure 4.3d). The proportion of Fe content in illite estimated from XANES showed a reasonably strong ($p < 0.001$, $R^2 = 0.41$) relationship with the Fe proportion estimated from EXAFS (Supplementary Figure 4.3e), with a couple of outliers. The proportion of Fe content in kaolinite estimated by XANES ranged from 4 – 23 % (Table 4.6), with about 0.17 – 1.84 % (median = 0.51 %) of the total Fe content present in this mineral in the soil samples. Iron has been reported to be substituted in the structure of kaolinite in soils, particularly highly weathered soil where about 2 % of Fe have been present in the kaolinite structure (Jepson and Rowse, 1975; Singh and Gilkes, 1992; Melo *et al.*, 2001).

Overall, our results confirmed the combination of XANES and EXAFS a valuable tool to estimate Fe proportion in different minerals using whole soil samples. Although XANES analysis perhaps better for identifying and estimating Fe^{2+} phases in soils based on our results, EXAFS estimated values appeared more accurate than XANES in the bulks soil samples used in this study. These predictions could be further improved by including reference minerals and compounds matching closely with the phases present in soils.

There are some drawbacks of the techniques, such as inability to detect low concentration of Fe in kaolinite in some samples including the two standard mixtures. The EXAFS spectrum of kaolinite was very noisy, and an unusual peak existed in the sample, hence kaolinite could not be estimated by the LCF analysis of EXAFS data. The detection for Fe complexed with OM was rather poor, which suggested that Fe(III) citrate did not represent the OM complexed Fe in the soil samples. Despite these drawbacks, the combination of XANES and EXAFS is a valuable tool for the identification and quantification of Fe in different minerals using bulk soil samples and it should be further explored on other soil types.

4.4 Conclusions

Iron K-edge XANES and EXAFS were used to identify Fe minerals and other phases and to quantify the Fe content in the identified phases, in 36 soil samples representing several soil types. LCF analysis of the XANES showed ferrihydrite contained most Fe (median 33%), followed by illite, goethite and hematite (all ~20%) and about 15% Fe was complexed with OM. The results obtained from the LCF of EXAFS spectra were more closely related than XANES with the chemically extracted Fe data. The summed Fe content in various minerals and Fe complexed with OM was well correlated with the DCB extracted Fe. The estimates for Fe content in ferrihydrite were reasonable using both XANES and EXAFS data. However, the predictions for Fe complexed with OM may not be accurate due to the lack of matching reference samples. Fe K-edge XAS demonstrated capability to identify various Fe forms and approximate portion of the total Fe present in various phases in bulk soils. It can be further refined using better matching reference phases and potentially used as a routine procedure for identifying and quantifying Fe phases in soils, especially given the emergence of bench top laboratory based XAS spectrometers where longer acquisition time is affordable.

4.5 Supplementary Information

Supplementary Table 4.1. *Parameters of the first five components obtained by principal component analysis.*

Component	Eignevalues	Variance	Cumulative variance
1	37.734673	0.993017	0.993017
2	0.231721	0.006098	0.999115
3	0.020665	0.000544	0.999659
4	0.010469	0.000275	0.999935
5	0.002071	0.000054	0.999989

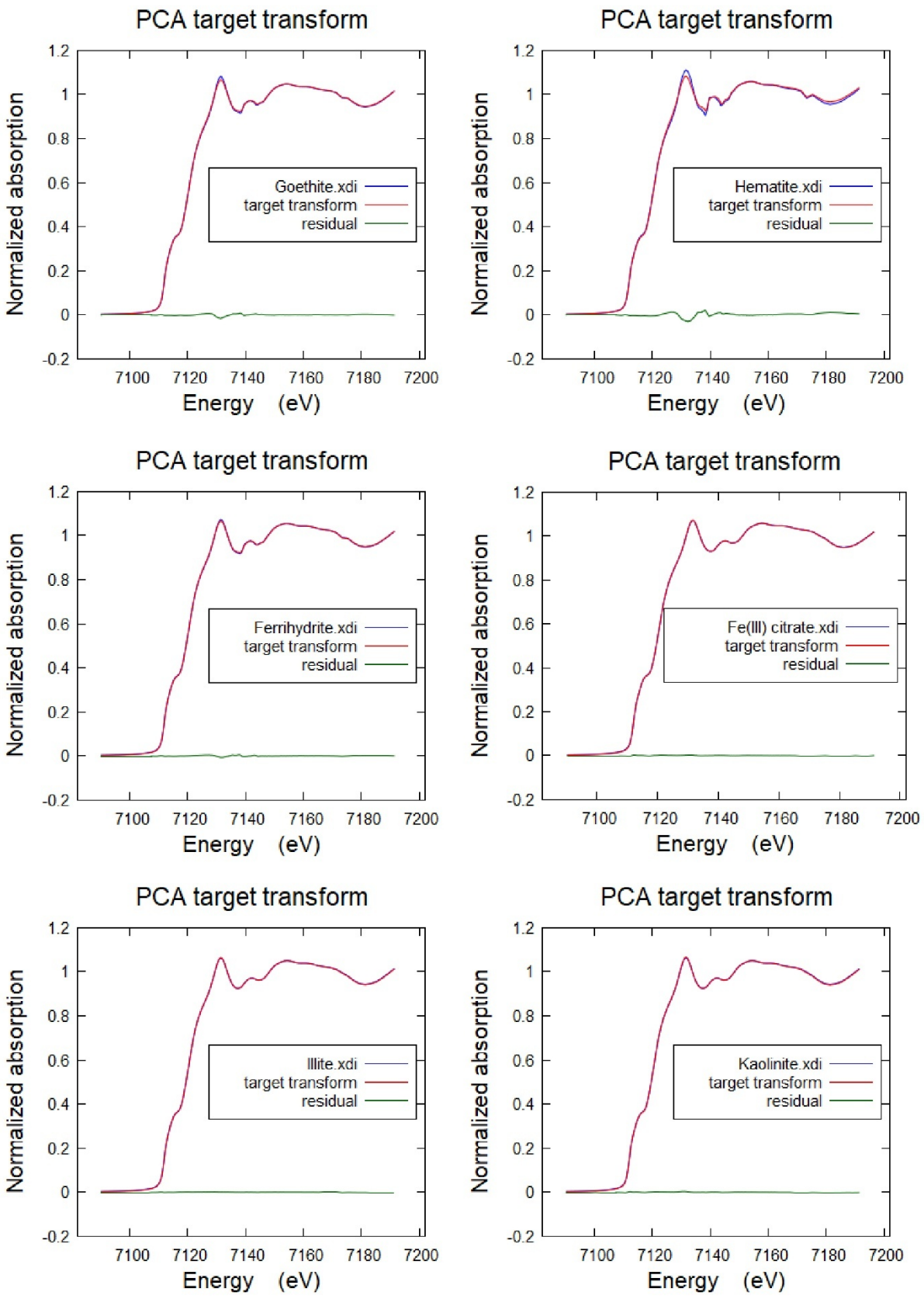

Supplementary Figure 4.1. *Target transformation and the residuals on each reference minerals as advised by principal component analysis.*

Supplementary Table 4.2. *Values of coefficients with their respective confidence intervals along with a probability level (α = 0.05) obtained from regression equations (y = a + bx).*

Term	Estimate	Standard Error	Lower 95%	Upper 95%	Estimate	Standard Error	Lower 95%	Upper 95%
	XANES				EXAFS			
Intercept	-0.14	0.38	-0.91	0.63	-0.15	0.33	-0.82	0.51
Fe_{DCB}	1.75	0.12	1.51	1.98	1.93	0.10	1.73	2.14
Intercept	-0.47	0.47	-1.44	0.49	0.15	0.40	-0.67	0.97
Fe_{OX}	2.40	0.51	1.34	3.45	2.47	0.44	1.57	3.37
Intercept	0.56	0.16	0.22	0.90	0.93	0.12	0.70	1.17
Fe_{PP}	-0.14	0.91	-2.02	1.75	-0.54	0.78	-2.13	1.05

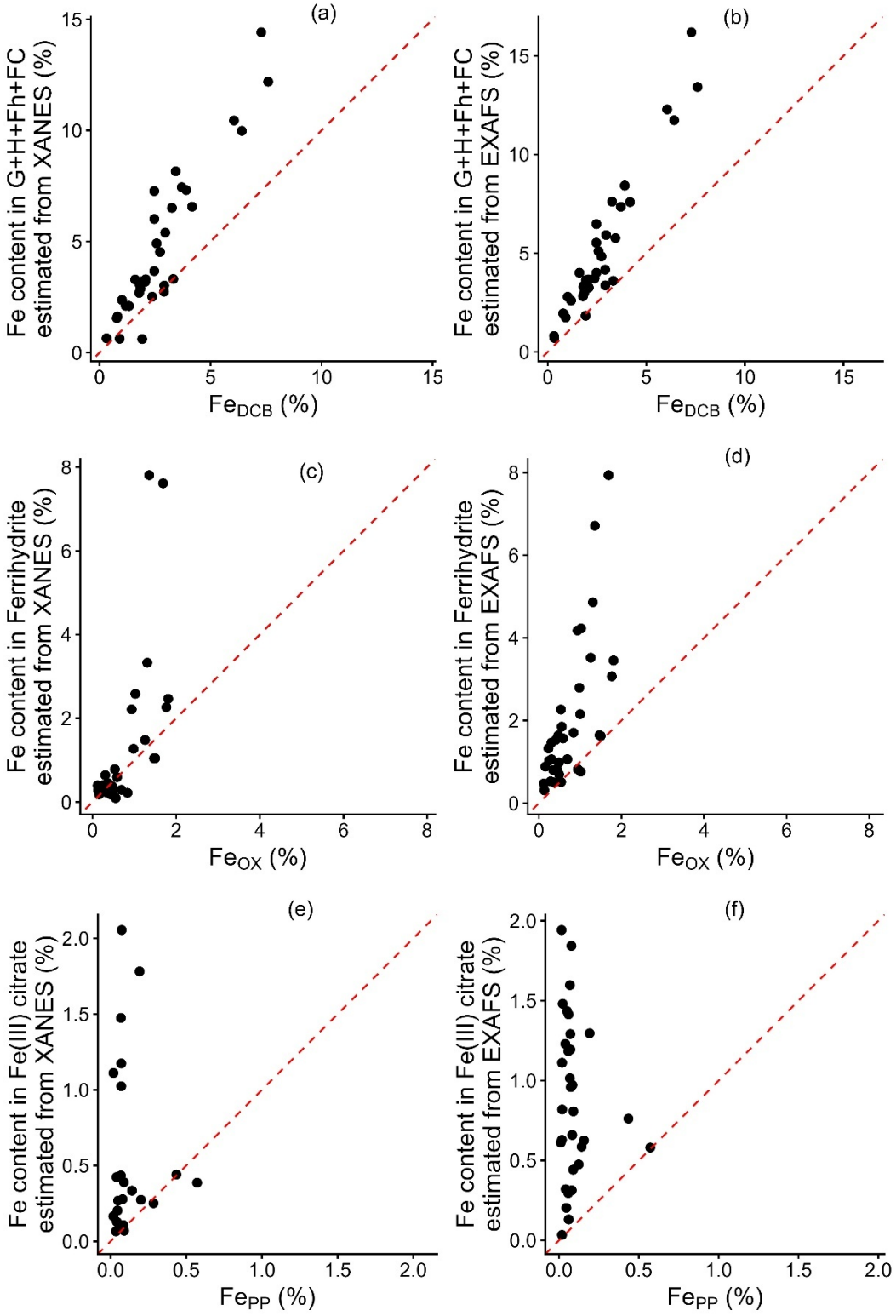

Supplementary Figure 4.2. *Pairwise 1:1 relationship between dithionite citrate bicarbonate extractable iron (Fe_{DCB}) content and summed Fe content present in goethite (G), hematite (H), ferrihydrite (Fh) and Fe (III) citrate (FC) estimated from (a) XANES and (b) EXAFS. Pairwise 1:1 relationship between ammonium oxalate extractable iron (Fe_{OX}) content and Fe content present in ferrihydrite as estimated from (c) XANES and (d) EXAFS, and sodium pyrophosphate extractable iron (Fe_{PP}) content and Fe content present in Fe complexed with organic matter estimated from (e) XANES and (f) EXAFS.*

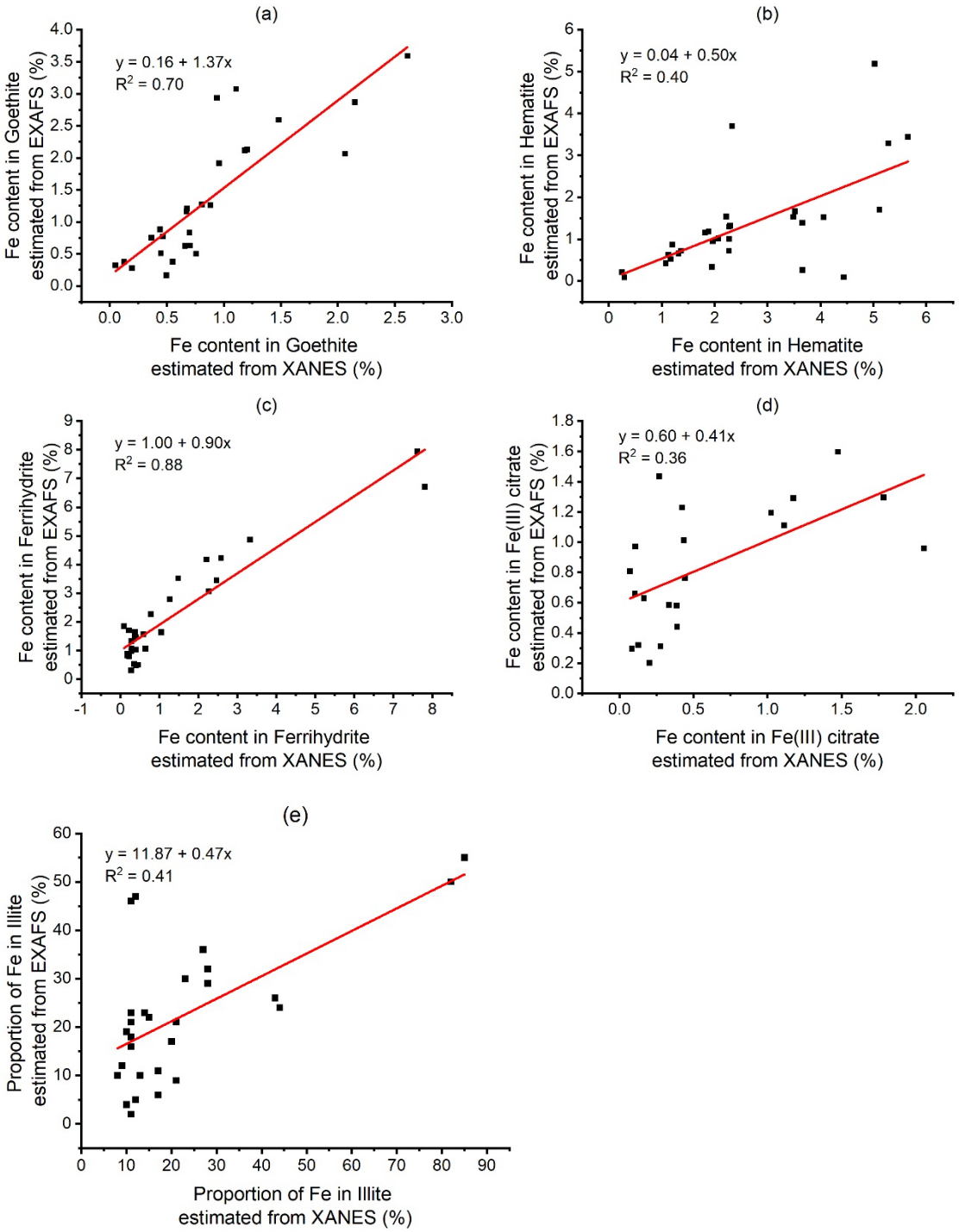

Supplementary Figure 4.3. *Relationship between Fe content in different Fe phases estimated by LCF analysis of XANES and EXAFS data. (a) goethite, (b) hematite, (c) ferrihydrite, (d) Fe(III) citrate and (e) illite.*

4.6 Acknowledgements

I acknowledge the **Soil Science Challenge Grants Program** funded by the Australian Government Department of Agriculture, Fisheries and Forestry and this article contributes towards the **National Soil Strategy** and the implementation of the **National Soil Action Plan**. X-ray absorption spectroscopy data were collected on the MEX-1 beamline at the Australian Synchrotron operated by the Australian Nuclear Science and Technology Organisation, enabled by the University of Sydney's membership of the BRiGHT Program. Data were collected with the assistance of Sydney Analytical, a Core Research Facility of the University of Sydney. I thank Jeremy Wykes from Australian Synchrotron, who helped with useful information during and after the beamtime, Ahmadi Jaya Permana from School of Chemistry and Xun Geng from Sydney Analytical for their help at the beamline.

I also thank Samuel Duyker for his assistance with XRD and XRF analysis that was carried out at Sydney Analytical, a core research facility at the University of Sydney

I am thankful to the Tertiary Education Trust Fund (TETFund), Nigeria for the financial support in tuition fees and living expenses.

References

Adams, W., and Kassim, J. (1984) Iron oxyhydroxides in soils developed from Lower Palaeozoic sedimentary rocks in mid-Wales and implications for some pedogenetic processes. *Journal of Soil Science* **35**, 117-126.

Amenkhienan, B. E., Dijkstra, F., Warren, C., and Singh, B. (2024) Understanding extractable metal species relationships with phosphorus sorption and organic carbon in soils. *Soil Research* **62**.

Ashida, K., Watanabe, T., Urayama, S., Hartono, A., Kilasara, M., Mvondo Ze, A. D., Nakao, A., Sugihara, S., and Funakawa, S. (2021) Quantitative relationship between organic carbon and geochemical properties in tropical surface and subsurface soils. *Biogeochemistry* **155**, 77-95.

Bascomb, C. L. (1968) Distribution of Pyrophosphate-Extractable Iron and Organic Carbon in Soils of Various Groups. *Journal of Soil Science* **19**, 251-268.

Bigham, J., Fitzpatrick, R. W., and Schulze, D. (2002) Iron oxides. *In* "Soil mineralogy with environmental applications" (J. Dixon and D. Schulz, eds.), Vol. 7, pp. 323-366. Soil Science Society of America Book Series.

Bigham, J., Golden, D., Bowen, L., Buol, S., and Weed, S. (1978) Iron Oxide Mineralogy of Well-drained Ultisols and Oxisols: I. Characterization of Iron Oxides in Soil Clays by Mössbauer Spectroscopy, X-ray Diffractometry, and Selected Chemical Techniques. *Soil Science Society of America Journal* **42**, 816-825.

Blume, H., and Schwertmann, U. (1969) Genetic evaluation of profile distribution of aluminum, iron, and manganese oxides. *Soil Science Society of America Journal* **33**, 438-444.

Brown, G., and Brindley, G. (1980) X-ray diffraction procedures for clay mineral identification.

Campbell, A., and Schwertmann, U. (1984) Iron oxide mineralogy of placic horizons. *Journal of Soil Science* **35**, 569-582.

Carlson, L. t., and Schwertmann, U. (1981) Natural ferrihydrites in surface deposits from Finland and their association with silica. *Geochimica et Cosmochimica Acta* **45**, 421-429.

Chen, Z., Zhang, L., Hou, F., and Xie, J. (2020) Verifying the feasibility of using Hand-Held X-ray fluorescence spectrometer to analyze Linqing brick: evaluation of the influencing factors and assessing reliability. *Heritage Science* **8**.

Childs, C. (1985) Towards understanding soil mineralogy. II. *Notes on ferrihydrite. NZ Soil Bureau Laboratory Report CM7. Lower Hutt, NZ.*

Cornell, R., and Schwertmann, U. (1979) Influence of organic anions on the crystallization of ferrihydrite. *Clays and Clay Minerals* **27**, 402-410.

Cornell, R. M., and Schwertmann, U. (2003) "The iron oxides: structure, properties, reactions, occurrences, and uses," Wiley-vch Weinheim.

Coward, E. K., Thompson, A. T., and Plante, A. F. (2017) Iron-mediated mineralogical control of organic matter accumulation in tropical soils. *Geoderma* **306**, 206-216.

De Faria, D. L., Venâncio Silva, S., and de Oliveira, M. T. (1997) Raman microspectroscopy of some iron oxides and oxyhydroxides. *Journal of Raman Spectroscopy* **28**, 873-878.

De Faria, D. L. A., and Lopes, F. N. (2007) Heated goethite and natural hematite: Can Raman spectroscopy be used to differentiate them? *Vibrational Spectroscopy* **45**, 117-121.

Diakonov, I., Khodakovsky, I., Schott, J., and Sergeeva, E. (1994) Thermodynamic properties of iron oxides and hydroxides; I, Surface and bulk thermodynamic properties of goethite (alpha -FeOOH) up to 500 K. *European Journal of Mineralogy* **6**, 967-983.

Dräger, G., Frahm, R., Materlik, G., and Brümmer, O. (1988) On the multipole character of the X-ray transitions in the pre-edge structure of Fe K absorption spectra. An experimental study. *physica status solidi (b)* **146**, 287-294.

Farmer, V., Russell, J., and Smith, B. (1983) Extraction of inorganic forms of translocated Al, Fe and Si from a podzol Bs horizon. *Journal of Soil Science* **34**, 571-576.

Fitzpatrick, R. W., and Schwertmann, U. v. (1982) Al-substituted goethite—an indicator of pedogenic and other weathering environments in South Africa. *Geoderma* **27**, 335-347.

Formenti, P., Caquineau, S., Chevaillier, S., Klaver, A., Desboeufs, K., Rajot, J.-L., Belin, S., and Briois, V. (2014) Dominance of goethite over hematite in iron oxides of mineral dust from Western Africa: Quantitative partitioning by X-ray absorption spectroscopy. *Journal of Geophysical Research: Atmospheres* **119**, 12,740-12,754.

Frey, P. A., and Reed, G. H. (2012) The ubiquity of iron. *ACS Chemical Biology* **7**, 1477-1481.

Galoisy, L., Calas, G., and Arrio, M. A. (2001) High-resolution XANES spectra of iron in minerals and glasses: structural information from the pre-edge region. *Chemical Geology* **174**, 307-319.

Giannetta, B., Cassetta, M., Oliveira de Souza, D., Mariotto, G., Aquilanti, G., and Zaccone, C. (2022) Coupling X-ray Absorption and Raman Spectroscopies to Characterize Iron Species in a Karst Pedosedimentary Record. *Soil Systems* **6**, 24.

Hanesch, M. (2009) Raman spectroscopy of iron oxides and (oxy) hydroxides at low laser power and possible applications in environmental magnetic studies. *Geophysical Journal International* **177**, 941-948.

Heckman, K., Lawrence, C. R., and Harden, J. W. (2018) A sequential selective dissolution method to quantify storage and stability of organic carbon associated with Al and Fe hydroxide phases. *Geoderma* **312**, 24-35.

Higashi, T., De Coninck, F., and Gelaude, F. (1981) Characterization of some spodic horizons of the Campine (Belgium) with dithionite-citrate, pyrophosphate and sodium hydroxide-tetraborate. *Geoderma* **25**, 131-142.

IUSS Working Group WRB (2022) World Reference Base for Soil Resources 2014, International Soil Classification System for Naming Soils and Creating Legends for Soil Maps, World Soil Resources Reports No. 106. UN Food and Agriculture Organization Rome.

Jackson, M. L., Lim, C. H., and Zelazny, L. W. (1986) Oxides, hydroxides, and aluminosilicates. *In "Methods of soil analysis. Part 1. Physical and mineralogical methods"* (A. Klute, ed.), pp. 101-150. Soil Science Society of America: Madison Wisconsin.

Jeanroy, E., and Guillet, B. (1981) The occurrence of suspended ferruginous particles in pyrophosphate extracts of some soil horizons. *Geoderma* **26**, 95-105.

Jepson, W., and Rowse, J. (1975) The composition of kaolinite—an electron microscope microprobe study. *Clays and Clay Minerals* **23**, 310-317.

Kaiser, K., and Guggenberger, G. (2000) The role of DOM sorption to mineral surfaces in the preservation of organic matter in soils. *Organic Geochemistry* **31**, 711-725.

Kämpf, N., and Schwertmann, U. (1983) Goethite and hematite in a climosequence in southern Brazil and their application in classification of kaolinitic soils. *Geoderma* **29**, 27-39.

Kirsten, M., Mikutta, R., Vogel, C., Thompson, A., Mueller, C. W., Kimaro, D. N., Bergsma, H. L. T., Feger, K. H., and Kalbitz, K. (2021) Iron oxides and aluminous clays selectively control soil carbon storage and stability in the humid tropics. *Scientific Reports* **11**.

Kleber, M., Eusterhues, K., Keiluweit, M., Mikutta, C., Mikutta, R., and Nico, P. S. (2015) Mineral–organic associations: formation, properties, and relevance in soil environments. *Advances in Agronomy* **130**, 1-140.

Kraft, S., Stümpel, J., Becker, P., and Kuetgens, U. (1996) High resolution x-ray absorption spectroscopy with absolute energy calibration for the determination of absorption edge energies. *Review of scientific instruments* **67**, 681-687.

Loeppert, R., and Inskeep, K. (1996) Methods of Soil Analysis: Part III. Chemical Methods. (A. L. P. D.L. Sparks, P.A. Helmke, R.H. Loeppert, P.N. Soltanpour, M.A. Tabatabai, C.T. Johnston, M.E. Sumner, ed.), pp. 639-664. *Soil Science Society of America*, Madison, WI.

Mansfeldt, T., Schuth, S., Häusler, W., Wagner, F. E., Kaufhold, S., and Overesch, M. (2012) Iron oxide mineralogy and stable iron isotope composition in a Gleysol with petrogleyic properties. *Journal of soils and sediments* **12**, 97-114.

McKeague, J. (1967) An evaluation of 0.1 M pyrophosphate and pyrophosphate-dithionite in comparison with oxalate as extractants of the accumulation products in podzols and some other soils. *Canadian Journal of Soil Science* **47**, 95-99.

McKeague, J., and Day, J. (1966) Dithionite-and oxalate-extractable Fe and Al as aids in differentiating various classes of soils. *Canadian Journal of Soil Science* **46**, 13-22.

Mehra, O., and Jackson, M. (1960) Iron oxide removal from soils and clays by a dithionite–citrate system buffered with sodium bicarbonate. *In* "*Clays and clay minerals*", pp. 317-327. *Elsevier*.

Melo, V. F., Singh, B., Schaefer, C. E. G. R., Novais, R. F., and Fontes, M. P. F. (2001) Chemical and Mineralogical Properties of Kaolinite-Rich Brazilian Soils. *Soil Science Society of America Journal* **65**, 1324-1333.

Murad, E. (2010) Mossbauer spectroscopy of clays, soils and their mineral constituents. *Clay Minerals* **45**, 413-430.

Murad, E., and Fischer, W. R. (1988) The geobiochemical cycle of iron. *In* "Iron in soils and clay minerals", pp. 1-18. Springer.

O'day, P. A., Rivera Jr, N., Root, R., and Carroll, S. A. (2004) X-ray absorption spectroscopic study of Fe reference compounds for the analysis of natural sediments. *American Mineralogist* **89**, 572-585.

Parfitt, R., and Childs, C. (1988) Estimation of forms of Fe and Al-a review, and analysis of contrasting soils by dissolution and Mossbauer methods. *Soil Research* **26**, 121-144.

Parfitt, R., Childs, C., and Eden, D. (1988) Ferrihydrite and allophane in four Andepts from Hawaii and implications for their classification. *Geoderma* **41**, 223-241.

Parfitt, R., and Henmi, T. (1982) Comparison of an oxalate-extraction methon and an infrared spectroscopic method for determining allophane in soll clays. *Soil Science and Plant Nutrition* **28**, 183-190.

Prasetyo, B., and Gilkes, R. (1994) Properties of iron-oxides from red soils derived from volcanic tuff in West Java. *Soil Research* **32**, 781-794.

Prietzel, J., Thieme, J., Eusterhues, K., and Eichert, D. (2007) Iron speciation in soils and soil aggregates by synchrotron-based X-ray microspectroscopy (XANES, μ-XANES). *European Journal of Soil Science* **58**, 1027-1041.

Ravel, B., and Newville, M. (2005) ATHENA, ARTEMIS, HEPHAESTUS: data analysis for X-ray absorption spectroscopy using IFEFFIT. *Journal of Synchrotron Radiation* **12**, 537-541.

Scheinost, A., and Schwertmann, U. (1999) Color identification of iron oxides and hydroxysulfates: use and limitations. *Soil Science Society of America Journal* **63**, 1463-1471.

Scheinost, A. C., and Singh, B. (2023) Metal oxides. *In* "Encyclopedia of Soils in the Environment (Second Edition)" (M. J. Goss and M. Oliver, eds.), pp. 135-148. Academic Press, Oxford.

Schwertmann, U. (1964) Differenzierung der eisenoxide des bodens durch extraktion mit ammoniumoxalat-Lösung. *Zeitschrift für Pflanzenernährung, Düngung, Bodenkunde* **105**, 194-202.

Schwertmann, U. (1988) Occurrence and formation of iron oxides in various pedoenvironments. *In* "Iron in soils and clay minerals" (J. Stocki, ed.), pp. 267-308. Springer, Dordrecht, Netherlands.

Schwertmann, U. (1993) Relationships between iron oxides, soil color, and soil formation. *In* "Soil Color. SSSA Special Publication" (J. Bigham and E. Ciolkosz, eds.), Vol. 31, pp. 51-69. Soil Science Society of America, Madison, Wisconsin.

Schwertmann, U., and Cornell, R. M. (2008) "Iron oxides in the laboratory: preparation and characterization," John Wiley & Sons.

Schwertmann, U., and Fischer, W. (1973) Natural "amorphous" ferric hydroxide. *Geoderma* **10**, 237-247.

Schwertmann, U., and Lentze, W. (1966) Bodenfarbe und eisenoxidform. *Zeitschrift für Pflanzenernährung, Düngung, Bodenkunde* **115**, 209-214.

Schwertmann, U., Schulze, D., and Murad, E. (1982) Identification of ferrihydrite in soils by dissolution kinetics, differential x-ray diffraction, and Mössbauer spectroscopy. *Soil Science Society of America Journal* **46**, 869-875.

Schwertmann, U., and Taylor, R. M. (1989) Iron oxides. *Minerals in Soil Environments* **1**, 379-438.

Ségalen, P. (1971) Metallic oxides and hydroxides in soils of the warm and humid areas of the world: formation, identification, evolution. *Soils and Tropical Weathering. UNESCO, Paris*.

Singh, B., and Gilkes, R. (1992) Properties and distribution of iron oxides and their association with minor elements in the soils of south-western Australia. *Journal of Soil Science* **43**, 77-98.

Singh, B., Gräfe, M., Kaur, N., and Liese, A. (2010) Applications of synchrotron-based X-ray diffraction and X-ray absorption spectroscopy to the understanding of poorly crystalline and metal-substituted Iron oxides. *In* "Developments in Soil Science", Vol. 34, pp. 199-254. Elsevier.

Skjemstad, J., Bushby, H., and Hansen, R. (1990) Extractable Fe in the surface horizons of a range of soils from Queensland. *Soil Research* **28**, 259-266.

Sun, J., Mailloux, B. J., Chillrud, S. N., van Geen, A., Thompson, A., and Bostick, B. C. (2018) Simultaneously quantifying ferrihydrite and goethite in natural sediments using the method of standard additions with X-ray absorption spectroscopy. *Chemical geology* **476**, 248-259.

Sundman, A., Karlsson, T., Laudon, H., and Persson, P. (2014) XAS study of iron speciation in soils and waters from a boreal catchment. *Chemical Geology* **364**, 93-102.

ThomasArrigo, L. K., and Kretzschmar, R. (2022) Iron speciation changes and mobilization of colloids during redox cycling in Fe-rich, Icelandic peat soils. *Geoderma* **428**, 116217.

Viscarra Rossel, R., Bui, E., De Caritat, P., and McKenzie, N. (2010) Mapping iron oxides and the color of Australian soil using visible–near-infrared reflectance spectra. *Journal of Geophysical Research: Earth Surface* **115**.

von Fromm, S. F., Jungkunst, H. F., Amenkhienan, B., Hall, S. J., Georgiou, K., Pries, C. H., Montaño-López, F., Quesada, C. A., Rasmussen, C., Schrumpf, M., Singh, B., Thompson, A., Wagai, R., and Fiedler, S. (2025) Moisture and soil depth govern relationships between soil organic carbon and oxalate-extractable metals at the global scale. *Biogeochemistry* **168**, 20.

Walker, A. L. (1983) The Effects of Magnetite on Oxalate- and Dithionite-Extractable Iron. *Soil Science Society of America Journal* **47**, 1022-1026.

Westre, T. E., Kennepohl, P., DeWitt, J. G., Hedman, B., Hodgson, K. O., and Solomon, E. I. (1997) A multiplet analysis of Fe K-edge 1s→ 3d pre-edge features of iron complexes. *Journal of the American Chemical Society* **119**, 6297-6314.

Wilke, M., Farges, F., Petit, P.-E., Brown Jr, G. E., and Martin, F. (2001) Oxidation state and coordination of Fe in minerals: An Fe K-XANES spectroscopic study. *American Mineralogist* **86**, 714-730.

Yamamoto, T. (2008) Assignment of pre-edge peaks in K-edge x-ray absorption spectra of 3d transition metal compounds: electric dipole or quadrupole? *X-Ray Spectrometry* **37**, 572-584.

Chapter Five

Competitive adsorption between phosphate and dissolved organic carbon in iron rich soils

5.0 Abstract

The competitive adsorption between phosphate and dissolved organic carbon (DOC) have been reported in Andosols and podzols. However, the published results on the competitive adsorption between P and DOC are unclear and sometimes contradictory. Phosphate and DOC competition for adsorption sites on minerals may be quite different in the surface and subsurface soils. In this study we used surface and subsurface soils with substantial Fe oxides contents from two sites i.e., Wagga Wagga and Tumbarumba to evaluate the adsorption of phosphate and DOC behaviour. Adsorption data were fitted into linear initial mass (IM) isotherm. The results showed that both surface and subsurface soils from Tumbarumba had a greater phosphate adsorption capacity than the soils from Wagga Wagga. Phosphate adsorption was greater for the subsurface (m = 0.72) than the surface (m = 0.82) soil from Tumbarumba. The trend for surface and subsurface was opposite for Wagga Wagga soils, where phosphate adsorption capacity was greater for surface (m = 0.55) than the subsurface (m = 0.37) soils. The greatest capacity for DOC adsorption in both studied soils occurred in the subsurface soils. In the mixed solution of P and DOC, phosphate adsorption promoted DOC desorption in the surface and subsurface soils from Wagga Wagga and Tumbarumba. The results of this study have crucial implications on the sustainability of Fe-rich soils. The adsorption of phosphate promoted DOC desorption in these soils, which may impair OC sequestration and stabilisation and therefore enhance microbial decomposition of OC in these soils. Furthermore, phosphate might play a major role in influencing the microbial stability of OC adsorption in these soils.

Keywords: Phosphate, DOC, soils, adsorption, desorption, linear initial mass isotherm

5.1 Introduction

Phosphorus (P) is an essential plant nutrient that is indispensable for several physiological and biochemical processes including photosynthesis, respiration, enzymes regulation and biosynthesis of structures such as cell membranes, DNA and RNA (Hawkesford *et al.*, 2023). Despite the presence of considerable total P content in most soils, crop productivity of agricultural soils is often limited by P availability, because a very small portion (< 1%) of the total P is present in soluble forms (Bünemann *et al.*, 2011; Balemi and Negisho, 2012). Phosphorus is particularly the most commonly limiting nutrient in highly weathered soils of tropical and subtropical regions because of their high P adsorption capacity and low levels of P availability (Singh and Gilkes, 1991; Tiessen, 2005; De Campos *et al.*, 2016).

Plant roots absorb P as $H_2PO_4^-$ and HPO_4^{2-} ions, which are the predominant orthophosphate species in soil solution (Tiessen, 2005). Phosphate concentration in soil solution is controlled by several reactions that have been considered under three categories: (i) adsorption-desorption, (ii) dissolution-precipitation, and (iii) mineralisation-immobilisation (Sims and Pierzynski, 2005; Bünemann, 2015; Roberts and Johnston, 2015). The availability of phosphate in soils is affected by root characteristics, soil properties (such as pH, clay and organic matter (OM) contents, iron (Fe) and aluminium (Al) oxides including hydroxides, oxyhydroxides and oxides) and environmental conditions (Singh and Gilkes, 1991; Brennan *et al.*, 1994; Börling *et al.*, 2001; Burt *et al.*, 2002). Soluble P can undergo different chemical reactions in soils; however, the solution P concentration is primarily controlled by adsorption-desorption reactions with soil minerals, in particular Fe/Al oxides and edge sites of phyllosilicates (Hinsinger, 2001; Devau *et al.*, 2009). Variable charge soils (e.g., Andisols) and highly weathered soils (e.g., Oxisols and Ultisols) often have greater P adsorption capacity than younger and less weathered soils such as Inceptisols (Yang and Post, 2011; Brenner *et al.*, 2018). Some studies have reported that P adsorption is mostly influenced by Fe oxides in the

tropical and subtropical soils (Borggaard, 1983; Peña and Torrent, 1984; Borggaard *et al.*, 1990; Agbenin, 2003). Contrary to this, other studies have observed that Al oxides play a more dominant role than Fe oxides in P adsorption capacity of both temperate (Lopez-Hernandez and Burnham, 1974; Börling *et al.*, 2001) and tropical soils (Fontes and Weed, 1996; De Campos *et al.*, 2016). Phosphate adsorption capacity has been closely related to crystalline Fe oxides (dithionite citrate bicarbonate extractable Fe) and amorphous Fe and Al oxides (ammonium oxalate extractable Fe and Al) in soils from different regions (Ballard and Fiskell, 1974; Borggaard, 1983; Peña and Torrent, 1984; Ryan *et al.*, 1985; Loganathan *et al.*, 1987; Singh and Gilkes, 1991; Sanyal *et al.*, 1993; Agbenin, 2003; Wiriyakitnateekul *et al.*, 2005).

Both Fe and Al oxides possess a large specific surface area (SSA) and positive charge at typical field pH, which are important characteristics for P adsorption in soils (Bigham *et al.*, 1978; Peña and Torrent, 1984; Fontes and Weed, 1996). The process of phosphate adsorption onto variable charge surfaces such as Fe/Al oxides primarily occurs through phosphate exchange with hydroxyl (OH^-), so called ligand exchange reaction, that results in the formation of inner-sphere surface complexes (Parfitt *et al.*, 1975; Goldberg and Sposito, 1985). The inner-sphere surface complexes can either be binuclear or mononuclear surface complexes (Atkinson *et al.*, 1974; Barron *et al.*, 1988; Arai and Sparks, 2001). In the binuclear surface complex formation, single-coordinated hydroxyl (OH) groups on the surfaces of Fe oxides is exchanged or replaced by phosphate (Parfitt and Atkinson, 1976; Borggaard *et al.*, 1990; Torrent *et al.*, 1992). In the mononuclear surface complex formation, phosphate is coordinated in a monodentate mode to the OH group on the surfaces of Fe oxides (Persson *et al.*, 1996).

Dissolved organic carbon (DOC) is abundant in terrestrial and aquatic environments. Although DOC forms only a small part of the total organic carbon in soils, it is highly reactive and labile (McGill *et al.*, 1986; Kalbitz *et al.*, 2000; Kalbitz and Kaiser, 2003). It is operationally defined as the fraction of organic C in solution that passed through a 0.45 μm pore size filter (Kalbitz

et al., 2000; Zsolnay, 2003; Bolan *et al.*, 2011). DOC actively influences many biogeochemical processes such as, mineral weathering, leaching, nutrient translocation, microbial activity, soil formation, and transport of metals and pollutants (Kaiser and Zech, 1998; Kalbitz *et al.*, 2000; Mavi *et al.*, 2012). Adsorption of DOC onto Fe oxides has been recognised as an important process in the accumulation and preservation of organic carbon in soils (Parfitt *et al.*, 1977). Thus similar to phosphate, DOC concentration in soil solution is controlled mainly by adsorption processes onto mineral surfaces (Kaiser and Zech, 1998). DOC adsorption on minerals can occur via ligand exchange surface complexation, cation bridging, anion exchange, hydrogen bonding, and hydrophobic interactions (Gu *et al.*, 1994; Sposito, 2004). However, Fe and Al oxides have been reported to adsorb DOC preferentially through ligand exchange reactions (Parfitt *et al.*, 1977; Tipping, 1981; Davis, 1982; Gu *et al.*, 1994).

Considering the similar nature of their adsorption reactions, phosphate and DOC may compete for adsorption sites in soils (Guppy *et al.*, 2005; Spohn *et al.*, 2022). Different observations have been made on the competitive adsorption of DOC and phosphate in soils. Many studies have observed that DOC including, high molecular weight organic compounds (HOCs), such as humic acid (HA) and fulvic acids (FA), competed strongly with phosphate for adsorption sites and caused a significant decrease in phosphate adsorption (Sibanda and Young, 1986; Ohno and Crannell, 1996; Guppy *et al.*, 2005; Hunt *et al.*, 2007; Fu *et al.*, 2013; Chase *et al.*, 2018; Yang *et al.*, 2019). Yang *et al.* (2019) reported that increasing SOM decreased the strength of P adsorption, thereby increased P availability in soils. Some other studies have shown that low molecular weight organic acids (LOAs), such as citrate, oxalate, polygalacturonate, acetate, malate, tartrate and protocatechuate, significantly decreased P adsorption (Nagarajah *et al.*, 1970; Earl *et al.*, 1979; Lopez-Hernandez *et al.*, 1986; Hue, 1991; Bolan *et al.*, 1994; Violante and Gianfreda, 2023). In contrast, several studies have found that organic compounds and organic matter do not compete with phosphate for adsorption sites

(Harter, 1969; Hinga, 1973; Appelt *et al.*, 1975; Borggaard *et al.*, 1990). Appelt *et al.* (1975) suggested that in Andosol, formation of Al (OH)-HA complexes exposed new sites for phosphate adsorption, therefore HA adsorption did not block the adsorption of phosphate. Harter (1969) suggested that OM is important for initial adsorption of phosphate (by anion exchange mechanism) that was subsequently transformed into less soluble Fe and Al phosphates. Spohn *et al.* (2022) observed that adsorption and desorption of organic compounds were greatly influenced by changes in concentration of P in the soil solution. Phosphate adsorption promoted OM desorption thereby increasing DOC concentration, thus phosphate ions competed more effectively for reactive sites than DOC (Spohn and Schleuss, 2019; Spohn *et al.*, 2022). Increased desorption of OC may further lead to destabilisation of OC and enhanced microbial decomposition of OM in soils (Beck *et al.*, 1999; Kahle *et al.*, 2004; Spohn and Schleuss, 2019; Li *et al.*, 2020). Adsorption of P is reported to promote the desorption of LOAs, such as malate, oxalate, phthalic acid (Afif *et al.*, 1995; Liu *et al.*, 1999; Guan *et al.*, 2006). Phosphate adsorption not only promoted DOC desorption, but also occupied the sorption sites thereby prevented DOC adsorption in soils (Gu *et al.*, 1994; Kaiser and Zech, 1997; Hur and Schlautman, 2004; Kahle *et al.*, 2004; Guppy *et al.*, 2005; Hunt *et al.*, 2007; Schneider *et al.*, 2010).

Most earlier studies have considered competitive adsorption between LOAs, HA, FA, DOC and phosphate in Andosols and podzols. However, the published results on the competitive adsorption between P and DOC are unclear and sometimes contradictory. Although, most agricultural soils in Australia are naturally P-deficient, but P accumulation has occurred in these soils with the long history of P fertiliser application including the historic excess addition of P fertilisers (Williams, 1950; McLaughlin *et al.*, 1992; Weaver and Wong, 2011). With growing focus on increasing OC in soils, research is needed to understand the interaction between DOC and P in Australian soils, many of which have high Fe (and Al) oxides contents. Furthermore,

little or no attention has been paid to understand the competitive DOC and phosphate adsorption behaviour in subsurface soils that have much less organic matter and greater number of reactive sites such as in Luvisols. Thus, phosphate and DOC competition for adsorption sites on minerals may be quite different in the surface and subsurface soils. Therefore, the aim of this study was to evaluate the adsorption of phosphate and DOC behaviour in surface and subsurface soils with substantial Fe oxides contents. We hypothesised that phosphate or DOC adsorption will be greater in the subsurface soils than the surface soils. Furthermore, we hypothesised that DOC would inhibit phosphate adsorption in both surface and subsurface soils.

5.2 Materials and Methods

5.2.1 Soil samples selection

Surface (0 – 20 cm) and Subsurface (20 – 40 cm) samples were collected from Wagga Wagga (35.03^{o} S, 147.33^{o} E) and Tumbarumba (35.74^{o} S, 147.98^{o} E) in New South Wales, Australia. The climate for Wagga Wagga is humid subtropical to temperate. The mean minimum annual temperature is 9.1^{o}C and mean maximum temperature is 22.3^{o}C while the mean annual rainfall is 573.4 mm. The climate for Tumbarumba is humid subtropical to temperate with an average rainfall of 977.9 mm. The mean minimum annual temperature is 5.7^{o}C and the mean maximum annual temperature is 19.8^{o}C. Wagga Wagga site was bare fallow that had earlier been cropped with wheat, while Tumbarumba site had native pasture. The soils collected from Wagga Wagga and Tumbarumba are classified as a Luvisol and a Ferralsol, respectively, according to the IUSS Working Group WRB (2022). Soil samples were air-dried, crushed, passed through a 2 mm sieve and stored at room temperature for laboratory analysis and adsorption experiments.

5.2.2 Soil analyses

Soil chemical and physical properties are shown in Table 5.1. Soil pH was measured in 1:5 of soil and 0.01 M calcium chloride ($CaCl_2$) using a glass electrode pH meter (Rayment and Lyons, 2011). Total C (TC) in soils was analysed using a vario MACRO cube Elementar CHN analyser and considering the acidic pH of both soils, the total carbon was assumed to be all organic C. Particle size analysis (PSA) was determined by the hydrometer method (Gee and Or, 2002). Cation exchange capacity (CEC) was determined by the silver thiourea method (Rayment and Lyons, 2011). The total free Fe oxides content was determined using the dithionite-citrate-bicarbonate (DCB) extraction procedure described by Mehra and Jackson (1960). The content of short-range ordered and poorly crystalline Fe oxides was measured by extracting with ammonium oxalate (OX) at pH 3.0 in dark for 4 h (McKeague and Day, 1966). Organic matter complexed with Fe was determined using sodium pyrophosphate (PP) extraction procedure described by McKeague (1967).

Oriented clays X-ray diffraction (XRD) patterns were obtained using a PANalytical X'Pert PRO instrument (40 kV and 40 mA) with CuKa radiation for the identification of phyllosilicate minerals in the clay fraction of soils. Random powder XRD patterns were obtained using a STOE Stadi P instrument (50 kV and 40 mA) with MoKα radiation for the identification of all minerals in the clay fraction of soils.

Table 5.1. *Selected chemical and physical properties of soils used in the study*

Properties	Wagga Wagga		Tumbarumba	
	Surface soil	Subsurface soil	Surface soil	Subsurface soil
pH $_{(1:5\ CaCl_2)}$	4.48	4.75	4.19	4.32
Organic C (g/kg)	12.4	9.8	20.3	18.5
CEC ($mmol_c/kg$)	96.4	97.6	97.9	98
Sand (%)	68	60	36	32
Silt (%)	10	4	12	12
Clay (%)	22	36	52	56
Fe_{OX} (g/kg)	1.75	1.59	7.69	7.38
Fe_{DCB} (g/kg)	12.83	17.93	41.70	39.05
Fe_{PP} (g/kg)	0.45	0.18	0.71	0.19
Al_{OX} (g/kg)	1.61	1.90	7.38	7.66
Al_{DCB} (g/kg)	1.25	1.57	5.64	6.01
Al_{PP} (g/kg)	0.94	0.74	2.65	2.44
Extractable $DOC_{0.01M\ CaCl2}$ (mmol/L)	1.23	0.93	1.47	0.52
Extractable $P_{0.01M\ CaCl2}$ (mmol/L)	0.89	<0.01	0.14	0.01
Minerals in the clay fraction	Goethite, hematite, kaolinite, illite, quartz		Goethite, hematite, kaolinite, smectite, traces of illite	

5.2.3 Phosphate adsorption experiment

2.0 g of surface and subsurface soil samples were weighed in duplicates and transferred into 50 mL centrifuge tubes. The soil samples were equilibrated with 40 mL of different P concentrations (up to 10 concentrations for each soil), ranging from 0 to 2.58 mmol/L for Wagga Wagga and 0 to 8.1 mmol/L for Tumbarumba using potassium dihydrogen phosphate (KH_2PO_4) in a 0.01 M calcium chloride ($CaCl_2$) matrix. Before adding P solutions to soil, the solution pH was adjusted to 6.0 using 0.1 M sodium hydroxide (NaOH). Three drops of chloroform were added into each centrifuge tubes to inhibit microbial activity. The centrifuge tubes were shaken on a rotary laboratory shaker at 19 ± 1°C for 17 hours, centrifuged at 1800 ×*g* for 15 minutes and supernatants were filtered through 0.45 µm PTFE syringe membrane filter. Supernatant pH was measured and P concentration in solution was analysed colorimetrically using the ascorbic acid method (Murphy and Riley, 1962).

5.2.4 DOC adsorption experiment

Dissolved organic carbon (DOC) used for the adsorption experiment was extracted from decomposed residues of pine (*Pinus radiata*), which is commonly used in timber plantations in Australia. For DOC extraction, 100 g of decomposed residues was soaked in 1000 mL of deionised water, and the suspension was shaken on a rotary shaker for 1 hour. Then the mixture was allowed to stand for 24 hours at 19 ± 1ºC. The mixture was then centrifuged at 3280 ×*g* for 20 minutes and supernatant was filtered through 0.45 µm Millipore white gridded membrane filter using a vacuum suction unit. The DOC concentration in the solution was ~200 mg /L and the pH was 5.79.

Similar to P adsorption, DOC adsorption experiments were carried out in duplicates for both surface and subsurface soil samples. Briefly, 3 g soil was mixed with 30 mL 0.01 M $CaCl_2$ solution (up to 10 solutions for each soil) containing a range of DOC concentration (0 to 11.65 mmol C/L) in 50 mL centrifuge tubes. The solution pH was adjusted to 6.0 before adding to soil samples. The suspensions were then placed on a rotary shaker for 17 hours at 19 ± 1ºC. The suspensions were then allowed to settle for 30 minutes before filtering through 0.45 µm PTFE syringe membrane filter. After filtration, the pH of the supernatants was measured. The DOC concentration in the initial and equilibrium solutions (supernatants) were analysed using a Shimadzu TOC-L total C analyser.

5.2.5 Phosphate-DOC competitive adsorption experiment

Batch adsorption experiment was conducted using 2.0 g of air-dried surface and subsurface soil samples (in duplicates) into 50 mL centrifuge tubes. Solutions containing different P and OC concentrations (up to 9 concentrations of each P and DOC for each soil), with P concentration ranging from 0 to 4 mmol/L using potassium dihydrogen phosphate (KH_2PO_4) and DOC concentration ranging from 0 to 5 mmol/L in a 0.01 M $CaCl_2$ solution. The soil samples were

equilibrated with 40 mL of the mixture solutions, with the solution pH adjusted to 6.0 before adding to soil samples. The suspensions were placed on a rotary shaker for 17 hours at 19 ± 1°C. The suspensions were then allowed to settle for 30 minutes and filtered through 0.45 µm PTFE syringe membrane filter. After filtration, the pH of the supernatants was measured. The initial and final P and DOC concentrations in solution were analysed as described earlier.

5.2.6. Fitting of adsorption data

The Langmuir and Freundlich equations did not fit the adsorption very well (R^2 = 0.35 and R^2 = 0.72). In systems where the solute (or adsorbate) to be adsorbed is already present in the adsorbent (such as, for the adsorption of phosphate and DOC on soils), the use of initial mass isotherm has been recommended to describe the adsorption data (Nodvin *et al.*, 1986). In essence, initial mass isotherm is a linear adsorption isotherm that accounts for a solute initially present within the adsorbent. Hence the adsorption data were fitted into linear initial mass (IM) isotherm:

$$RE = mX_i - b$$

where RE is the amount of P or DOC removed from or released into the solution normalised for soil mass (mmol/kg), X_i is the initial P and DOC concentrations in the solution, normalised to mass of soil, m (slope of the linear regression) is the partition coefficient of the initial mass isotherm and - b (intercept) is the desorption term.

The m of the linear IM isotherm was used to determine the distribution coefficient (K_d).

$$K_d = \left(\frac{m}{1-m}\right) \times \frac{V}{M}$$

Where V is the volume of solution and M is the mass of soil.

The slope (m) and intercept (– b) were used to determine reactive soil pool (RSP) of solute.

$$RSP = \frac{b}{(1-m)}$$

5.3 Results

5.3.1 Phosphate adsorption

The linear IM model described all the adsorption data very well (R^2 = 0.98 and R^2 = 0.99). The isotherm plots for surface and subsurface samples of the two soils are shown in Figure 5.1, and the model parameters are presented in Table 5.2. The surface soil from Wagga Wagga did not adsorb P from solutions until the initial P loadings of up to 32 mmol/kg, rather, P was desorbed at loadings lower than this. The amount of P desorbed decreased with increasing initial P concentration, and the P desorption estimated from the intercept was -18.3±0.53 mmol/kg (Figure 5.1a and Table 5.2). Tumbarumba soil showed greater capacity for P adsorption than Wagga Wagga soil, indicated by steeper slope (m) and higher distribution coefficient (K_d) values (Table 5.2). The trend for surface and subsurface was opposite for the two soils, with the Wagga-Wagga surface soil showing greater capacity for phosphate adsorption than the corresponding subsurface soil, whereas the phosphate adsorption capacity was greater for the subsurface soil than the surface soil from Tumbarumba (Table 5.2). The reactive soil pool (RSP) of phosphate was very high (40.6 mmol/kg) in the surface soil from Wagga Wagga, and low (1.00 mmol/kg) in the surface soil from Tumbarumba, and the subsurface samples had negligible or no RSP (Table 5.2). The equilibrium solution pH in all samples decreased from the initial adjusted pH value (6.0). Wagga Wagga surface and subsurface soils had a mean equilibrium pH value of 4.83 and 5.37, respectively and Tumbarumba surface and subsurface soils had a mean equilibrium pH value of 4.72 and 5.16, respectively. However, a small unit increase (0.1 – 0.4) in the equilibrium pH was observed with phosphate adsorption in the subsurface soil from Wagga Wagga and the surface and subsurface soils from Tumbarumba. Phosphate adsorption resulted in DOC desorption in all samples, varying between 6 and 8 mmol/kg in Wagga Wagga soils, and between 24 and 36 mmol/kg in Tumbarumba soils. The

desorption of DOC was greater in subsurface soil as compared to surface soil for both sites (Supplementary Figure 5.1). The plots of the phosphate adsorption or desorption data in relation to the equilibrium P concentration for surface and subsurface soils from Wagga Wagga and Tumbarumba are shown in Supplementary Figure 5.2.

The P adsorption coefficient showed a tendency to increase with increasing contents of clay, OC, Fe_{OX}, Fe_{DCB}, Al_{OX}, Al_{DCB}, Fe_{DCB}+Al_{DCB} and Fe_{OX}+Al_{OX} and decrease with increasing soil pH (Supplementary Figure 5.3).

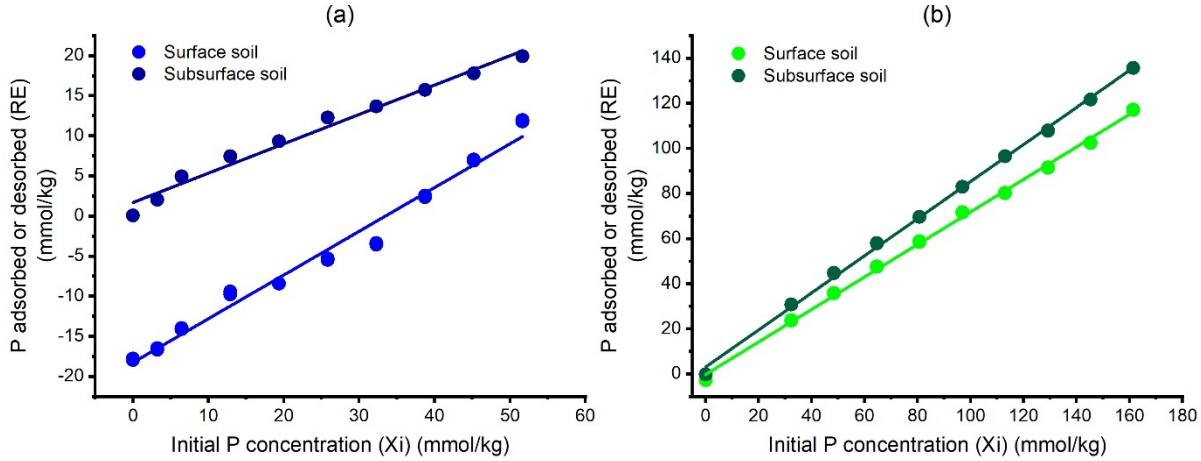

Figure 5.1. *Linear initial mass isotherms for phosphate adsorption or desorption on surface and subsurface soils from (a) Wagga Wagga, and (b) Tumbarumba. Positive RE values indicate adsorption and negative RE values indicates desorption.*

Table 5.2. *Regression parameters derived from the linear initial mass isotherms of phosphate adsorption onto surface and subsurface soils from Wagga Wagga and Tumbarumba*

Location	Depth (cm)	m±se	-b±se (mmol/kg)	K_d±se (10^{-5} m^3/g)	RSP (mmol/kg)	R^2
Wagga Wagga	0-20	0.55±0.02	-18.3±0.53	2.44±0.20	40.6	0.98
	20-40	0.37±0.01	1.68±0.34	1.17±0.05	-2.67	0.98
Tumbarumba	0-20	0.72±0.01	-0.28±0.72	5.14±0.26	1.00	0.99
	20-40	0.82±0.01	3.03±0.71	9.11±0.62	-16.8	0.99

5.3.3 DOC adsorption

The linear IM isotherms for DOC adsorption are shown in Figure 5.2. The surface and subsurface soil of Wagga Wagga and Tumbarumba did not adsorb DOC from the initial DOC

concentrations ranging between 1 mmol/kg and 15 mmol/kg, rather DOC was desorbed. The amount of DOC desorbed decreased with increasing initial DOC concentration. The linear IM isotherm parameters are shown in Table 5.3. The partition coefficient (slope) and distribution coefficient showed that both surface and subsurface soils from Tumbarumba had a greater capacity for DOC adsorption than the Wagga Wagga soils. Also, the subsurface soils from both sites had greater adsorption capacity than their corresponding surface soils.

All soil samples had a substantial RSP of DOC, with the highest value in the surface soil from Tumbarumba that is consistent with its highest OC concentration. The equilibrium solution pH in all samples decreased from the initial adjusted pH value (6.0). Wagga Wagga surface and subsurface soils had a mean equilibrium pH value of 4.62 and 5.04, respectively and Tumbarumba surface and subsurface soils had a mean equilibrium pH value of 4.35 and 5.40, respectively. However, a small unit increase of 0.1 in the equilibrium solution pH was observed with DOC adsorption in the surface soil from Wagga Wagga and the surface and subsurface soils from Tumbarumba. The adsorption DOC resulted in little desorption of P in both soils, with about 0.7 mmol/kg in Wagga Wagga soils, and < 0.05 mmol/kg in Tumbarumba soils. The desorption of P was greater in surface soil as compared to subsurface soil for both sites (Supplementary Figure 5.4). The plots of the DOC adsorption or desorption data in relation to the equilibrium DOC concentration for surface and subsurface soils from Wagga Wagga and Tumbarumba are shown in Supplementary Figure 5.5.

The DOC adsorption coefficient showed a tendency to increase with increasing contents of clay, OC, Fe_{OX}, Fe_{DCB}, Al_{OX}, Al_{DCB}, Fe_{DCB}+Al_{DCB} and Fe_{OX}+Al_{OX} and decrease with increasing soil pH (Supplementary Figure 5.6).

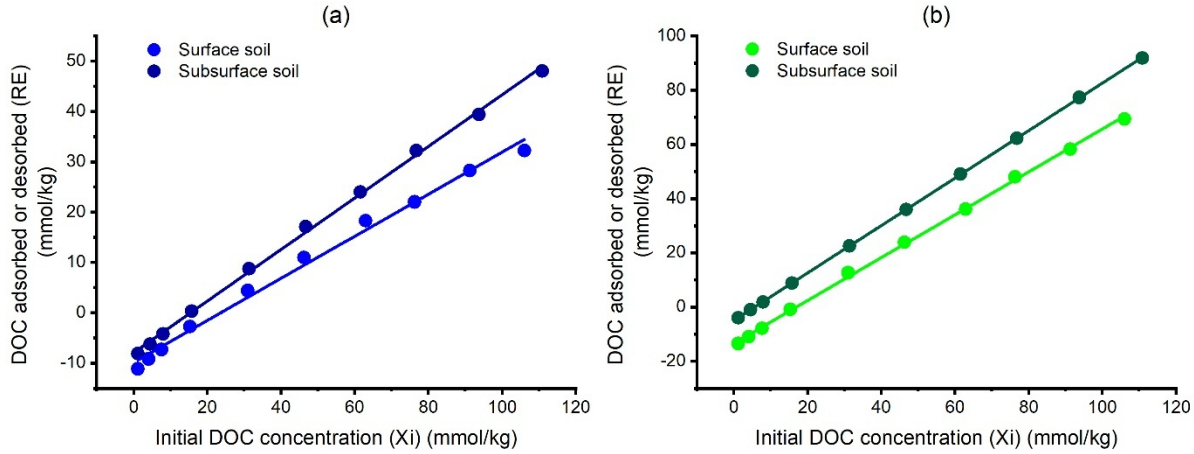

Figure 5.2. *Linear initial mass isotherms for dissolved organic carbon (DOC) adsorption or desorption on surface and subsurface soils from (a) Wagga Wagga, and (b) Tumbarumba. Positive RE values indicate adsorption and negative RE values indicates desorption.*

Table 5.3. *Regression parameters derived from the linear initial mass isotherms of DOC adsorption onto surface and subsurface soils from Wagga Wagga and Tumbarumba*

Location	Depth (cm)	m±se	-b±se (mmol/kg)	K_d±se (10^{-5} m^3/g)	RSP (mmol/kg)	R^2
Wagga Wagga	0-20	0.42±0.01	-9.88±0.49	1.45±0.06	17.0	0.99
	20-40	0.51±0.004	-7.93±0.26	2.08±0.03	16.2	0.99
Tumbarumba	0-20	0.79±0.01	-13.5±0.33	7.25±0.45	64.1	0.99
	20-40	0.88±0.001	-4.98±0.05	14.7±0.14	41.5	0.99

5.3.4 Competitive adsorption of phosphate and DOC

The linear IM isotherm for phosphate adsorption from mixed solution of P and DOC are presented in Figure 5.3, and the isotherm parameters are shown in Table 5.4. Tumbarumba soil showed greater capacity for phosphate adsorption than Wagga Wagga soil, indicated by steeper slope and higher distribution coefficient values. The trend for surface and subsurface was opposite for the two soils, with the Wagga-Wagga surface soil showing greater adsorption capacity than the corresponding subsurface soil, whereas the phosphate adsorption capacity was greater for the subsurface soil than the surface soil from Tumbarumba (Table 5.4). This was similar to the trend observed from the solution of only P as mentioned earlier. However, the slope and distribution coefficient values obtained from the mixed solution of P and DOC was higher than the values obtained from the solution of only P. The RSP of phosphate was

higher in the surface soil (22.50 mmol/kg) than in the subsurface (12.76 mmol/kg) from Wagga Wagga. Nevertheless, Tumbarumba soils had negligible or no RSP (Table 5.4). The plot of the phosphate adsorption or desorption data in relation to the equilibrium P concentration from mixed solution of P and DOC on surface and subsurface soils from Wagga Wagga and Tumbarumba is shown in Supplementary Figure 5.7.

The linear IM isotherm for DOC adsorption from mixed solution of P and DOC are presented in Figure 5.4, and the isotherm parameters are shown in Table 5.4. The surface and subsurface soils of Wagga Wagga did not adsorb DOC from mixed P and DOC solutions rather DOC was desorbed, but adsorption occurred on the subsurface soil at 32 mmol/kg. Similarly, the surface and subsurface soil of Tumbarumba did not adsorb DOC from the mixed P and DOC solutions, however, adsorption occurred on the subsurface soil from 22 mmol/kg. The partition coefficient and distribution coefficient showed that both surface and subsurface soils from Tumbarumba had a greater capacity for DOC adsorption than the Wagga Wagga soils. Also, the subsurface soils from both sites had greater adsorption capacity than their corresponding surface soils (Table 5.4). This was similar to the trend observed from the solution of only DOC as mentioned earlier. Nevertheless, the isotherm parameters obtained from the solution of only DOC was higher than the isotherm parameters obtained from the mixed solution of P and DOC.

The equilibrium solution pH in all samples decreased from the initial pH value (6.0), with varying degree depending on the initial soil pH. However, the equilibrium solution pH values of both soils increased with increasing depth. The mean equilibrium solution pH value for surface and subsurface soils of Wagga Wagga was 4.77 and 5.09, respectively and surface and subsurface soils of Tumbarumba was 4.63 and 4.95 respectively. Moreso, the adsorption of phosphate or DOC made no substantial change in the equilibrium solution pH values. The plot of the DOC adsorption or desorption data in relation to the equilibrium DOC concentration

from mixed solution of P and DOC on surface and subsurface soils from Wagga Wagga and Tumbarumba is shown in Supplementary Figure 5.8.

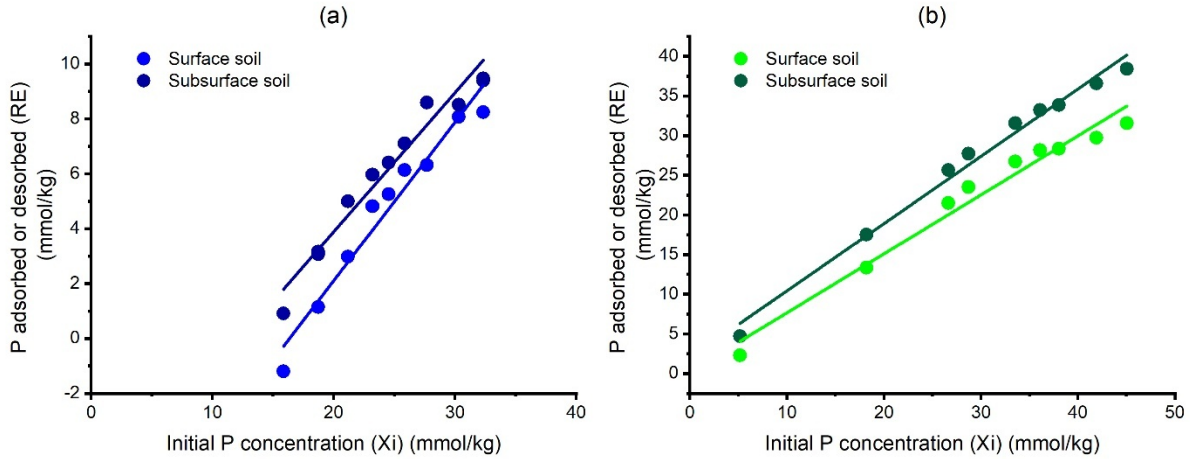

Figure 5.3. *Linear initial mass isotherms for phosphate adsorption or desorption from mixed solutions of P and DOC on surface and subsurface soils from (a) Wagga Wagga (b) Tumbarumba. Positive RE values indicate adsorption and negative RE values indicates desorption.*

Table 5.4. *Regression parameters derived from the linear initial mass isotherms of phosphate and DOC adsorption from mixed solution of P and DOC onto soils.*

Location	Depth (cm)	m±se	b±se (mmol/kg)	K_d±se ($10^{-5}m^3/g$)	RSP	R^2
			Phosphate adsorption			
Wagga Wagga	0-20	0.58±0.03	-9.45±0.77	2.76±0.34	22.5	0.96
	20-40	0.51±0.03	-6.25±0.71	2.08±0.25	12.8	0.95
Tumbarumba	0-20	0.74 ±0.03	0.21±1.03	5.69±0.89	-0.81	0.97
	20-40	0.85±0.02	1.93±0.79	11.3±1.78	-12.9	0.99
			Dissolved organic carbon adsorption			
Wagga Wagga	0-20	0.34±0.01	-14.4±0.20	1.03±0.05	21.9	0.98
	20-40	0.40±0.02	-11.1±0.28	1.33±0.11	18.4	0.97
Tumbarumba	0-20	0.22±0.01	-25.6±0.24	0.56±0.03	32.8	0.94
	20-40	0.55±0.01	-9.58±0.22	2.44±0.10	21.3	0.99

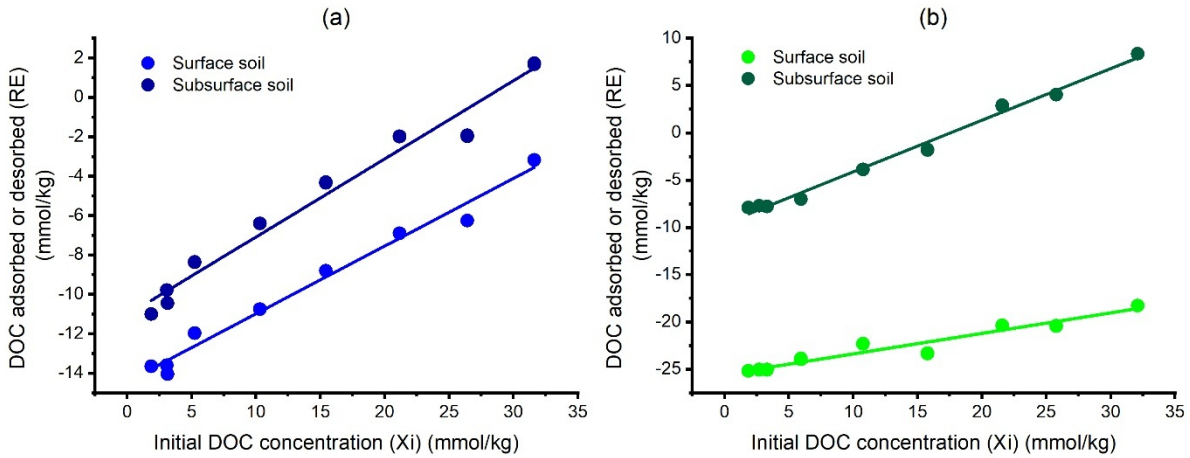

Figure 5.4. *Linear initial mass isotherms for dissolved organic carbon (DOC) adsorption or desorption from mixed solutions of P and DOC on surface and subsurface soils from (a) Wagga Wagga (b) Tumbarumba. Positive RE values indicate adsorption and negative RE values indicates desorption.*

5.4 Discussion

5.4.1 Adsorption studies

The surface charge of an adsorbent has effects on adsorption processes. Iron oxides are effective adsorbent of phosphate (Peña and Torrent, 1984; Singh and Gilkes, 1991). Iron oxides adsorb phosphate and DOC via ligand exchange reactions where a singly coordinated hydroxyl (OH) groups on the oxides surfaces are exchanged by the adsorbate (Borggaard *et al.*, 1990; Torrent *et al.*, 1992; Kaiser and Guggenberger, 2000; Watanabe, 2017). The linear IM isotherm parameters revealed that phosphate adsorption was greater in the subsurface soil than the surface soil from Tumbarumba. This support our hypothesis that phosphate adsorption will be greater in the subsurface soils than the surface soils. However, the isotherm parameters obtained from Wagga Wagga soils did not support our hypothesis, rather phosphate adsorption was greater in the surface soil than the subsurface soil from Wagga Wagga.

The surface and subsurface soils from Tumbarumba had the greatest capacity for phosphate adsorption than the surface and subsurface soils of Wagga Wagga. This result was expected considering that Tumbarumba soils had higher contents of Fe_{OX}, Fe_{DCB}, Fe_{PP}, Al_{OX}, Al_{DCB} and Al_{PP} than Wagga Wagga soils. The positive linear relationships between P adsorption partition coefficient and extractable forms of Fe and Al indicated possible influence of these soil

properties on phosphate adsorption. The Fe_{OX} showed a stronger relationship ($R^2 = 0.81$) with P adsorption partition coefficient than Fe_{DCB} ($R^2 = 0.68$). This implied that poorly crystalline Fe (Fe_{OX}) contributed more to phosphate adsorption than the crystalline Fe (Fe_{DCB}), possible due to greater SSA of poorly crystalline Fe than well crystalline phases. Several studies have reported significant and positive relationships between phosphate adsorption and Fe_{OX} and Fe_{DCB} (Syers *et al.*, 1971; Udo and Uzu, 1972; Jones, 1981; Karim and Adams, 1984; Peña and Torrent, 1984; Singh and Gilkes, 1991; Agbenin and Tiessen, 1994; Agbenin, 2003; Wiriyakitnateekul *et al.*, 2005). Furthermore, Al_{OX} and Al_{DCB} also showed strong relationships ($R^2 = 0.81$ and 0.80) with P adsorption partition coefficient, which suggested their significant role in influencing P adsorption in these soils. Some studies have reported 3 to 5 times greater contribution of Al_{DCB} in P adsorption than Fe_{DCB} in acid soil from Australia (Bromfield, 1965; Singh and Gilkes, 1991). During DCB extraction, Al substituting for Fe in the structure of goethite and hematite is extracted, in addition to the forms of Al extracted by OX solution (Singh and Gilkes, 1991). Aluminium substitution for Fe is common in soils, with about one-third in goethite half of the one-third in hematite (Singh and Gilkes, 1992). The crystal size of Fe oxides is known to decrease with increasing Al substitution and in turn increases SSA and phosphate adsorption capacity (Borggaard, 1983; Schwertmann, 1988). Therefore, Al_{DCB} indirectly contributed to more reactive surfaces for phosphate adsorption than Fe_{DCB} (Peña and Torrent, 1990). Several studies have reported significant relationships between phosphate adsorption and forms of extractable Al (Bromfield, 1965; Singh and Gilkes, 1991; Agbenin and Tiessen, 1994; Agbenin, 2003; Wiriyakitnateekul *et al.*, 2005). In this study, $Fe_{OX} + Al_{OX}$ showed a stronger positive relationship ($R^2 = 0.81$) with P adsorption partition coefficient than $Fe_{DCB} + Al_{DCB}$ ($R^2 = 0.70$), which indicated that poorly crystalline Fe and Al oxides played more important roles in influencing phosphate adsorption than their well crystalline forms in

these soils. The clay content of Tumbarumba soils also positively influenced P adsorption, however, Fe/Al oxides formed a significant portion of the clay fraction.

The desorption of large amount of P that occurred in the surface soil from Wagga Wagga was expected owing to the long history of P fertiliser application including the historic excess addition of P fertilisers to Australian soils (Williams, 1950; McLaughlin *et al.*, 1992; Weaver and Wong, 2011). Hence, P was highly accumulated in the surface soil from Wagga Wagga. The equilibrium solution pH decreased in all samples, and all samples were trying to reverse to their original soil pH values. However, the small unit increase in equilibrium solution pH with P adsorption was expected as in ligand exchange process, where single-coordinated OH group on the surfaces of Fe/Al oxides are replaced by phosphate (Parfitt *et al.*, 1975; Goldberg and Sposito, 1985; Borggaard *et al.*, 1990). The pH of all soil samples was acidic and well below the point of zero charge (PZC) of Fe/Al oxides, so no pH effect was observed in the studied soils. Several studies have reported an increase phosphate sorption with increasing pH in soils (Anderson *et al.*, 1974; Mokwunye, 1975; Agbenin, 1995).

The isotherm parameters showed that DOC adsorption was greater in the subsurface soil than the surface soil from Wagga Wagga and Tumbarumba. This support our hypothesis that DOC adsorption will be greater in the subsurface soils than the surface soils. The surface and subsurface soils from Tumbarumba favoured DOC adsorption than the surface and subsurface soils from Wagga Wagga. This was possible owing to the higher content of Fe/Al oxides present in the Tumbarumba soils than Wagga Wagga soils. However, surface and subsurface soils of Tumbarumba favours DOC adsorption than surface and subsurface soils of Wagga Wagga. Similar to that of P adsorption, the adsorption of DOC and their relative affinity for surfaces of mineral are closely linked to Fe and Al oxides in soils (Kaiser and Zech, 1998). The strong positive relationships between DOC adsorption partition coefficient and different fractions of extractable Fe and Al indicated that both extractable Fe and Al are important soil properties

influencing DOC adsorption. A significant positive relationship between Fe_{DCB} and Al_{DCB} with DOC adsorption partition coefficient suggested that the adsorption of DOC is influenced by pedogenic Fe and Al oxides. Other studies have observed such a positive correlation between DOC adsorption and Fe_{DCB} (Kaiser *et al.*, 1996; Kahle *et al.*, 2003; Kahle *et al.*, 2004). The positive relationship showed between Fe_{OX} and Al_{OX} with DOC adsorption partition coefficient indicated that poorly crystalline Fe and Al oxides also contributed to the DOC adsorption. These results are consistent with previous studies (Kothawala *et al.*, 2009; Pengerud *et al.*, 2014). The small increase in equilibrium DOC solution pH with DOC adsorption was expected as during ligand exchange reactions, coordinative OH groups on the surfaces of Fe/Al oxides are replaced by organic anion (Parfitt *et al.*, 1977; Tipping, 1981; Davis, 1982; Gu *et al.*, 1994). The pH of all soil samples was acidic and below the PZC of Fe/Al oxides, thus supporting the sorption of anionic species, including dissociated organic acids. Tipping (1981) reported that greatest sorption of humic substances by iron oxides occurred at pH 5.

Our results showed that DOC did not have any influence on P adsorption from the mixed solution of P and DOC. The adsorption of P promoted DOC desorption in the surface and subsurface soils from Wagga Wagga and Tumbarumba. In this study, results suggested that P competed more effectively than DOC for sorption sites on mineral surfaces (Violante and Gianfreda, 1993; Afif *et al.*, 1995; Fransson and Jones, 2007; Schneider *et al.*, 2010; Spohn and Schleuss, 2019; Spohn, 2020; Spohn *et al.*, 2022). It also indicated DOC was adsorbed by weaker interaction on Fe/Al oxides. This result did not support our hypothesis that DOC would inhibit phosphate adsorption in both surface and subsurface soils. Phosphate addition in the studied soils may affect the adsorption and desorption of DOC, causing the destabilisation of OC, which may increase mineralisation of OC (Kaiser and Zech, 1997; Spohn *et al.*, 2022). Further, continuous phosphate addition can lead to increase in the release of DOC, and thus makes OC available for microbial decomposition in the studied soils (Spohn and Schleuss,

2019). Hur and Schlautman (2004) reported a significant reduction on sorption of DOC onto hematite in the presence of P. Kahle *et al.* (2004) observed that the blocking of OH groups on minerals surfaces with phosphate significantly reduced DOC adsorption. Our findings showing increased phosphate concentration promoted DOC desorption is in line with previous studies findings in soils (Kaiser and Zech, 1999; Zhang and Zhang, 2010; Scott *et al.*, 2015; Spohn and Schleuss, 2019; Li *et al.*, 2020; Spohn *et al.*, 2022).

5.5 Implications

The results of this study have crucial implications on the sustainability of Fe-rich soils. The adsorption of phosphate promoted DOC desorption in these soils, which may lead to destabilisation of OC. Consequently, OC destabilisation may impair OC sequestration and enhance microbial decomposition in these soils. However, the effect of phosphate addition on DOC desorption may depend on different soil environmental conditions which may vary from one soil type to another. More so, phosphate might play a major role in influencing the microbial stability of OC adsorption in these soils. On the contrary, it had been shown that DOC competed strongly with phosphate for adsorption sites and significantly inhibited phosphate adsorption, which can increase the bioavailability of P in soils.

5.6 Conclusions

This study shows that the surface and subsurface soils from Tumbarumba had the greater affinity for phosphate adsorption than the soils from Wagga Wagga, which is due to the higher content Fe and Al oxides present soils from Tumbarumba. Phosphate adsorption was greater in the subsurface than the surface soil from Tumbarumba. This support our first hypothesis which state that phosphate adsorption will be greater in the subsurface than the surface soils. However, soils from Wagga Wagga did not support the hypothesis since phosphate adsorption was greater

in the surface than in subsurface soils. The affinity for DOC was greater in subsurface than in surface soils. In contrast to our hypothesis, we found that in the mixed solution of P and DOC, phosphate adsorption promoted DOC desorption in the surface and subsurface soils from Wagga Wagga and Tumbarumba. This suggest that phosphate outcompeted DOC for the adsorption sites on soil mineral surfaces.

In conclusion, extractable Fe and Al explained well the phosphate and DOC adsorption behaviour in the studied soils and may serve as suitable routine predictors of P and DOC adsorption capacity in surface and subsurface soils.

5.7 Supplementary information

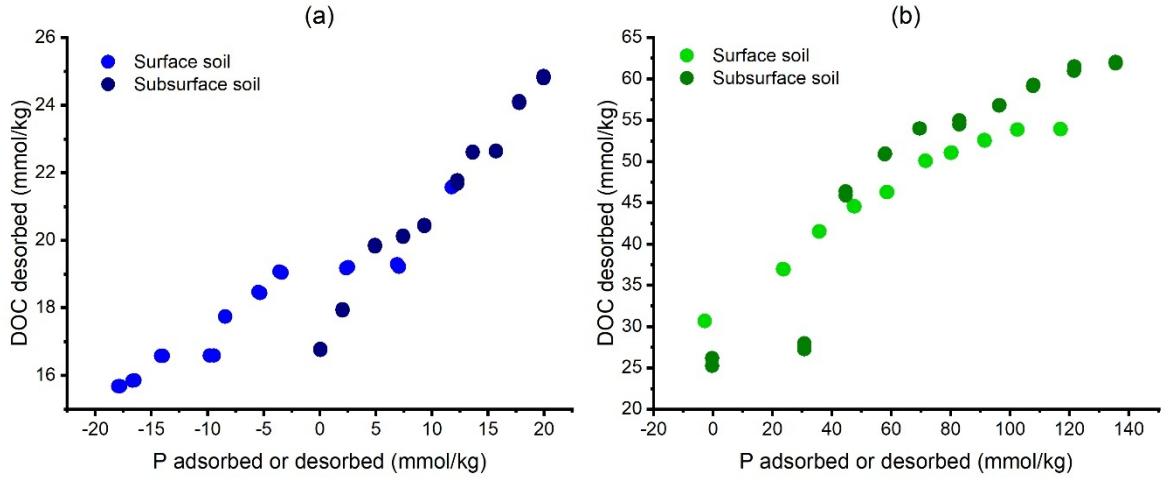

Supplementary Figure 5.1. *Dissolved organic carbon (DOC) desorption in relation to phosphate adsorption or desorption for surface and subsurface soils from (a) Wagga Wagga (b) Tumbarumba*

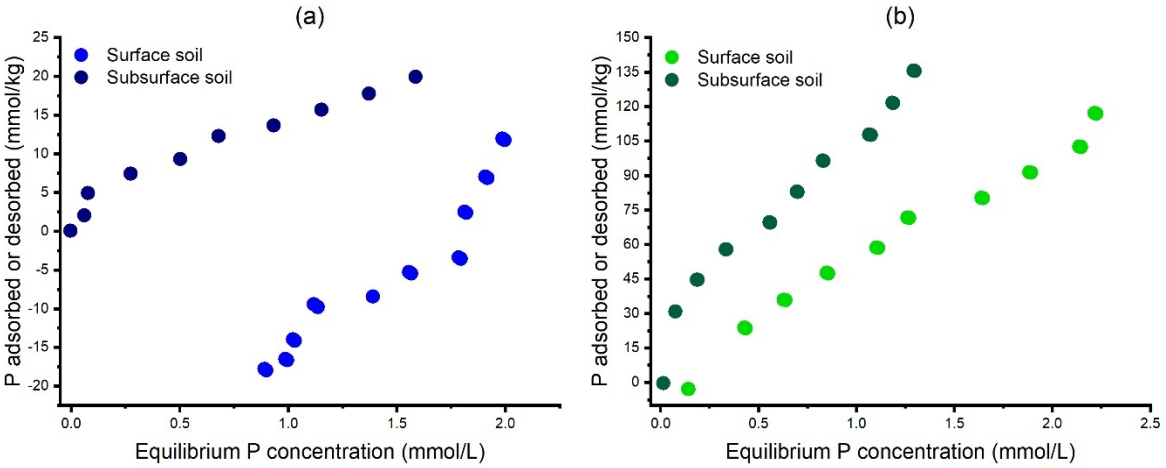

Supplementary Figure 5.2*. Phosphate adsorption or desorption in relation to equilibrium P concentration for surface and subsurface soils from (a) Wagga Wagga (b) Tumbarumba.*

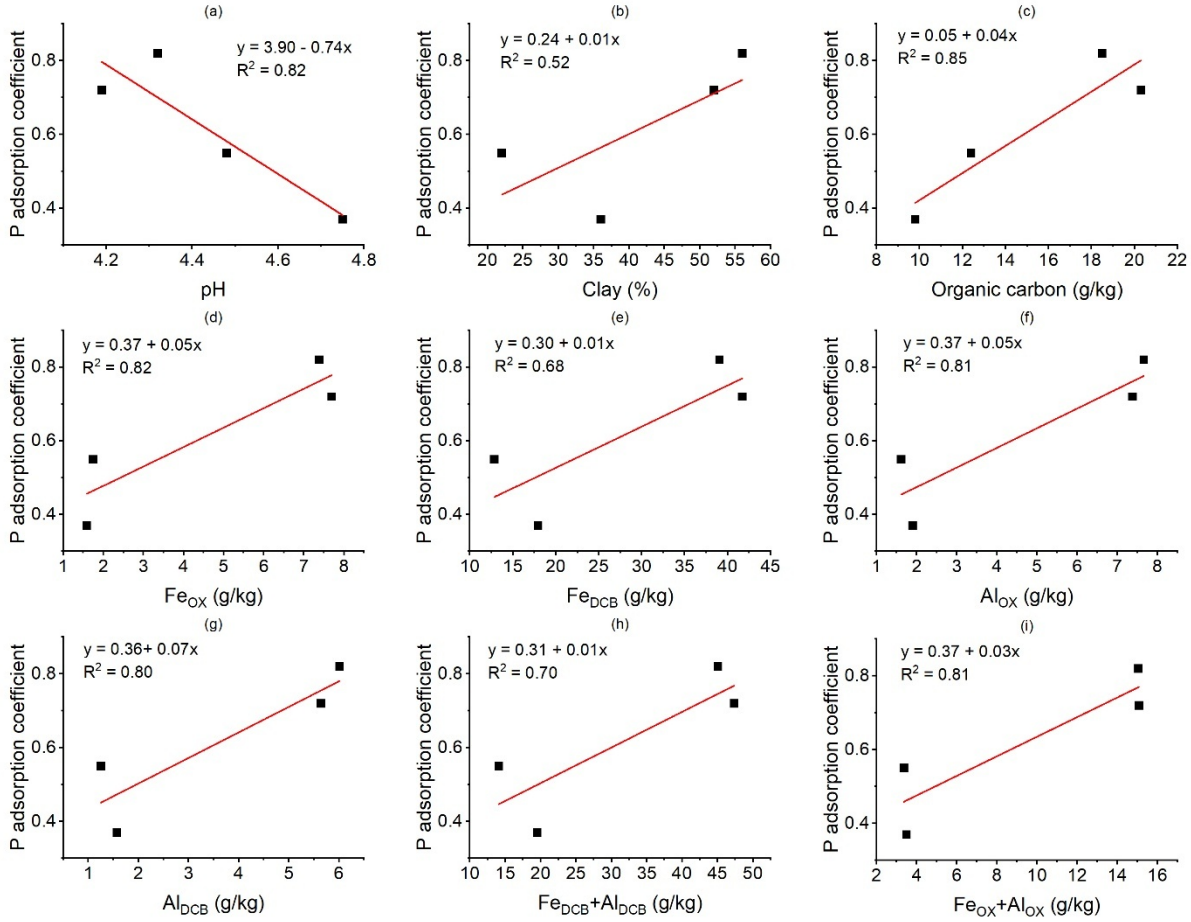

Supplementary Figure 5.3. *Relationship between phosphate partition coefficient (m) and some properties of soils from Wagga Wagga and Tumbarumba.*

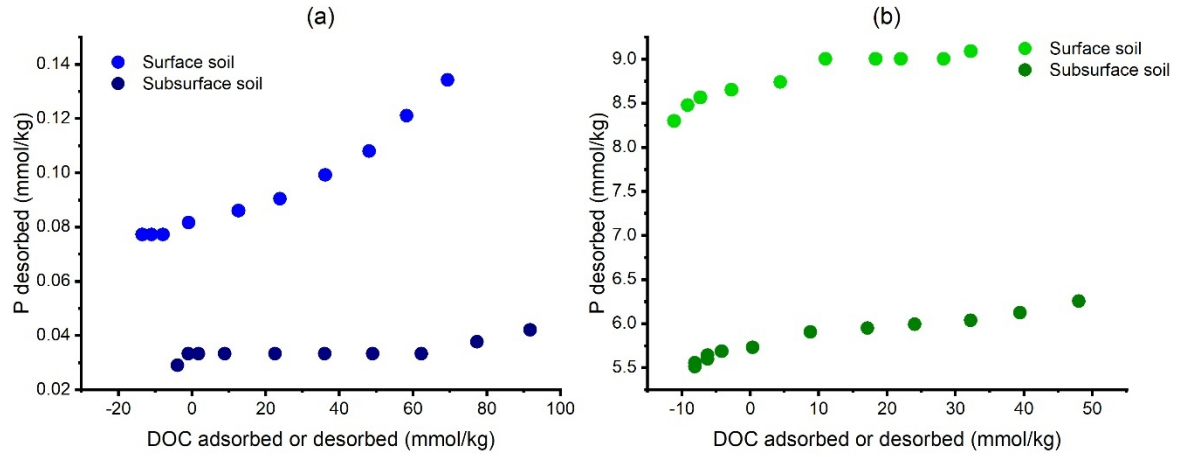

Supplementary Figure 5.4. *Phosphate desorption in relation to DOC adsorption or desorption for surface and subsurface soils from (a) Wagga Wagga (b) Tumbarumba*

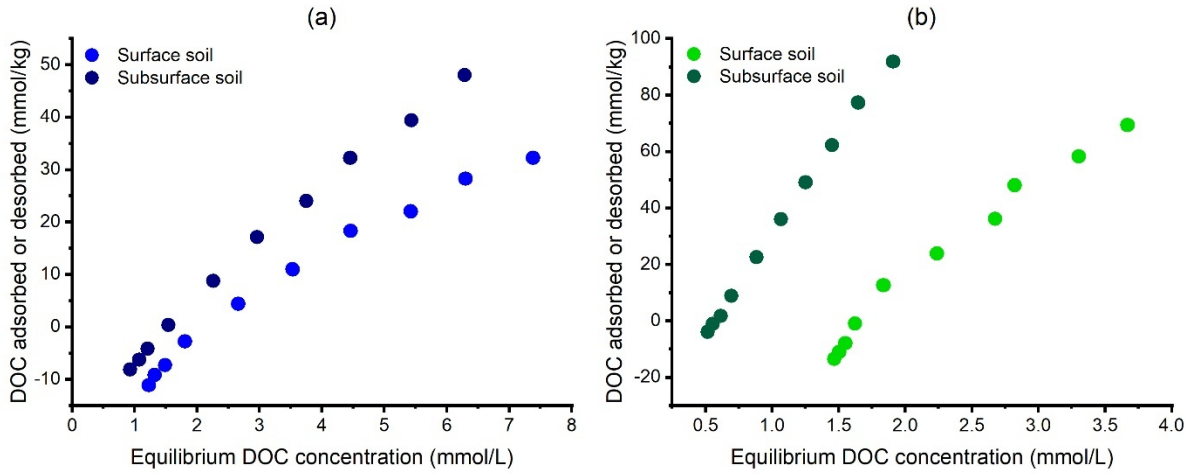

Supplementary Figure 5.5. *Dissolved organic carbon (DOC) adsorption or desorption in relation to equilibrium DOC concentration for surface and subsurface soils from (a) Wagga Wagga (b) Tumbarumba.*

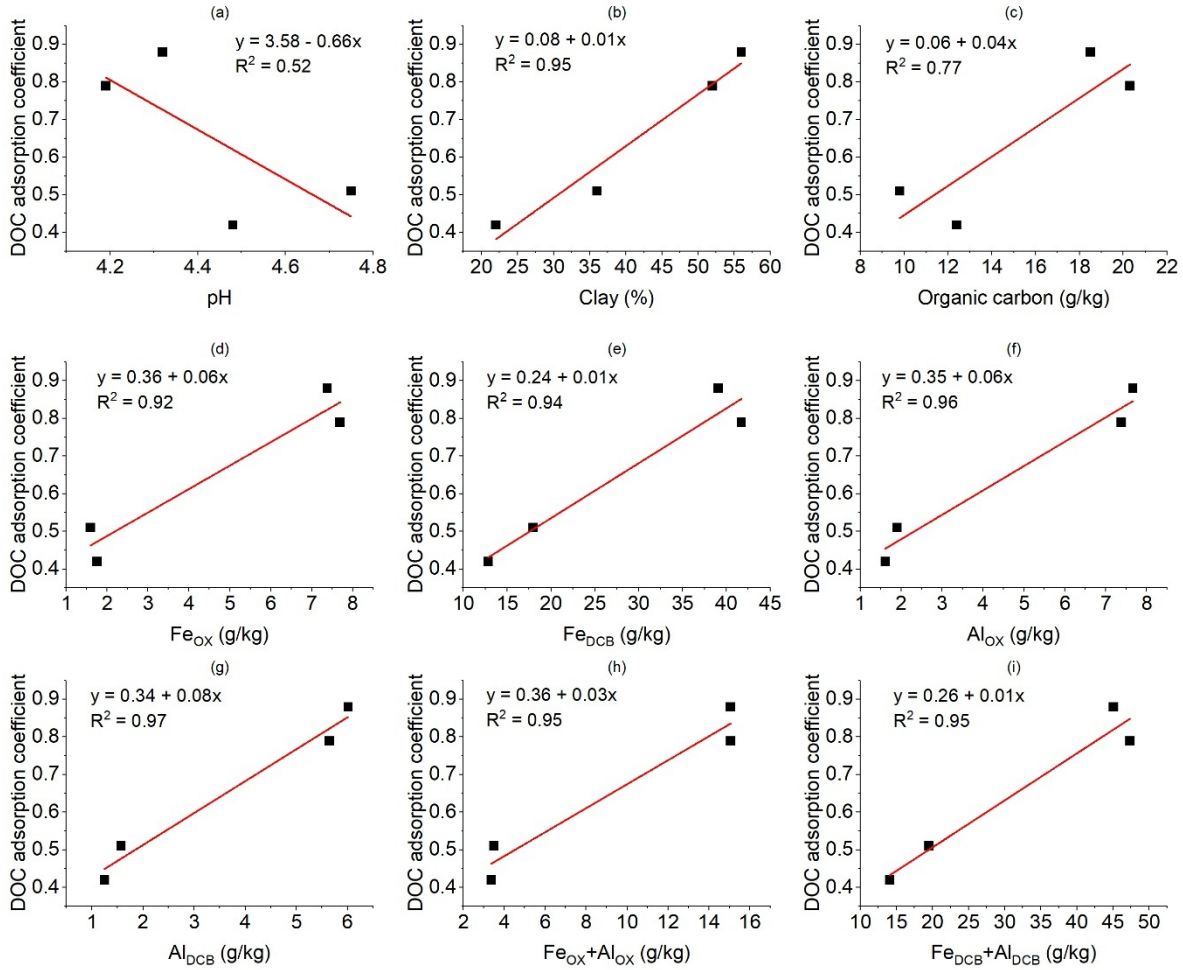

Supplementary Figure 5.6. *Relationship between DOC partition coefficient (m) and some properties of soils from Wagga Wagga and Tumbarumba.*

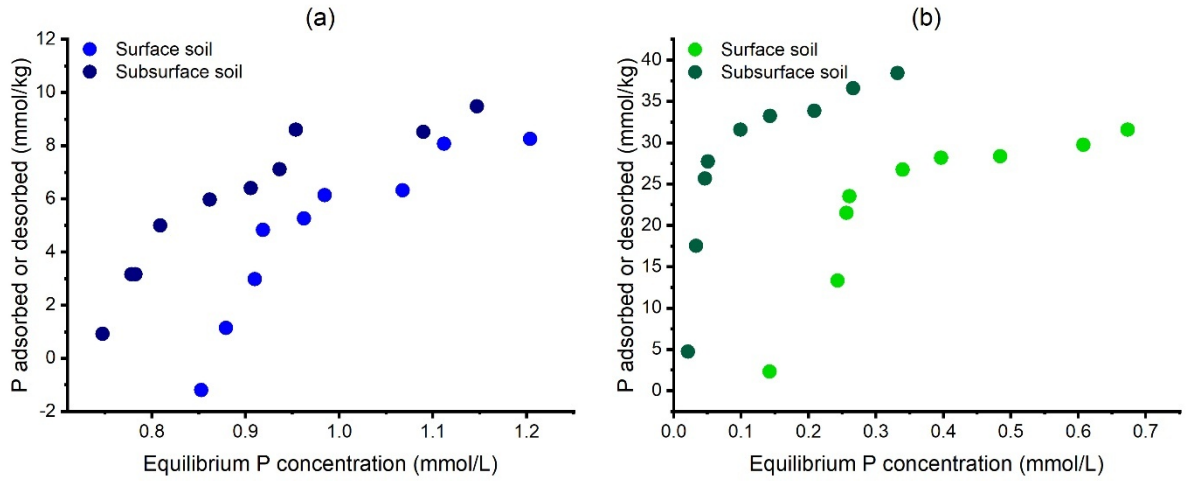

Supplementary Figure 5.7. *Phosphate adsorption or desorption in relation to the equilibrium P concentration from mixed solution of P and DOC on surface and subsurface soils from (a) Wagga Wagga (b) Tumbarumba.*

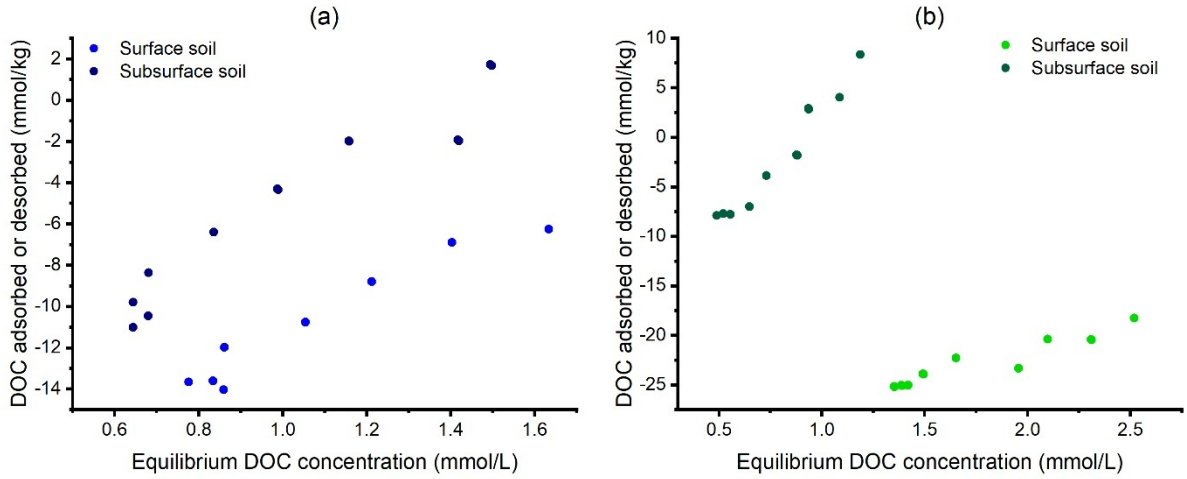

Supplementary Figure 5.8. *Dissolved organic carbon (DOC) adsorption or desorption in relation to the equilibrium DOC concentration from mixed solution of P and DOC on surface and subsurface soils from (a) Wagga Wagga (b) Tumbarumba.*

5.8 Acknowledgements

I acknowledge the **Soil Science Challenge Grants Program** funded by the **Australian Government Department of Agriculture, Fisheries and Forestry** and this article contributes towards the **National Soil Strategy** and the implementation of the **National Soil Action Plan**. I am thankful to the Tertiary Education Trust Fund (TETFund), Nigeria for the financial support in tuition fees and living expenses.

References

Afif, E., Barrón, V., Torrent, J., 1995. Organic matter delays but does not prevent phosphate sorption by Cerrado soils from Brazil. *Soil Science* **159**, 207-211.

Agbenin, J., 1995. Phosphorus sorption by three cultivated savanna Alfisols as influenced by pH. *Fertilizer research* **44**, 107-112.

Agbenin, J., Tiessen, H., 1994. The effects of soil properties on the differential phosphate sorption by semiarid soils from Northeast Brazil. *Soil Science* **157**, 36-45.

Agbenin, J.O., 2003. Extractable iron and aluminum effects on phosphate sorption in a savanna Alfisol. *Soil Science Society of America Journal* **67**, 589-595.

Anderson, G., Williams, E., Moir, J.O., 1974. A comparison of the sorption of inorganic orthophosphate and inositol hexaphosphate by six acid soils. *Journal of Soil Science* **25**, 51-62.

Appelt, H., Coleman, N.T., Pratt, P.F., 1975. Interactions Between Organic Compounds, Minerals, and Ions in Volcanic-ash-derived Soils: II. Effects of Organic Compounds on the Adsorption of Phosphate. *Soil Science Society of America Journal* **39**, 628-630.

Arai, Y., Sparks, D.L., 2001. ATR–FTIR spectroscopic investigation on phosphate adsorption mechanisms at the ferrihydrite–water interface. *Journal of colloid and interface science* **241**, 317-326.

Atkinson, R.J., Parfitt, R.L., Smart, R.S.C., 1974. Infra-red study of phosphate adsorption on goethite. *Journal of the Chemical Society, Faraday Transactions 1: Physical Chemistry in Condensed Phases* **70**, 1472-1479.

Balemi, T., Negisho, K., 2012. Management of soil phosphorus and plant adaptation mechanisms to phosphorus stress for sustainable crop production: a review. *Journal of soil science and plant nutrition* **12**, 547-562.

Ballard, R., Fiskell, J.G., 1974. Phosphorus retention in coastal plain forest soils: I. Relationship to soil properties. *Soil Science Society of America Journal* **38**, 250-255.

Barron, V., Herruzo, M., Torrent, J., 1988. Phosphate adsorption by aluminous hematites of different shapes. *Soil Science Society of America Journal* **52**, 647-651.

Beck, M., Robarge, W., Buol, S., 1999. Phosphorus retention and release of anions and organic carbon by two Andisols. *European journal of soil science* **50**, 157-164.

Bigham, J., Golden, D., Bowen, L., Buol, S., Weed, S., 1978. Iron Oxide Mineralogy of Well-drained Ultisols and Oxisols: I. Characterization of Iron Oxides in Soil Clays by Mössbauer Spectroscopy, X-ray Diffractometry, and Selected Chemical Techniques. *Soil Science Society of America Journal* **42**, 816-825.

Bolan, N.S., Adriano, D.C., Kunhikrishnan, A., James, T., McDowell, R., Senesi, N., 2011. Chapter One - Dissolved Organic Matter: Biogeochemistry, Dynamics, and Environmental Significance in Soils. In: Sparks, D.L. (Ed.), Advances in Agronomy. Academic Press, Vol. 110, pp. 1-75.

Bolan, N.S., Naidu, R., Mahimairaja, S., Baskaran, S., 1994. Influence of low-molecular-weight organic acids on the solubilization of phosphates. *Biology and Fertility of Soils* **18**, 311-319.

Borggaard, O., 1983. The influence of iron oxides on phosphate adsorption by soil. *Journal of Soil Science* **34**, 333-341.

Borggaard, O.K., Jdrgensen, S.S., Moberg, J.P., Raben-Lange, B., 1990. Influence of organic matter on phosphate adsorption by aluminium and iron oxides in sandy soils. *Journal of Soil Science* **41**, 443-449.

Börling, K., Otabbong, E., Barberis, E., 2001. Phosphorus sorption in relation to soil properties in some cultivated swedish soils. *Nutrient Cycling in Agroecosystems* **59**, 39-46.

Brennan, R.F., Bolland, M.D.A., Jeffery, R.C., Allen, D.G., 1994. Phosphorus adsorption by a range of Western Australian soils related to soil properties. *Communications in Soil Science and Plant Analysis* **25**, 2785-2795.

Brenner, J., Porter, W., Phillips, J.R., Childs, J., Yang, X., Mayes, M.A., 2018. Phosphorus sorption on tropical soils with relevance to Earth system model needs. *Soil research* **57**, 17-27.

Bromfield, S.M., 1965. Studies of the relative importance of iron and aluminium in the sorption of phosphate by some Australian soils. *Australian Journal of Soil Research* **3**, 31-44.

Bünemann, E.K., 2015. Assessment of gross and net mineralization rates of soil organic phosphorus–A review. *Soil Biology and Biochemistry* **89**, 82-98.

Bünemann, E.K., Oberson, A., Frossard, E., 2011. Phosphorus in action: Biological processes in soil phosphorus cycling. *Soil Biology* **26**.

Burt, R., Mays, M.D., Benham, E.C., Wilson, M.A., 2002. Phosphorus characterization and correlation with properties of selected benchmark soils of the United States. *Communications in Soil Science and Plant Analysis* **33**, 117-141.

Chase, A.J., Erich, M.S., Ohno, T., 2018. Bioavailability of phosphorus on iron (oxy) hydroxide not affected by soil amendment–derived organic matter. *Agricultural and Environmental Letters* **3**, 170042.

Davis, J.A., 1982. Adsorption of natural dissolved organic matter at the oxide/water interface. *Geochimica et cosmochimica acta* **46**, 2381-2393.

De Campos, M., Antonangelo, J.A., Alleoni, L.R.F., 2016. Phosphorus sorption index in humid tropical soils. *Soil and Tillage Research* **156**, 110-118.

Devau, N., Le Cadre, E., Hinsinger, P., Jaillard, B., Gérard, F., 2009. Soil pH controls the environmental availability of phosphorus: experimental and mechanistic modelling approaches. *Applied Geochemistry* **24**, 2163-2174.

Earl, K., Syers, J., McLaughlin, J., 1979. Origin of the effects of citrate, tartrate, and acetate on phosphate sorption by soils and synthetic gels. *Soil Science Society of America Journal* **43**, 674-678.

Fontes, M.P.F., Weed, S.B., 1996. Phosphate adsorption by clays from Brazilian Oxisols: relationships with specific surface area and mineralogy. *Geoderma* **72**, 37-51.

Fransson, A.M., Jones, D.L., 2007. Phosphatase activity does not limit the microbial use of low molecular weight organic-P substrates in soil. *Soil Biology and Biochemistry* **39**, 1213-1217.

Fu, Z., Wu, F., Song, K., Lin, Y., Bai, Y., Zhu, Y., Giesy, J.P., 2013. Competitive interaction between soil-derived humic acid and phosphate on goethite. *Applied Geochemistry* **36**, 125-131.

Gee, G.W., Or, D., 2002. 2.4 Particle-size analysis. *Methods of soil analysis: part 4 physical methods* **5**, 255-293.

Goldberg, S., Sposito, G., 1985. On the mechanism of specific phosphate adsorption by hydroxylated mineral surfaces: A review. *Communications in Soil Science and Plant Analysis* **16**, 801-821.

Gu, B., Schmitt, J., Chen, Z., Liang, L., McCarthy, J.F., 1994. Adsorption and desorption of natural organic matter on iron oxide: mechanisms and models. *Environmental Science & Technology* **28**, 38-46.

Guan, X.-H., Shang, C., Chen, G.-H., 2006. Competitive adsorption of organic matter with phosphate on aluminum hydroxide. *Journal of Colloid and Interface Science* **296**, 51-58.

Guppy, C.N., Menzies, N., Moody, P.W., Blamey, F., 2005. Competitive sorption reactions between phosphorus and organic matter in soil: a review. *Soil Research* **43**, 189-202.

Harter, R.D., 1969. Phosphorus Adsorption Sites in Soils. *Soil Science Society of America Journal* **33**, 630-632.

Hawkesford, M.J., Cakmak, I., Coskun, D., De Kok, L.J., Lambers, H., Schjoerring, J.K., White, P.J., 2023. Chapter 6 - Functions of macronutrients. This chapter is a revision of the third edition chapter by M. Hawkesford, W. Horst, T. Kichey, H. Lambers, J. Schjoerring, I. Skrumsager Møller, and P. White, pp. 135–189. DOI: https://doi.org/10.1016/B978-0-12-384905-2.00006-6. In: Rengel, Z., Cakmak, I., White, P.J. (Eds.), Marschner's Mineral Nutrition of Plants (Fourth Edition). *Academic Press*, San Diego, pp. 201-281.

Hinga, G., 1973. Phosphate sorption capacity in relation to properties of several types of Kenya soil. *East African Agricultural and Forestry Journal* **38**, 400-404.

Hinsinger, P., 2001. Bioavailability of soil inorganic P in the rhizosphere as affected by root-induced chemical changes: a review. *Plant and soil* **237**, 173-195.

Hue, N., 1991. Effects of organic acids/anions on P sorption and phytoavailability in soils with different mineralogies. *Soil science* **152**, 463-471.

Hunt, J.F., Ohno, T., He, Z., Honeycutt, C.W., Dail, D.B., 2007. Inhibition of phosphorus sorption to goethite, gibbsite, and kaolin by fresh and decomposed organic matter. *Biology and Fertility of Soils* **44**, 277-288.

Hur, J., Schlautman, M.A., 2004. Effects of pH and phosphate on the adsorptive fractionation of purified Aldrich humic acid on kaolinite and hematite. *Journal of colloid and interface science* **277**, 264-270.

IUSS Working Group WRB (2022) World Reference Base for Soil Resources 2014, International Soil Classification System for Naming Soils and Creating Legends for Soil Maps, World Soil Resources Reports No. 106. UN Food and Agriculture Organization Rome.

Jones, R., 1981. X-Ray Diffraction Line Profile Analysis Vs. Phosphorus Sorption by 11 Puerto Rican Soils. *Soil Science Society of America Journal* **45**, 818-825.

Kahle, M., Kleber, M., Jahn, R., 2003. Retention of dissolved organic matter by illitic soils and clay fractions: Influence of mineral phase properties. *Journal of Plant Nutrition and Soil Science* **166**, 737-741.

Kahle, M., Kleber, M., Jahn, R., 2004. Retention of dissolved organic matter by phyllosilicate and soil clay fractions in relation to mineral properties. *Organic Geochemistry* **35**, 269-276.

Kaiser, K., Guggenberger, G., 2000. The role of DOM sorption to mineral surfaces in the preservation of organic matter in soils. *Organic Geochemistry* **31**, 711-725.

Kaiser, K., Guggenberger, G., Zech, W., 1996. Sorption of DOM and DOM fractions to forest soils. *Geoderma* **74**, 281-303.

Kaiser, K., Zech, W., 1997. Competitive sorption of dissolved organic matter fractions to soils and related mineral phases. *Soil Science Society of America Journal* **61**, 64-69.

Kaiser, K., Zech, W., 1998. Rates of dissolved organic matter release and sorption in forest soils. *Soil Science* **163**, 714-725.

Kaiser, K., Zech, W., 1998. Soil dissolved organic matter sorption as influenced by organic and sesquioxide coatings and sorbed sulfate. *Soil Science Society of America Journal* **62**, 129-136.

Kaiser, K., Zech, W., 1999. Release of natural organic matter sorbed to oxides and a subsoil. *Soil Science Society of America Journal* **63**, 1157-1166.

Kalbitz, K., Kaiser, K., 2003. Ecological aspects of dissolved organic matter in soils. *Geoderma* **113**, 177-178.

Kalbitz, K., Solinger, S., Park, J.-H., Michalzik, B., Matzner, E., 2000. Controls on the dynamics of dissolved organic matter in soils: a review. *Soil science* **165**, 277-304.

Karim, M.I., Adams, W.A., 1984. Relationships between Sesquioxides, Kaolinite, and Phosphate Sorption in a Catena of Oxisols in Malawi. *Soil Science Society of America Journal* **48**, 406-409.

Kothawala, D., Moore, T., Hendershot, W., 2009. Soil properties controlling the adsorption of dissolved organic carbon to mineral soils. *Soil Science Society of America Journal* **73**, 1831-1842.

Li, Y., Wang, T., Camps-Arbestain, M., Suárez-Abelenda, M., Whitby, C.P., 2020. Lime and/or phosphate application affects the stability of soil organic carbon: Evidence from changes in quantity and chemistry of the soil water-extractable organic matter. *Environmental science & technology* **54**, 13908-13916.

Liu, F., He, J., Colombo, C., Violante, A., 1999. Competitive adsorption of sulfate and oxalate on goethite in the absence or presence of phosphate. *Soil Science* **164**, 180-189.

Loganathan, P., Isirimah, N., Nwachuku, D., 1987. Phosphorus sorption by Ultisols and Inceptisols of the Niger delta in southern Nigeria. *Soil science* **144**, 330-338.

Lopez-Hernandez, D., Burnham, C.P., 1974. The covariance of phosphate sorption with other soil properties in some British and tropical soils. *Journal of Soil Science* **25**, 196-206.

Lopez-Hernandez, D., Siegert, G., Rodriguez, J., 1986. Competitive adsorption of phosphate with malate and oxalate by tropical soils. *Soil Science Society of America Journal* **50**, 1460-1462.

Mavi, M.S., Sanderman, J., Chittleborough, D.J., Cox, J.W., Marschner, P., 2012. Sorption of dissolved organic matter in salt-affected soils: Effect of salinity, sodicity and texture. *Science of The Total Environment* **435-436**, 337-344.

McGill, W.B., Cannon, K.R., Robertson, J.A., Cook, F.D., 1986. Dynamics of soil microbial biomass and water-soluble organic C in Breton L after 50 years of cropping to two rotations. *Canadian Journal of Soil Science* **66**, 1-19.

McKeague, J., 1967. An evaluation of 0.1 M pyrophosphate and pyrophosphate-dithionite in comparison with oxalate as extractants of the accumulation products in podzols and some other soils. *Canadian Journal of Soil Science* **47**, 95-99.

McKeague, J., Day, J., 1966. Dithionite-and oxalate-extractable Fe and Al as aids in differentiating various classes of soils. *Canadian Journal of Soil Science* **46**, 13-22.

McLaughlin, M.J., Fillery, I.R., Till, A.R., 1992. Operation of the phosphorus, sulphur and nitrogen cycles. In: Gifford, R.W., Barson, M.M. (Eds.), Australia's Renewable Resources: Sustainability and Global Change. Bureau of Rural Resources, Canberra, pp. 67-116.

Mehra, O., Jackson, M., 1960. Iron oxide removal from soils and clays by a dithionite–citrate system buffered with sodium bicarbonate. *Clays and clay minerals*. *Elsevier*, pp. 317-327.

Mokwunye, U., 1975. The influence of pH on the adsorption of phosphate by soils from the Guinea and Sudan savannah zones of Nigeria. *Soil Science Society of America Journal* **39**, 1100-1102.

Murphy, J., Riley, J.P., 1962. A modified single solution method for the determination of phosphate in natural waters. *Analytica chimica acta* **27**, 31-36.

Nagarajah, S., Posner, A., Quirk, J., 1970. Competitive adsorption of phosphate with polygalacturonate and other organic anions on kaolinite and oxide surfaces. *Nature* **228**, 83-85.

Nodvin, S.C., Driscoll, C.T., Likens, G.E., 1986. Simple partitioning of anions and dissolved organic carbon in a forest soil. *Soil Science* **142**, 27-35.

Ohno, T., Crannell, B.S., 1996. Green and animal manure-derived dissolved organic matter effects on phosphorus sorption. Wiley Online Library.

Parfitt, R., Fraser, A., Farmer, V., 1977. Adsorption on hydrous oxides. III. Fulvic acid and humic acid on goethite, gibbsite and imogolite. *Journal of soil science* **28**, 289-296.
Parfitt, R.L., Atkinson, R.J., 1976. Phosphate adsorption on goethite (α-FeOOOH). *Nature* **264**, 740-742.
Parfitt, R.L., Atkinson, R.J., Smart, R.S.C., 1975. The mechanism of phosphate fixation by iron oxides. *Soil Science Society of America Journal* **39**, 837-841.
Peña, F., Torrent, J., 1984. Relationships between phosphate sorption and iron oxides in Alfisols from a river terrace sequence of Mediterranean Spain. *Geoderma* **33**, 283-296.
Peña, F., Torrent, J., 1990. Predicting phosphate sorption in soils of mediterranean regions. *Fertilizer Research* **23**, 173-179.
Pengerud, A., Johnsen, L.K., Mulder, J., Strand, L.T., 2014. Potential adsorption of dissolved organic matter in poorly podzolised, high-latitude soils. *Geoderma* **226**, 39-46.
Persson, P., Nilsson, N., Sjöberg, S., 1996. Structure and bonding of orthophosphate ions at the iron oxide–aqueous interface. *Journal of colloid and interface science* **177**, 263-275.
Rayment, G.E., Lyons, D.J., 2011. *Soil chemical methods: Australasia*. CSIRO publishing.
Roberts, T.L., Johnston, A.E., 2015. Phosphorus use efficiency and management in agriculture. *Resources, conservation and recycling* **105**, 275-281.
Ryan, J., Hasan, H., Baasiri, M., Tabbara, H., 1985. Availability and transformation of applied phosphorus in calcareous Lebanese soils. *Soil Science Society of America Journal* **49**, 1215-1220.
Sanyal, S., Chan, P., De Datta, S., 1993. Phosphate sorption-desorption behavior of some acidic soils of south and southeast Asia. *Soil Science Society of America Journal* **57**, 937-945.
Schneider, M.P.W., Scheel, T., Mikutta, R., van Hees, P., Kaiser, K., Kalbitz, K., 2010. Sorptive stabilization of organic matter by amorphous Al hydroxide. *Geochimica et Cosmochimica Acta* **74**, 1606-1619.
Schwertmann, U., 1988. Some properties of soil and synthetic iron oxides. Iron in soils and clay minerals. Springer, pp. 203-250.
Scott, J., Lambie, S., Stevenson, B., Schipper, L., Parfitt, R., McGill, A., 2015. Carbon and nitrogen leaching under high and low phosphate fertility pasture with increasing nitrogen inputs. *Agriculture, Ecosystems & Environment* **202**, 139-147.
Sibanda, H.M., Young, S.D., 1986. Competitive adsorption of humus acids and phosphate on goethite, gibbsite and two tropical soils. *Journal of Soil Science* **37**, 197-204.
Sims, T.J., Pierzynski, G.M., 2005. Chemistry of phosphorus in soils. *Chemical processes in soils* **8**, 151-192.
Singh, B., Gilkes, R., 1991. Phosphorus sorption in relation to soil properties for the major soil types of south-western Australia. *Soil Research* **29**, 603-618.
Singh, B., Gilkes, R., 1992. Properties and distribution of iron oxides and their association with minor elements in the soils of south-western Australia. *Journal of Soil Science* **43**, 77-98.
Spohn, M., 2020. Phosphorus and carbon in soil particle size fractions: A synthesis. *Biogeochemistry* **147**, 225-242.
Spohn, M., Diáková, K., Aburto, F., Doetterl, S., Borovec, J., 2022. Sorption and desorption of organic matter in soils as affected by phosphate. *Geoderma* **405**, 115377.
Spohn, M., Schleuss, P.-M., 2019. Addition of inorganic phosphorus to soil leads to desorption of organic compounds and thus to increased soil respiration. *Soil Biology and Biochemistry* **130**, 220-226.
Sposito, G., 2004. The surface chemistry of natural particles. Oxford University Press.
Syers, J., Evans, T., Williams, J., Murdock, J., 1971. Phosphate sorption parameters of representative soils from Rio Grande do Sul, Brazil. *Soil Science* **112**, 267-275.

Tiessen, H., 2005. Phosphorus Dynamics in Tropical Soils. Phosphorus: Agriculture and the Environment, pp. 253-262.
Tipping, E., 1981. The adsorption of aquatic humic substances by iron oxides. *Geochimica et cosmochimica acta* **45**, 191-199.
Torrent, J., Schwertmann, U., Barrón, V., 1992. Fast and slow phosphate sorption by goethite-rich natural materials. *Clays and Clay Minerals* **40**, 14-21.
Udo, E.J., Uzu, F.O., 1972. Characteristics of Phosphorus Adsorption by Some Nigerian Soils. *Soil Science Society of America Journal* **36**, 879-883.
Violante, A., Gianfreda, L., 1993. Competition in adsorption between phosphate and oxalate on an aluminum hydroxide montmorillonite complex. *Soil Science Society of America Journal* **57**, 1235-1241.
Violante, A., Gianfreda, L., 2023. Adsorption of phosphate on variable charge minerals: competitive effect of organic ligands. Environmental impacts of soil component interactions. CRC Press, pp. 29-38.
Watanabe, T., 2017. Significance of active aluminum and iron on organic carbon preservation and phosphate sorption/release in tropical soils. In: Funakawa, S. (Ed.), Soils, Ecosystem Processes, and agricultural development: Tropical Asia and Sub-Saharan Africa. *Springer* Tokyo, Japan, pp. 103-125.
Weaver, D.M., Wong, M.T., 2011. Scope to improve phosphorus (P) management and balance efficiency of crop and pasture soils with contrasting P status and buffering indices. *Plant and Soil* **349**, 37-54.
Williams, C.H., 1950. Studies on soil phosphorus. II. The nature of native and residual phosphorus in some South Australian soils. *The Journal of Agricultural Science* **40**, 243-256.
Wiriyakitnateekul, W., Suddhiprakarn, A., Kheuruenromne, I., Gilkes, R.J., 2005. Extractable iron and aluminium predict the P sorption capacity of Thai soils. *Soil Research* **43**, 757-766.
Yang, F., Zhang, S., Song, J., Du, Q., Li, G., Tarakina, N.V., Antonietti, M., 2019. Synthetic humic acids solubilize otherwise insoluble phosphates to improve soil fertility. *Angewandte Chemie* **131**, 18989-18992.
Yang, X., Chen, X., Yang, X., 2019. Effect of organic matter on phosphorus adsorption and desorption in a black soil from Northeast China. *Soil and Tillage Research* **187**, 85-91.
Yang, X., Post, W.M., 2011. Phosphorus transformations as a function of pedogenesis: A synthesis of soil phosphorus data using Hedley fractionation method. *Biogeosciences* **8**, 2907-2916.
Zhang, M., Zhang, H., 2010. Co-transport of dissolved organic matter and heavy metals in soils induced by excessive phosphorus applications. *Journal of Environmental Sciences* **22**, 598-606.
Zsolnay, Á., 2003. Dissolved organic matter: Artefacts, definitions, and functions. *Geoderma*, pp. 187-209.

Chapter Six

Conclusions and outlook

The review of literature (Chapter 2) provided a comprehensive understanding of the relationships among the different fractions of extractable Fe and Al with P sorption capacity and SOC concentration. The analysis of the data from published literature showed that ammonium oxalate extractable aluminium (Al_{ox}) and dithionite-citrate-bicarbonate extractable aluminium (Al_d) are strong predictor variables of P sorption capacity of soils, but Al_d was a better predictor variable. Further, a positive (and 1:1) relationship between Al_{ox} and Al_d, suggested that Al dissolved by ammonium oxalate and dithionite-citrate-bicarbonate (DCB) was nearly similar. A statistically significant and strong relationship was found between ammonium oxalate extractable Fe (Fe_{ox}) and Al_{ox}, and SOC concentration, but the relationship of Al_{ox} was the strongest. This may be due to chemical interactions of SOC with Al oxides, which can directly or indirectly influence P sorption capacity in soils. These results suggested that DCB and OX extractable Fe (and Al) that represent Fe in crystalline and poorly crystalline, or amorphous form of Fe/Al, respectively, may be used as a routine soil test to predict P sorption capacity and SOC preservation potential of soils, particularly acid soils. The published literature data did not show any relationship between P sorption capacity and SOC concentration. Further research is needed to evaluate the complex relationship between P sorption capacity and SOC concentration (and accounting for the influence of climate, geochemical variables, vegetation types, and soil depth) particularly in acid soils at a global scale, using various approaches e.g. random forest model, generalized additive mixed effect model and linear mixed effect model.

In Chapter 3, a comprehensive study determined the role of different extractable forms of metal(loid)s in the association of OC in top and sub-soils of NSW, Australia. The results showed that SOC was extracted in the sequence: $C_{PP} > C_{DCB} > C_{OX}$, with mean of 62 %, 41 %

and 28 % C, respectively, of the TC in soils. C_{PP} and C_{DCB} were significantly greater in the topsoils than the subsoils. The extraction sequence for Fe was: $Fe_{DCB} > Fe_{OX} > Fe_{PP}$, with mean of 49 %, 9 % and 3 %, respectively, of the total Fe. Fe_{PP} was significantly greater in the topsoils than the subsoils. The sequence for Al was: $Al_{DCB} > Al_{OX} > Al_{PP}$, with mean of 4 %, 3.9 % and 2 %, respectively, of the total Al. Manganese was extracted in the sequence - $Mn_{OX} > Mn_{DCB} > Mn_{PP}$, with an average of 78 %, 65 % and 43 %, respectively, of the total Mn. All forms of extractable Mn were significantly greater in the topsoils than the subsoils. All extractants dissolved < 1% of the total Si. The results also showed that among the elements extracted, the concentration of Fe_{DCB} was the highest in the both top- and sub-soils. All extractable forms of Fe and Al showed significant positive correlations with extractable C, which suggested their role in the preservation of SOC. The large fraction (62 %) of total OC extracted by PP was present in organic-Fe/Al complexes and about 28 % of the total OC was associated with SRO and poorly crystalline Fe oxides in the studied soils. A relatively small proportion of total OC extracted by DCB was present in crystalline Fe/Al oxides indicating a limited role of crystalline Fe/Al oxides in the OC preservation. DCB and OX extracted almost similar Al concentrations, which might indicate release of additional Al, that substituted for Fe in the structure of Fe oxides, during DCB extraction. Crystalline Fe oxides (i.e., goethite and hematite) were dominant in both topsoils and subsoils, and SRO of Al and Si were absent in the soils. Organic carbon in the studied soils was preserved via both organo-metal complexes and adsorption processes. The findings from this study are important in providing valuable insights for farmers, climate modelers, land managers and researchers in soil science in making informed decisions on the prediction of SOC. Extraction techniques offer the best option for the evaluation of OC association with Fe, Al, Mn and Si. However, there some overlaps and non-selectivity in using extraction methods. Further research should explore the use of synchrotron based high-energy X-ray diffraction and pair distribution functions for assessment of OC

associated with Fe, Al, Mn and Si. The technique enables the characterisation of poorly crystalline forms of Fe, Al, and Mn (Carrero *et al.*, 2017; Wang *et al.*, 2017; Wang *et al.*, 2018; Rennert, 2019). The techniques may possibly be able to examine the pertinence of extraction methods.

In Chapter 4 XANES and EXAFS at Fe-K edge were used to quantify Fe-minerals containing minerals and Fe complexed with OM in 36 bulk soil samples representing several soil types. LCF analysis of the XANES and EXAFS data revealed that crystalline Fe oxides (i.e., hematite and goethite) accounted for 60 % and 40 %, respectively, of the total Fe in the bulk soil samples. The predictions for ferrihydrite were reasonable from both XANES and EXAFS. The results obtained from the LCF of EXAFS spectra were more closely related than XANES with the chemically extracted Fe data. XAS predicted Fe content in various Fe phases was well correlated with the DCB extractable Fe. EXAFS predicted Fe contents in different phases better than XANES in bulk soils. Fe K-edge XAS showed good results for the quantification of Fe phases in bulk soils, which can be improved using closely matching reference materials in the analysis. The procedure could potentially be used in routine soil analysis considering the emergence of bench top laboratory based XAS spectrometers.

Nevertheless, there are some drawbacks of the techniques, such as inability to detect low concentration of Fe in kaolinite in some samples including the two standard mixtures. The EXAFS spectrum of kaolinite was very noisy, and an unusual peak existed in the sample, hence kaolinite could not be estimated by the LCF analysis of EXAFS data. The detection for Fe complexed with OM was rather poor, which suggested that Fe(III) citrate did not represent the OM complexed Fe in the soil samples. Despite these drawbacks, the combination of XANES and EXAFS showed good potential for the identification and quantification of Fe in different minerals using bulk soil samples and it should be further explored using closely matching reference phases in the analysis.

In Chapter 5, adsorption of phosphate and DOC separately, and competitive adsorption of phosphate and DOC from mixed solutions of P and DOC in soils was studied. Surface and subsurface soils containing substantial Fe oxides from Tumbarumba and Wagga Wagga were used in these experiments. The surface and subsurface soils from Tumbarumba had the greater capacity for phosphate adsorption than the surface and subsurface soils of Wagga Wagga, which may be due to the higher content Fe and Al oxides in the soils from Tumbarumba. Phosphate adsorption was greater in the subsurface than the surface soil from Tumbarumba. However, in soils from Wagga Wagga, phosphate adsorption was greater in the surface than the subsurface soils. The greatest adsorption capacity for DOC in both studied soils occurred in the subsurface soils. We found that in the mixed solution of P and DOC, phosphate adsorption promoted DOC desorption in the surface and subsurface soils from Wagga Wagga and Tumbarumba. This was due to effective competitive effect from phosphate than DOC for adsorption sites on mineral surfaces. Extractable Fe and Al strongly influenced phosphate and DOC adsorption capacity in the studied soils and can be used as a routine soil test to predict P and DOC adsorption capacity in surface and subsurface soils. Furthermore, the optimal P fertilisation may be estimated from extractable Fe and Al without considering the content of OC in the studied soils. The results of this study have crucial implications on the sustainability of Fe-rich soils. The adsorption of phosphate promoted DOC desorption in these soils, may lead to destabilisation of OC. Consequently, OC destabilisation may impair OC sequestration and enhance microbial decomposition in these soils. Nevertheless, the effect of P addition on DOC desorption may depend on different soil environmental conditions which may vary from one soil type to another. More so, phosphate might play a major role in influencing the microbial stability of OC adsorption in these soils. On the contrary, it had been shown that DOC competed strongly with phosphate for adsorption sites and significantly inhibited phosphate adsorption, which can increase the bioavailability of P in soils. Further research is needed to explore the competitive

adsorption of phosphate and DOC behaviour in tropical soils with high and low Fe oxide content and low P content. Further research should also be explored on the competitive adsorption of phosphate and DOC behaviour in subsurface soils that have no impact OM. In addition, long-term field experiment research should be conducted in tropical soils to determine the effect of P additions on OC sequestration.

References

Carrero, S., Fernandez-Martinez, A., Pérez-López, R., Nieto, J.M., 2017. Basaluminite Structure and its Environmental Implications. *Procedia Earth and Planetary Science* **17**, 237-240.

Rennert, T., 2019. Wet-chemical extractions to characterise pedogenic Al and Fe species–a critical review. *Soil Research* **57**, 1-16.

Wang, Q., Yang, P., Zhu, M., 2018. Structural transformation of birnessite by fulvic acid under anoxic conditions. *Environmental Science & Technology* **52**, 1844-1853.

Wang, X., Hu, Y., Tang, Y., Yang, P., Feng, X., Xu, W., Zhu, M., 2017. Phosphate and phytate adsorption and precipitation on ferrihydrite surfaces. *Environmental Science: Nano* **4**, 2193-2204.

Appendices

Appendix 5.1. Initial P concentration, equilibrium P pH, equilibrium P concentration, P adsorbed, equilibrium DOC desorbed concentration and DOC desorbed for surface and subsurface soils from Wagga Wagga.

		Wagga Wagga surface soil					Wagga Wagga subsurface soil				
Initial P concentration (mg/L)	Replicates	Equilibrium P pH	Equilibrium P concentration (mmol/L)	P adsorbed (mmol/kg)	Equilibrium DOC desorbed concentration (mmol/L)	DOC desorbed (mmol/kg)	Equilibrium P pH	Equilibrium P concentration (mmol/L)	P adsorbed (mmol/kg)	Equilibrium DOC desorbed concentration (mmol/L)	DOC desorbed (mmol/kg)
0	1	5.23	0.89	-17.79	0.78	15.68	5.31	0.00	0.05	0.84	16.75
0	2	5.24	0.90	-17.97	0.78	15.68	5.30	0.00	0.05	0.84	16.79
5	1	4.72	1.00	-16.67	0.79	15.85	5.27	0.06	2.04	0.90	17.92
5	2	4.73	0.99	-16.50	0.79	15.85	5.31	0.06	2.04	0.90	17.95
10	1	4.72	1.02	-13.97	0.83	16.58	5.33	0.08	4.91	0.99	19.82
10	2	4.71	1.03	-14.14	0.83	16.57	5.33	0.08	4.91	0.99	19.87
20	1	4.78	1.12	-9.44	0.83	16.59	5.37	0.27	7.42	1.00	20.10
20	2	4.77	1.14	-9.79	0.83	16.59	5.36	0.27	7.42	1.01	20.13
30	1	4.75	1.39	-8.42	0.89	17.75	5.39	0.50	9.32	1.02	20.42
30	2	4.76	1.39	-8.42	0.89	17.74	5.39	0.50	9.32	1.02	20.45
40	1	4.77	1.56	-5.30	0.92	18.43	5.38	0.68	12.27	1.08	21.68
40	2	4.78	1.57	-5.48	0.92	18.47	5.39	0.68	12.27	1.09	21.78
50	1	4.74	1.78	-3.40	0.95	19.03	5.39	0.93	13.64	1.13	22.60
50	2	4.75	1.79	-3.58	0.95	19.07	5.37	0.93	13.64	1.13	22.61
60	1	4.81	1.82	2.35	0.96	19.17	5.39	1.15	15.71	1.13	22.63
60	2	4.80	1.81	2.53	0.96	19.20	5.40	1.15	15.71	1.13	22.65
70	1	4.85	1.91	7.05	0.96	19.22	5.41	1.37	17.78	1.20	24.06
70	2	4.82	1.92	6.88	0.96	19.28	5.45	1.37	17.78	1.21	24.11
80	1	4.81	2.00	11.76	1.08	21.57	5.45	1.59	19.94	1.24	24.86
80	2	4.80	1.99	11.93	1.08	21.62	5.45	1.59	19.94	1.24	24.80

Appendix 5.2. Initial P concentration, equilibrium P pH, equilibrium P concentration, P adsorbed, equilibrium DOC desorbed concentration and DOC desorbed for surface and subsurface soils from Tumbarumba.

		Tumbarumba surface soil					Tumbarumba subsurface soil				
Initial P concentration (mg/L)	Replicates	Equilibrium P pH	Equilibrium P concentration (mmol/L)	P adsorbed (mmol/kg)	Equilibrium DOC desorbed concentration (mmol/L)	DOC desorbed (mmol/kg)	Equilibrium P pH	Equilibrium P concentration (mmol/L)	P adsorbed (mmol/kg)	Equilibrium DOC desorbed concentration (mmol/L)	DOC desorbed (mmol/kg)
0	1	4.73	0.14	-2.82	1.53	30.67	4.88	0.01	-0.27	1.31	26.19
0	2	4.72	0.14	-2.83	1.54	30.72	4.82	0.01	-0.26	1.26	25.23
50	1	4.62	0.43	23.76	1.85	36.94	5.06	0.07	30.79	1.36	27.24
50	2	4.63	0.44	23.59	1.85	36.97	5.05	0.08	30.77	1.40	27.96
75	1	4.66	0.64	35.69	2.08	41.52	5.13	0.19	44.64	2.29	45.88
75	2	4.67	0.63	35.87	2.08	41.55	5.14	0.19	44.73	2.32	46.38
100	1	4.66	0.85	47.63	2.23	44.56	5.17	0.33	57.95	2.55	50.94
100	2	4.68	0.86	47.45	2.23	44.60	5.16	0.34	57.86	2.54	50.87
125	1	4.70	1.10	58.68	2.31	46.28	5.17	0.56	69.62	2.70	53.99
125	2	4.69	1.11	58.51	2.31	46.29	5.18	0.56	69.53	2.70	53.97
150	1	4.73	1.26	71.67	2.50	50.04	5.20	0.70	82.86	2.72	54.47
150	2	4.74	1.27	71.49	2.50	50.09	5.18	0.70	82.95	2.75	54.95
175	1	4.75	1.65	80.09	2.55	51.02	5.18	0.83	96.38	2.84	56.74
175	2	4.76	1.64	80.27	2.55	51.09	5.22	0.83	96.46	2.84	56.82
200	1	4.78	1.88	91.50	2.63	52.52	5.24	1.07	107.70	2.96	59.12
200	2	4.77	1.89	91.32	2.63	52.59	5.26	1.06	107.87	2.96	59.27
225	1	4.78	2.15	102.38	2.69	53.84	5.25	1.18	121.65	3.07	61.50
225	2	4.76	2.14	102.55	2.69	53.87	5.24	1.19	121.56	3.05	60.98
250	1	4.78	2.22	117.12	2.70	53.91	5.30	1.29	135.60	3.10	62.01
250	2	4.77	2.23	116.94	2.70	53.94	5.29	1.30	135.51	3.09	61.85

Appendix 5.3. Initial DOC concentration, equilibrium DOC pH, equilibrium DOC concentration, DOC adsorbed, equilibrium P desorbed concentration and P desorbed for surface and subsurface soils from Wagga Wagga.

		Wagga Wagga surface soil					Wagga Wagga subsurface soil				
Initial DOC concentration (mg/L)	Replicates	Equilibrium DOC pH	Equilibrium DOC concentration (mmol/L)	DOC adsorbed (mmol/kg)	Equilibrium P desorbed concentration (mmol/L)	P desorbed (mmol/kg)	Equilibrium DOC pH	Equilibrium DOC concentration (mmol/L)	DOC adsorbed (mmol/kg)	Equilibrium P desorbed concentration (mmol/L)	P desorbed (mmol/kg)
0	1	4.55	1.23	-11.10	0.83	8.30	5.11	0.93	-8.10	0.56	5.55
0	2	4.56	1.23	-11.13	0.83	8.30	5.10	0.93	-8.11	0.55	5.51
5	1	4.58	1.32	-9.16	0.85	8.48	5.03	1.07	-6.23	0.56	5.64
5	2	4.57	1.32	-9.17	0.85	8.48	5.01	1.07	-6.24	0.56	5.60
10	1	4.58	1.49	-7.28	0.86	8.56	4.97	1.21	-4.17	0.57	5.69
10	2	4.57	1.49	-7.30	0.86	8.56	4.98	1.21	-4.16	0.57	5.69
20	1	4.6	1.81	-2.74	0.87	8.65	5.00	1.54	0.35	0.57	5.73
20	2	4.59	1.81	-2.76	0.87	8.65	4.99	1.54	0.34	0.58	5.73
40	1	4.58	2.66	4.40	0.87	8.74	5.06	2.26	8.78	0.59	5.91
40	2	4.59	2.66	4.37	0.87	8.74	5.04	2.26	8.77	0.59	5.91
60	1	4.64	3.53	10.99	0.90	9.00	4.99	2.96	17.14	0.59	5.95
60	2	4.65	3.53	10.97	0.90	9.00	5.01	2.96	17.13	0.59	5.95
80	1	4.66	4.46	18.33	0.90	9.00	5.03	3.75	24.05	0.60	5.99
80	2	4.65	4.46	18.30	0.90	9.00	5.01	3.75	24.04	0.60	5.99
100	1	4.67	5.42	22.04	0.90	9.00	5.05	4.45	32.21	0.60	6.04
100	2	4.68	5.42	22.01	0.90	9.00	5.02	4.45	32.20	0.60	6.04
120	1	4.67	6.30	28.28	0.90	9.00	5.09	5.43	39.42	0.61	6.12
120	2	4.68	6.30	28.27	0.90	9.00	5.08	5.43	39.41	0.61	6.12
140	1	4.68	7.38	32.24	0.91	9.09	5.06	6.29	48.00	0.63	6.26
140	2	4.67	7.38	32.22	0.91	9.09	5.08	6.29	48.01	0.62	6.26

Appendix 5.4. Initial DOC concentration, equilibrium DOC pH, equilibrium DOC concentration, DOC adsorbed, equilibrium P desorbed concentration and P desorbed for surface and subsurface soils from Tumbarumba.

		Tumbarumba surface soil					Tumbarumba subsurface soil				
Initial DOC concentration (mg/L)	Replicates	Equilibrium DOC pH	Equilibrium DOC concentration (mmol/L)	DOC adsorbed (mmol/kg)	Equilibrium P desorbed concentration (mmol/L)	P desorbed (mmol/kg)	Equilibrium DOC pH	Equilibrium DOC concentration (mmol/l)	DOC adsorbed (mmol/kg)	Equilibrium P desorbed concentration (mmol/L)	P desorbed (mmol/kg)
0	1	4.33	1.47	-13.49	0.01	0.08	5.24	0.52	-3.98	0.003	0.03
0	2	4.32	1.47	-13.50	0.01	0.08	5.22	0.52	-3.98	0.003	0.03
5	1	4.32	1.50	-10.97	0.01	0.08	5.41	0.55	-1.06	0.003	0.03
5	2	4.33	1.51	-11.00	0.01	0.08	5.43	0.55	-1.05	0.003	0.03
10	1	4.32	1.55	-7.90	0.01	0.08	5.46	0.61	1.79	0.003	0.03
10	2	4.33	1.55	-7.91	0.01	0.08	5.43	0.61	1.78	0.003	0.03
20	1	4.31	1.62	-0.91	0.01	0.08	5.42	0.69	8.83	0.003	0.03
20	2	4.32	1.62	-0.92	0.01	0.08	5.42	0.69	8.82	0.003	0.03
40	1	4.33	1.84	12.64	0.01	0.09	5.42	0.88	22.53	0.003	0.03
40	2	4.34	1.84	12.60	0.01	0.09	5.42	0.88	22.54	0.003	0.03
60	1	4.35	2.24	23.91	0.01	0.09	5.44	1.07	36.05	0.003	0.03
60	2	4.36	2.24	23.89	0.01	0.09	5.41	1.07	36.06	0.003	0.03
80	1	4.35	2.67	36.18	0.01	0.10	5.44	1.25	49.00	0.003	0.03
80	2	4.36	2.68	36.15	0.01	0.10	5.43	1.25	49.02	0.003	0.03
100	1	4.35	2.82	48.06	0.01	0.11	5.43	1.45	62.23	0.003	0.03
100	2	4.36	2.82	48.03	0.01	0.11	5.45	1.45	62.25	0.003	0.03
120	1	4.37	3.30	58.26	0.01	0.12	5.40	1.65	77.29	0.004	0.04
120	2	4.38	3.30	58.24	0.01	0.12	5.40	1.65	77.29	0.004	0.04
140	1	4.39	3.67	69.37	0.01	0.13	5.36	1.91	91.80	0.004	0.04
140	2	4.38	3.67	69.33	0.01	0.13	5.38	1.91	91.77	0.004	0.04

Appendix 5.5. Initial DOC concentration, initial P concentration, equilibrium P and DOC pH, equilibrium P concentration, equilibrium DOC concentration, P adsorbed, and DOC adsorbed for surface and subsurface soil from Wagga Wagga.

Wagga Wagga surface soil								Wagga Wagga subsurface soil				
Initial DOC concentration (mg/L)	Initial P concentration (mg/L)	Replicates	Equilibrium P+DOC pH	Equilibrium P concentration (mmol/L)	P adsorbed (mmol/kg)	Equilibrium DOC concentration (mmol/L)	DOC adsorbed (mmol/kg)	Equilibrium P+DOC pH	Equilibrium P concentration (mmol/L)	P adsorbed (mmol/kg)	Equilibrium DOC concentration (mmol/L)	DOC adsorbed (mmol/kg)
1.12	24.57	1	5.26	0.85	-1.19	0.78	-13.66	5.60	0.75	0.91	0.64	-11.01
1.12	24.57	2	5.25	0.85	-1.19	0.78	-13.65	5.60	0.75	0.91	0.64	-11.01
1.85	28.99	1	4.75	0.88	1.14	0.83	-13.60	5.09	0.78	3.16	0.64	-9.80
1.85	28.99	2	4.74	0.88	1.14	0.83	-13.60	5.09	0.78	3.16	0.64	-9.79
1.89	32.80	1	4.70	0.91	2.98	0.86	-14.04	5.09	0.81	5.00	0.68	-10.45
1.89	32.80	2	4.71	0.91	2.98	0.86	-14.04	5.09	0.81	5.00	0.68	-10.46
3.15	35.92	1	4.70	0.92	4.83	0.86	-11.97	5.01	0.86	5.97	0.68	-8.36
3.15	35.92	2	4.71	0.92	4.83	0.86	-11.97	5.01	0.86	5.97	0.68	-8.37
6.20	37.96	1	4.71	0.96	5.26	1.05	-10.76	5.00	0.91	6.41	0.84	-6.40
6.20	37.96	2	4.72	0.96	5.26	1.05	-10.76	5.00	0.91	6.41	0.84	-6.40
9.28	40.00	1	4.67	0.98	6.14	1.21	-8.80	5.00	0.94	7.11	0.99	-4.34
9.28	40.00	2	4.68	0.98	6.14	1.21	-8.80	5.00	0.94	7.11	0.99	-4.30
12.71	42.85	1	4.67	1.07	6.32	1.40	-6.89	5.01	0.95	8.60	1.16	-1.98
12.71	42.85	2	4.69	1.07	6.32	1.40	-6.89	5.01	0.95	8.60	1.16	-2.00
15.86	46.93	1	4.72	1.11	8.07	1.63	-6.26	5.01	1.09	8.51	1.42	-1.93
15.86	46.93	2	4.73	1.11	8.07	1.63	-6.26	5.01	1.09	8.51	1.42	-1.98
18.99	50.05	1	4.75	1.20	8.25	1.74	-3.18	5.03	1.15	9.48	1.49	1.73
18.99	50.05	2	4.75	1.20	8.25	1.74	-3.18	5.03	1.15	9.48	1.50	1.67

Appendix 5.6. Initial DOC concentration, initial P concentration, equilibrium P and DOC pH, equilibrium P concentration, equilibrium DOC concentration, P adsorbed, and DOC adsorbed for surface and subsurface soil from Tumbarumba.

Tumbarumba surface soil								Tumbarumba subsurface soil				
Initial DOC concentration (mg/L)	Initial P concentration (mg/L)	Replicates	Equilibrium P+DOC pH	Equilibrium P concentration (mmol/L)	P adsorbed (mmol/kg)	Equilibrium DOC concentration (mmol/L)	DOC adsorbed (mmol/kg)	Equilibrium P+DOC pH	Equilibrium P concentration (mmol/L)	P adsorbed (mmol/kg)	Equilibrium DOC concentration (mmol/L)	DOC adsorbed (mmol/kg)
1.12	7.99	1	4.87	0.14	2.32	1.35	-25.18	5.09	0.02	4.73	0.49	-7.91
1.12	7.99	2	4.86	0.14	2.32	1.35	-25.19	5.08	0.02	4.73	0.49	-7.92
1.63	28.18	1	4.53	0.24	13.34	1.39	-25.04	4.89	0.03	17.53	0.52	-7.73
1.63	28.18	2	4.54	0.24	13.34	1.39	-25.08	4.90	0.03	17.53	0.52	-7.73
2.00	41.22	1	4.60	0.26	21.50	1.42	-25.03	4.94	0.05	25.69	0.56	-7.78
2.00	41.22	2	4.59	0.26	21.50	1.42	-25.07	4.95	0.05	25.69	0.56	-7.78
3.58	44.48	1	4.51	0.26	23.52	1.49	-23.89	4.96	0.05	27.71	0.65	-7.01
3.58	44.48	2	4.52	0.26	23.52	1.49	-23.94	4.97	0.05	27.71	0.65	-7.01
6.46	51.96	1	4.59	0.34	26.76	1.65	-22.30	4.93	0.10	31.57	0.73	-3.88
6.46	51.96	2	4.58	0.34	26.76	1.65	-22.30	4.94	0.10	31.57	0.73	-3.88
9.48	55.90	1	4.65	0.40	28.17	1.96	-23.33	4.90	0.14	33.24	0.88	-1.79
9.48	55.90	2	4.64	0.40	28.17	1.96	-23.35	4.91	0.14	33.24	0.88	-1.84
12.96	58.89	1	4.59	0.48	28.34	2.10	-20.38	4.92	0.21	33.85	0.93	2.90
12.96	58.89	2	4.60	0.48	28.34	2.10	-20.38	4.92	0.21	33.85	0.94	2.85
15.48	64.86	1	4.69	0.61	29.74	2.31	-20.42	4.97	0.27	36.57	1.09	4.03
15.48	64.86	2	4.68	0.61	29.74	2.31	-20.45	4.98	0.27	36.57	1.09	4.03
19.27	69.76	1	4.62	0.67	31.59	2.52	-18.27	4.96	0.33	38.41	1.19	8.34
19.27	69.76	2	4.61	0.67	31.59	2.52	-18.27	4.97	0.33	38.41	1.19	8.34